Train Trajectory Optimization Methods for Energy-Efficient Railway Operations

Wang, Pengling

DOI
10.4233/uuid:ce04a07d-89fc-470a-9d1a-b6fae9182dae

Publication date
2017

Document Version
Final published version

Citation (APA)
Wang, P. (2017). *Train Trajectory Optimization Methods for Energy-Efficient Railway Operations*. [Dissertation (TU Delft), Delft University of Technology]. TRAIL Research School. https://doi.org/10.4233/uuid:ce04a07d-89fc-470a-9d1a-b6fae9182dae

Train Trajectory Optimization Methods for Energy-Efficient Railway Operations

Pengling Wang

Delft University of Technology, 2017

This thesis is in partial funded by the Chinese Scholarship Council (CSC) and the Dutch railway manager ProRail.
The Netherlands Research School for Transport, Infrastructure and Logistics TRAIL is greatly acknowledged.

Cover illustration: Pengling Wang

Train Trajectory Optimization Methods for Energy-Efficient Railway Operations

Proefschrift

ter verkrijging van de graad van doctor

aan de Technische Universiteit Delft,

op gezag van de Rector Magnificus prof. ir. K.C.A.M. Luyben,

voorzitter van het College voor Promoties,

in het openbaar te verdedigen op woensdag 6 december 2017 om 10:00 uur

door

Pengling WANG

Bachelor of Engineering in Electrical Engineering and Automation,

Southwest Jiaotong University (China)

geboren te Haian, Jiangsu, China.

This dissertation has been approved by the promotor:
Prof. dr. ir. S.P. Hoogendoorn
Prof. dr. R.M.P. Goverde

Composition of the doctoral committee:

Rector Magnificus	Chairman
Prof. dr. ir. S.P. Hoogendoorn	Delft University of Technology, promotor
Prof. dr. R.M.P. Goverde	Delft University of Technology, promotor

Independent members:

Prof. dr. ir. A. Verbraeck	Delft University of Technology
Prof. dr. ir. B. De Schutter	Delft University of Technology
Prof. Dr. -Ing. L. Ma	Southwest Jiaotong University
Dr. R. Liu	University of Leeds
Dr. R. Lentink	Netherlands Railways

TRAIL Thesis Series no. T2017/12, the Netherlands TRAIL Research School

TRAIL
P.O. Box 5017
2600 GA Delft
The Netherlands
E-mail: info@rsTRAIL.nl

ISBN: 978-90-5584-231-5

Printed in the Netherlands

”竣实扬华 自强不息”

”Challenge the Future”

Preface

In 2011, I chose "Optimizing Train Trajectory for Energy Efficiency using Genetic Algorithms" as the research topic for my Bachelor thesis. It is the very beginning of my research on improving the energy efficiency of railway operations. It has been a pleasant experience for me to study in Delft for three years to pursue a PhD degree. I would like to take this opportunity to thank the people who have been important to me during my PhD life.

Foremost, I would like to express my sincere gratitude to my daily supervisor Prof. Rob M.P. Goverde for the continuous support of my Ph.D. study and research. In 2013, I decided to come abroad and expand my horizon. I applied for TU Delft because the railway group at TU Delft enjoyed great popularity for their outstanding works. In that year, I had my first interview Skype meeting with Rob. I was diffident, nervous, and barely able to speak one complete sentence since that was my first time to talk to a non-Chinese, who is also a famous figure in our field! It was not easy in the beginning of my study here. Our first paper went through FIVE times of major revisions before it was accepted. I had to extend my knowledge, think more creatively, and improve my English and writing skills to meet reviewers' requirements. Rob was patient and taught me a lot during that period. The research got much smooth afterwards. I got many chances to attend conferences and meet experts in our field; I got some papers accepted by high-quality journals; and, most importantly, I got my knowledge and skills grown. Then I realized that it is all the challenges and difficulties I met during the PhD study that make me a PhD. Nevertheless, all these cannot happen without Rob's help. Many thanks for his patience, motivation, enthusiasm, and immense knowledge. Many congratulations to him for becoming a full professor in this year.

Besides my supervisor, I would like to thank Prof. Lei Ma and Prof. Serge Hoogendoorn. As my promotor in China, Lei is always supportive and gives me a lot of wise advice in career development. As my promotor in the Netherlands, Serge always gives me positive and encouraging feedbacks, which makes me feel so warm to study in the Netherlands. I would also like to thank the rest of committee members: Prof. B. De Schutter, Prof. A. Verbaeck, Dr. R. Liu, and Dr. R. Lentink, for their encouragement, insightful comments and questions. Thank Ingo Hansen for knowing me and introducing me to Rob. Without you, I am not able to be here. I also appreciate your critical and detailed advice on my research.

My sincere thanks also go to Jelle van Luipen from ProRail, for offering me the opportunities of working for the NEO project, by which I was able to put my theoretical works into practical implementations and developed a prototype driver advisory system named ETO. I thank my previous supervisors in China, Qingyuan Wang and Xiaoyun Feng, for leading me into the exciting field of railway operation optimization research.

I thank my officemates: Nikola, Nadjla, Fei, Yongqiu, and Gerben, for all the struggles and funs we have had in 4.17. I thank my roommates: Shuai, Hai, and Hongzhi, for giving me a sweet "family" in the Netherlands. I thank Xiao Lin for teaching me swimming. Thank Kai Yuan, Rong Zhang, Lei Xie, Qu Hu, Liang Xiao, Wenhua, Anqi, and Qingxi, for giving me great time in Paris, Belgium and Barcelona. Thank Yao, Yihong, and Yu for the days we hung out. Thank Na Chen, Haopeng, Xiao Li, Jiateng and Yande for giving me happy memories in tennis fields. Thank my colleagues of T&P: Yushen, Meng, Yufei, Yaqing, Lin, Xiaochen, Vincent, Ding, Meiqi, Mo, Priscilla, Francesco, Bernat, Silvia, Xavier and Freddy. Finally, I would like to thank all technical and administrative staff of T&P and TRAIL Research School for taking care of many practical issues, which allowed me to fully focus on the project.

Last but not least, I'd like to thank my family and Song, for their love and unconditional support during the last three years. Your love, full understanding, and wise encouragements helped me go through tough moments and brought me peace and joy in these years.

Delft, October 2017

Pengling Wang

Contents

Chapter 1

Introduction

1.1 Background

In many countries, railway systems play a critical role in carrying passengers and cargo. Even though rail is more energy efficient than most other transport modes, the enhancement of energy efficiency is an important issue for railways to reduce their contributions to climate change further as well as to save and enhance the competition advantages involved.

One promising means of improving energy efficiency is to optimize train operations by using energy-efficient driving strategies. Even with a small amount of energy saved by each train operation, the total energy costs saved by the whole railway network are huge. Research on finding the optimal energy-efficient driving strategies has been done since 1960s. The main focus has been to use optimal control theory to find the optimal trajectory (speed-distance curves and time-distance curves along the train's journey), which assure a safe, on-time, comfortable and energy-saving train operation (Howlett and Pudney, 1995; Albrecht et al., 2016a,b; Scheepmaker et al., 2017). The process of finding the optimal trajectory is called train trajectory optimization (TTO). The optimized trajectory is the foundation for the Automatic Train Operation (ATO) systems to control train movements, as well as the train Driver Advisory Systems (DASs) to provide driving advice, such as advised speeds and control regimes, which helps train drivers to drive the train in a safe and efficient manner.

The ideal train movement is to follow its pre-designed timetable. It is unavoidable that unexpected events may cause the train to deviate from its timetable. In that case, the delayed train should get back to its schedule as soon as possible to avoid train conflicts and delay propagation. However, it is more energy-efficient if the delay is reduced gradually during the remaining journey (Albrecht et al., 2011). How to balance the urgency of delay recovery and energy-efficient driving is an important issue for the real-time delay recovery problem.

Meanwhile, energy-efficient driving relies on the time supplements provided by the timetables. The time supplement refers to the extra running time from one stop to another compared to the minimal technical running time (Hansen and Pachl, 2014; Goverde et al., 2016). That extra running time provides the possibility for energy-efficient train operations, such as coasting or cruising at a low speed. How to design a good timetable by providing more time supplements without influencing the railway capacity is essential for energy-efficient train operations.

This dissertation investigates the approaches of energy-efficient railway operations. More specifically, the research is explored from three aspects to improve energy efficiency of train operations: train trajectory optimization, energy-efficient delay recovery and energy-efficient timetabling problem.

In the remainder of this chapter, Section 1.2 presents the remaining challenges of the train trajectory optimization, energy-efficient delay recovery and timetabling problem. Section 1.3 presents the questions to be solved in this dissertation. Section 1.4 summarizes the main contributions of this dissertation. Finally, Section 1.5 provides an outline of this dissertation, as well as brief introductions of every chapter in the remainder of this dissertation.

1.2 Challenges for energy-efficient railway operations

In this section, we describe the main challenges in energy-efficient railway operations that will be addressed in this dissertation.

1.2.1 Train trajectory optimization problem

The purpose of the train trajectory optimization is to find a trajectory that reduces the use of energy caused by train movements while maintaining schedule (Howlett and Pudney, 1995). The traditional TTO research focuses on optimizing an individual train movement from one stop to another. Pontryagin's Maximum Principle (PMP) has been widely used to analyze the optimal control strategy to achieve an energy-efficient train movement. According to the application of PMP, the optimal control regimes consist of maximum power, cruise, coasting and maximum braking. The optimal control strategy is a sequence of these optimal regimes (Milroy, 1980; Cheng and Howlett, 1992; Howlett and Pudney, 1995; Howlett, 2016). Given this knowledge of the optimal driving regimes, most train control algorithms then aim at finding the optimal switching points between the regimes. Another different approach to the TTO problem is by discretizing the continuous-time optimal control model to a static nonlinear programming model, after which nonlinear programming solvers are adopted to directly solve the problem (Wang et al., 2013, 2014; Ye and Liu, 2016, 2017; Haahr et al., 2017). Only recently this direct approach has been considered

for solving the TTO problem and has shown some advantages over the PMP-based methods (Wang et al., 2014; Ye and Liu, 2016, 2017; Haahr et al., 2017). The research on the TTO problem already got some achievements, however there are still some bottlenecks.

First, current TTO models are not able to fully characterize train operation constraints and objectives. The general TTO problem focuses on a single train moving between two stops within a given running time. TTO models use minimizing energy costs as the objective, and take into account the train movement constraints, speed limit constraints, vehicle characteristic constraints (maximum power, force, etc.) and arrival/departure time constraints. However, there are more factors that need to be taken into account by TTO models. First, the train trajectory should respect more time/speed constraints than just the arrival/departure time constraints at two stops, to satisfy the timetables. The additional constraints could be the arrival/departure/passing-through time or speed targets at intermediate stations and conflict points. Second, the train trajectory is restricted by some time and speed constraints at certain signalling locations. For instance, certain headway times between adjacent trains are required at some signals for the safety issue, yellow signals mandatorily demand the train to reduce its speed. Last but not least, if a train got delayed, the primary goal of the train operation is to reduce delays instead of energy consumption. The optimization objective changes to minimizing train delays in that circumstance.

The second drawback of current TTO methods is that the TTO requires a fast computation time since it is an important part of the DASs for real-time trajectory computation. However, the current existing PMP-based methods may consume long computation times since they have difficulties in finding the optimal switch points with complex speed limits and gradients (Albrecht et al., 2016a,b). The TTO requires more efficient solution methods for varying conditions.

In short, accurate modelling and efficient solution methods of the TTO problem are the bottleneck of the performance of the DASs. Therefore, research on TTO is important in improving train operations.

1.2.2 Energy-efficient delay recovery problem

Unexpected events might occur and impact train operations and result in train delays. How to efficiently control train movements while getting the train back to schedule is a difficult question even for experienced drivers. It is necessary to provide an optimal trajectory to help drivers, and that this trajectory provides the solution of energy-efficient delay recovery.

The first challenge of finding that energy-efficient delay recovery trajectory is to take into account the influences of signal systems. In the case that train operations are interrupted by unexpected events, it is all too common that a train approaches a station or junction at a time when its required platform or route is blocked by another train.

The consequence of this is that the signalling system sends a yellow or a red signal, which makes the train to brake to a low speed or stop on the approach to the station or junction. The train is allowed to accelerate again when the conflicting train has moved away. This brake/re-accelerate running is not energy efficient. If an approach can be devised to predict signal states ahead, and provide the optimal trajectory with consideration of signal states to train drivers, this realizes benefits of reducing energy consumption, avoiding conflicts and reducing the brake/re-accelerate behavior.

Furthermore, if the trains are able to cooperate to avoid conflicts and yellow (red) signals initiatively, this will also help reducing the brake/re-accelerate behavior. Optimizing multi-train trajectory together is a solution to achieve this target of the multi-train cooperation. Current train trajectory optimization methods focus on an individual train movement (Scheepmaker et al., 2017), while the TTO method for multiple trains is lacking. To distinguish the two concepts, the TTO method for a single train is called Single-Train Trajectory Optimization (STTO), while the TTO method for multiple trains called Multi-Train Trajectory Optimization (MTTO). There are two challenges to develop a MTTO method. Firstly, different trains using different routes and tracks, different speed limits, and different rolling stock compositions increase the difficulty of computing multi-train trajectory together. Secondly, the multi-train trajectory must take into account the interactions between trains and avoid train conflicts. It is challenging to operationalise the two concepts and develop a new MTTO method to improve train behaviors under delay situations.

1.2.3 Energy-efficient timetabling problem

Although energy efficiency is an important concern to railway infrastructure managers and railway undertakings, only little literature focuses on energy-efficient timetabling (Scheepmaker et al., 2017; Yang et al., 2016a,b; Zhou et al., 2017). Current timetable design approaches care more about journey time efficiency, feasibility, and robustness, while energy consumption is a secondary objective, which can therefore be considered as a fine-tuning step after the time allowances have been set based on feasibility and robustness (Goverde et al., 2016).

The performance of train operations depends highly on the quality of the timetable. A too tight timetable has no benefits for delay recovery, since it is not easy for a delayed train to catch up and get back to its planned timetable. A tight timetable is also not convenient for energy-efficiency because there is no room for energy-efficient train operation, i.e. there is no time for coasting. Instead, a certain amount of time supplement provides the possibility for coasting operations and absorbing small delays by running at faster speeds.

Both optimizing train trajectory and timetables can improve the railway energy efficiency. Past studies typically consider these two problems separately (Hansen and Pachl, 2014; Scheepmaker et al., 2017). However, the train trajectory and timetable are

closely related and both of them have a direct influence on energy-efficiency, so this separate optimization method is suboptimal. Integrating train trajectory optimization and timetable design improves the accuracy of the model and contributes to global optimality. Among the limited references about an integrated model to jointly optimize the timetable and speed profiles, researchers take into account the speed profile calculation in the timetable design (Kraay et al., 1991; Li and Lo, 2014a,b). The train trajectory optimization model is approximated and merged into a mixed integer programming model for timetable design, which however produces inaccurate speed profiles as well as a computational hard programming model. On the contrary, the train trajectory optimization models produce accurate speed profiles, which can be extended to solving the energy-efficient timetable design problem.

1.3 Research objectives and questions

The main objectives of this dissertation are to develop modelling and solution methods for the train trajectory optimization problem to improve model accuracy and shorten computation time, to apply the methods in a train driver advisory system development, and to develop a multi-train trajectory optimization method to solve the delay recovery and the energy-efficient timetabling problem.

To achieve the research objectives, the following research questions will be answered
1. How to formulate an accurate model for the train trajectory optimization problem?
2. Which solution approach can be used to solve the train trajectory optimization in short time?
3. What are feasible modelling and solution methods for the multi-train trajectory optimization problem?
4. How can we ensure a single train get back to its schedule with less energy consumption, as well as efficiently respond to signal systems, when the train is delayed?
5. How can we avoid yellow and red signals and the brake/re-accelerate behavior with a multi-train cooperation method, when the train operations are interrupted by unexpected events?
6. How can we improve the timetable's energy efficiency with the train trajectory optimization method?
7. How can we implement the proposed train trajectory optimization method into a driver advisory system?

1.4 Thesis contributions

This section summarizes the main contributions of this dissertation. A distinction is made between contributions that are of a scientific nature (either theoretical or methodological) and contributions that are of a societal nature.

1.4.1 Scientific contributions

The main scientific contributions of this thesis are as follows:

1. *A modelling method (the multiple-phase optimal control problem formulation) for the TTO problem*

   The TTO problem is formulated as a multiple-phase optimal control problem (Chapter 2), that enables an accurate and flexible formulation of varying speed limits and gradients, time (speed) constraints at timetable points and signal locations, and multi-objectives of energy-efficient driving and delay recovery.

2. *A multi-train trajectory optimization approach*

   A multi-train trajectory optimization approach is proposed (Chapter 3, 4 and 5), which optimizes multi-train trajectories simultaneously with consideration of every single train's operational constraints and conflict-avoiding constraints.

3. *A single-train delay recovery method with consideration of signalling constraints*

   A single-train delay recovery method is proposed (Chapter 2). The delay recovery method is on the basis of the TTO method with reducing delay as the optimization objective, meanwhile considering the influences from signalling systems. A signal response policy is proposed to ensure that the train makes correct and quick responses to different signalling aspects. A green wave policy is developed to avoid inefficient stop/start behaviors in case that a full prediction is available about the signal aspect timings in rear of the train ahead.

4. *An energy-efficient delay recovery method using the MTTO approach*

   A multi-train delay recovery method is proposed based on the MTTO approach (Chapter 3 and Chapter 4). The method reduces delay propagation and energy consumptions, as well as avoids inefficient stop/start behaviors, with the idea of multi-train cooperation.

5. *An energy-efficient timetabling method using the TTO approach*

   A novel timetabling method based on the TTO that optimises timetables by shifting arrival and departure times so that the time supplements are optimally allocated for energy efficient operation (Chapter 5).

6. *Development of a train driver advisory system that provides continuous energy-efficient and on-time driving advice*

   A prototype DAS named ETO (Energy-efficient Train Operation) is developed with the application of the proposed TTO method, which provides energy-efficient and on-time advice and responds to deviations from the advised time-distance path (Chapter 6).

1.4.2 Societal contributions

The main contributions to society of this thesis are as follows:

1. *This research focuses on improving the energy efficiency of railway operations.* Energy-efficient TTO methods are developed, which have practical relevance. They provide the railway undertakings a way to reducing energy costs of railway operations, both on the timetable plan level and on the train operation level. They can also be useful in advising safe, comfortable, and punctual train operations.

2. *For industry (including railway managers, operators, etc.), the energy-efficient TTO methods can be used as part of the timetable design and the DAS development.* The TTO methods can support timetable designers to improve a timetable's energy efficiency. TTO methods can also be adopted into the DASs to advise train drivers an energy-efficient driving behavior while maintaining the train schedule. Our work shows the flexibility of the TTO methods in practical applications and the generality of the ETO framework, which are desired features for DAS developers.

3. *From a driver's or passenger's perspective, our work shows that the TTO methods and the DASs can help train drivers in train control under multiple criteria and constraints.* It also is beneficial for the passengers by providing more punctual and cheaper services. The DASs can be developed to enhance safety, comfort, punctuality and energy efficiency.

1.5 Outline of the dissertation

This dissertation consists of seven chapters. A road map of the dissertation is presented in Figure 1.1, which clarifies the connections between the chapters. Chapter 2 investigates the STTO problem. Chapter 3, 4 and 5 can be grouped into a coherent content focusing on the MTTO problems. Chapter 6 presents a practical application of the proposed TTO method in the DAS development. Chapter 7 concludes the dissertation with the main contributions and directions for future research.

The main contents are in Chapters 2-7:

Chapter 2 presents the modelling and solution methods of STTO by the multiple-phase optimal control problem formulation and the pseudospectral method. This chapter studies the STTO problem which considers the general constraints (varying infrastructure characteristics and timetable constraints) and the influences from signal aspects and automatic train protection (ATP). The signal response policy and the green wave policy are developed in this chapter to dynamically respond to signals and to avoid yellow signals.

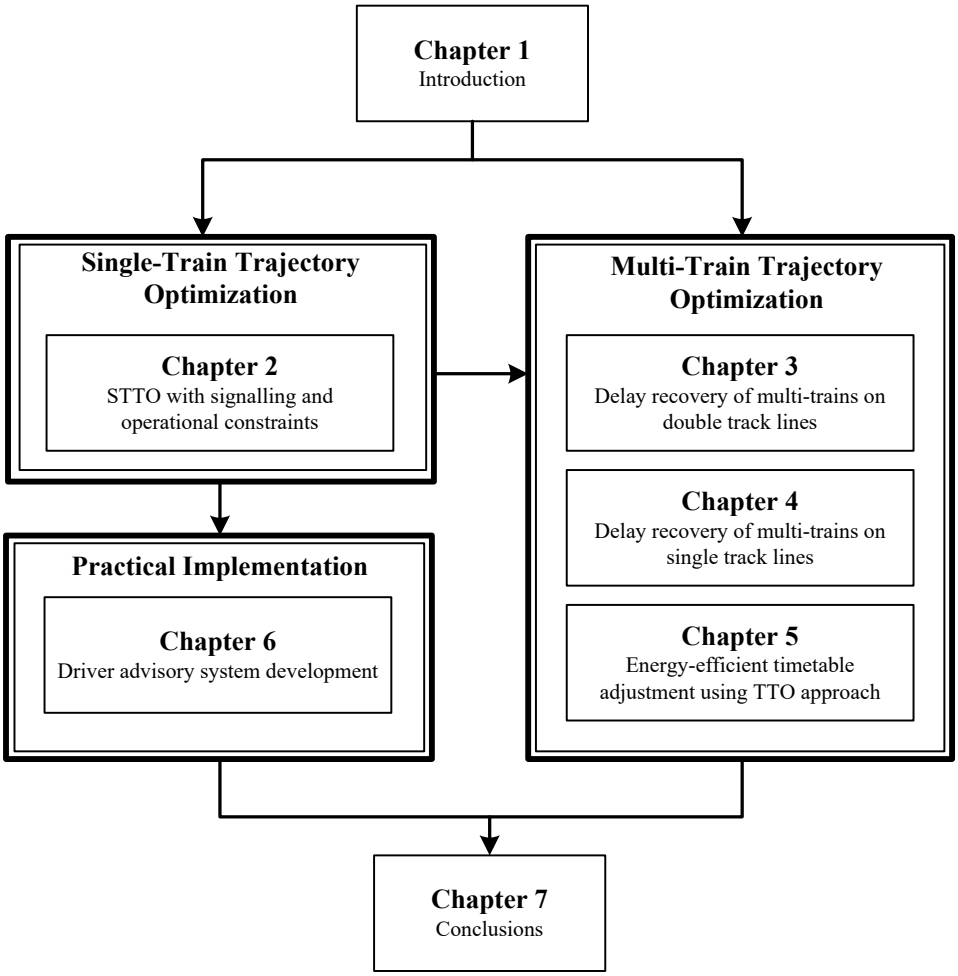

Figure 1.1: Flowchart of this dissertation structure.

The contents of Chapter 2 have been published as *P. Wang and R. M. P. Goverde, "Multiple-phase train trajectory optimization with signalling and operational constraints," Transportation Research Part C: Emerging Technologies, 69, 255–275, 2016*.

Chapter 3 presents the delay recovery problem of two successive trains in the same direction. The MTTO method is adopted to solve this problem, which takes into account not only each train's operational constraints, but also the constraints on keeping safe distances between the two trains. The green wave policy is adopted to ensure that the trains run safely under all green signals to avoid frequent stop/start behavior and thus improving train operation efficiency.

The contents of Chapter 3 have been published as *P. Wang and R. M. P. Goverde, "Two-train trajectory optimization with a green-wave policy," Transportation Research Record: Journal of the Transportation Research Board, 2546, 112–120, 2016*.

Chapter 4 proposes the delay recovery problem of opposite trains on single-track lines. We restrict our attention to delay cases, aiming to find a feasible schedule as well as energy-efficient speed profiles for multiple trains simultaneously. A MTTO model for opposite trains is proposed, which takes into account meet-and-pass constraints to avoid head-on conflicts. Three driving strategies of speed-up, energy-efficient and on-time driving, are proposed and combined in the optimization objective selection for different delay scenarios.

The contents of Chapter 4 have been published as *P. Wang and R. M. P. Goverde, "Multi-train trajectory optimization for energy efficiency and delay recovery on single-track railway lines," Transportation Research Part B: Methodological, 2017, 105: 340-361.*.

Chapter 5 implements the TTO methods in an energy-efficient timetable design, which is to improve the timetable's energy efficiency by adjusting running time allocation and optimizing trains' arrival and departure times of timetables. The timetables' fixed arrival and departure time targets are replaced with flexible arrival and departure time windows. The TTO methods compute the optimal arrival and departure times within those time windows. The optimized arrival and departure times are good for saving multi-trains' energy costs.

Chapter 6 introduces the driver advisory system ETO. The ETO system contains 5 core modules: data processor, train state monitor, trajectory calculator, trajectory processor, and advice generator. Chapter 6 provides an introduction to the framework of the ETO system as well as detailed descriptions of the five core modules. It also presents how to implement the proposed TTO method into the ETO system and the behavior in test scenarios with real-time instances of the Netherlands railways.

Finally, **Chapter 7** presents the conclusions of the dissertation. This chapter summarizes the main research findings and discusses their implications. In addition, it proposes directions for future research.

Bibliography

Albrecht, A., Howlett, P., Pudney, P., Vu, X., Zhou, P., 2016a. The key principles of optimal train control—part 1: Formulation of the model, strategies of optimal type, evolutionary lines, location of optimal switching points. Transportation Research Part B: Methodological 94, 482–508.

Albrecht, A., Howlett, P., Pudney, P., Vu, X., Zhou, P., 2016b. The key principles of optimal train control—part 2: Existence of an optimal strategy, the local energy minimization principle, uniqueness, computational techniques. Transportation Research Part B: Methodological 94, 509–538.

Albrecht, A., Koelewijn, J., Pudney, P., 2011. Energy-efficient recovery of delays in a rail network. In: Proceedings of 2011 Australasian Transport Research Forum. Adelaide, Australia.

Cheng, J., Howlett, P., 1992. Application of critical velocities to the minimisation of fuel consumption in the control of trains. Automatica 28 (1), 165–169.

Goverde, R. M. P., Bešinović, N., Binder, A., Cacchiani, V., Quaglietta, E., Roberti, R., Toth, P., 2016. A three-level framework for performance-based railway timetabling. Transportation Research Part C: Emerging Technologies 67, 62–83.

Haahr, J. T., Pisinger, D., Sabbaghian, M., 2017. A dynamic programming approach for optimizing train speed profiles with speed restrictions and passage points. Transportation Research Part B: Methodological 99, 167–182.

Hansen, I. A., Pachl, J., 2014. Railway timetabling and operations. Eurailpress.

Howlett, P., 2016. A new look at the rate of change of energy consumption with respect to journey time on an optimal train journey. Transportation Research Part B: Methodological 94, 387–408.

Howlett, P., Pudney, P., 1995. Energy-efficient train control. Springer.

Kraay, D., Harker, P. T., Chen, B., 1991. Optimal pacing of trains in freight railroads: model formulation and solution. Operations Research 39 (1), 82–99.

Li, X., Lo, H. K., 2014a. An energy-efficient scheduling and speed control approach for metro rail operations. Transportation Research Part B: Methodological 64, 73–89.

Li, X., Lo, H. K., 2014b. Energy minimization in dynamic train scheduling and control for metro rail operations. Transportation Research Part B: Methodological 70, 269–284.

Milroy, I. P., 1980. Aspects of automatic train control. Ph.D. thesis, Loughborough University, Leicestershire, UK.

Scheepmaker, G. M., Goverde, R. M. P., Kroon, L. G., 2017. Review of energy-efficient train control and timetabling. European Journal of Operational Research 257 (2), 355–376.

Wang, Y., De Schutter, B., van den Boom, T. J., Ning, B., 2013. Optimal trajectory planning for trains–a pseudospectral method and a mixed integer linear programming approach. Transportation Research Part C: Emerging Technologies 29, 97–114.

Wang, Y., De Schutter, B., van den Boom, T. J., Ning, B., 2014. Optimal trajectory planning for trains under fixed and moving signaling systems using mixed integer linear programming. Control Engineering Practice 22, 44–56.

Yang, X., Chen, A., Ning, B., Tang, T., 2016a. A stochastic model for the integrated optimization on metro timetable and speed profile with uncertain train mass. Transportation Research Part B: Methodological 91, 424–445.

Yang, X., Li, X., Ning, B., Tang, T., 2016b. A survey on energy-efficient train operation for urban rail transit. IEEE Transactions on Intelligent Transportation Systems 17 (1), 2–13.

Ye, H., Liu, R., 2016. A multiphase optimal control method for multi-train control and scheduling on railway lines. Transportation Research Part B: Methodological 93, 377–393.

Ye, H., Liu, R., 2017. Nonlinear programming methods based on closed-form expressions for optimal train control. Transportation Research Part C: Emerging Technologies 82, 102–123.

Zhou, L., Tong, L. C., Chen, J., Tang, J., Zhou, X., 2017. Joint optimization of high-speed train timetables and speed profiles: A unified modeling approach using space-time-speed grid networks. Transportation Research Part B: Methodological 97, 157–181.

Chapter 2

Multiple-phase train trajectory optimization with signalling and operational constraints

---

Apart from minor updates, this chapter has been published as:
P. Wang and R. M. P. Goverde, "Multiple-phase train trajectory optimization with signalling and operational constraints," *Transportation Research Part C: Emerging Technologies*, 69, 255–275, 2016.

2.1 Introduction

Improving transport capacity and saving energy consumption are the most urgent challenges faced by modern railway transportation all around the world. Optimizing train operation is one promising method, which does not need extra infrastructure, but improves rail traffic efficiency by optimizing train speed and control trajectories. One core function of train operation optimization is train trajectory calculation, which uses optimal control theory to calculate the optimal speed profiles and control regimes, aiming at safe, on-time and energy saving train operation. These profiles are used to generate driving advice to support train drivers in train control.

Research on train trajectory calculation started in the 1960s. The solution methods of the train trajectory optimization problem can be divided into two categories: indirect methods and direct methods. The indirect approach solves the problem indirectly by converting the optimal control problem to a boundary-value problem. The direct method finds the optimal solution by transcribing a continuous optimization problem to a nonlinear programming problem (NLP). Researchers who focus on indirect methods are interested largely in solving differential equations, while researchers who focus

on direct methods are interested more in optimization techniques (Betts, 1998; Rao, 2009). Pontryagin's Maximum Principle is a typical indirect method. The optimal train control strategy following from application of Pontryagin's Maximum Principle to a long journey on flat track with sufficient running time supplement consists of the sequence Maximum Power–Cruising–Coasting–Maximum Braking (Cheng and Howlett, 1992; Howlett and Pudney, 2012; Milroy, 1980). For a train operating on a track with varying speed limits and gradients the optimal control strategy is a sequence of these optimal regimes where the succession of regimes and their switching points also depends on the speed limits and gradients (Howlett, 1996; Khmelnitsky, 2000; Liu and Golovitcher, 2003; Pudney and Howlett, 1994). Finding the optimal switching points is a difficult problem except for simple cases such as a single speed limit and flat track (Albrecht et al., 2016a,b). Direct approaches transform the optimal control problem into a mathematical programming problem. Wang et al. (2013), Wang et al. (2015) and Wang and Goverde (2016) reformulate the problem as a multiple-phase optimal control model, and solve it with Pseudospectral methods (Gong et al., 2008; Rao, 2003; Ross and Fahroo, 2004; Ross and Karpenko, 2012). Pseudospectral methods transcribe the continuous-time optimal control problem into a nonlinear programming problem, after which nonlinear programming solvers are adopted to directly solve the problem.

The classic single-train control problem focuses on one independent train from one station to the next under a scheduled traffic plan. Dynamic influences such as delays and signalling systems, are considered only recently. Delays or other disturbances cause deviations from the traffic plan, in which case the train may meet yellow or red signals, which require speed reductions and unscheduled stops. A rescheduling process is required to produce a new timetable when the deviation is big enough. As a result, the train trajectories also need to be adjusted accordingly. Albrecht et al. (2010) considered the influence of signalling and automatic train protection on the train trajectory optimization. This research is based on the optimal control regimes obtained from Pontryagin's Maximum Principle, and focuses on finding the optimal switching points to handle the influence of the signalling system. Albrecht et al. (2011) discuss energy-efficient delay recovery strategies for trains in opposite directions. They find a set of interaction times that allows each affected train to recover from delays as well as to save energy consumption, but energy-efficient train trajectory calculation is not discussed. Albrecht et al. (2015) study the safe separation problem for two trains travelling in the same direction. To satisfy the safe separation for two following trains. An optimal set of specified intermediate clearance times for each section is calculated, which also aims at minimizing total energy consumption. Wang et al. (2014) consider the train trajectory planning problem under fixed and moving block signalling systems. They transform the optimal control problem into a mixed-integer linear programming problem. The nonlinear train dynamic movement model is simplified into a linear model, which speeds up the computation process but degrades the solutions' accuracy.

This paper gives several contributions to the literature. First, a rescheduling process

may change the train's traffic plan, which requires adjustment of the train speed to track the new timetable. Second, a safe separation between trains running on the same line should be guaranteed. Third, an accurate calculation taking into account operational and signalling constraints is necessary since the train trajectory is designed to help train drivers in practical operation. Based on these three points, this paper formulates the real-time traffic plan for each train as a train path envelope (TPE), which was proposed first by Albrecht et al. (2013), see also ON-TIME (2014). Similar to the quadratic time geography theory (Ma et al., 2016; Zhou et al., 2015), train path envelopes set bounds to feasible trajectory ranges, including time and/or speed ranges at specific points. These time and/or speed ranges are available in real operations along a train run, within which the train can move without running late with respect to the timetable and hindering other trains' operations. If the timetable is changed by a rescheduling process, a new train path envelope must be generated and sent to the train trajectory calculation module. Based on this, new speed and control profiles are calculated.

Train separation is guaranteed by a signalling system. Generally speaking, if the train operation deviates from a conflict-free timetable, it might meet yellow or red signals. The influence from the signalling system cannot be ignored when calculating train trajectories, and in particular the information available about the future signal aspects affects the train trajectory calculation. Two different scenarios are proposed about the amount of signal information available to the trajectory optimization. In the first scenario, we assume that only information is available about the next signal aspect. An optimization strategy called *signal response policy* is developed to ensure that the train makes correct and quick responses to different signalling aspects. In the other scenario, we assume that a full prediction is available about the signal aspect timings in rear of the train ahead. A *green wave policy* (Corman et al., 2009) is then used to avoid yellow signals and thus separate successive trains. The focus of this paper is on successive trains in the same direction over the same line. The signalling system discussed is the Dutch signalling system, which is a variant of a three-aspect two-block system with additional speed indications together with a continuous ATP system. The method is however generic and any signalling system can be taken into account. Moreover, the work assumes an advanced traffic management environment such as the ON-TIME real-time railway traffic management framework (Quaglietta et al., 2016). Within such a framework, real-time communication is possible for real-time train trajectory optimization.

For accurate calculations, a nonlinear model is used for the train movement formulation with accurate varying speed limits and gradients. The train trajectory optimization problem is built as a multiple-phase optimal control model, and solved with a Pseudospectral method. The multiple-phase optimal control model and Pseudospectral method have been used before for modelling the train trajectory optimization problem in our previous works (Wang and Goverde, 2016; Wang et al., 2015). This paper extends it to real-time train trajectory optimization with consideration of signalling and operational constraints.

The paper is organized as follows: Section 2.2 introduces the basic train dynamic movement model and the train path envelope and shows how to formulate the problem into a multiple-phase optimal control problem and solve it with a Pseudospectral method. In Section 2.3, the train trajectory calculation with consideration of delays is developed with respect to two optimization policies incorporating the impact of the signalling system and the online information available. Section 2.4 illustrates the approach in a case study, and finally Section 2.5 ends the paper with conclusions.

2.2 Train trajectory optimization modeling and solving method

2.2.1 Basic train trajectory optimization model

The movement of a railway vehicle is determined by a set of physical constraints such as the timetable, speed limits, and other vehicle-related factors. The general equation of train motion can be written as follows (Hansen and Pachl, 2014; Wang et al., 2015):

$$\frac{dv(s)}{ds} = \frac{\theta_1 f(s) - \theta_2 b(s) - R_{train}(v) - R_{line}(s)}{\rho \cdot m \cdot v(s)}, \tag{2.1}$$

$$\frac{dt(s)}{ds} = \frac{1}{v(s)}, \tag{2.2}$$

where s the traversed path [m], $v(s)$ is the train velocity [m/s], ρ the rotating mass factor, m the train mass [t], $f(s)$ the traction force [kN], $b(s)$ the braking force [kN], $R_{train}(v)$ the train resistance force [kN], $R_{line}(s)$ the line resistance force [kN], $t(s)$ the traversed time [s], and $\theta_1, \theta_2 \in \{0,1\}$ two binary parameters with $\theta_1 \cdot \theta_2 = 0$. Distance is chosen as the independent variable because gradients and speed limits occur as functions of distance rather than of time.

The train resistance $R_{train}(v)$ comprises rolling, bearing, dynamic and wind resistances (Hansen and Pachl, 2014), and can be described as

$$R_{train}(v) = 0.001 \cdot \rho \cdot m \cdot g \cdot (\alpha + \beta \cdot v + \gamma \cdot v^2), \tag{2.3}$$

where g is the acceleration of gravity, and α, β and γ are constant coefficients. The line resistance $R_{line}(s)$ is a function of position and consists of two components: grade resistance $R_{grade}(s)$ and curve resistance $R_{curve}(s)$,

$$R_{line}(s) = R_{grade}(s) + R_{curve}(s). \tag{2.4}$$

Train traction and braking power are limited by the adhesion between the wheels and the rails as well as the maximum power possible to be produced by the engine, so that

$$0 \leq f(s) \leq F_{\max}, \tag{2.5}$$

$$0 \leq b(s) \leq B_{\max}, \tag{2.6}$$

$$0 \leq f(s) \cdot v(s) \leq P_{\max}, \tag{2.7}$$

where $F_{\max}$, $B_{\max}$ and $P_{\max}$ are the upper bounds on traction force, braking force and traction power.

The train speed cannot exceed the speed limits, i.e.,

$$0 \leq v(s) \leq V_{\max}(s), \tag{2.8}$$

where $V_{\max}(s)$ is the train speed limit at position s, including static and temporary speed restrictions.

The riding comfort is usually measured by train acceleration, which should satisfy

$$A_{\min} \leq \frac{dv(s)}{dt(s)} \leq A_{\max}, \tag{2.9}$$

where $A_{\min}$ and $A_{\max}$ are the lower and upper bound of acceptable riding comfort, respectively.

For a train running between two stops, the timetable restricts the departure and arrival time, which can be formulated as

$$v(s_0) = 0, \qquad t(s_0) = T_0, \qquad v(s_f) = 0, \qquad t(s_f) = T_f, \tag{2.10}$$

where s_0 and s_f are the positions of the departure and arrival stations, respectively, and T_0 and T_f are the scheduled departure and arrival time assigned by the timetable.

Generally, the train trajectory optimization problem is to find a series of control laws for the train traction and braking forces that minimizes train energy consumption, i.e.,

$$J = \int_{s_0}^{s_f} f(s)\, ds. \tag{2.11}$$

The problem can be formulated as a generic optimal control problem with the train speed and time as the state variables and the traction and braking force as the control variables. Define the state vector $x = [x_1, x_2]' = [v, t]'$ and the control vector $u = [u_1, u_2]' = [f, b]'$. Then (2.1)–(2.11) can be written as the generic optimal control problem:

$$\begin{cases} \text{Minimize} & J = \int_{s_0}^{s_f} \ell(x(s), u(s), s)\, ds & \text{(Cost function)} \\ \text{subject to} & \dot{x}(s) = f(x(s), u(s), s) & \text{(Dynamic constraints)} \\ & g_{\min} \leq g(x(s), u(s), s) \leq g_{\max} & \text{(Path constraints)} \\ & e(x_0, x_f, s_0, s_f) = E & \text{(Boundary constraints)} \end{cases} \tag{2.12}$$

where $x_0 = x(s_0)$ and $x_f = x(s_f)$. The cost function is minimizing the energy consumption (2.11), the dynamic constraints consist of (2.1)–(2.2), the path constraints represent (2.5)–(2.9), and the boundary constraints are (2.10).

2.2.2 Train path envelope

Model (2.12) only considers the departure and arrival time constraints in (2.10), while more time constraints exist such as passing-through times at junctions or non-served stations. A train path envelope is used to describe those time and speed allowances. A train path envelope is a series of targets for each train at specific positions such as station platform stops or signals, based on estimated earliest and latest passing times and speed limits. The targets are defined by triples of position, time and speed information. Two kinds of targets are distinguished:

1. Target points (p,t,v): indicating that a train must reach target position p at the specified time t and speed v,
2. Target windows $(p,[t_{\min},t_{\max}],[v_{\min},v_{\max}])$: indicating that a train must reach target position p within a time window $[t_{\min},t_{\max}]$ and speed window $[v_{\min},v_{\max}]$.

The target windows may also be specified for a fixed time or speed, in which case the lower and upper bound of the window are equal. With this notation, the train path envelope for a given train i can be written as a series of target points and windows

$$TPE_i = \left\{(p_{i,j},[t_{i,j,\min},t_{i,j,\max}],[v_{i,j,\min},v_{i,j,\max}])\right\}_{j=1}^{m}$$

where m is the number of target positions along train's route, $p_{i,j}$ refers to the j-th target points for train i, $j \in \{1,2,\ldots,m\}$, and $p_{i,j} < p_{i,j+1}$. $t_{i,j,\min}$, $t_{i,j,\max}$, $v_{i,j,\min}$ and $v_{i,j,\max}$ are respectively the minimum and maximum time and speed limits for train i at $p_{i,j}$.

The target positions can be stations, junctions, signal positions, and route release points. The target speed for stop points is defined as $v = 0$. For other target positions speed information is optional. Only some crucial positions need speed restrictions to assure the speed limits or operational constraints such as minimum speeds before slopes or tunnels. The upper bounds of the time targets in the train path envelope need to be bigger than the minimal technical running time under consideration of the speed limits, maximum traction and braking power, and lower than some maximal running time. In addition, the train path envelopes of the various trains must be mutually exclusive so that the trains have no conflicts as long as they stay within their envelopes. This means that sufficient headway times are required between the envelopes of adjacent trains.

In the following we will discuss the time restrictions at stations and junctions. Since a wide range of situations may occur, we only present four typical examples (Fig. 2.1). In these examples, we assume for simplicity local minimum headway times independent of the train orders, although in practice the minimum headway times depend on the location and order of the train sequence.

Stops: The real-time traffic plan for each train indicates fixed arrival and departure times at their stops (Albrecht and Dasigi, 2014). Even slight delays might be perceived

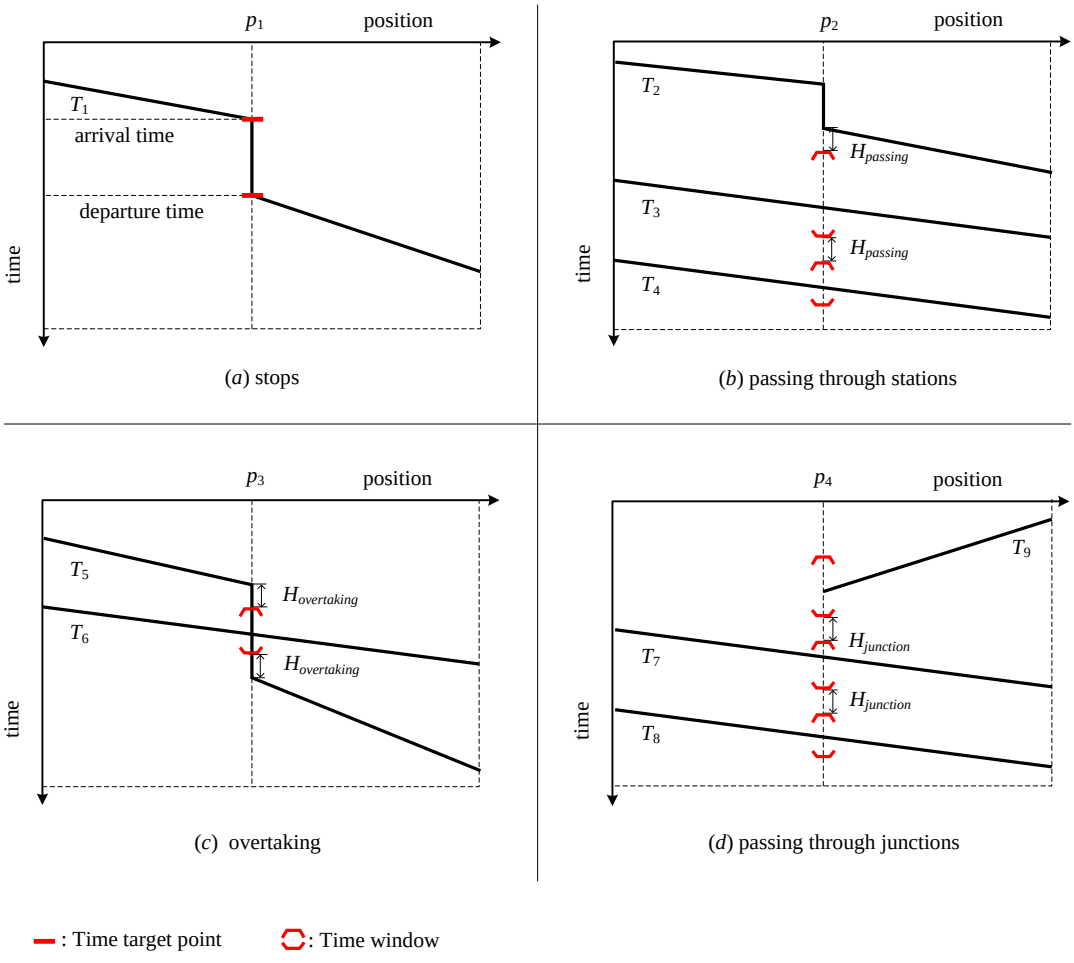

Figure 2.1: Time-distance diagrams of example target time points and time windows.

directly by customers. Therefore, the arrival and departure times are modelled as target points. In Fig. 2.1 (a), the target points of train T_1 at station p_1 can be formulated as $(p_1, A_{T_1}^{p_1}, 0)$ and $(p_1, D_{T_1}^{p_1}, 0)$, where $A_{T_1}^{p_1}$ and $D_{T_1}^{p_1}$ are respectively the scheduled arrival and departure time of train T_1 at stop position p_1, and the target speeds are 0.

Passing through stations: Each passing event has its own passing time which is assigned by the timetable. A small time deviation without impacting other trains and passengers is acceptable. Fig. 2.1 (b) shows an example of three trains T_2, T_3 and T_4 around a station at position p_2. Train T_2 has a scheduled stop at the station while train T_3 and T_4 are non-stop. The passing times at the station for trains T_3 and T_4 are modelled as target time windows. The time window is computed in such a way that no two different trains have overlapping windows and a minimum headway time is maintained between two successive trains. Taking train T_3 in Fig. 2.1 (b) as an example, the time window is calculated as $[D_{T_2}^{p_2} + H_{passing}, (P_{T_3}^{p_2} + P_{T_4}^{p_2} - H_{passing})/2]$, where $D_{T_2}^{p_2}$ is the departure time of train T_2 at p_2, $P_{T_3}^{p_2}$ and $P_{T_4}^{p_2}$ are the scheduled passing through times of train T_3 and T_4 at p_2, and $H_{passing}$ is the minimum headway time.

Overtaking: Overtaking is similar with passing through a station for a non-stop train. The passing time can be modelled as a time window respecting the given flexibility in the timetable. Consider the situation in Fig. 2.1 (c), where train T_6 overtakes train T_5 at a station at position p_3. The overtaking time of train T_6 should be kept within a range, otherwise the overtaken train T_5 has to wait and is delayed. The minimum headway times for overtaking must be respected by train T_6 resulting in the target time window $[A_{T_5}^{p_3} + H_{overtaking}, D_{T_5}^{p_3} - H_{overtaking}]$, where $A_{T_5}^{p_3}$ and $D_{T_5}^{p_3}$ are the scheduled arrival and departure time of train T_5 at p_3, and $H_{overtaking}$ is the minimum overtaking headway time.

Passing through junctions: Junctions are locations where different lines cross or merge, but none of the trains has a planned stop. Train operations at junctions may result in knock-on delays, so that a passing time window for each train is adopted to avoid interactions. Consider the situation shown in Fig. 2.1 (d). The time window of the passing time of train T_7 at junction p_4 can be calculated as $[(P_{T_7}^{p_4} + P_{T_9}^{p_4} + H_{junction})/2, (P_{T_7}^{p_4} + P_{T_8}^{p_4} - H_{junction})/2]$, where $P_{T_7}^{p_4}$, $P_{T_8}^{p_4}$ and $P_{T_9}^{p_4}$ are the passing through times of train T_7, T_8 and T_9 indicated by the timetable, and $H_{junction}$ is the minimum headway.

Above four cases show how to transform the timetable into detailed formulation of time and speed constraints in train path envelope. It can be adopted easily for the computations related to train speed trajectory optimization and control. An application example is shown in Section 2.4. Note all the time windows above should intersect with the minimum and maximum running time constraints. Time constraints at stations and junctions might be changed in case of delays. Besides, more time constraints might be present at signal positions, which is discussed in Section 2.3.

2.2.3 Multiple-phase optimal control model

It is difficult to use model (2.12) in Section 2.2.1 for solving the trajectory optimization problem, since the speed limits and gradients change along the railway track. Besides, not only the arrival and departure time constraints considered in (2.12) should be respected by train operation, but also more time and/or speed limits from train path envelope should be considered. So we re-formulate the problem in a multiple-phase optimal control model. The advantages of this model is accurate illustration of changing speed limits, gradients and time/speed constraints from train path envelope.

In a multiple-phase optimal control model, the trajectory consists of a collection of phases (Rao (2003)). A phase is any segment of the complete trajectory, where any particular phase of an optimal control problem has its own cost function, dynamic model, path constraints, and boundary conditions. The complete trajectory is then obtained by properly linking adjacent phases via linkage conditions. The total cost function is the sum of the cost functions within each phase. The optimal trajectory is then found by minimizing the total cost functional subject to the constraints within each phase and the linkage constraints connecting adjacent phases.

Since the speed limits and gradients change along the rail track, the complete train trajectory can be divided into several segments by the critical points of speed limits and gradients, so that each phase has a unique speed limit and line resistance. Consider a train trajectory that consists of R distinct phases, let the independent variable in phase $r \in \{1,\dots,R\}$ lie in the interval $s \in [s_0^{(r)}, s_f^{(r)}]$ and denote the state and control in phase r as $x^{(r)} = [x_1^{(r)}, x_2^{(r)}]' = [v^{(r)}, t^{(r)}]'$ and $u^{(r)} = [u_1^{(r)}, u_2^{(r)}]' = [f^{(r)}, b^{(r)}]'$. The dynamic constraints in phase $r \in \{1,\dots,R\}$ are given as

$$\dot{x}^{(r)}(s) = f^{(r)}(x^{(r)}(s), u^{(r)}(s), s), \qquad (r \in \{1,\dots,R\}). \tag{2.13}$$

where

$$f^{(r)}(x^{(r)}(s), u^{(r)}(s), s) = \begin{bmatrix} \dfrac{\theta_1 u_1^{(r)} - \theta_2 u_2^{(r)} - R_{train}^{(r)}(x_1^{(r)}) - R_{line}^{(r)}(s)}{\rho \cdot m \cdot x_1^{(r)}} \\ \dfrac{1}{x_1^{(r)}} \end{bmatrix}, \tag{2.14}$$

and the value of $R_{line}^{(r)}(s)$ changes from phase to phase depending on the value of the gradient and curve in phase r. The path constraints in phase $r \in \{1,\dots,R\}$ are given as

$$g_{\min}^{(r)} \le g^{(r)}(x^{(r)}(s), u^{(r)}(s), s) \le g_{\max}^{(r)}, \qquad (r \in \{1,\dots,R\}). \tag{2.15}$$

where

$$g_{\min}^{(r)} = \begin{bmatrix} 0 \\ 0 \\ 0 \\ 0 \\ A_{\min} \end{bmatrix}, \quad g^{(r)}(x^{(r)}(s), u^{(r)}(s), s) = \begin{bmatrix} u_1^{(r)} \\ u_2^{(r)} \\ u_1^{(r)} \cdot x_1^{(r)} \\ x_1^{(r)} \\ \dot{x}_1^{(r)} / \dot{x}_2^{(r)} \end{bmatrix}, \quad g_{\max}^{(r)} = \begin{bmatrix} F_{\max} \\ B_{\max} \\ P_{\max} \\ V_{\max}^{(r)} \\ A_{\max} \end{bmatrix}. \tag{2.16}$$

Here, $g^{(r)}$ includes the constraints of train traction, braking force, engine power, speed limit and riding comfort. Note that $V_{\max}^{(r)}$ is the maximum speed allowance from $s_0^{(r)}$ to $s_f^{(r)}$, which is a constant value in phase r, but might have different values in different phases.

The trajectory is also partitioned into more phases by the target positions of the train path envelope. For each target position of the train path envelope a time and speed allowance is needed to restrain train operations, which can be formulated as the boundary constraints. For example, assume target position s_p of the train path envelope is the linkage point of phase r and $r+1$ ($r \in \{1,\ldots,R-1\}$). If there is a target point constraint at s_p, we have

$$x(s_p) = \begin{bmatrix} V_{s_p} \\ T_{s_p} \end{bmatrix}, \tag{2.17}$$

where V_{s_p} are T_{s_p} are the target speed and time at s_p, and if the constraint is a flexible target window we have

$$\begin{bmatrix} V_{s_p,\min} \\ T_{s_p,\min} \end{bmatrix} \leq x(s_p) \leq \begin{bmatrix} V_{s_p,\max} \\ T_{s_p,\max} \end{bmatrix}, \tag{2.18}$$

where $V_{s_p,\min}$, $V_{s_p,\max}$, $T_{s_p,\min}$ and $T_{s_p,\max}$ are the minimum and maximum speed and time at s_p, repectively. Since s_p is the boundary between two adjacent phases, constraints (2.17)–(2.18) work as the terminal boundary constraints for phase r as well as the initial boundary constraints for phase $r+1$. In general, the boundary constraints (if any) in phase $r \in \{1,\ldots,R\}$ are given as

$$e_{\min}^{(r)} \leq e^{(r)}(x_0^{(r)}, s_0^{(r)}, x_f^{(r)}, s_f^{(r)}) \leq e_{\max}^{(r)}, \qquad (r \in \{1,\ldots,R\}). \tag{2.19}$$

where the lower and upper bound in $e_{\min}^{(r)}$ and $e_{\max}^{(r)}$ are equal if the constraint is a target point.

The whole train trajectory is divided into multiple segments with critical points of speed limits or gradients and curves, and target positions of the train path envelope. For each two consecutive phases k and $k+1$, $k \in \{1,\ldots,R-1\}$, a set of conditions is used to connect the trajectories in phase k and $k+1$. In particular, the state variables must be continuous at the boundary between phase k and phase $k+1$. Therefore, the following linkage conditions must be satisfied for all $k \in \{1,\ldots,R-1\}$:

$$s_f^{(k)} - s_0^{(k+1)} = 0, \quad x(s_f^{(k)}) - x(s_0^{(k+1)}) = 0. \tag{2.20}$$

An exception occurs if the linkage point of phase k and $k+1$ is the stop point, in which case $x_2(s_f^{(k)})$ and $x_2(s_0^{(k+1)})$ represent the arrival and departure time, and thus

$$x_2(s_0^{(k+1)}) - x_2(s_f^{(k)}) = D_{s_f^{(k)}}, \tag{2.21}$$

where $D_{s_f^{(k)}}$ is the dwell time of the train at $s_f^{(k)}$ (or $s_0^{(k+1)}$). The general linkage conditions can be formulated as

$$l(x_f^{(k)}, s_f^{(k)}, x_0^{(k+1)}, s_0^{(k+1)}) = L, \qquad (k \in \{1,\ldots,R-1\}). \tag{2.22}$$

The cost function $J^{(r)}$ in phase $r \in \{1,\ldots,R\}$ can be the energy consumption given as

$$J^{(r)} = \int_{s_0^{(r)}}^{s_f^{(r)}} \ell^{(r)}(x^{(r)}(s), u^{(r)}(s), s)\, ds, \tag{2.23}$$

with $\ell^{(r)}(x^{(r)}(s), u^{(r)}(s), s) = u_1^{(r)}(s)$, although later we also include delay. The objective of the multiple-phase train trajectory optimization problem is to minimize the cost function over all phases

$$J = \sum_{r=1}^{R} J^{(r)}, \tag{2.24}$$

subject to the dynamic constraints (2.13), path constraints (2.15), boundary constraints (2.19), and the linkage conditions (2.22).

2.2.4 Pseudospectral method

The multiple-phase optimal control model in Section 2.2.3 is solved by a Pseudospectral method. Pseudospectral method transcribes the continuous-time optimal control problem into a nonlinear programming problem. The state and control functions are approximated using a set of orthogonal polynomials (Chebyshev or Lagrange polynomials), where specified collocation points are used for collocation of the dynamics and a quadrature approximation of the integrated Lagrange cost term. The Pseudospectral method has a simple structure and converges exponentially. The most well-developed Pseudospectral methods are the Gauss Pseudospectral Method (GPM) (Benson, 2005; Huntington, 2007), the Radau Pseudospectral Method (RPM) (Garg, 2011), and the Lobatto Pseudospectral Method (LPM) (Elnagar et al., 1995).

For the Radau Pseudospectral Method, the multiple-phase train trajectory optimization model described into the previous section is transcribed to a NLP as follows. The first step is to map the physical domain $s \in [s_0^{(r)}, s_f^{(r)}]$ to a computational domain $\sigma^{(r)} \in [-1,1]$ by means of the affine transformation

$$\sigma^{(r)} = \frac{2s}{s_f^{(r)} - s_0^{(r)}} - \frac{s_f^{(r)} + s_0^{(r)}}{s_f^{(r)} - s_0^{(r)}}. \tag{2.25}$$

Next, let $N^{(r)}$ be the number of Legendre-Gauss-Radau (LGR) points $\sigma_j^{(r)}$ in phase $r \in \{1,\ldots,R\}$, with $\sigma_j^{(r)} \in [-1,1)$, $j \in \{1,\ldots,N^{(r)}\}$, and $\sigma_1^{(r)} = -1$ and $\sigma_{N^{(r)}}^{(r)} < 1$. Let $\sigma_{N^{(r)}+1}^{(r)} = 1$, which is a non-collocation point. Then the state and control of phase $r \in \{1,\ldots,R\}$ are approximated by a basis of Lagrange interpolating polynomials

$$x^{(r)}(\sigma^{(r)}) \approx X^{(r)}(\sigma^{(r)}) = \sum_{j=1}^{N^{(r)}+1} X_j^{(r)} L_j^{(r)}(\sigma^{(r)}), \tag{2.26}$$

$$u^{(r)}(\sigma^{(r)}) \approx U^{(r)}(\sigma^{(r)}) = \sum_{j=1}^{N^{(r)}} U_j^{(r)} \widetilde{L}_j^{(r)}(\sigma^{(r)}), \tag{2.27}$$

where $X_j^{(r)} = X^{(r)}(\sigma_j^{(r)})$, $U_j^{(r)} = U^{(r)}(\sigma_j^{(r)})$, and the Lagrange polynomials $L_j^{(r)}(\sigma^{(r)})$ ($j \in \{1,\ldots,N^{(r)}+1\}$) and $\widetilde{L}_j^{(r)}(\sigma^{(r)})$ ($j \in \{1,\ldots,N^{(r)}\}$) are defined as

$$L_j^{(r)}(\sigma^{(r)}) = \prod_{i=1, i\neq j}^{N^{(r)}+1} \frac{\sigma^{(r)} - \sigma_i^{(r)}}{\sigma_j^{(r)} - \sigma_i^{(r)}} \qquad \text{and} \qquad \widetilde{L}_j^{(r)}(\sigma^{(r)}) = \prod_{i=1, i\neq j}^{N^{(r)}} \frac{\sigma^{(r)} - \sigma_i^{(r)}}{\sigma_j^{(r)} - \sigma_i^{(r)}}. \quad (2.28)$$

Note that $L_j^{(r)}(\sigma_j^{(r)}) = 1$ and $L_j^{(r)}(\sigma_i^{(r)}) = 0$ for $i \neq j$, and likewise for $\widetilde{L}_j^{(r)}(\sigma^{(r)})$, so that $X_j^{(r)} = x^{(r)}(\sigma_j^{(r)})$ is exact at the LGR points and the additional point $\sigma_{N^{(r)}+1}^{(r)}$ used in the state approximation, and likewise $U_j^{(r)} = u^{(r)}(\sigma_j^{(r)})$ is exact at the LGR points.

Next, the derivative of the state (2.13) and cost function (2.23) are approximated. Let $\omega^{(r)}$ and $D^{(r)}$ be the weights and differentiation matrix in phase $r \in \{1,\ldots,R\}$ corresponding to the choice of $N^{(r)}$. The collocated dynamics at the $N^{(r)}$ LGR collocation points are expressed as

$$\sum_{j=1}^{N^{(r)}+1} D_{ij}^{(r)} X_j^{(r)} - \frac{s_f^{(r)} - s_0^{(r)}}{2} f^{(r)}(X_i^{(r)}, U_i^{(r)}, \sigma_i^{(r)}; s_0^{(r)}, s_f^{(r)}) = 0, \quad (2.29)$$

$$D_{ij}^{(r)} = \dot{L}_j(\sigma_i^{(r)}), \quad (i \in \{1,\ldots,N^{(r)}\}). \quad (2.30)$$

The cost function in phase r is

$$J^{(r)} = \frac{s_f^{(r)} - s_0^{(r)}}{2} \sum_{i=1}^{N^{(r)}} \omega_i^{(r)} \ell^{(r)}(X_i^{(r)}, U_i^{(r)}, \sigma_i^{(r)}; s_0^{(r)}, s_f^{(r)}). \quad (2.31)$$

Likewise, with approximations of the path constraints (2.15), boundary constraints (2.19), and linkage conditions (2.22) (Rao (2003), Garg (2011)), the multiple-phase optimal control problem can be rewritten as

$$\begin{cases} \text{Minimize} & J = \sum_{r=1}^{R} J^{(r)} \\ \text{subject to} & \sum_{j=1}^{N^{(r)}+1} D_{ij}^{(r)} X_j^{(r)} - \frac{s_f^{(r)} - s_0^{(r)}}{2} f^{(r)}(X_i^{(r)}, U_i^{(r)}, \sigma_i^{(r)}; s_0^{(r)}, s_f^{(r)}) = 0 \\ & g_{\min}^{(r)} \leq g^{(r)}(X_i^{(r)}, U_i^{(r)}, \sigma_i^{(r)}; s_0^{(r)}, s_f^{(r)}) \leq g_{\max}^{(r)} \\ & e_{\min}^{(r)} \leq e^{(r)}(X_1^{(r)}, s_0^{(r)}, X_{N^{(r)}+1}^{(r)}, s_f^{(r)}) \leq e_{\max}^{(r)} \\ & l(X_{N^{(k)}+1}^{(k)}, s_f^{(k)}, X_1^{(k+1)}, s_0^{(k+1)}) = L, \end{cases} \quad (2.32)$$

where the constraints range in $r \in \{1,\ldots,R\}$, $i \in \{1,\ldots,N^{(r)}\}$, and $k \in \{1,\ldots,R-1\}$.

In this way, the continuous optimal problem is transformed into a nonlinear programming problem. The resulting nonlinear programming problem can be solved by nonlinear optimization algorithms (Gill et al., 2002). There are several well-developed packages that implement the Pseudospectral method, in which GPOPS is a Matlab-based open source tool that uses the Radau Pseudospectral Method to solve the multiple-phase optimal control problem (Darby et al., 2011; Rao et al., 2010).

2.3 Train trajectory optimization in case of delays

Section 2.2 describes the basic modeling and solving methods for the train trajectory optimization problem following planned timetables. This section discusses the train trajectory optimization in case of disturbances.

2.3.1 Problem description

In the presence of disturbances a rescheduling process may produce a new conflict-free timetable by changing the reference times and speeds for particular points or track sections, train routes, or even train sequences. The train path envelope then must also be updated accordingly with the adjusted times and route characteristics. The central issue of the train trajectory calculation is to respect and follow the new train path envelope. The detailed process of train trajectory calculation in case of disturbances is as follows: The train path envelope for each train is first determined based on the new timetable with the method from Section 2.2.2. New time and speed constraints of the train path envelope as well as train parameters, track gradients, curves, speed limits and energy saving requirements are considered by the new trajectory calculation. The method of calculating the new trajectory is the same as the one in Section 2.2.3 and 2.2.4.

If rescheduling is not necessary, the delayed trains may have to speed up to get back to the timetable. Furthermore, it is also important to reduce the impact of delays on other trains. The train path envelope for each train is first checked on whether minimum running times are satisfied or not. When delayed trains do not have enough time to reach the next target position, a free time supplement is added. The arrival and departure time constraints at stops change into flexible target windows instead of mandatory target points because there is no guarantee that the delayed train can arrive at (depart from) stops on time. However the train is not expected to arrive (depart) earlier than its scheduled time. So the flexible time window of the arrival (departure) event can be $[t_a, t_a + t_s]$ ($[t_d, t_d + t_s]$), where t_a and t_d are the scheduled arrival and departure time, and t_s is an extra time supplement. The lower bounds make sure that the trains do not arrive (depart) early, while the upper bounds make sure that the trains have enough running time. Dwell times can be reduced to make up delay, but the minimum dwell time at a stop should be respected. This minimum dwell constraint is included into the multiple phase optimal control model, that is

$$x_2(s_0^{(k+1)}) - x_2(s_f^{(k)}) \geq D_{s_f^{(k)},\min}, \tag{2.33}$$

where phase k and $k+1$ are two two sequential phases where the connecting point is a stop point. $D_{s_f^{(k)},\min}$ is the minimum dwell time there. (2.21) is adopted for non-delayed trains, and (2.33) for delayed trains.

The optimization objective of delayed trains is no longer just energy-efficient driving. Another important issue is to minimize delays to stimulate that the train paths will get back to the scheduled ones as soon as possible. So the cost function for each phase is now given as

$$J^{(r)} = w_1 \cdot x_2(s_f^{(r)}) + \int_{s_0^{(r)}}^{s_f^{(r)}} u_1^{(r)}(s^{(r)})\, ds, \tag{2.34}$$

where $x_2(s_f^{(r)})$ is the time to be optimized at position $s_f^{(r)}$ and w_1 is a nonnegative weight factor. The first item is to reduce the arrival time at the terminal point of each phase. In turn, it is to minimize the arrival time at stations. On the other hand, a time window constraint $[t_a, t_a + t_s]$ is used to make sure that the train cannot arrival at stations earlier than the scheduled arrival time. So the objective function makes the arrival time get close to the scheduled one, that in turn reduces train delays. In all, the first item aims at reducing delays by minimizing the running times in each phase, while the second term aims at saving energy consumption. The weight w_1 reflects the trade-off between these two objectives. Different values of w_1 result in different optimization solutions. The effect of w_1 is discussed by Wang and Goverde (2016). In this paper, we use $w_1 = 10^3$.

Delay changes headway between successive trains and train path conflicts might occur if the scheduled buffer time between train paths is not big enough. In practice this means that a train will meet yellow or even red signals, and has to decelerate to a restricted speed and possibly wait in rear of a stop signal. Signalling influences are complicated and should be taken into account the train trajectory calculation.

2.3.2 Signalling influences

The response to signals depends on the specific signalling system and characteristics of the ATP system, and can be quite different. In this paper, we consider the Dutch signalling system NS'54 with the Dutch ATP system ATB (*Automatische Trein Beïnvloeding*). NS'54 operates by wayside light signals that give speed commands to drivers such that trains can always brake before a signal at danger (Goverde et al., 2013). Normally, NS'54 is a three-aspect two-block system with clear (Green, G), approach (Yellow, Y) and stop (Red, R) aspects. In case of a green signal aspect, the train is unaffected by the signalling system and can proceed with its normal operational speed. A yellow signal orders to reduce speed to a restricted speed of 40 km/h and prepare to stop before a red signal. A red signal is a stop order, which implies that the train should stop before the signal. Near stations also short blocks are applied which have a length shorter than the maximum braking distance from the line speed by which trains can follow at a shorter headway. In that case, NS'54 indicates already one (or more) signals before that the train has to slow down to an indicated speed that must be reached before the next signal, so that the train will enter the short block with a lower speed associated to the short block length. This progressive speed signalling is given by a Yellow signal plus a white numeral indicating the permitted speed at the

next signal. For instance, 'Yellow 8' (Y8) indicates that the train has to reduce speed to 80 km/h before the next signal.

Moreover, Dutch trains are equipped with the ATB system, which supervises braking after an approach aspect as well as certain ceiling speeds and intervenes with an emergency brake to standstill if the driver does not obey the braking or supervised speed limits forced upon the train. So after a speed reduction order the driver has to apply the brakes until the permitted speed is reached. In the case of a yellow signal the driver has to reduce speed to a restricted speed of 40 km/h and then drive on-sight for the remainder of the block. If a driver does not brake sufficiently after a speed reduction order then ATB warns the driver and if the driver still does not react ATB will intervene with an emergency brake to standstill. The train is able to re-accelerate after an improved signal aspect ahead, otherwise it has to stop in rear of the signal and wait until a new proceed aspect (green or yellow) is given.

Signalling influences cannot be ignored during train trajectory calculation. An important part is that information about the current and future signalling state is required. The train trajectory calculation strategies in case of two different scenario assumptions about available information are discussed below. The first scenario assumes that the driver only gets information from the signal aspect at the beginning of a block. This scenario simulates the limited information that train drivers can receive based on current commutation systems. A *signal response policy* then is developed considering train trajectory optimization assuming only this limited signalling information. Another assumption is that the states of the upcoming signals along the running track can be predicted. This assumption is based on advanced train control and commutation systems. The future states of signals are predicted by the movements of previous trains. A *green wave policy* is developed for this case. The following two sections give detailed illustrations of signal response policy and green wave policy.

2.3.3 Signal response policy

The signal response policy first calculates an optimal speed trajectory from the current location to the next stop before the train leaves the station. Because of limited information about the signal aspects, the optimal trajectory is calculated with the method in Section 2.2 if the train is not delayed or the method in Section 2.3.1 if the train is delayed. The trajectory is followed until meeting a yellow or red signal aspect. A yellow or red signal means that the train should decelerate or stop, so the train can not just follow the old trajectory calculated. A new train trajectory is re-calculated for the remaining journey, which should make proper responses to signal aspects. The train follows the new trajectory until meeting another yellow or red signal aspect, or the first green signal aspect after yellow or red. Then a proper trajectory is calculated again. Hence, the signal response policy keeps detecting the signal state when the train reaches the sight distance of a signal. Once a yellow or red signal aspect, or the first

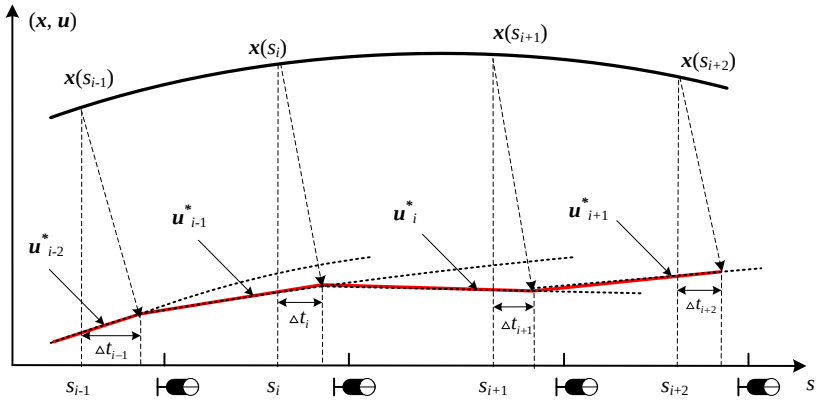

Figure 2.2: Illustration of the signal response policy with the calculated optimal controls at each step (black dotted lines) and the actual used control (red solid line).

green signal aspect after yellow or red is detected, a new trajectory is required. Fig. 2.2 shows an example of re-calculating a train trajectory after meeting a yellow signal:

At sight distance before the signal, information about the signal aspect ahead is available. Then a measurement of the train speed and time is taken. Denote by s_i the sight distance before the signal, and $x(s_i)$ the state of the train speed and time at s_i. Based on the measurement, an optimal trajectory from s_i to $s_{i,end}$ is calculated, where s_i and $s_{i,end}$ are respectively the start and end points of the new trajectory. $s_{i,end}$ depends on which kind of signal aspect is detected at s_i. Denote $u_i^*(s_i, s_{i,end})$ as the optimal control trajectory calculated at s_i. Suppose that u_i^* is available after time $t(s_i) + \Delta t_i$, where Δt_i is a computational delay and $t(s_i)$ is the travelled time at s_i. Then the new trajectory u_i^* is applied after $t(s_i) + \Delta t_i$. When the train gets close to the next signal s_{i+1}, the signal aspect ahead is available, and a new trajectory might be calculated if the signal at s_{i+1} is yellow or red, or the first green signal aspect after yellow or red. To simplify the problem, a reasonable assumption is made that the calculation time of the new trajectory is small enough so that the system can get a new trajectory before the train passes the signal, i.e., within the sight and reaction time before the signal which is usually about 12 s.

The calculation of the optimal controller depends on the signal aspect. As an example of the section between s_i and s_{i+1}. If the signal aspect is Yellow, then the train has to reduce speed to an approach speed ($v_{approach} = 40$ km/h in the Dutch railways). Braking has to start immediately after passing the yellow signal because of the ATB system. In view of this, the new trajectory after the yellow signal is calculated as follows. The first step is to calculate the decelerating curve with maximum braking force until the restricted speed $v_{approach}$ is reached (Fig. 2.3 (a)). If speed $v(s_i)$ at s_i is lower than $v_{approach}$, skip this step (Fig. 2.3 (b)). The yellow signal means that the next signal is red; therefore a stop curve is calculated after the decelerating curve. The stop curve starts with the end point of the decelerating curve $s_{i,y}$ (Fig. 2.3 (a)) or s_i (Fig. 2.3 (b)) and ends at the next signal $s_{i+1,signal}$ (we assume s_{i+1} is the sight distance

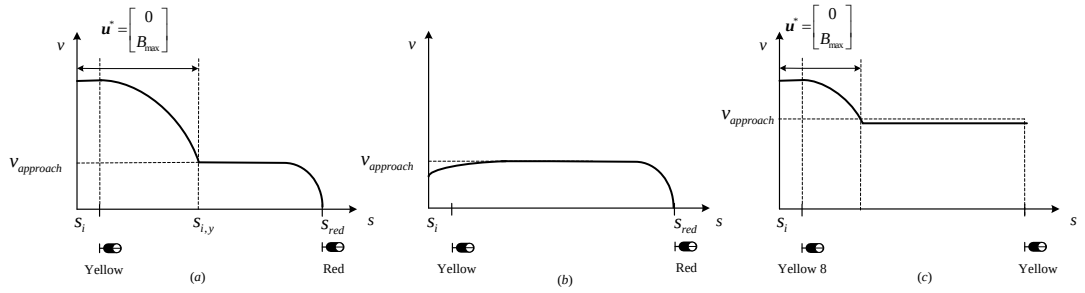

Figure 2.3: Illustrative speed-distance diagrams to optimization strategies in face of a yellow signal aspect.

before signal $s_{i+1,signal}$). The terminal speed at $s_{i+1,signal}$ is zero. A new trajectory is calculated with the multiple-phase optimal control model and pseudospectral method solver. $v_{approach}$ is taken as the speed limit for all phases and (2.34) is chosen as the objective function since braking after yellow signals wastes time. In summary, the controller $u_i^*(s_i, s_{i,end})$ consists of a deceleration stage (if any) and a stop stage, and $s_{i,end} = s_{i+1,signal}$.

In case of a Yellow 8 aspect, the train must reduce speed to $v_{approach} = 80$ km/h (and similar for other speed indications). If speed $v(s_i)$ at s_i is higher than 80 km/h then first a decelerating curve to the indicated speed must be computed with the maximum braking force as shown in Fig. 2.3 (c). If $v(s_i)$ is lower than 80 km/h then this step can be skipped. The second step is to calculate the optimal curve over the remaining sections, from the end point of the decelerating curve (or the train's current position if there is none) to the next signal $s_{i+1,signal}$. This curve assumes that the maximum operation speed over the remaining section may not exceed 80 km/h, that is, the speed limit of each phase and point should be lower or equal to 80 km/h. With this new speed limit the optimal train trajectory is calculated using the Pseudospectral method.

When the signal aspect at s_i is Red, the stop curve calculated after the yellow signal aspect at s_{i-1} is followed until standstill. The train keeps waiting in rear of the signal until the signal aspect improves.

If the signal at s_i is Green, the train can proceed if the planned train trajectory covers train operation in the section between s_i and s_{i+1}. The green signal may also appear after yellow or red signals. In that case, a new trajectory is calculated. $s_{i,end}$ is set as the closest next stop point. A multiple phase train trajectory model is generated with the method in Section 2.2.3 and solved with the Pseudospectral method with (2.34) as the objective function for each phase to minimize delay and energy consumption.

2.3.4 Green wave policy

The signal response policy above has a proper response to the different signal aspects. But this also means that the train has to decelerate to a lower speed when meeting

yellow signal aspects and sometimes needs to re-accelerate when the signal aspect improves, energy-efficiency and riding comfort are not guaranteed. In practice, we like to avoid frequent deceleration and re-acceleration, and have the train operate in a more smooth way in order to improve passenger comfort and save energy consumption. The green wave policy is a train operation strategy which avoids yellow signals and has the train operate under green signals for energy-efficient operation. The green wave policy makes the trains only encounter green signals and ultimately the railway network achieves smoother operations and as additional benefits, reduced energy consumption and reduced risk of signals passed at danger (Caimi et al., 2012; Corman et al., 2009).

It is based on the assumption that the states of the upcoming signals along the running track can be predicted. Signalling states include the changes of signal aspects and corresponding changing times. Take one signal p_s along the train journey as an example, and denote the predicted time that the signal aspect changes to green as $T_{p_s,\min}$. A green wave means that the train will only pass through the signal with a green aspect. So $T_{p_s,\min}$ is the earliest possible time for the train to pass through signal p_s. That is

$$t(p_s) \geq T_{p_s,\min}, \tag{2.35}$$

where $t(p_s)$ is the time for the train to pass through signal p_s.

Every signal along the train journey has such a time constraint in the green wave policy. Those constraints are included in the train path envelope. In other words, the train path envelope not only consists of the time and speed constraints at timetable points but also the time constraints at signals.

For the train trajectory calculation with green wave policy, the train journey is partitioned into multiple phases by critical points of speed limits or gradients and curves and target positions of the TPE, including signal positions. The target windows (2.35) are the boundary conditions at the phases that start or end at a signal. (2.34) is adopted as the cost function for each phase since the train is delayed. The optimal model is then solved using a Pseudospectral method.

2.4 Case studies

This section demonstrates the approach with some case studies. The optimization model and solution algorithm are implemented in Matlab based on GPOPS 4.1 (Rao et al., 2010). The calculations were carried out on a laptop equipped with a 3.2 GHz Pentium R processor. The Dutch corridor between Utrecht and 's Hertogenbosch is adopted for the case studies, which is a 50 km long double-track line with some multiple-track parts with traffic in both directions having their own tracks (Fig. 2.4). Eight stations are located along this corridor: Utrecht (Ut), Utrecht Lunetten (Utl), Houten (Htn), Houten Castellum (Htnc), Culemborg (Cl), Geldermalsen (Gdm), Zaltbommel (Zbm) and 's Hertogenbosch (Ht). The infrastructure characteristics

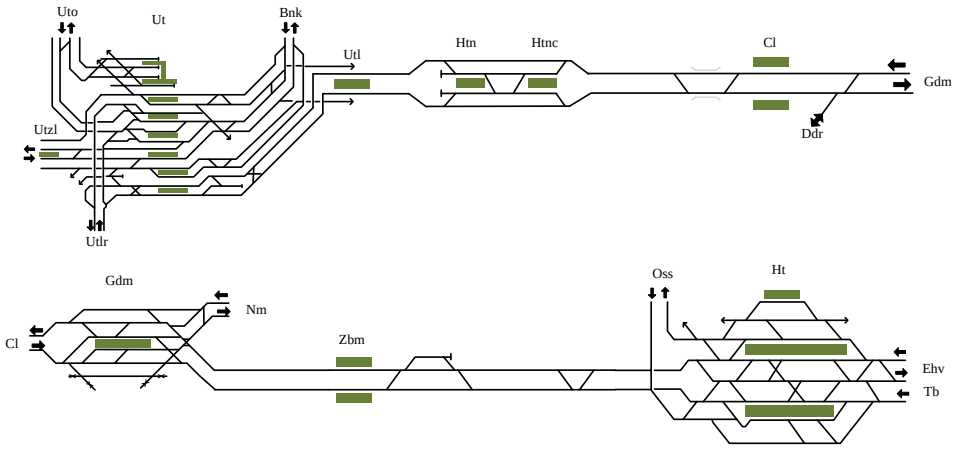

Figure 2.4: The infrastructure between Utrecht and 's Hertogenbosch.

Table 2.1: Characteristics of Sprinter and Intercity train.

Characteristic	Value	
	Sprinter	Intercity
Train mass [t]	220	391
Rotating mass factor	1.06	1.06
Train length [m]	138	162
Maximum traction power [kW]	1918	2157
Maximum traction force [kN]	170	214
Maximum braking rate [m/s^2]	-0.8	-0.66

consist of an accurate description of all track sections, points, speed signs, gradients, and signals over the entire track layout from Utrecht until 's Hertogenbosch.

We consider two different passenger train types running on the corridor in the direction from Utrecht to 's Hertogenbosch: a local train (Sprinter) and an Intercity. The characteristics of the Sprinter and Intercity are shown in Table 2.1, including train mass, rotating mass factor, train length, maximum traction force and power, and maximum braking rate. Since the braking rate is the only accessible data characterizing the braking behavior, we set the braking force equal to the braking rate times train mass. The assumed traction force and train resistance curves of both trains are shown in Fig. 2.5.

Fig. 2.6 shows the timetable for the direction from Utrecht to 's Hertogenbosch within a basic hour. This timetable is based on the practical timetable in use in 2015. Sprinter train stops at every station while the Intercity only stops in Utrecht and 's Hertogenbosch. Each 15 minutes a pair of a Sprinter and an Intercity departs from Utrecht, while the Sprinter is overtaken by the Intercity at Gdm. The scheduled dwell times of the Sprinter at all stations is assumed 1 minute except for the dwell time in Gdm which is 6 minutes. The minimum dwell time for the Sprinter train in Gdm remains 6 minutes while the minimum dwell times in the other stations are all assumed

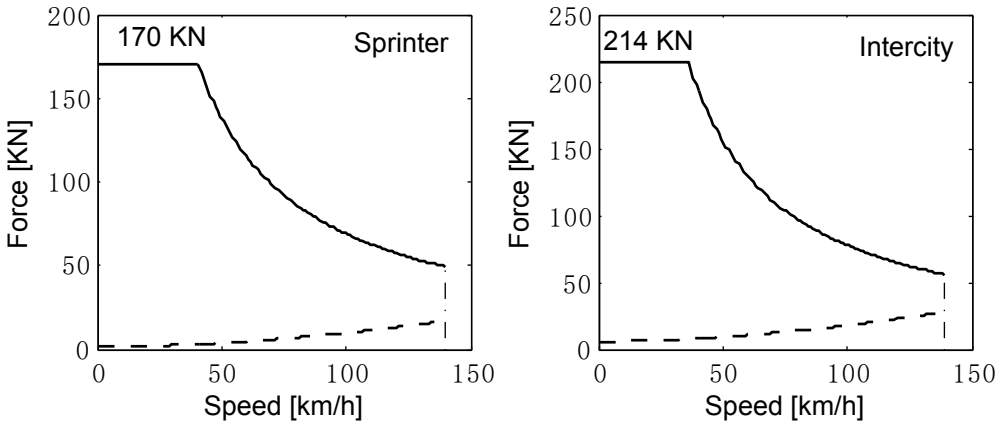

Figure 2.5: Traction force (solid line) and train resistance (dashed line) of Sprinter and Intercity.

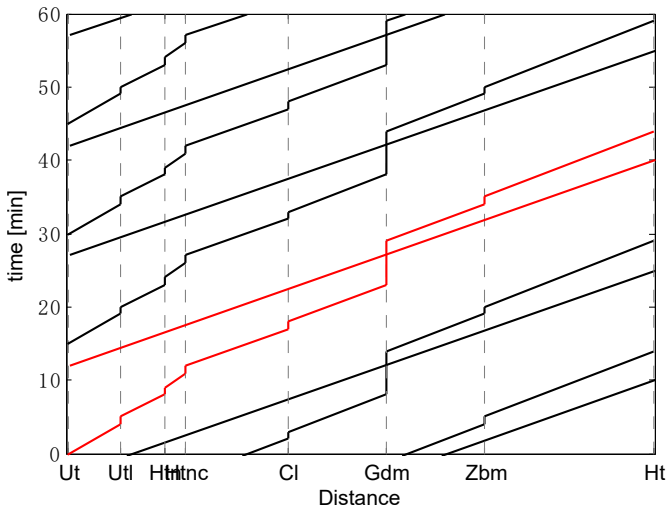

Figure 2.6: Timetable for the corridor from Utrecht to 's Hertogenbosch within a basic hour pattern.

0.5 minutes. Table 2.2 shows the arrival and departure times of a pair of Sprinter and Intercity (red lines in Fig. 2.6) within the basic hour pattern.

2.4.1 Case A: trajectory optimization for scheduled conditions

The first case study is about train trajectory optimization for scheduled conditions. We discuss the train trajectory optimization based on a conflict-free traffic plan without consideration of delays or disturbances. Assume that the Sprinter and Intercity trains follow the timetable of Table 2.2, the focus of Case A is to calculate the optimal speed profiles for one Sprinter and one Intercity train using the method from Section 2.2. The steps of building up train path envelope and multiple phase optimal control model are introduced in detail.

Table 2.2: Basic arrival and departure times (mm:ss) of the Sprinter and Intercity from Ut to Ht (repeating each 15 min).

Station	Sprinter		Intercity	
	Arrival time	Departure time	Arrival time	Departure time
Ut	- -:- -	00:00	- -:- -	12:00
Utl	04:00	05:00	- -:- -	- -:- -
Htn	08:00	09:00	- -:- -	- -:- -
Htnc	11:00	12:00	- -:- -	- -:- -
Cl	17:00	18:00	- -:- -	- -:- -
Gdm	23:00	29:00	- -:- -	- -:- -
Zbm	34:00	35:00	- -:- -	- -:- -
Ht	44:00	45:00	40:00	- -:- -

The first step of the optimal trajectory calculation is to transform the timetable into a train path envelope. Table 2.2 shows the Sprinter has 8 stops. Its train path envelope uses a series of target points indicating the departure and arrival times and speed at stop points. $TPE_{sprinter} = \{$(244, 0, 0), (4574, 240, 0), (4574, 300, 0), (8193, 480, 0), (8193, 540, 0), (9934, 660, 0), (9934, 720, 0), (18366, 1020, 0), (18366, 1080, 0), (26554, 1380, 0), (26554, 1740, 0), (34737, 2040, 0), (34737, 2100, 0), (48707, 2640, 0),(48707, 2700, 0)$\}$. Each target point constraint is a triple which consists of the stop position [m], the scheduled departure or arrival time [s], and the speed target [m/s]. Speed target equals 0 everywhere because the Sprinter stops at each station. For the Intercity, there is one departure event at Ut, one overtaking event at Gdm and one arrival event at Ht. So the train path envelope includes two target points and one flexible target window. Assuming the minimum overtaking headway time at Gdm is 2 minutes, the time window of the Intercity to pass through Gdm is calculated as $[1500, 1620]$ s based on the method presented in Section 2.2.2. $TPE_{intercity} = \{$(244, 720, 0), (26554, [1500, 1620], [0, 140]), (48707, 2400, 0)$\}$.

The second step is to build the multiple-phase train trajectory optimal control model. Both train trajectories are partitioned into multiple phases by the critical points of speed limits or gradients, the signals, and the target positions of the train path envelope. For example, Fig. 2.7 shows the partitioning of the Sprinter's journey from Utrecht to Houten into 22 phases. The lower black solid lines are the gradients, the red upper solid lines are the speed limits. The low speed limits before a speed increase are extended by the train length (cyan speed lines) which models that the train will only accelerate after its rear has safely passed low speed limit. The dotted lines with circles indicate the stop positions: Utrecht, Utrecht Lunetten and Houten, which are the target points of the train path envelope. The dotted lines with crosses are the signal positions, and the other dotted lines are the critical points of speed limits or gradients. Each segment between two dotted lines is a phase in the multiple-phase optimal control model, with a unique speed limit and gradient. The entire corridor from Ut to Ht is partitioned into 125 phases for the Sprinter, while the Intercity route is partitioned into 90 phases.

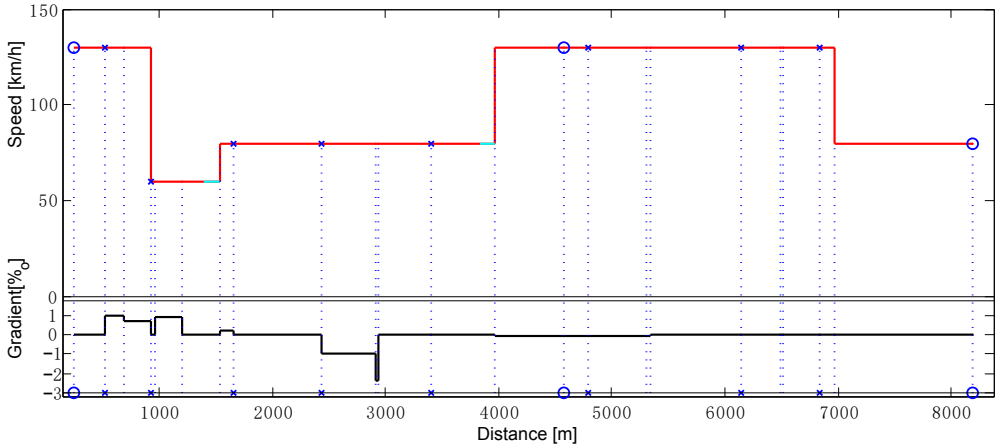

Figure 2.7: Illustration of route partitioning into multiple phases.

The optimized results of state and control trajectories for the Sprinter and Intercity trains are shown in Fig. 2.8 and 2.9, respectively. In each figure, the upper plot shows the optimized speed profiles (solid black lines) and the static speed limits (red horizontal lines). The lower plot shows the optimized forces, where the solid lines refer to the traction force and the dotted lines are the braking force curves. The speed profiles show that both train speeds stay below the speed limits and the trains stop at the planned stop target positions, which means that safety and accurate stops are ensured. The control regimes include using maximum traction during the outbound processes, maximum braking force for the inbound processes, cruising at maximum speeds, and coasting before braking to save energy, which matches the theoretical Maximum Power-Cruising-Coast-Maximum Brake optimal control regimes. Moreover, the speed profiles show that the trains are able to regulate their speed at the varying speed limits via decelerating before low speed limits and accelerating before high speed limits, where the trains only accelerate after the entire train passed the low speed limits. From the traction and braking force curves, we can see that the maximum traction force is used during the outbound processes. The traction force reduces gradually once the maximum power has been reached. In the cruising regimes the traction force constantly adjusts to maintain the optimal cruising speed, while it becomes zero during the coasting regimes so that no energy consumption is produced. The maximum value of the traction and braking force is kept within a range since the optimization algorithm also takes riding comfort as a constraint.

Table 2.3 shows the results of the train trajectory optimization for the scheduled conflict-free case. The 1st column indicates the train type, the 2nd column is the running section in the corridor. The 3rd column shows the computed running times within that section, which are equal to the scheduled ones implying that the train trajectories ensure punctuality as well. The 4th column gives the energy consumption. The 5th column is the number of phases in the multiple-phase optimal control models and the 6th column gives the computation times. These last two columns indicate that the computation time grows with the number of phases in this case. For the total 50

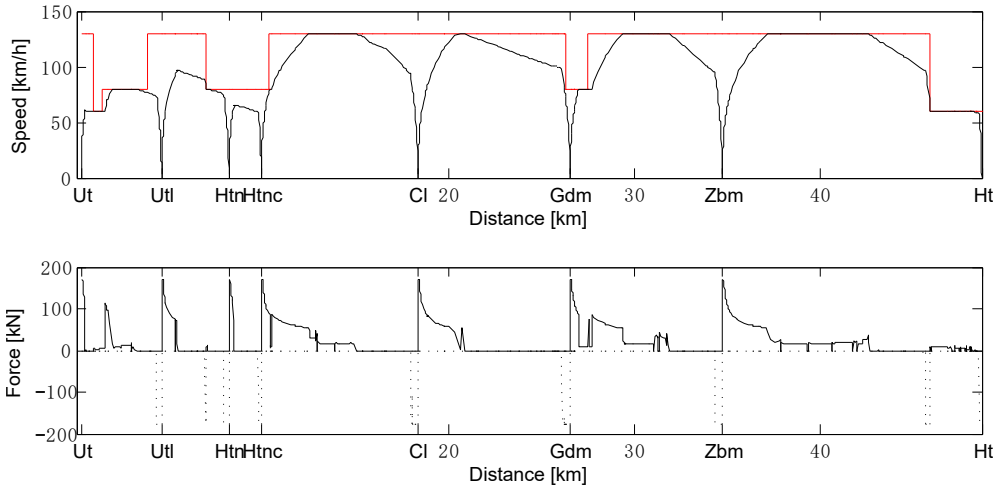

Figure 2.8: Optimal speed trajectories (top) and traction and braking force curves (bottom) of the Sprinter train.

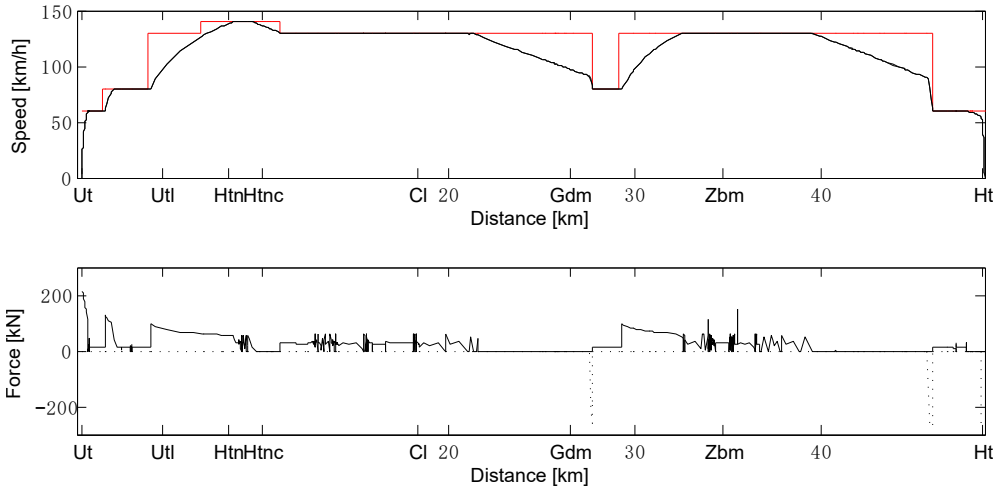

Figure 2.9: Optimal speed trajectories (top) and traction and braking force curves (bottom) of the Intercity train.

Table 2.3: The results of the train trajectory optimization for the scheduled conflict-free case.

Train	Section	Running time [s]	Energy consumption [J]	Number of phases	Computation time [s]
Sprinter	Ut – Utl	240	7.0923×10^7	13	3.80
	Utl – Htn	180	8.5819×10^7	9	2.20
	Htn – Htnc	120	3.7637×10^7	4	1.01
	Htnc – Cl	300	2.3219×10^8	18	6.29
	Cl – Gdm	300	1.6357×10^8	22	7.75
	Gdm – Zbm	300	2.2234×10^8	21	6.75
	Zbm – Ht	540	2.9830×10^8	38	17.25
Intercity	Ut –Ht	1680	1.2023×10^9	90	46.60

km train trajectory, the computation time is limited within 1 minute.

2.4.2 Case B: trajectory optimization with signalling constraints

Section 2.3 shows the method of train trajectory calculation under disruptions and small disturbances. A rescheduling process might produce a new timetable in case of small disruptions. The new generated timetable is conflict-free, which means signalling system would not influence train operation if the train is controlled according to the train path envelope based on the new timetable. So a new train trajectory can be calculated with the method in Section 2.2 without using a signal response policy or a green wave policy. However in the presence of small delays, trains need to recover from delays and get back to the original timetable by regulating their own speed. Signalling influences are obvious since the headway between successive trains might become small because of delays. Hence the focus of this case study is small delay situations and the interactions between trains and signals. We assume that the Sprinter with scheduled departure from Ut at :00 is delayed at this station. Both the signal response policy and green wave policy are used to calculate the train trajectories for the delayed Sprinter. The trajectories between every two stops are calculated separately.

For the signal response policy, a trajectory is calculated each time before the Sprinter departs from a station. If the Sprinter has a delay, objective (2.34) is chosen to minimize the energy consumption as well as the delay. Meanwhile, the arrival time constraint is changed into a time window, where the lower bound is the scheduled arrival time and the upper bound is the scheduled arrival time plus an extra time supplement. The objective (2.34) makes the Sprinter reach the next station as soon as possible, while the new arrival time constraint provides enough running time and ensures that the train cannot arrive earlier than the scheduled time. With the two cost terms, the new trajectory is able to recover the delay and have the train path return to the scheduled one. The minimum dwell times are used when the Sprinter train is

delayed. When the Sprinter has recovered from the delay, objective (2.23) is chosen to concentrate on energy saving only.

During the train run, the signal response policy checks every signal aspect at the sight distance before the signal. If the Sprinter meets a yellow signal aspect, the trajectory is recalculated with the method from Section 2.3.3. The new trajectory may include a decelerating curve in face of a yellow signal, a stop curve to stop the train before a red signal, and a re-acceleration curve when the next signal aspect improves.

The green wave policy calculates the train trajectory every time before the Sprinter departs from a station. The states of the upcoming signal aspects along the track are predicted with the train trajectory of the train running in front of the delayed Sprinter. With the predicted signalling information, additional time constraints at the signal positions are added to make the Sprinter run under all green signals. The optimal trajectories are computed using the Pseudospectral method with (2.34) as the cost function for each phase.

Delayed Sprinter may cause a train path conflict to the Intercity that overtakes the Sprinter at Gdm, which means that the Intercity might meet yellow signals during the section between Ut to Gdm. New Intercity's trajectory is re-calculated by the signal response policy and the green wave policy. For the signal response policy, a trajectory between Ut to Ht is calculated at once before the Intercity departs from Ut with (2.23) as the objective because there is no delay of the Intercity at Ut. During the train run, the signal response policy checks each signal aspect at sight distance before the signals. Proper responses are made in face of different signal aspects with the signal response policy. For the green wave policy, the signal states over the track from Ut to Gdm are predicted with the trajectory of the delayed Sprinter. The corresponding time constraints at signals are added to ensure safe separations between the two trains. After station Gdm the Intercity train becomes the leading train of the delayed Sprinter. The time constraints of the signals for the Intercity in the section between Gdm and Ht depend on a previous Sprinter train in front of the Intercity instead of the delayed one. Moreover, the Sprinter's delay may be propagated to the Intercity at Gdm, which means that the overtaking time of the Intercity at Gdm is changed, since the overtaking time window for the green wave policy depends on the arrival and departure times of the delayed Sprinter. Furthermore, the arrival time constraint at Ht becomes a flexible target window constraint, using the scheduled arrival time as the lower bound and the scheduled arrival time plus an extra time supplement as the upper bound. The arrival time window is to ensure a sufficient running time to reach Ht. With the new time constraints for signals, overtaking, and arrival events, the green wave policy calculates the Intercity's optimal trajectory between Ut and Gdm with objective function (2.34) aiming at minimizing delays and energy consumption.

Fig. 2.10-2.12 show the train trajectories of the Sprinter and Intercity trains in case of three different initial delays of the Sprinter at Ut: 210 s, 270 s and 330 s. The red lines are the static speed limits and the black lines are the optimized speed profiles. The trajectories are calculated with both the signal response policy (Fig. 2.10(a), 2.11(a)

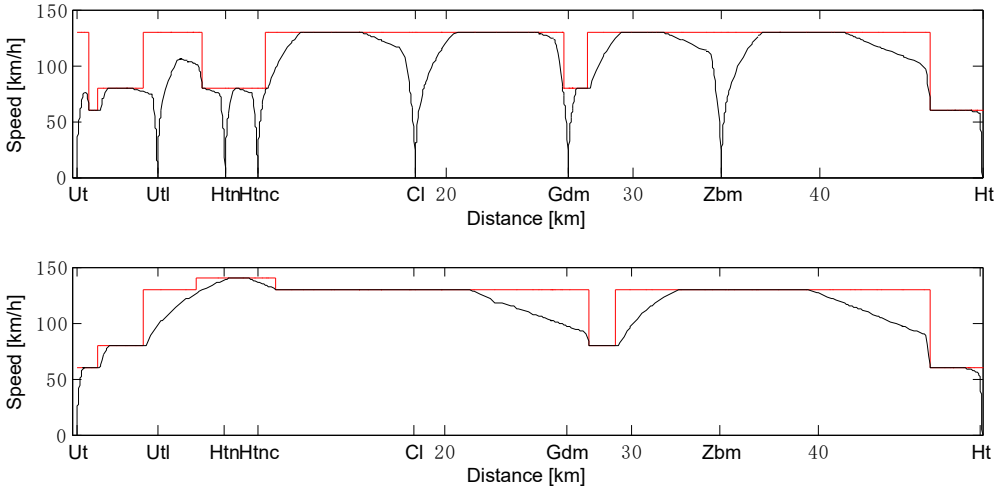

(a) Optimal speed trajectories of the Sprinter (top) and Intercity (bottom) using the signal response policy.

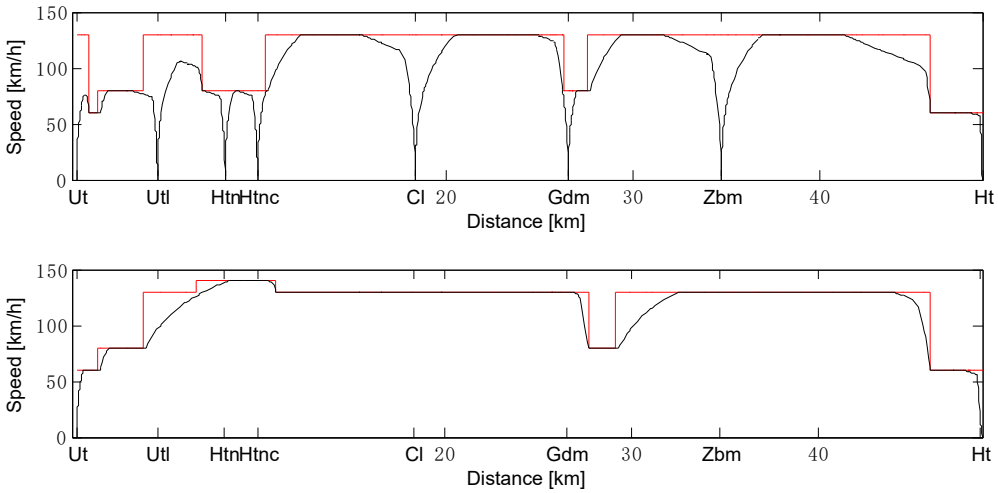

(b) Optimal speed trajectories of the Sprinter (top) and Intercity (bottom) using the green wave policy.

Figure 2.10: Optimal speed trajectories of the Sprinter and Intercity in case of 210 s departure delay of the Sprinter from Utrecht.

and 2.12(a)) and the green wave policy (Fig. 2.10(b), 2.11(b) and 2.12(b)). Table 2.4 gives the resulting energy consumptions from Ut to Ht and the delays at Ht for the two trains, the three different initial delays, and the two policies.

In the case of 210 s delay of the Sprinter from Ut (Fig. 2.10), the Sprinter applies less coasting but cruises more at the maximum speed in the early several sections. The delay decreases gradually by the increased average speed and reduced dwell times. Compared with the energy consumption for the Sprinter travelling from Ut to Ht in Case A, which in total is 1.1108 $\times 10^9$ J, more energy consumption is required to recover from the delay. The delay at station Ht is zero, which means that the Sprinter has entirely recovered from the delay and is back on schedule. The Intercity's speed profile using the signal response policy is the same as the one shown in Fig. 2.9. The Intercity does not meet yellow signals in this case, so the speed profile remains

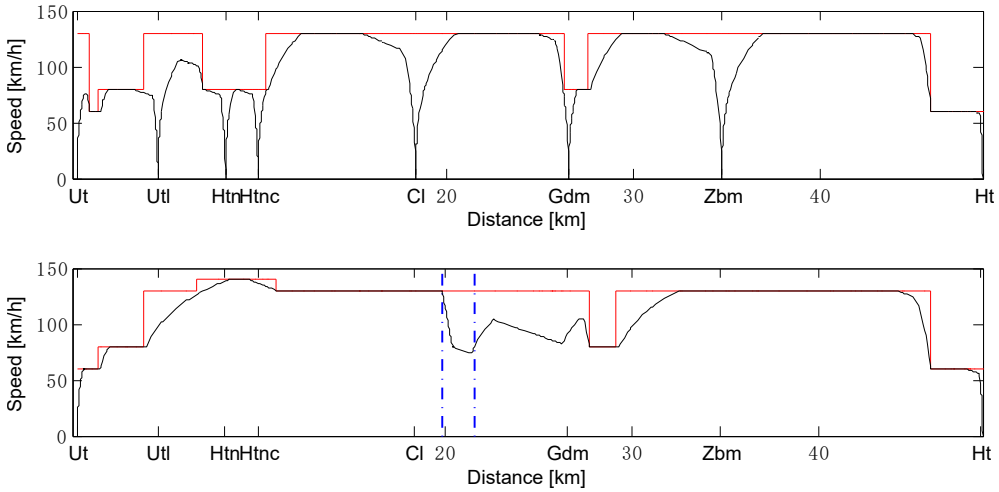

(a) Optimal speed trajectories of the Sprinter (top) and Intercity (bottom) using the signal response policy.

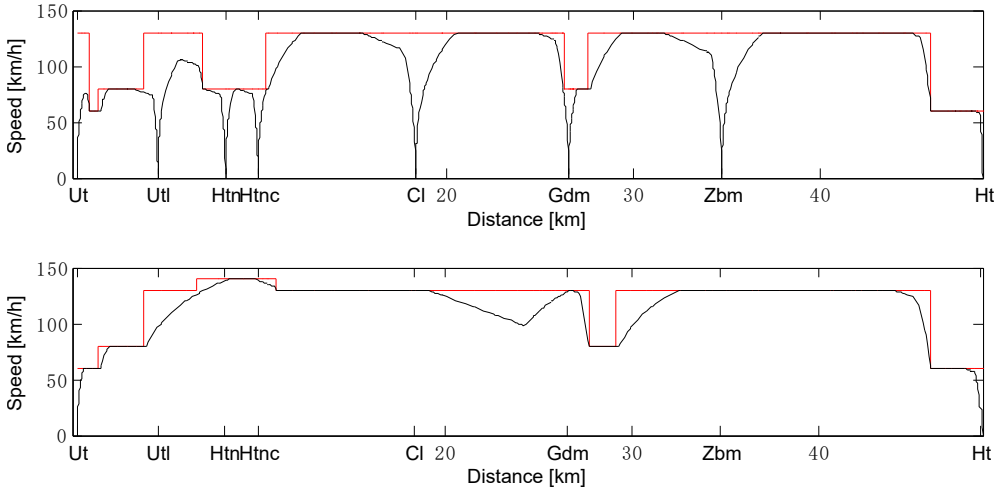

(b) Optimal speed trajectories of the Sprinter (top) and Intercity (bottom) using the green wave policy.

Figure 2.11: Optimal speed trajectories of the Sprinter and Intercity in case of 270 s departure delay of the Sprinter from Utrecht.

Table 2.4: Optimization results for various Sprinter delays from Utrecht (SR: signal response policy, GW: green wave policy).

	Initial Delay at Ut [s]	Energy Consumption [J]		Delays at Ht [s]	
		SR	GW	SR	GW
Sprinter	210	1.2045×10^9	1.2041×10^9	0	0
	270	1.2052×10^9	1.2052×10^9	50.81	50.81
	330	1.2052×10^9	1.2052×10^9	110.92	110.92
Intercity	210	1.2023×10^9	1.4951×10^9	0	0
	270	1.5938×10^9	1.4428×10^9	25.93	0
	330	1.6329×10^9	1.3732×10^9	85.53	46.88

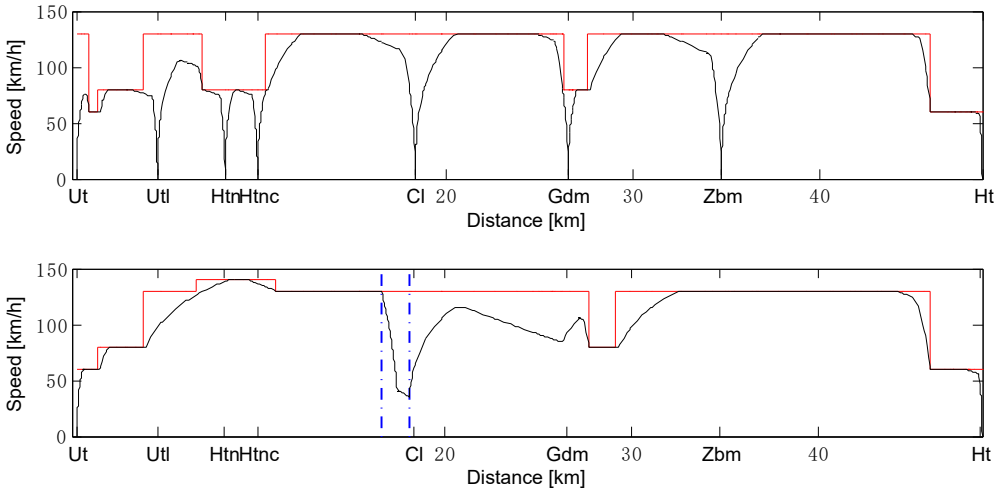

(a) Optimal speed trajectories of the Sprinter (top) and Intercity (bottom) using the signal response policy.

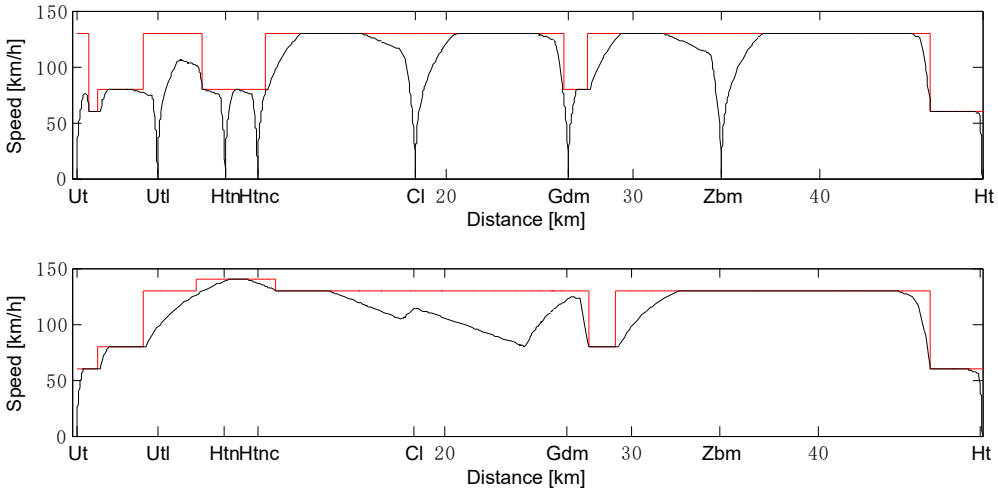

(b) Optimal speed trajectories of the Sprinter (top) and Intercity (bottom) using the green wave policy.

Figure 2.12: Optimal speed trajectories of the Sprinter and Intercity in case of 330 s departure delay of the Sprinter from Utrecht.

the same as the one planned before departing from Ut. However, the speed trajectory obtained with the green wave policy is different. The train uses less coasting and thus consumes more energy compared to the result of the signal response policy. This is because the objective function of the green wave policy is (2.34), which trades off minimizing energy consumptions as well as delays, while the objective function of the signal response policy in the first stage is (2.23), which aims at minimizing the energy consumption without consideration of delays. Moreover, the green wave policy adds more time constraints at signal positions, which also changes the speed profile.

In the case of 270 s initial delay of the Sprinter from Ut (Fig. 2.11), more power is used by the Sprinter to improve its average speed and reduce running time, but still some delay remains at Ht station. The objective (2.34) is used both in the signal response policy and green wave policy. As a result of the trade-off between minimizing energy consumption and delay still coasting regimes are included in the Sprinter's speed profile. The Intercity gets affected by the signalling system because the headway with the Sprinter becomes small in the section between Ut and Gdm due to the Sprinter's delay. Fig. 2.11(a) shows that the Intercity train meets a Yellow 8 signal aspect (blue dashed lines) in the signal response policy, so that the train has to decelerate to the approach speed (80 km/h) and proceed with a speed lower than that 80 km/h until the next signal aspect improves. After this braking, the train re-accelerates to make up for the delay caused by the unscheduled braking but still has some delay at Ht. Instead, the green wave policy makes the train coast to a lower speed before the critical signals, as shown in Fig. 2.11(b). Hence, the green wave policy avoids the yellow signals, and in doing so avoids a delay in Ht and consumes less energy consumption, see Table 2.4.

Fig. 2.12 shows the speed trajectories in the case that the Sprinter has 330 s delay from Ut. The optimized speed trajectories and energy consumption for the Sprinter are the same as the results for 270 s initial delay. The speed profiles show that the Sprinter applies full power for almost the whole corridor from Ut to Ht, with some minor coasting regimes. The delay is again not fully recovered at Ht, and is about 60 s more than in the case of 270 s delay. With the signal response policy, the intercity meets a yellow signal followed by a green signal afterwards (blue dashed lines in Fig. 2.12(a)). So the train decelerates to 40 km/h and then accelerates again. Moreover, the overtaking time is affected by the Sprinter's delay at Gdm. The results show that the Intercity uses coasting to consume time before passing through Gdm station for a smooth overtaking. The speed profile with the green wave policy is different. It shows that the train uses coasting to avoid a yellow signal and for smooth overtaking as well. This saves energy consumption, but results in a small delay in Ht, but less than with the signal response policy.

The Sprinter's trajectories with respect to the signal response policy and the green wave policy are more or less the same. This is because the Sprinter is not affected by yellow or red signals. During the runs between Ut and Gdm, sufficient separation between the Sprinter and the previous Intercity makes sure that there is no path conflict between the two trains. After Gdm, the Sprinter train runs after the next Intercity, but

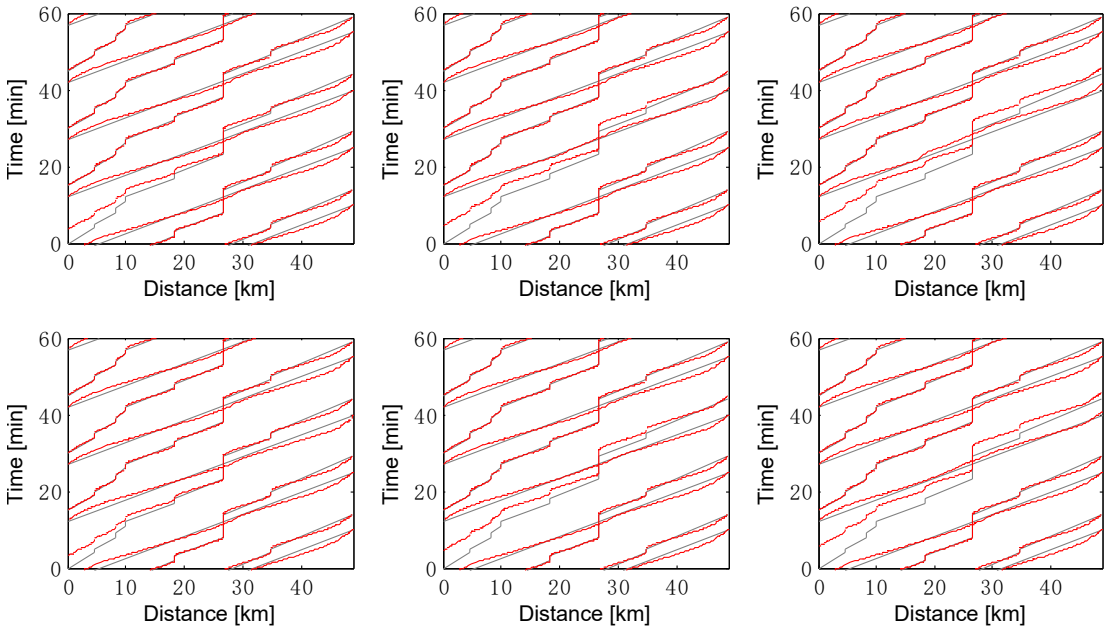

Figure 2.13: The scheduled (gray) and optimized (red) train paths of the Sprinters and Intercities from Ut-Ht during an hour, including three initially delayed Sprinters by 210 s (left), 270 s (middle) and 330 s (right). The upper and lower plots correspond to the signal response and green wave policy, respectively.

the 2 min overtaking headway is sufficient for the Sprinter to again meet no yellow and red signals after Gdm. Besides, the signal response policy and green wave policy use the same objective function in case of delays. So the optimization results with the two policies are very similar. The results show that although the delay is absorbed gradually, it is not entirely recovered and the bigger the initial delay, the more stations get a delay. Furthermore, the delay can also be propagated to other trains. Fig. 2.11 and 2.12 show that the Intercity is delayed because of unplanned braking caused by yellow signals and late overtaking. The energy consumption in case of delays is larger than the one in case of the scheduled conditions.

The trajectories of the next and previous Sprinters and Intercities have also been calculated. Fig. 2.13 shows the time-distance paths for an hour horizon, where the gray lines are the scheduled time-distance paths and the red lines are the optimization results obtained using the signal response policy (top) and the green wave policy (bottom). From left to right, the subfigures show the results in case of 210 s, 270 s, and 330 s departure delay of the Sprinter from Ut. The other train runs are not affected by the delays except for the IC train overtaking the delayed Sprinter at Gdm. The distance-time paths show that they track their scheduled paths well. So sufficient buffer time is available to prevent further delay propagation for these initial delays up to 330 s. The delay of the Sprinter reduces gradually in each policy and delay scenario. Only small delays can be found for the IC train that overtakes the delayed Sprinter.

2.5 Conclusions

This paper presented a model for the train trajectory optimization problem. We formulated the real-time traffic plan as a train path envelope. The train path envelope provides a convenient formulation of time and speed allowances at timetable points and signals, witch can be used easily in the train trajectory calculation and updated with changes of the timetable. Train trajectories based on the up-to-date train path envelope ensure that the train can track the new timetable after the rescheduling process. The train trajectory optimization problem was formulated as a multiple-phase optimal control model, which provides an accurate train movement model with varying speed limits and gradients along the route as well as time and/or speed constraints from the train path envelope. A Pseudospectral method was adopted for problem solving, while case studies show that the algorithm was able to find solutions within short times.

In addition, the train trajectory calculation in case of delays was discussed. In the presence of disturbances, a rescheduling process may adjust the timetable. As a consequence, the train path envelope needs to be updated and the train trajectory is re-calculated based on the new train path envelope. Alternatively, trains may need to recover from delays and get back to the timetable by regulating their own speed. The trains may meet yellow or red signals since the headway between successive trains might become small because of the delays. Two optimization strategies were developed –the signal response policy and the green wave policy–which take different responses to the signalling into account. The signal response policy is based on a limited information scenario corresponding to only the signal aspect of the next signal. The idea is to ensure that the train makes correct and quick responses to different signalling aspects. On the other hand, the green wave policy is based on a full information scenario corresponding to an accurate prediction of the leading train's dynamic behavior. Predictions of yellow or red signals can be used in target windows to avoid early arrivals to signals and thus have a train running according to a green wave. Results show the benefit of the predictive information of the leading train on energy consumption and train delay.

This work has been designed for real-time train trajectory calculation to support a driver advisory system. So smooth control profiles are the next target of our optimization. The work is also useful for timetable optimization (Zhou et al., 2017) or traffic flow and delay propagation analysis (Su et al., 2013) in railway networks. Future work will be devoted to improve the computation times to seconds. Train trajectory optimization is an important module in developing driver advisory system, which requires fast computation times. Currently this work is based on an existing pseudospectral tool. More work is needed to further improve the solution time for real-time applications.

Acknowledgements

The authors thank the Dutch Infrastructure Manager ProRail for making available the infrastructure data. This work was partially supported by the China Scholarship Council CSC (No. 201407000015).

Bibliography

Albrecht, A., Howlett, P., Pudney, P., Vu, X., Zhou, P., 2016a. The key principles of optimal train control—part 1: Formulation of the model, strategies of optimal type, evolutionary lines, location of optimal switching points. Transportation Research Part B: Methodological 94, 482–508.

Albrecht, A., Howlett, P., Pudney, P., Vu, X., Zhou, P., 2016b. The key principles of optimal train control—part 2: Existence of an optimal strategy, the local energy minimization principle, uniqueness, computational techniques. Transportation Research Part B: Methodological 94, 509–538.

Albrecht, A., Koelewijn, J., Pudney, P., 2011. Energy-efficient recovery of delays in a rail network. In: Proceedings of 2011 Australasian Transport Research Forum. Adelaide, Australia.

Albrecht, A. R., Howlett, P. G., Pudney, P. J., Vu, X., Zhou, P., 2015. Energy-efficient train control: the two-train separation problem on level track. Journal of Rail Transport Planning & Management 5 (3), 163–182.

Albrecht, T., Binder, A., Gassel, C., 2013. Applications of real-time speed control in rail-bound public transportation systems. IET Intelligent Transport Systems 7 (3), 305–314.

Albrecht, T., Dasigi, M., 2014. On-time: A framework for integrated railway network operation management. Transport Research Arena.

Albrecht, T., Gassel, C., Binder, A., van Luipen, J., 2010. Dealing with operational constraints in energy efficient driving. In: IET Conference on Railway Traction Systems. Birmingham, UK, 13-15 April 2010.

Benson, D., 2005. A gauss pseudospectral transcription for optimal control. Ph.D. thesis, Massachusetts Institute of Technology, Cambridge, USA.

Betts, J. T., 1998. Survey of numerical methods for trajectory optimization. Journal of guidance, control, and dynamics 21 (2), 193–207.

Caimi, G., Fuchsberger, M., Laumanns, M., Lüthi, M., 2012. A model predictive control approach for discrete-time rescheduling in complex central railway station areas. Computers & Operations Research 39 (11), 2578–2593.

Cheng, J., Howlett, P., 1992. Application of critical velocities to the minimisation of fuel consumption in the control of trains. Automatica 28 (1), 165–169.

Corman, F., D'Ariano, A., Pacciarelli, D., Pranzo, M., 2009. Evaluation of green wave policy in real-time railway traffic management. Transportation Research Part C: Emerging Technologies 17 (6), 607–616.

Darby, C. L., Hager, W. W., Rao, A. V., 2011. An *hp*-adaptive pseudospectral method for solving optimal control problems. Optimal Control Applications and Methods 32 (4), 476–502.

Elnagar, G., Kazemi, M., Razzaghi, M., et al., 1995. The pseudospectral legendre method for discretizing optimal control problems. IEEE Transactions on Automatic Control 40 (10), 1793–1796.

Garg, D., 2011. Advances in global pseudospectral methods for optimal control. Ph.D. thesis, University of Florida, Gainesville, USA.

Gill, P. E., Murray, W., Saunders, M. A., 2002. SNOPT: an SQP algorithm for large-scale constrained optimization. SIAM Journal on Optimization 12 (4), 979–1006.

Gong, Q., Ross, I. M., Kang, W., Fahroo, F., 2008. Connections between the covector mapping theorem and convergence of pseudospectral methods for optimal control. Computational Optimization and Applications 41 (3), 307–335.

Goverde, R. M. P., Corman, F., D'Ariano, A., 2013. Railway line capacity consumption of different railway signalling systems under scheduled and disturbed conditions. Journal of Rail Transport Planning & Management 3 (3), 78–94.

Hansen, I. A., Pachl, J., 2014. Railway timetabling and operations. Eurailpress.

Howlett, P., 1996. Optimal strategies for the control of a train. Automatica 32 (4), 519–532.

Howlett, P., Pudney, P., 2012. Energy-efficient train control. Springer.

Huntington, G. T., 2007. Advancement and analysis of a gauss pseudospectral transcription for optimal control problems. Ph.D. thesis, Massachusetts Institute of Technology, Cambridge, USA.

Khmelnitsky, E., 2000. On an optimal control problem of train operation. IEEE Transactions on Automatic Control 45 (7), 1257–1266.

Liu, R., Golovitcher, I. M., 2003. Energy-efficient operation of rail vehicles. Transportation Research Part A: Policy and Practice 37 (10), 917–932.

Ma, J., Li, X., Zhou, F., Park, B. B., 2016. Parsimonious shooting heuristic for trajectory control of connected automated traffic part II: computational issues and optimization. Transportation Research Part B: Methodological.

Milroy, I. P., 1980. Aspects of automatic train control. Ph.D. thesis, Loughborough University, Leicestershire, UK.

ON-TIME, 2014. Best practice, recommendations and standardisation. Deliverable ONT-WP01-DEL-003.

Pudney, P., Howlett, P., 1994. Optimal driving strategies for a train journey with speed limits. The Journal of the Australian Mathematical Society. Series B. Applied Mathematics 36 (01), 38–49.

Quaglietta, E., Pellegrini, P., Goverde, R. M. P., Albrecht, T., Jaekel, B., Marlière, G., Rodriguez, J., Dollevoet, T., Ambrogio, B., Carcasole, D., et al., 2016. The ON-TIME real-time railway traffic management framework: a proof-of-concept using a scalable standardised data communication architecture. Transportation Research Part C: Emerging Technologies 63, 23–50.

Rao, A. V., 2003. Extension of a pseudospectral legendre method to non-sequential multiple-phase optimal control problems. In: AIAA Guidance, Navigation, and Control Conference and Exhibit. Austin, USA, pp. 11–14.

Rao, A. V., 2009. A survey of numerical methods for optimal control. Advances in the Astronautical Sciences 135 (1), 497–528.

Rao, A. V., Benson, D. A., Darby, C., Patterson, M. A., Francolin, C., Sanders, I., Huntington, G. T., 2010. Algorithm 902: GPOPS, a matlab software for solving multiple-phase optimal control problems using the gauss pseudospectral method. ACM Transactions on Mathematical Software 37 (2), 22.

Ross, I. M., Fahroo, F., 2004. Pseudospectral knotting methods for solving nonsmooth optimal control problems. Journal of Guidance, Control, and Dynamics 27 (3), 397–405.

Ross, I. M., Karpenko, M., 2012. A review of pseudospectral optimal control: from theory to flight. Annual Reviews in Control 36 (2), 182–197.

Su, S., Li, X., Tang, T., Gao, Z., 2013. A subway train timetable optimization approach based on energy-efficient operation strategy. IEEE Transactions on Intelligent Transportation Systems 14 (2), 883–893.

Wang, P., Goverde, R. M. P., 2016. Two-train trajectory optimization with a green-wave policy. Transportation Research Record: Journal of the Transportation Research Board (2546), 112–120.

Wang, P., Goverde, R. M. P., Ma, L., 2015. A multiple-phase train trajectory optimization method under real-time rail traffic management. In: 2015 IEEE 18th International Conference on Intelligent Transportation Systems (ITSC). Las Palmas, Spain, pp. 771–776.

Wang, Y., De Schutter, B., van den Boom, T. J., Ning, B., 2013. Optimal trajectory planning for trains–a pseudospectral method and a mixed integer linear programming approach. Transportation Research Part C: Emerging Technologies 29, 97–114.

Wang, Y., De Schutter, B., van den Boom, T. J., Ning, B., 2014. Optimal trajectory planning for trains under fixed and moving signaling systems using mixed integer linear programming. Control Engineering Practice 22, 44–56.

Zhou, F., Li, X., Ma, J., 2015. Parsimonious shooting heuristic for trajectory control of connected automated traffic part I: Theoretical analysis with generalized time geography. arXiv:1511.04810.

Zhou, L., Tong, L. C., Chen, J., Tang, J., Zhou, X., 2017. Joint optimization of high-speed train timetables and speed profiles: A unified modeling approach using space-time-speed grid networks. Transportation Research Part B: Methodological 97, 157–181.

Chapter 3

Two-train trajectory optimization with a green wave policy

Apart from minor updates, this chapter has been published as:
P. Wang and R. M. P. Goverde, "Two-train trajectory optimization with a green-wave policy," *Transportation Research Record: Journal of the Transportation Research Board*, 2546, 112–120, 2016.

3.1 Introduction

Optimization of train speed trajectory is an essential research topic of train operation optimization and control, which uses optimal control theory to calculate a speed trajectory over the running section to generally ensure punctual, safe, and energy-efficient train behavior. The research on train trajectory optimization problem began in the 1960s, where mostly Pontryagin's Maximum Principle is applied to solve the optimal control problem with energy saving as the objective (Howlett, 1996; Howlett and Pudney, 2012). Pontryagin's Maximum Principle proved that the optimal control consists of four regimes, i.e., maximum traction, cruising, coasting, and maximum (service) braking. The optimal speed profile of the train is a sequence of these optimal regimes where the succession of regimes and their switching points depend on constraints such as speed limits and gradients. Finding these optimal switching points is a difficult problem except for simple cases such as a single speed limit and flat track. Most works assume that there is a static timetable and focus on the single-train trajectory from its current location to the next stop. In practice, the train operations environment is complicated. For instance, a train does not always follow the scheduled timetable. Unexpected events could cause train delays while the delayed trains may interact on other trains' operations. Albrecht et al. (2011) studied the energy-efficient recovery of delays with consideration of the interactions between trains. They aim at

finding the interaction times that allow each affected train to finish on time but they ignore the impact from the signalling systems. For trains operating on the same line, the following trains are not directly interacting with the leading trains, but instead the signalling system displays specific aspects informing trains to slow down. So the influence from signalling systems should be taken into account while studying multiple-train operations.

This paper studies the train trajectory optimization of two successive trains on the same line. The multiple-phase optimal control model is used for modelling the two-train trajectory optimization problem. This model has already been used for the single-train trajectory optimization problem (Wang et al., 2015a,b). This paper extends this work to a two-train trajectory optimization method which is able to calculate the multiple train trajectories simultaneously. In case of delays, a delay recovery strategy is developed with minimizing the delays as one of the objectives. A green-wave (GW) policy is used to make sure that all trains proceed safely under all green signals.

The paper is organized as follows. First the basic optimal control model for a single train is formulated, followed by a description of the GW policy and the two-train trajectory optimization model. Then an optimization strategy for recovery from delays is presented, followed by a case study of an 18-km corridor to verify the effectiveness of our implemented method. The paper ends with conclusions.

3.2 The single-train optimal control problem

In this section, we introduce the basic optimal control model of the dynamic movement of a single train. Distance is adopted as the independent variable, and speed and time as the state variables. The model of a train moving along a railway line can be formulated as (Wang et al., 2015a)

$$\frac{dv}{ds} = \frac{\theta_1 f - \theta_2 b - R_{train}(v) - R_{line}(s)}{\rho \cdot m \cdot v} \tag{3.1}$$

$$\frac{dt}{ds} = \frac{1}{v}, \tag{3.2}$$

where

v = train velocity (m/s),
s = traversed path (m),
m = train mass (t),
ρ = rotating mass factor,
f = traction force (kN),
b = braking force (kN),
$R_{train}(v)$ = train resistance force (kN),
$R_{line}(s)$ = line resistance force (kN),

t = traversed time (s), and
$\theta_1, \theta_2 \in \{0,1\}$ = two binary parameters with $\theta_1 \cdot \theta_2 = 0$.

The train resistance $R_{train}(v)$ consists of rolling, bearing, dynamic and wind resistances. The line resistance $R_{line}(s)$ is a function of position and consists of two components: grade and curve resistance. They can be described as

$$R_{train}(v) = 0.001 \cdot m \cdot g \cdot (\alpha + \beta \cdot v + \gamma \cdot v^2) \tag{3.3}$$

$$R_{line}(s) = R_{grade}(s) + R_{curve}(s), \tag{3.4}$$

where

g = acceleration of gravity,
α, β, γ = constant coefficients,
$R_{grade}(s)$ = grade resistance, and
$R_{curve}(s)$ = curve resistance.

Train traction and braking power are limited by the adhesion between the wheels and the rails as well as the maximum power from the engine, so that

$$0 \leq f \leq F_{\max} \tag{3.5}$$

$$0 \leq b \leq B_{\max} \tag{3.6}$$

$$0 \leq f \cdot v \leq P_{\max}, \tag{3.7}$$

where

$F_{\max}$ = upper bound on the traction force,
$B_{\max}$ = upper bound on the braking force, and
$P_{\max}$ = upper bound on the traction power.

The train speed cannot exceed the speed limitation, as defined in Equation (3.8)

$$0 \leq v \leq V_{\max}(s), \tag{3.8}$$

where $V_{\max}(s)$ is the train speed limit, including static and temporary speed restrictions. The riding comfort is usually measured by train acceleration, which should satisfy

$$A_{\min} \leq a \leq A_{\max}, \tag{3.9}$$

where

$A_{\min}$ = lower bound of acceptable riding comfort,
a = acceleration (calculated as dv/dt), and
$A_{\max}$ = upper bound of acceptable riding comfort.

Each train has its own traffic plan, indicated by the timetable, which restrains train arrival, departure and passing times at timetable points (stations, junctions, etc.). These times can be modeled as a series of time and speed constraints at specific positions, called the *Train Path Envelope* (TPE) (ON-TIME, 2014). The TPE contains two kinds of constraints:

- Mandatory target points, which indicate that a train must reach a target position exactly at a specified time and speed given by a triple (p,t,v), where p is the global coordinate of the target position, and t and v are respectively the specified time and speed.
- Flexible target windows, which indicate that a train must reach a target position within a specific time and speed window given by $(p,[t_{\min},t_{\max}],[v_{\min},v_{\max}])$, where p is the global coordinate of the target position, and $[t_{\min},t_{\max}]$ and $[v_{\min},v_{\max}]$ are respectively the specified time and speed window.

TPE models have been considered before by Wang et al. (2015a); Albrecht et al. (2013). The timetable points along a train's route are modeled as the target positions of the TPE, with their scheduled event time and speed set as their target times and speeds. The scheduled event times at stops can be regarded as mandatory target points. The passing times for a train to pass a specific station or junction are usually not limited to an exact time or speed. So passing events can be modelled as flexible target windows.

The general problem for train trajectory optimization aims at minimizing the energy consumption as well as ensure the riding comfort, which can be formulated as

$$\text{minimize} \int_{s_0}^{s_f} (\omega_1 f + \omega_2 a)\, ds, \tag{3.10}$$

where

$s_0 =$ initial and terminal position,
$s_f =$ terminal position, and
$\omega_1, \omega_2 =$ weight factors.

The first term in Equation (3.10) models the energy consumption from the traction force and the second term models the riding comfort. The weights ω_1, ω_2 can be used to balance between the two objectives.

3.3 Green wave policy

The signalling system ensures the safety of railway traffic by guaranteeing that the block section between two signals can host only one train. The Dutch signalling system NS'54 uses a three-aspect two-block system with a clear (Green, G), approach (Yellow,

Y) and stop (Red, R) aspect (Figure 3.1(a)). In case of a green signalling aspect, the train is unaffected by the signalling system and can proceed with its normal operational speed. A yellow signal orders a reduction in speed to a restricted speed of 40 km/h and prepare to stop before a red signal. In addition, some short blocks are applied which have a length shorter than the maximum braking distance from the line speed. The NS'54 indicates progressive speed reductions before short blocks. The train has to slow down to an indicated speed so that the train will enter the short block with a lower speed associated to the short block length. This speed signalling is given by a yellow signal plus a white numeral indicating the permitted speed at the next signal. For instance in Figure 3.1(b), 'Yellow 8' (Y8) indicates that the train has to reduce speed to 80 km/h before the next signal, S_6.

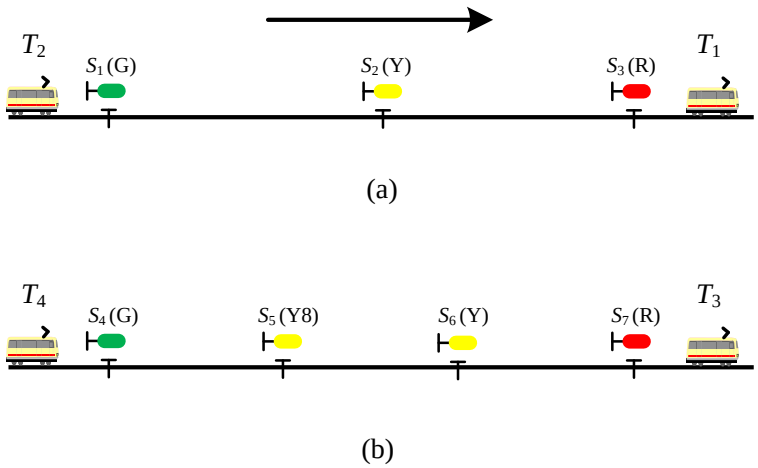

Figure 3.1: Examples of Dutch signaling system.

On a heavily loaded railway network, a train-required platform or route might be blocked by another train. As a consequence, the train has to reduce speed or stop for a while, and then re-accelerate again after the conflicting train has departed. This situation results in an inefficient operation. The GW policy is a method to avoid these inefficient decelerations and reaccelerations (Corman et al., 2009). This policy makes the trains operate only on green signal aspects, with the objective that the railway system achieves smooth, safe, punctual and energy efficient operations. To ensure the GW policy is followed, a suitable distance is required between two successive trains. For instance, in Figure 3.1(a), two empty blocks ahead are required to ensure the following train, T_2, operates under all green signals, while, for train T_4, three empty blocks ahead are required. A feasible control rule for the GW policy is to keep a desired time headway between two successive trains, called the time headway rule. Let H_s be the time headway of two successive trains passing through a signal s. Then, it must hold that

$$H_s \geq R_{T,s,s'} + H_0, \tag{3.11}$$

where

$R_{T,s,s'}$ = running time of the previous train T from signal s to s', with blocks between signals s to s' being the required empty blocks to ensure that the GW policy is followed;

H_0 = the sum of the time for clearing and setting up signals s and s', a certain time for the driver to view the signal s, the overlap with full length of the train at signal s', and the release time to "unlock" the block in rear of signal s'; and

$R_{T,s,s'} + H_0$ = the so-called blocking time of train T of the block before signal s' (Hansen and Pachl, 2014).

3.4 Optimization model for two-train trajectory

A multiple-phase optimal control model is one in which the trajectory consists of a collection of phases. Each phase has its own cost function, dynamic model, path constraints and boundary conditions. The complete trajectory is obtained by properly linking adjacent phases via linkage conditions. The total cost function is the sum of the cost functions within each phase. The optimal trajectory is found by minimizing the total cost function subject to the constraints within each phase and the linkage constraints connecting adjacent phases. In the current model, the trajectory is separated into multiple phases because of changing gradients and speed limits and specific time or speed constraints at the TPE points. The linkage points can be: (*a*) target positions of the TPE, (*b*) critical points of speed limits or gradients and curves, and (*c*) signal positions.

Consider two successive trains, T_1 and T_2 (T_1 being the leading train and T_2 the following one), moving along a railway line. For each phase, let the independent variable in phase $r \in \{1,\ldots,R\}$ lie in the interval $s \in [s_0^{(r)}, s_f^{(r)}]$. Let $x^{(r)} = [v_1^{(r)}, v_2^{(r)}, t_1^{(r)}, t_2^{(r)}]$ and $u^{(r)} = [f_1^{(r)}, f_2^{(r)}, b_1^{(r)}, b_2^{(r)}]$ be, respectively, the state and control vectors in phase r, where $v_1^{(r)}, t_1^{(r)}, f_1^{(r)}, b_1^{(r)}$ and $v_2^{(r)}, t_2^{(r)}, f_2^{(r)}, b_2^{(r)}$ are the speed, run time, traction force and braking force of train T_1 and T_2. The dynamic equations in phase $r \in \{1,\ldots,R\}$ are

$$\frac{dx_1^{(r)}}{ds} = \frac{\theta_1 u_1^{(r)} - \theta_2 u_3^{(r)} - R_{train,1}^{(r)}(x_1^{(r)}) - R_{line,1}^{(r)}(s)}{\rho \cdot m_1 \cdot x_1^{(r)}} \tag{3.12}$$

$$\frac{dx_2^{(r)}}{ds} = \frac{\theta_1 u_2^{(r)} - \theta_2 u_4^{(r)} - R_{train,2}^{(r)}(x_2^{(r)}) - R_{line,2}^{(r)}(s)}{\rho \cdot m_2 \cdot x_2^{(r)}} \tag{3.13}$$

$$\frac{dx_3^{(r)}}{ds} = \frac{1}{x_1^{(r)}} \tag{3.14}$$

$$\frac{dx_4^{(r)}}{ds} = \frac{1}{x_2^{(r)}}, \tag{3.15}$$

where

$R^{(r)}_{train,1}(x^{(r)}_1)$ = train resistances of train T_1 in $s \in [s^{(r)}_0, s^{(r)}_f]$,
$R^{(r)}_{line,1}(s)$ = line resistances of train T_1 in $s \in [s^{(r)}_0, s^{(r)}_f]$,
m_1 = mass of train T_1,
$R^{(r)}_{train,2}(x^{(r)}_2)$ = train resistances of train T_2 in $s \in [s^{(r)}_0, s^{(r)}_f]$,
$R^{(r)}_{line,2}(s)$ = line resistances of train T_2 in $s \in [s^{(r)}_0, s^{(r)}_f]$, and
m_2 = mass of train T_2.

The trains behavior in phase $r \in \{1, \ldots, R\}$ should also satisfy the path constraints in Equations (3.5) through (3.9). Additional details can be found in Wang et al. (2015b).

The boundary of each phase could be the target positions of the TPE, the critical points of speed limits or gradients and curves, or signal positions. The critical points of speed limits or gradients and curves have no specific boundary constraints; however, each phase has its own specific values of speed limit, gradient and curve. For each target point of the TPE, a time and speed allowance is needed to restrain train operations, and this allowance can be formulated as the boundary constraints. Take train T_1 and target points p_t as an example, where p_t is the boundary between two adjacent phases r_t and $r_t + 1$, $r_t \in \{1, \ldots, R-1\}$. If a mandatory target point constraint exists at p_t, then

$$x_1(p_t) = v_{T_1,p_t}, \quad x_3(p_t) = t_{T_1,p_t}, \tag{3.16}$$

where v_{T_1,p_t} is the target speed of train T_1 at p_t, and t_{T_1,p_t} is the target time of train T_1 at p_t.

If a flexible target window constraint exists at p_t, then

$$v_{T_1,p_t,\min} \le x_1(p_t) \le v_{T_1,p_t,\max}, \quad t_{T_1,p_t,\min} \le x_3(p_t) \le t_{T_1,p_t,\max}, \tag{3.17}$$

where $v_{T_1,p_t,\min}$, $v_{T_1,p_t,\max}$, $t_{T_1,p_t,\min}$ and $t_{T_1,p_t,\max}$ are the minimum and maximum speed and time for train T_1 at p_t.

Because p_t is the boundary between two adjacent phases, Constraints (3.16) and (3.17) work as the terminal boundary constraints for phase r_t as well as the initial boundary constraints for phase $r_t + 1$. Likewise, Constraints (3.16) and (3.17) also hold for the TPE target points of train T_2 with different values.

Additional boundary constraints at signal positions are needed to ensure that both train operate under all green signals (i.e., keep sufficient time headway). For example, at signal p_s, with p_s the boundary between two adjacent phases r_s and $r_s + 1$, $r_s \in \{1, \ldots, R-1\}$, we have

$$x_4(p_s) - x_3(p_s) \ge R_{T_1,p_s,p'_s} + H_0, \tag{3.18}$$

where R_{T_1,p_s,p'_s} is the estimated running time of train T_1 from signal p_s to p'_s, which are the signals before and after the empty blocks to ensure the GW policy. Constraint

(3.18) works as the terminal boundary constraint for phase r_s as well as the initial boundary constraint for phase r_s+1.

For each two sequential phases r and $r+1$, a set of conditions is used to connect the trajectories in phase r and $r+1$. In most cases, the state variables must be continuous at the boundary between phase r and phase $r+1$. Therefore, the following linkage conditions must be satisfied for $r \in \{1,\ldots,R-1\}$:

$$s_f^{(r)} - s_0^{(r+1)} = 0 \tag{3.19}$$

$$x(s_f^{(r)}) - x(s_0^{(r+1)}) = 0. \tag{3.20}$$

One exception occurs if the linkage point of phase r and $r+1$ is the stop point for a train. Take train T_1 as an example, if $s_f^{(r)}$ (or $s_0^{(r+1)}$) is a stop point of train T_1, then $x_3(s_f^{(r)})$ and $x_3(s_0^{(r+1)})$ represent, respectively, the arrival and departure time of train T_1 and, in normal cases

$$x_3(s_0^{(r+1)}) - x_3(s_f^{(r)}) = D_{T_1,s_f^{(r)}}. \tag{3.21}$$

where $D_{T_1,s_f^{(r)}}$ is the dwell time of train T_1 at $s_f^{(r)}$ (or $s_0^{(r+1)}$).

In normal conditions, the objective is more smooth, punctual and energy-efficient train operation. With punctuality we mean that the train arrives at and departs from the stops at the times indicated by the timetable, which can be achieved by setting mandatory target arrival and departure times and speeds to the arrival and departure events. Smoothness and energy-efficient operation can be formulated in the objective function. The cost functional $J^{(r)}$ in phase $r \in \{1,\ldots,R\}$ is

$$J^{(r)} = \int_{s_0^{(r)}}^{s_f^{(r)}} \left[\omega_1 \left(u_1^{(r)} + u_2^{(r)}\right) + \omega_2 \left(a_1^{(r)} + a_2^{(r)}\right)\right] ds, \tag{3.22}$$

where a_1 and a_2 are, respectively, the acceleration of train T_1 and T_2.

In case of delays, the objective is to recover from the delays as well as save energy consumption and operate in a smooth way. In this case the objective function $J^{(r)}$ in phase $r \in \{1,\ldots,R\}$ becomes

$$J^{(r)} = \omega_3 \left(x_3(s_f^{(r)}) + x_4(s_f^{(r)})\right) + \int_{s_0^{(r)}}^{s_f^{(r)}} \left[\omega_1 \left(u_1^{(r)} + u_2^{(r)}\right) + \omega_2 \left(a_1^{(r)} + a_2^{(r)}\right)\right] ds, \tag{3.23}$$

where ω_3 is a weight factor for the delay.

In case of delays, the constraints at the stops become flexible target windows instead of mandatory target points because there is no guarantee that the delayed train can arrive at (or depart from) stops on time. However the train is not expected to arrive (or depart) earlier than its scheduled time. So the flexible time window of the arrival (or departure) event can be $[t_a,\infty]$ ($[t_d,\infty]$), where t_a and t_d are the scheduled arrival and departure time.

The minimum dwell time at a stop should be respected. Take train T_1 for example, for two sequential phases r and $r+1$ where the connecting point is a stop point for train T_1. Then a constraint is adopted for the dwell time:

$$D_{T_1,s_f^{(r)},\min} \leq x_3(s_0^{(r+1)}) - x_3(s_f^{(r)}) \leq D_{T_1,s_f^{(r)},\max}, \tag{3.24}$$

where $D_{T_1,s_f^{(r)},\min}$ and $D_{T_1,s_f^{(r)},\max}$ are the minimum and maximum dwell time of T_1 at $s_f^{(r)}$.

The objective of the R-phase problem of train trajectory optimization is to minimize the cost function over all phases:

$$J = \sum_{r=1}^{R} J^{(r)}, \tag{3.25}$$

subject to Dynamic constraints, Path constraints, Boundary constraints, and Linkage condition.

Pseudospectral methods can be applied for solving multiple-phase optimal control problems (Rao, 2003). There exist several commercial and free packages that implement the pseudospectral method. We adopt GPOPS (Rao et al., 2010) as the solver in this paper.

3.5 Case studies

The authors considered a case of two successive trains of the same type (T_1 being the leading train, T_2 the following train) operating on a railway line 18 km long that is based on the line from Houten to Geldermalsen in the Netherlands. The static parameters of the train type used in the case studies are listed in Table 3.1. The traction force and train resistance curves are shown in Figure 3.2. Because the braking deceleration is the only accessible data for the braking characteristic, the braking force equals braking deceleration times train mass. The trains depart from station S1, where the line from S1 to S4 includes 4 stations (S1, S2, S3 and S4), 15 signals, 6 short blocks and 8 long blocks (Figure 3.3). The trains serve each station with a scheduled dwell time of 1 min. The minimum dwell times are 0.5 min. The departure headway time at station S1 is 4 min, while the running times of both trains are the same. The running times between S1 and S2, S2 and S3, and S3 and S4 are 2, 5 and 5 min, respectively. The proposed method was tested in four cases. In the first, the two trains operate according to the timetable, while in the other three different input delays are added to train T_1 at departure station S1 to test the delay recovery ability. The calculation has been carried out with GPOPS 4.1 on a laptop equipped with a 3.2 GHz Pentium R processor.

Table 3.1: Basic parameters Of the train

Property	Value
Train mass: m [t]	220
Mass factor: ρ	1.06
Maximum traction power: $P_{f,\max}$ [kW]	1918
Maximum traction force: $F_{\max}$ [kN]	170
Maximum braking deceleration: $A_{\min}$ [m/s^2]	-0.8

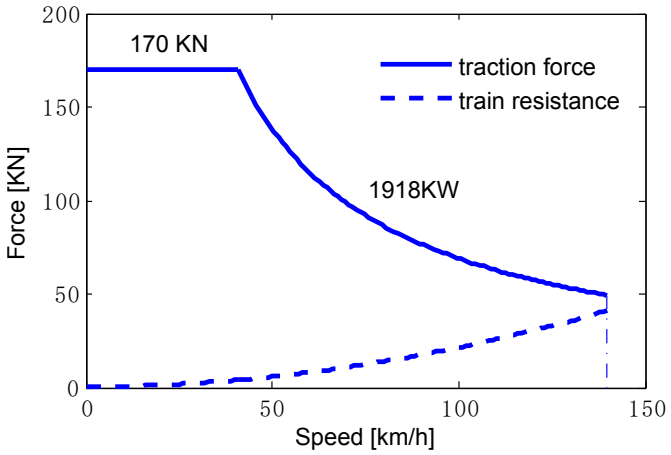

Figure 3.2: Traction force (solid line) and train resistance (dashed line) of the train.

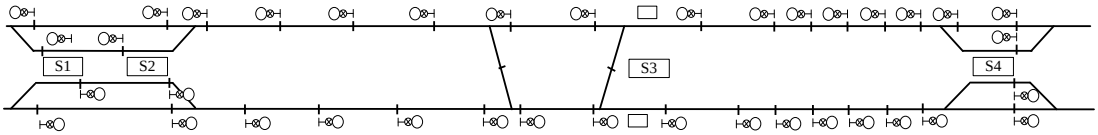

Figure 3.3: The infrastructure structure.

Figure 3.4 shows the trajectories of both trains for the four different cases. Figure 3.4 (a) and (b) shows, respectively, the optimized speed distance profiles for train T_1 and T_2, where the red line indicates the speed limits. In Figure 3.4(c), the red dashed lines are the (linearized) scheduled timetable of both trains, while the solid lines are the real time-distance paths for train T_1 and T_2. For the first case, Equation (3.22) is chosen as the objective function with $\omega_1 = 1$ and $\omega_2 = 100$. These weights give more priority to energy consumption than to riding comfort (note the difference in scale of force and acceleration). The speeds are clearly below the maximum speed limits, and the arrival and departure times at each stop are equal to the scheduled ones. Moreover, both trains use coasting regimes between almost every two stations to make full use of the given running times and ensure a smooth operation. Because the departure headway time is large enough, the following train T_2 is not affected by the first train and the speed-distance curves of both trains are the same.

In the delayed cases, three delays (1, 2 and 3 min) are added to train T_1 at station S1. Equation (3.23) is chosen as the objective function with $\omega_1 = 1$, $\omega_2 = 100$ and

Table 3.2: The results Of the two-train trajectory optimization

Train	Total running time [s]	Total dwell time [s]	Input Delay [s]	Output Delay [s]	Energy consumption [J]	Computation time [s]
Case I						
T_1	720	120	0	0	1.4281×10^9	58.26
T_2	720	120	0	0		
Case II						
T_1	706.86	73.14	60	0	1.4607×10^9	93.42
T_2	711.70	119	9.30	0		
Case III						
T_1	687.54	60	120	27.53	1.5246×10^9	126.79
T_2	711.93	60	68.06	0		
Case IV						
T_1	683.76	60	180	83.76	1.5437×10^9	99.47
T_2	701.92	60	128.74	50.66		

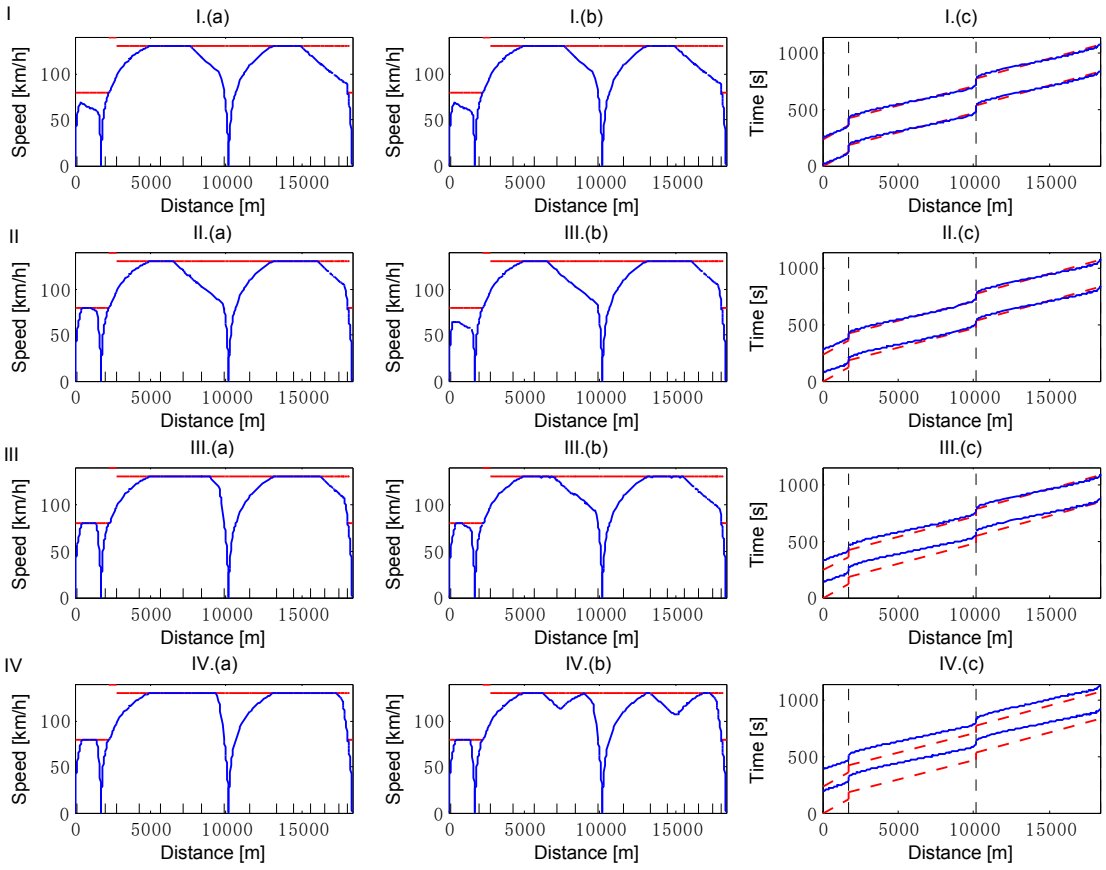

Figure 3.4: The optimized trajectories of train T_1 and T_2 in case of 0 min (I), 1 min (II), 2 min (III), and 3 min (IV) initial delay of train T_1; (a) The optimized speed-distance of train T_1, (b) The optimized speed-distance of train T_2, and (c) The time-distance paths of train T_1 and T_2.

$\omega_3 = 1000$, and makes a tradeoff between the objectives of energy saving, riding comfort and delay recovery. Figure 3.4 shows that the delayed train tends to use less coasting and more power to overcome delays and that the following train is influenced because the headway between the two train becomes small in case of delays. Table 3.2 shows the corresponding total running time, total dwell time, energy consumption and computation times. The four rows correspond to initial delays of 0, 1, 2, and 3 min. The third column shows the total running time between station S1 and S4, and the fourth column gives the cumulative dwell time at station S2 and S3. The fifth column shows the delays of both trains at station S1 compared with the scheduled departure time. The delay of train T_1 is the input while the delay of train T_2 is caused by the delay of train T_1. The sixth column reports the delays of both trains at station S4. The last two columns are the energy consumption and the computation times.

Comparison of the input and output delays of train T_1 shows that the delayed train T_1 tends to use less coasting and reduced dwell times to recover from delays. The following train, T_2, is influenced by the delayed previous train because a certain headway is required between the two successive trains to ensure safety and the GW policy constraints (Equation (3.18)). The delay is reduced gradually by reducing the

dwell and running times. Comparison of the energy consumption of the four different cases in Table 3.2 shows that more energy consumption is required when the trains tend to recover from delays. This is because the trains use less coasting for energy saving in case of delays. The computation times of the four cases are shown in Table 3.2, and they range between 1 to 2 min.

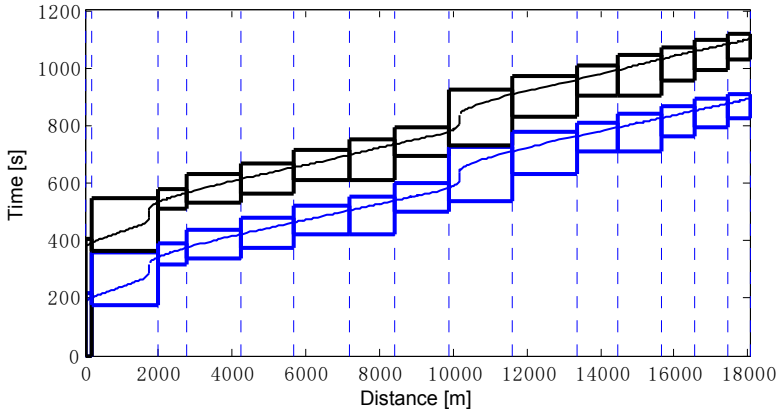

Figure 3.5: Blocking time diagram of train T_1 (blue) and T_2 (black).

In some cases (Figure 3.4 IV.(b)), train T_2 needs to decelerate for a while before some signals to make sure that those signals show green aspects when the train passes. Otherwise, train T_2 will meet yellow signal aspects and should brake and proceed at a restricted speed of 40 or 80 km/h. Figure 3.5 shows the blocking time diagram of both trains in case of a 3-min delay of train T_1 at station S1. The blocking times of both trains don't overlap each other, which proves that the two trains have no conflicts, and the following train T_2 proceeds under all-green signals.

Instead of optimizing both train trajectories simultaneously, an alternative approach can be pursued in which, first, the leading train is optimized and, then, the following train using the GW policy. The result can then be compared with the global optimization. The authors use the single-train trajectory optimization method with consideration of signalling constraints proposed by Wang et al. (2015b). First the leading train was optimized with objective function (3.23) using $\omega_1 = 1$, $\omega_2 = 100$ and $\omega_3 = 1000$, and then the following train was optimized with the signalling constraints from the leading train. The case of the two trains running from S1 to S4 with train T_1 having 3 min departure delay at station S1 was then considered. The result is shown in Figure 3.6. The speed profiles look smoother compared to the results of case IV in Figure 3.4. The delays of the trains at station S4 are now 80 s and 70.3 s, and the energy consumption of both trains is 1.594×10^9 J. The delay of the leading train is now slightly smaller, but the delay of the following train and the total energy consumption are larger. The distance between the two trains using the joint trajectory optimization method is smaller than the one obtained from the successive optimization. With smaller distance headway, the delay time of the following train is smaller than the result calculated by the successive optimization. The computation times for the joint

and successive optimization are similar. More tests are required to see how the models scale up to multiple trains and different corridors.

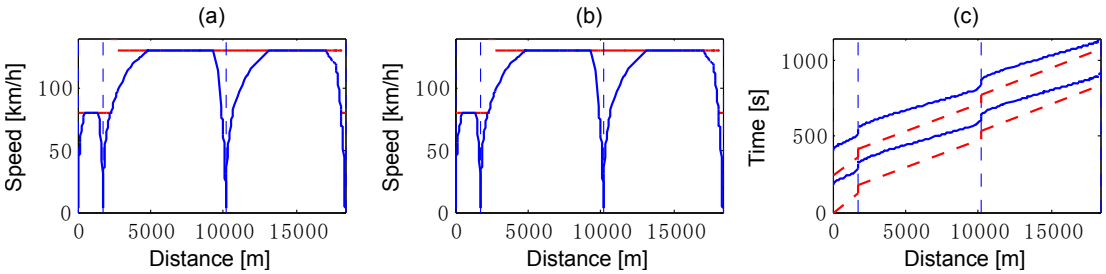

Figure 3.6: The optimized trajectories of train T_1 and T_2 in case of 3 min initial delay of train T_1 by optimizing the train trajectories one by one; (a) The optimized speed-distance of train T_1, (b) The optimized speed-distance of train T_2, and (c) The time-distance paths of train T_1 and T_2.

Different values of ω_1, ω_2 and ω_3 results in different optimal solutions. Figure 3.7 shows the results of the total delay at station S4 and the energy consumption with $\omega_1 = 1$, $\omega_2 = 100$ and different values for ω_3. The initial delay of train T_1 is 3 min. With increasing weight ω_3, delay is reduced while energy consumption increases. The delay reduction stabilizes for weights $\omega_3 \geq 1000$, with a fixed positive delay, which indicates that the time supplements are not sufficient to recover the 3-min initial delay entirely.

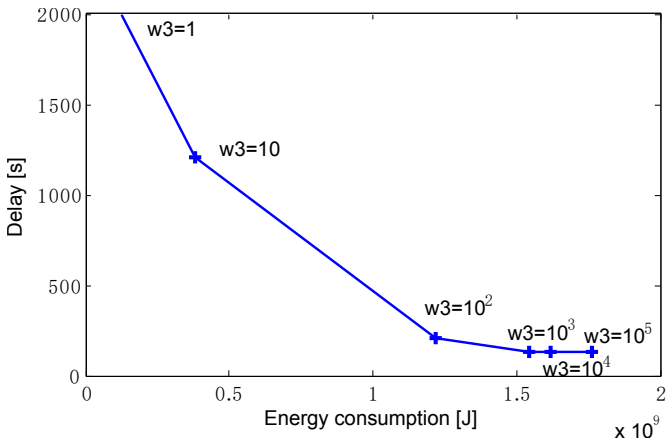

Figure 3.7: Delay and energy consumption for different ω_3.

3.6 Conclusions

This paper presented a model for the computation of optimal train trajectories of two successive trains on the same line. We described a detailed model for the single-train optimal control problem and extended it to a two-train optimal control problem

adopting a multiple-phase optimal control problem to formulate the dynamic behaviors of the two successive trains. The green wave policy was adopted to ensure that the trains proceed under all green signals. A method in case of delays was also developed by extending the objective functions and constraints. The objective was to ensure a smooth, safe, punctual and energy-efficient train operation. The multiple-phase optimal control problem was solved using the Gauss Pseudospectral Method. A case study of two successive trains running on a line with various initial delays showed the benefit of the green wave policy and the ability of delay recovery. Future work will be devoted to improve the computation times to seconds and consider more interactions (overtaking, meeting, etc.) and more trains simultaneously.

Bibliography

Albrecht, A., Koelewijn, J., Pudney, P., 2011. Energy-efficient recovery of delays in a rail network. In: Proceedings of 2011 Australasian Transport Research Forum. Adelaide, Australia.

Albrecht, T., Binder, A., Gassel, C., 2013. Applications of real-time speed control in rail-bound public transportation systems. IET Intelligent Transport Systems 7 (3), 305–314.

Corman, F., D'Ariano, A., Pacciarelli, D., Pranzo, M., 2009. Evaluation of green wave policy in real-time railway traffic management. Transportation Research Part C: Emerging Technologies 17 (6), 607–616.

Hansen, I. A., Pachl, J., 2014. Railway timetabling and operations. Eurailpress.

Howlett, P., 1996. Optimal strategies for the control of a train. Automatica 32 (4), 519–532.

Howlett, P., Pudney, P., 2012. Energy-efficient train control. Springer.

ON-TIME, 2014. Best practice, recommendations and standardisation. Deliverable ONT-WP01-DEL-003.

Rao, A. V., 2003. Extension of a pseudospectral legendre method to non-sequential multiple-phase optimal control problems. In: AIAA Guidance, Navigation, and Control Conference and Exhibit. Austin, USA, pp. 11–14.

Rao, A. V., Benson, D. A., Darby, C., Patterson, M. A., Francolin, C., Sanders, I., Huntington, G. T., 2010. Algorithm 902: GPOPS, a matlab software for solving multiple-phase optimal control problems using the gauss pseudospectral method. ACM Transactions on Mathematical Software 37 (2), 22.

Wang, P., Goverde, R. M. P., Ma, L., 2015a. A multiple-phase train trajectory optimization method under real-time rail traffic management. In: 2015 IEEE 18th International Conference on Intelligent Transportation Systems. IEEE, Las Palmas, Spain, pp. 771–776.

Wang, P., Goverde, R. M. P., Ma, L., 2015b. Train trajectory optimization with signalling constraints. In: 2015 Conference on Advanced Systems in Public Transport. Rotterdam, the Netherlands.

Chapter 4

Multi-trains trajectory optimization for energy efficiency and delay recovery on single-track railway lines

---

Apart from minor updates, this chapter has been published as:
P. Wang and R. M. P. Goverde, "Multi-trains trajectory optimization for energy efficiency and delay recovery on single-track railway lines," *Transportation Research Part B: Methodological*, 2017, 105: 340-361.

4.1 Introduction

Delays affect the performance of railway networks and the quality of service provided to passengers and shippers. When delays occur, drivers are responsible for getting the delayed trains back to the original or rescheduled timetable. The process of getting delayed trains back to schedule is called delay recovery. It is more energy-efficient to recover the delay gradually over several legs of the journey than to recover quickly (Albrecht et al., 2015). However, the delayed train will often interact with other trains, causing a further delay propagation through the system and thereby impacting the energy-efficiency of many trains. In particular, on single-track lines, trains have limited possibility of meeting and overtaking. Trains cannot enter the single-track lines that are occupied by opposite trains, and trains in the same directions must follow each other's path sequentially, until an overtaking or passing track is reached at stations or sometimes at loops. Those limitations increase the possibility of delay propagation. Therefore, even the experienced drivers find it hard to achieve an efficient train operation once the train is delayed or affected by delayed trains on the single-track lines.

To improve the performances of train drivers, train driver advisory systems (DASs) are proposed, which provide train drivers with information and driving advice and help them to drive the train in an efficient manner. A DAS needs an optimal train trajectory (speed-distance curve and time-distance curve along the train's journey), based on which driving advice is computed accordingly. The train trajectory optimization (TTO) problem is to find the optimal trajectory by optimal control theory. Generally, the optimization aims at minimising the energy consumption and maintaining the timetable, with consideration of the constraints of train characteristics, track gradients, curves and speed limits. In the last few decades, TTO has drawn a lot of attention in the literature. Wang et al. (2011), Albrecht et al. (2016a), and Scheepmaker et al. (2017) provide comprehensive surveys from different views. Wang et al. (2011) reviewed the numerical approaches for solving the train trajectory optimization problem. Albrecht et al. (2016a) focused on the state-of-the-art of using Pontryagin's Maximum Principle (PMP) to find the key principles of optimal train control. Scheepmaker et al. (2017) provided surveys on the energy-efficient train control and energy-efficient train timetable problems. The solution methods of the TTO problem can be divided into two categories: indirect methods and direct methods (Wang et al., 2011). PMP is a typical indirect method, which has been successfully used in train trajectory optimization (Albrecht et al., 2016a). With the application of PMP, the TTO problem is converted to a problem of finding the optimal sequence of optimal control regimes (maximum power, cruising, coasting, and maximum braking) and the switching points between the regimes for a range of different circumstances and train types. Finding the optimal sequence and switching points is a difficult problem except for simple cases such as a single speed limit and flat track (Albrecht et al., 2016b). Direct methods were developed more recently and expanded quickly because of their advantages over indirect methods (Scheepmaker et al., 2017). Direct methods transcribe a optimal control problem to a nonlinear programming problem (NLP), which is then solved by existing NLP solvers. For instance, pseudospectral methods have been successful applied by Wang et al. (2013); Wang and Goverde (2016a) and Ye and Liu (2016) in solving the TTO problem.

Under delay circumstances, the interactions from neighbouring trains cannot be ignored, which have drawn attention recently. Some researches reflect the interactions as dynamic speed limits on train movements imposed by signaling systems. Albrecht (2009) considered the driving strategies to move a train through conflict areas. The target was to slow down the train before critical conflicts (red signals) and then pass critical infrastructure elements with shortest possible delay, in this way, reducing energy costs and avoiding unscheduled stops. Three driving strategies – reactive driving, optimal anticipating driving, and safe anticipating driving – were proposed to achieve this target. Yun et al. (2011) provided solutions to identify the optimal approaching speed for the optimal anticipating driving strategy. The optimal speed enables the train to leave the conflict area as soon as possible. A heuristic method was then developed to attain the optimal speed trajectory. Wang and Goverde (2016a) focused on the single-train trajectory optimization problem with consideration

of dynamic speed limits imposed by the signalling system. Two different driving strategies, a signal response policy and green wave policy, were developed to respond to signals and to avoid yellow signals. The signal response policy refers to actively adjusting the train speed according to the signal aspects. A green wave policy means anticipating to slow down the train in front of a conflicting area to make the train face only green signal aspects. A different green wave policy was first proposed in (Corman et al., 2009), in which the green wave policy allows trains to wait only at their scheduled stops. Wang and Goverde (2016a) extended the green wave policy by allowing regulating speeds and running times for more efficient driving. The case studies in (Wang and Goverde, 2016a) show that a green wave policy saves more energy consumption than the signal response policy.

Other researchers optimize multi-train trajectories together with consideration of the interactions between neighbouring trains. Albrecht et al. (2011) provided a numerical algorithm to find interaction times that allows each affected train to finish on time wherever possible and minimises total energy consumption for the whole set of trains. The interaction times can be transmitted to DASs on each of the trains (trajectory optimization modules), which will set strategies to meet these times. Further work is required to extend to situations where interaction locations and sequences may change. Yang et al. (2012) provided a mathematical model for multiple trains on a railway network. The model aims at minimizing total energy consumption and running times of all trains, while satisfying the constraints to ensure the feasibility of multi-train operations, which include headway constraints, vehicle speed limit constraints, passenger riding comfort constraints, and dwell time constraints. The control strategies of every involved train are the decision variables of the multi-train model. A genetic algorithm (GA) integrated with simulation was designed to find the optimal control strategies. Zhao et al. (2015) studied the trajectory optimization problem of multi-trains, considering the trade-off between reduction in train energy usage against increases in delay. The research focused on following trains with a fixed block signaling system in a delayed situation. A multi-train simulator and three searching methods, namely, enhanced brute force, ant colony optimization, and a genetic algorithm, were adopted to find the optimal trajectories. A case study of four following trains showed that the algorithm is able to reduce energy consumption and interactions between trains. However, the three searching methods cost long computation times to find optimal solutions, which needs future improvement for real-time application. Yin et al. (2016, 2017) addressed the train schedule and reschedule problem with dynamic passenger demands, with consideration of multiple trains' energy-efficient speed profiles. Wang and Goverde (2016c) studied the delay recovery problem of the two successive trains in the same direction. Wang and Goverde (2016c) studied the delay recovery problem of the two successive trains in the same direction. A two-train trajectory optimization method was developed to compute two trains' trajectories simultaneously, which takes into account not only each train's operational constraints, but also the constraints on keeping safe distances between the two trains. The green wave policy was adopted to ensure that the trains run safely under all

green signals to avoid frequent stop/start behavior and thus improving train operation efficiency.

Summing up past research on trajectory optimization under delay circumstances, most of the previous studies focus on trains in the same direction. Certain headways between trains are necessary to avoid conflicts, while the energy efficiency relies on how do the trains pass through conflict areas (yellow and red signals). Nevertheless, the trajectory optimization for a train on single-track lines is more complex, because the train has additional restrictions of meeting and overtaking. Opposite trains cannot occupy a single-track section at the same time. In practice, the dispatching process is first used to determine optimal orders and meet-pass plans, after which drivers adjust the train speed to follow the new plan. Cacchiani et al. (2014) provided a review of recovery models and algorithms for real-time rescheduling. As for the single-track railway scheduling problem, one of the first researches started in the 1970's, with the work by Szpigel (1973). Szpigel (1973) developed a linear programming model to determine the best meeting and overtaking positions and used a branch and bound method to resolve the conflicts. Minimising the sum of the travel times was the objective and only small problems were tested. Jovanović and Harker (1991) introduced the Schedule Analysis System (SCAN), which deals with scheduling problems on single and double track segments. It is based on a compound method of optimization and simulation. Higgins et al. (1996) gave a mathematical programming model to schedule trains over a single line track. The objective function is to minimize a combination of delays and energy consumption. The priority of each train in a conflict depends on an estimate of the remaining crossing and overtaking delay, as well as the current delay. This priority is used in a branch and bound procedure to allow an optimal solution to reasonable size train scheduling problems to be determined efficiently. Meng and Zhou (2011) provided a dispatching model for a major service disruption on single-track lines. The model incorporates different probabilistic scenarios in the rolling horizon decision process. A multi-layer branching solution procedure was developed to generate and select meet-pass plans under different stochastic scenarios. Umiliacchi et al. (2016) introduced a simulation-based method that minimizes the effects of a single delay on the journeys of two trains and on the trains' energy consumption while satisfying time constraints on a single-track railway line.

It can be seen that the aim of rescheduling on single-track lines is to determine where trains will meet and pass to minimize train delays or deviations from the planned schedule while satisfying a set of operational constraints. The train movement process (train trajectory) is rarely taken into account during the dispatching process, which results in two major shortcomings: first, the way of driving a train may influence the decision to be made during the dispatching process. Second, the delays of a train after an initial delay are different for different driving strategies. A bad delay estimation may result in a bad prediction of future conflicts. D'Ariano et al. (2007); Mazzarello and Ottaviani (2007); Luthi (2009) and Caimi et al. (2011) proposed approaches for anticipating driving in the dispatching process, and showed that those approaches

contribute to further decreasing delays and increasing energy efficiency.

Recognizing that limited attention has been devoted to the anticipating driving in the dispatching process especially on single-track lines, this research restricts attention to opposite trains on a single-track line which meet at multiple-track stations, and aims to find a feasible meet plan and energy-efficient speed profiles for opposite trains under delayed conditions. It is assumed that trains in the same direction do not overtake, and the delays are relatively small so that the cancelation of trains in the timetable is not necessary, but the meet locations and the train sequences may change. The work is developed on the train trajectory optimization level. It firstly aims at finding feasible time windows at stations, which delayed trains are able to go through. The time windows and corresponding speed windows are formulated as timetable constraint sets (TCSs). Then a multi-train trajectory optimization (MTTO) method is developed to find trains' trajectories within the TCSs. The MTTO model takes into account not only every single train's constraints of dynamic movement equations, vehicle parameters, and varying speed limits and gradients, but also constraints to avoid conflicts between following trains and opposite trains. The MTTO method can calculate speed profiles for multiple trains simultaneously, and choose proper meeting locations for opposite trains for the benefit of reducing delays and energy costs.

The MTTO is formulated as a multiple-phase optimal control problem (Rao et al., 2003). The multiple-phase optimal control problem formulation has been used first in Wang et al. (2015); Wang and Goverde (2016a) for single-train trajectory optimization, in Wang and Goverde (2016c) for two following trains in the same direction, and then in Wang and Goverde (2016b) for two opposite trains on single-track lines. The multiple-phase optimal control problem has the advantage of accurately incorporating varying gradients, curves and speed limits, timetable constraints, and railway network topology. This work is an extension of Wang and Goverde (2016b), which dealt with two punctual opposite trains. This paper discusses the case of train trajectory optimization after a delay occurs. Compared with Wang and Goverde (2016b), the present paper has two improvements: (1) we relax the assumption that the train sequencing within single-track segments is fixed which works for on-time trains, but not for delayed conditions. So the formulation in this paper allows changing the train orders at the open tracks. (2), we relax the assumption of equal lengths of parallel station tracks and thus consider different lengths of station tracks, which provides a more accurate model for multiple-track stations and for train trajectory calculation. The multiple-phase optimal control problem is solved efficiently by a pseudospectral method (Rao et al., 2010), which transforms the problem into a nonlinear programming model that is solved by a nonlinear programming solver.

The MTTO model has two objectives: minimizing delays and saving energy consumption. The priorities of the two objectives are different under different circumstances. In order to select proper optimization objectives, three different driving strategies – the delay-recovery strategy, energy-saving strategy and on-time strategy – are proposed. A driving strategy selection algorithm is developed in order to find the best

driving strategy for each running section (The running section refers to a train route between two stops.). The proposed method is demonstrated by application to case studies of opposite-trains running on a Dutch partially single-track railway corridor with different initial delay scenarios. For simplicity, we mainly address a two-train trajectory optimization problem for two opposite trains on a single-track corridor and subsequently show a case of multi-trains. The results show that our method is able to produce optimal timetables and speed profiles of opposite trains simultaneously. The meeting locations and times are chosen during the optimization process automatically where energy-efficient and conflict-free driving as well as delay recovery requirements are considered.

The remainder of the paper is organized as follows: Section 4.2 provides a description of optimization objectives and operational constraints of train movements. Section 4.3 introduces the timetable constraint set formulation in case of delays. Section 4.4 formulates the multi-train trajectory optimization as a multiple-phase optimal control problem, and presents three driving strategies and a corresponding driving strategy selection algorithm. Section 4.5 illustrates the proposed approach in case studies. Finally Section 4.6 ends the paper with conclusions.

4.2 Problem description

A single-track railway line consists of a single-track line with intermediate multiple-track stations where trains can meet and overtake, see Fig. 4.1. Consider a single-track corridor between kilometer point K_0 and K_f $(K_0 < K_f)$. The stations in the direction from K_0 to K_f are named with successive numbers $1,2,\ldots,Z$. Denote by $\mathbf{Z} = \{1,2,...,Z\}$ the set of stations where Z is the number of stations between K_0 and K_f. Denote by $\mathbf{I}$ the set of trains operating on this corridor, $\mathbf{I_d}$ the set of trains in the downstream direction from station 1 to Z and $\mathbf{I_u}$ the set of trains in the upstream direction from station Z to 1, and $\mathbf{Z}_i$ the stations on train $i \in \mathbf{I}$'s journey.

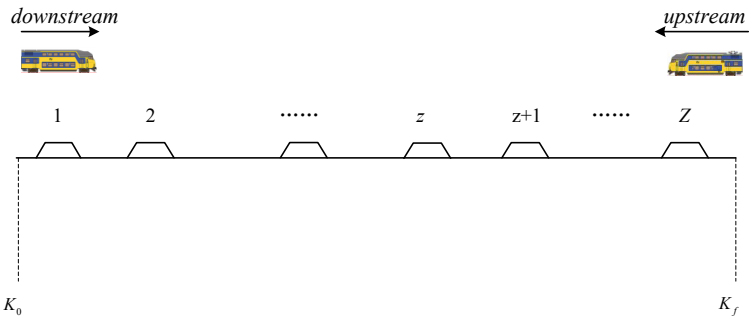

Figure 4.1: Opposite trains on a single-track railway line between K_0 and K_f.

For a train $i \in \mathbf{I}$, it is requested by the timetable to arrive at and depart from stations on specific times. Moreover, the passing-through times at non-stop stations should stay within specific time windows to avoid influences on other trains. For a mathematical

description, classify a train's event at a station into three types: arrival, departure and pass-through. Denote by e an event $e \in \{a,d,p\}$, where a refers to arrival, d refers to departure, and p refers to pass-through. For train $i \in \mathbf{I}$, the timetable constraint set (TCS) is written as

$$\mathbf{TCS}_i = \left\{ \left(k_{i,z,e}, [t_{i,z,e}^{\min}, t_{i,z,e}^{\max}], [v_{i,z,e}^{\min}, v_{i,z,e}^{\max}] \right) \right\}_{z \in \mathbf{Z}_i}, \tag{4.1}$$

where $k_{i,z,e}$ is the location for train i at station z of event e, and $t_{i,z,e}^{\min}$, $t_{i,z,e}^{\max}$, $v_{i,z,e}^{\min}$ and $v_{i,z,e}^{\max}$ are respectively the lower and upper bounds of time and speed for e at $k_{i,z,e}$. Define $\mathbf{K}_{\mathbf{TCS}_i}$ as the set of timetable points of train i. If $k_{i,z,e}$ is a stop station, the speed window $[v_{i,z,e}^{\min}, v_{i,z,e}^{\max}] = [0,0]$, and $k_{i,z,a} = k_{i,z,d}$.

Let distance be the independent variable because gradients and speed limits occur as functions of distance rather than of time. For train $i \in \mathbf{I}$, the generic equations of train motion can be written as follows:

$$\begin{cases} \dfrac{dv_i(s_i)}{ds_i} = \dfrac{\theta_1 f_i(s_i) - \theta_2 b_i(s_i) - R_{train,i}(v_i) - R_{line,i}(s_i)}{\rho_i \cdot m_i \cdot v_i(s_i)}, \\ \dfrac{dt_i(s_i)}{ds_i} = \dfrac{1}{v_i(s_i)}, \end{cases} \tag{4.2}$$

subject to

$$\begin{cases} 0 \le f_i(s_i) \le F_i^{\max}, \\ 0 \le b_i(s_i) \le B_i^{\max}, \\ 0 \le f_i(s_i) \cdot v_i(s_i) \le P_i^{\max}, \\ 0 \le v_i(s_i) \le V_i^{\max}(s_i), \\ A_i^{\min} \le \dfrac{dv_i(s_i)}{dt_i(s_i)}, \le A_i^{\max}, \end{cases} \tag{4.3}$$

$$\begin{cases} v_{i,z,e}^{\min} \le v_i(k_{i,z,e}) \le v_{i,z,e}^{\max}, \\ t_{i,z,e}^{\min} \le t_i(k_{i,z,e}) \le t_{i,z,e}^{\max}, \quad \forall\, z \in \mathbf{Z}_i,\ k_{i,z,e} \in \mathbf{K}_{\mathbf{TCS}_i}, \end{cases} \tag{4.4}$$

$$D_{i,z}^{\min} \le t_i(k_{i,z,d}) - t_i(k_{i,z,a}) \le D_{i,z}^{\max}, \quad \forall\, z \in \mathbf{Z}_i,\ k_{i,z,a}, k_{i,z,d} \in \mathbf{K}_{\mathbf{TCS}_i}. \tag{4.5}$$

Equations (4.2) present the dynamic equations of train i, where s_i is the traversed distance [m], $v_i(\cdot)$ is the train velocity [m/s], ρ_i is the rotating mass factor, m_i is the train mass [t], $f_i(\cdot)$ is the traction force [kN], $b_i(\cdot)$ is the braking force [kN], $R_{train,i}(v_i) = \alpha_i + \beta_i \cdot v_i + \gamma_i \cdot v_i^2$ is the train resistance force [kN] with coefficients α_i, β_i and γ_i, $R_{line,i}(s_i)$ is the line resistance force [kN], which is a function of position and consists of grade resistance and curve resistance, $t_i(\cdot)$ is the traversed time [s], and $\theta_1, \theta_2 \in \{0,1\}$ are two binary parameters with $\theta_1 \cdot \theta_2 = 0$. Inequalities (4.3) are the path constraints of train i's vehicle performance characteristics, speed limits and riding-comfort. $F_i^{\max}$, $B_i^{\max}$ and $P_i^{\max}$ are the maximum traction force, maximum braking force and maximum traction power of train i. $V_i^{\max}(s_i)$ is the speed limit at position s_i, including static and temporary speed restrictions. $A_i^{\min}$ and $A_i^{\max}$ are the

lower and upper bound of acceptable accelerations. Inequalities (4.4) are the TCS constraints which represent time and speed constraints of every timetable point in $\mathbf{K}_{\mathbf{TCS}_i}$. Inequality (4.5) is the dwell time constraint of train i at every stop station, where $D_{i,z}^{\min}$ and $D_{i,z}^{\max}$ are respectively the minimum and maximum dwell times.

In case a delay occurs, the train driver must get the delayed train back to the pre-defined timetable. The train trajectory optimization problem is to find a series of control laws for the train traction and braking forces and an optimal speed profile, which reduce delays as well as minimize the energy consumption, to guide drivers in train control. The train trajectory optimization problem for a single train $i \in \mathbf{I}$ can be formulated with a cost function

$$\min \quad J_i = \omega_i \cdot t_i(K_i^f) + \int_{K_i^0}^{K_i^f} f_i(s_i)\, ds_i, \tag{4.6}$$

subject to dynamic constraints (4.2), path constraints (4.3), TCS constraints (4.4), and dwell time constraints (4.5). The cost function (4.6) and constraints (4.2)-(4.5) constitute a single-train trajectory optimization (STTO) model for a train i. In Equation (4.6), K_i^0 and K_i^f are respectively the start and end positions of train i's journey between K_0 and K_f, $t_i(K_i^f)$ is the travelled time at K_i^f, and ω_i is a weight factor. The first item in Equation (4.6) aims at reducing total running time, which in turn reduces delays with the scheduled arrival time as the lower bound of the time window at K_i^f (see Section 4.4). The second term aims at saving energy consumption. The weight ω_i reflects the trade-off between the two objectives of delay recovery and energy efficiency. If $\omega_i = 0$ then J_i is used for energy-efficient driving.

In case train i runs on schedule, the TCS time constraints at stop stations are the scheduled arrival and departure time targets, while the time windows at non-stop stations equal the scheduled passing-through time windows. The STTO model focuses on reducing energy consumptions with $\omega_i = 0$. However, the delay circumstances are different. First, the TCS cannot be set according to the schedule times, because the train movement has deviated from its time plan and the scheduled TCS may be not feasible. The method of computing the TCS for delay cases is presented in Section 4.3. Second, the first priority of a delayed train is to recover from delays instead of to reduce energy consumption. Energy-efficient driving is possible in case the train has got back to the schedule, or in case the train is waiting for another train. Last but not least, a delayed train may impact other trains, causing conflicts and delay propagation. It is necessary to avoid conflicts and reduce delay propagation. In order to avoid conflicts, three more constraints should be noticed: (1) a time interval between every two adjacent trains in the same direction is required for safe train separation (Fig. 4.2 ①), (2) for opposite trains, there are two important types of headway requirements: (i) "depart-arrive" headway, the headway between the departure of a train and the arrival of an opposing train from the same line (Fig. 4.2 ②); and (ii) "arrive-depart" headway, the headway between the arrival of a train and the departure of an opposing train towards the same line (Fig. 4.2 ③), and (3) opposite trains cannot travel on a single-track section between two adjacent stations at the same time, otherwise a head-on conflict occurs (Fig 4.2. ④).

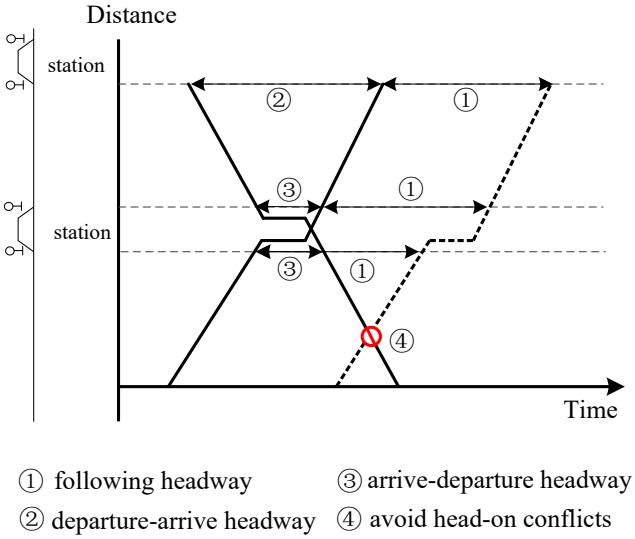

Figure 4.2: Necessary headways between trains.

Define the train sets $\mathbf{I_o} = \{(i,j)|\ i \text{ and } j \text{ are from opposite directions}, i,j \in \mathbf{I}\}$ and $\mathbf{I_s} = \{(i,j)|\ i \text{ and } j \text{ are in the same direction}, i,j \in \mathbf{I}\}$. Denote by $\mathbf{Signal}_{i,j}$ the set of signals on both train i and j's journeys for $i,j \in \mathbf{I_s}$, $\mathbf{StationSignal}_{i,j}$ the set of signals at station boundaries on both train i and j's journeys for $i,j \in \mathbf{I_o}$, $[l_0,l_f]$ a piece of single track (l_0 and l_f are the start and end locations), which opposite trains are allowed to use, and $\mathbf{SingleTrack}_{i,j}$ the set of single-tracks on both train i and j's journeys for $i,j \in \mathbf{I_o}$. The three constraints are formulated as:

$$\begin{cases} \big(t_i(q)-t_j(q)\big)^2 \geq h_s^2, & \forall (i,j) \in \mathbf{I_s}, q \in \mathbf{Signal}_{i,j}, \\ \big(t_i(q)-t_j(q)\big)^2 \geq h_o^2, & \forall (i,j) \in \mathbf{I_o}, q \in \mathbf{StationSignal}_{i,j}, \\ \big(t_i(l_0)-t_j(l_0)\big)\big(t_i(l_f)-t_j(l_f)\big) \geq \sigma, & \forall (i,j) \in \mathbf{I_o}, [l_0,l_f] \in \mathbf{SingleTrack}_{i,j}. \end{cases} \tag{4.7}$$

In the above, $t_i(q)$ and $t_j(q)$ refer to the time of train i and j passing through signal q. $t_i(l_0)$, $t_i(l_f)$, $t_j(l_0)$ and $t_j(l_f)$ refer to the time of train i and j passing through l_0 and l_f. h_s is the minimal headway time between two successive trains in the same direction. h_o is the minimum "arrive-depart" or "depart-arrive" headway time. σ is a positive value close to 0 representing a safe margin for train separation. The first inequality represents the safe following headway constraint for trains in the same direction. The second inequality is for safe "arrive-depart" or "depart-arrive" headway constraints. The point where the headway time applies is usually the station but we put the headway times at signals, which are at station boundaries, to simplify the formulation. The left hand sides of the two inequalities are squared to include the influence of train sequences. The third inequality in (4.7) is used to avoid any crossover of two trains' time-distance paths on single-track segments.

Constraints (4.7) should been taken into account to avoid conflicts between trains, especially in case a delay occurs. However, the constraints cannot be easily included in the STTO model presented above (minimize (4.6) subject to (4.2)-(4.5)) since the

STTO method only focuses on one train movement. Therefore, we propose a multi-train trajectory optimization (MTTO) model by optimizing multi-trains' trajectories simultaneously. The MTTO model is introduced in Section 4.4.

4.3 TCS computation

This section presents the method of computing TCSs for delayed or delay-affected trains. In case a delay occurs, the delayed or delay-affected trains might not be able to arrive at or depart from stations on time. In other words, there are no feasible trajectories within the scheduled TCSs. Therefore, specific TCSs for delayed or delay-affected trains are required.

The TCS indicates the time and speed window constraints at every timetable point along a train's route. For each timetable point, speed information is optional. Only some crucial positions need speed restrictions to assure the speed limits or operational constraints such as minimum speeds before slopes or tunnels. A typical example of a speed restriction is for stop points where the speed window is $[0,0]$, meaning that the train should stop. Time window constraints are mandatory. The time windows for delayed or delay-affected trains in this paper are designed based on three principles: drivability, feasibility, and energy efficiency. *Drivability* means that the time windows are reachable with minimal technical running (dwell) times and maximal advisable running (dwell) times. *Feasibility* means that the time windows allow conflict-free train movements. For trains in the same direction, adjacent trains' time windows should provide enough headway. For trains in opposite directions, the time windows should allow opposite trains to meet at stations. *Energy efficiency* means the time windows contain enough time supplements for energy-efficient driving. The time window computation follows three steps: Step 1: calculate a drivable time envelope for every train separately; Step 2: adjust time windows for feasibility; and Step 3: adjust time windows to improve energy efficiency.

The first step is to calculate a drivable time envelope for every train separately. The time windows at each station are computed one by one in the train's travelling direction with

$$t^{\min}_{i,y,a} = t^{\min}_{i,z,d} + R^{\min}_{i,z}, \qquad t^{\max}_{i,y,a} = t^{\max}_{i,z,d} + R^{\max}_{i,z}, \tag{4.8}$$

$$t^{\min}_{i,y,d} = \max\left\{t^{\min}_{i,y,a} + D^{\min}_{i,y}, S_{i,y,d}\right\}, \qquad t^{\max}_{i,y,d} = \max\left\{t^{\max}_{i,y,a} + D^{\max}_{i,y}, S_{i,y,d}\right\}, \tag{4.9}$$

where $i \in \mathbf{I}$, $z \in \mathbf{Z}_i$, y is the next station after z on train i's route. For $i \in \mathbf{I_d}$, $z \neq Z$, $y = z+1$. For $i \in \mathbf{I_u}$, $z \neq 1$, $y = z-1$. $R^{\min}_{i,z}$ and $R^{\max}_{i,z}$ are the minimal and maximal running times of train i from station z to y, and $D^{\min}_{i,y}$ and $D^{\max}_{i,y}$ are the minimal and maximal dwell times of train i at station y. $S_{i,y,e}$ is the scheduled time for event e of train i at station y, $e \in \{a,d,p\}$. For simplification, we consider the passing through event as a special case of a stop, where the dwell time equals 0, $t^{\min}_{i,y,p} = t^{\min}_{i,y,a} = t^{\min}_{i,y,d}$, and

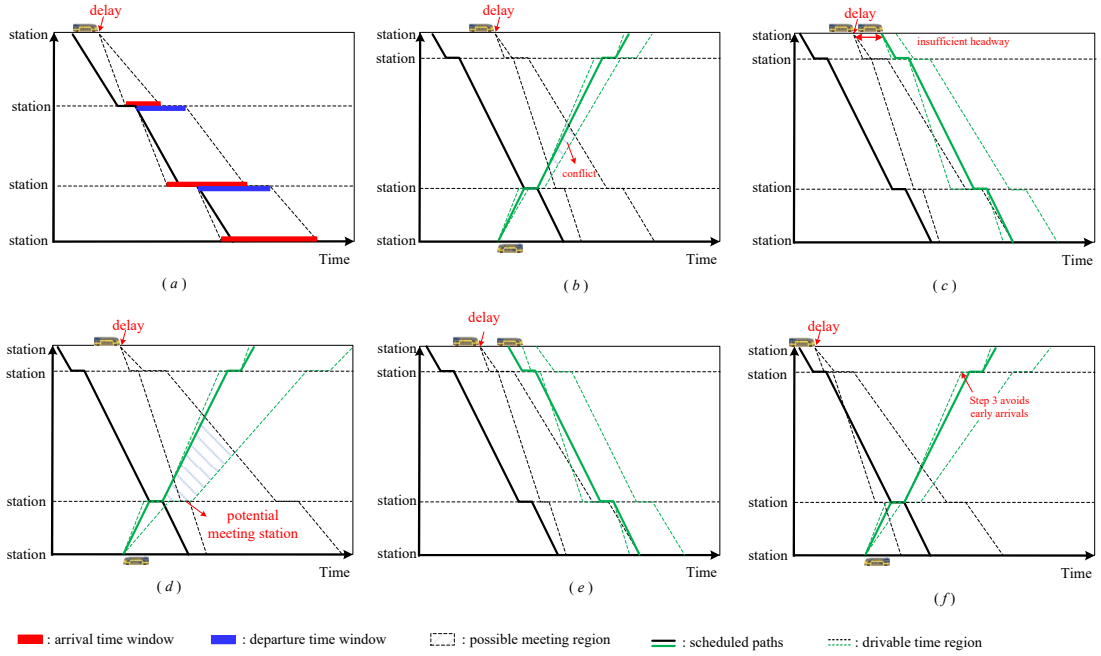

Figure 4.3: TCS time window examples.

$t^{\max}_{i,y,p} = t^{\max}_{i,y,a} = t^{\max}_{i,y,d}$. Equations (4.9) avoid departures earlier than scheduled otherwise the passengers would miss the train. An example of a single train's TCS is shown in Fig. 4.3 (a). The drivable time region is between the two dashed lines, where the train has the chance to get back to schedule (because the minimal running times are smaller than the scheduled running times) and also has enough supplements in case that the train gets delays (because maximal running times are bigger than the scheduled ones).

The second step is the TCS adjustment for feasibility. The time windows calculated in Step 1 can not guarantee feasible solutions. Take Fig. 4.3 (b) for instance, the overlap part of drivable regions of the two trains is the potential meeting region of the two opposite trains. The overlap region must include at least one multiple-track station, otherwise the two trains can only meet at single-track segments, which leads to a head-on conflict, as the dashed area in Fig. 4.3 (b). In Fig. 4.3 (c), the previous train is delayed so that the headway between the two trains is not sufficient, even if the preceding train goes with minimal running (dwell) times and the following train takes maximal running (dwell) times.

Step 2 is executed to adjust the time windows computed by Step 1 to avoid such potential conflicting meeting and following. First, Step 2 detects whether the headway between adjacent following trains are enough or not. For train $i, j \in \mathbf{I_s}$, i is a preceding train, and j is a following train. If $t^{\max}_{j,z,e} - t^{\min}_{i,z,e} < H^{\min}_{i,j,z}$, then

$$t^{\min}_{j,z,a} = t^{\min}_{i,z,a} + H^{\min}_{i,j,z}, \qquad t^{\max}_{j,z,a} = \max\{t^{\min}_{j,z,a} + W, t^{\max}_{j,z,a}\}, \tag{4.10}$$

$$t^{\min}_{j,z,d} = \max\{t^{\min}_{i,z,d} + H^{\min}_{i,j,z}, S_{j,z,d}\}, \qquad t^{\max}_{j,z,d} = \max\{t^{\min}_{j,z,d} + W, t^{\max}_{j,z,d}\}, \tag{4.11}$$

where $z \in \mathbf{Z}_i \cap \mathbf{Z}_j$, $H^{\min}_{i,j,z}$ refers to the minimal headway time from i to j at station z, and W makes sure $t^{\max}_{j,z,a} > t^{\min}_{j,z,a}$, $W > 0$.

Second, Step 2 detects potential conflicting meetings by checking the overlap regions of opposite trains. If there are potential meeting conflicts, then we enlarge the upper bounds of time windows of conflicting trains by

$$t^{\max}_{j,z,e} = \alpha \cdot t^{\max}_{j,z,e}, \quad z \in \mathbf{Z}_i \cap \mathbf{Z}_j,\ e \in \{a,d,p\}, \tag{4.12}$$

where j is a conflict train, $\alpha > 1$. α should be large enough to eliminate conflicting meetings. The results of Step 2 processing the time windows in Fig. 4.3 (b) and (c) are presented in Fig. 4.3 (d) and (e) respectively. In Fig. 4.3 (d), the potential meeting area of the two opposite trains includes at least one multiple-track station. In Fig. 4.3 (e), the lower bounds and upper bounds of the following train are extended so that it is possible to keep safe headway between the two trains.

The third step is to adjust the time windows for energy-efficiency. The time windows calculated in Step 1 and 2 allow early arrivals which is not beneficial for saving energy consumption. But a train may be suggested to arrive earlier than its scheduled time at potential meeting stations, so that an opposite delayed train can enter the single-track section just released by the early arriving train as soon as possible. In other cases it is unnecessary to arrive earlier than scheduled. Instead it is better to make full use of running times and coast more for energy saving purpose. Therefore Step 3 is executed to adjust lower bounds of arrival time windows to avoid unnecessary early arrivals with

$$t^{\min}_{i,z,a} = \max\left\{t^{\min}_{i,z,a}, S_{i,z,a}\right\}, \quad t^{\max}_{i,z,a} = \max\left\{t^{\max}_{i,z,a}, S_{i,z,a}\right\}, \quad \forall\, i \in \mathbf{I},\ z \in \mathbf{Z}_i,\ z \notin \mathbf{M}_i, \tag{4.13}$$

where $\mathbf{M}_i$ is the set of potential meeting stations of train $i \in \mathbf{I}$.

4.4 Multi-train trajectory optimization

The main idea behind the multi-train trajectory optimization is to minimize the total delay and energy consumption of multiple trains, with consideration of each train's operational constraints (dynamic movement constraints, vehicle characteristic constraints, speed limits, riding comfort, TCS constraints and dwell time constraints) and the constraints to avoid conflict between trains. The MTTO is formulated as a multiple-phase optimal control problem (Rao et al., 2003), and constructed by the following steps: multiple-phase division, independent variable unification, track length normalization, and multiple-phase optimal control problem formulation. In the following, each step is introduced in detail.

4.4.1 Multiple-phase division

The multiple-phase division step partitions the single-track corridor into multiple segments, in order to characterize the varying speed limits and time (and speed) constraints at timetable points and signals. The division points are one of three types:

1. *Critical points of speed limits and gradients.* The values of speed limits and gradients change along the track. It is assumed that the speed limits and gradients are piecewise constant functions. The points of changing speed limits or gradients are adopted to partition the whole corridor, so that each interval has a unique speed limit and gradient value.

2. *Timetable points* that have time or speed limitations indicated by the timetable.

3. *Signal positions in both directions*. The signaling system consists of a series of railway signals that divide a railway line into a series of blocks, which are important elements in managing train movements. Each block can only be occupied by one train at a time.

Fig.4.4 gives an illustration, where the single-track corridor is divided into 16 segments. The segment between any two adjacent division-points is a phase of the multiple-phase optimal control problem. Within each phase, the gradient and speed limit are constant, and the boundary points might be timetable points or signals, where time and/or speed restrictions apply on the train operations.

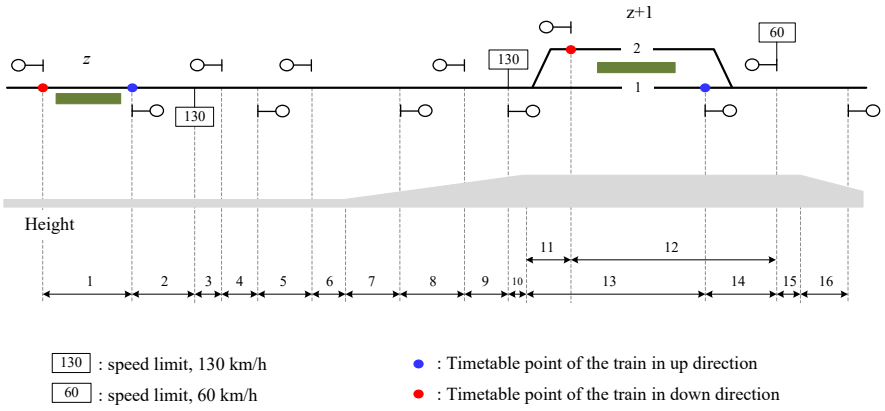

Figure 4.4: Example of partitioning in phases.

4.4.2 Independent variable unification

The STTO model presented in Section 4.2 takes train i's traversed distance as the independent variable because gradients and speed limits occur as functions of distance rather than of time (Equation (4.2)). The proposed MTTO model also uses trains' traversed distances as the independent variables in order to characterize every single train's dynamic movement constraints. However different trains' traversed distances are not the same since they are in different directions or follow different routes. However, the MTTO model needs a unified independent variable to formulate multi-train movements together. This paper let distance s be the independent variable of the MTTO model, which increases in the downstream direction. Let

$$ds_i = ds, ds_j = -ds, \quad \forall i \in \mathbf{I_d}, j \in \mathbf{I_u}.$$

$ds_j = -ds$ because train j is in the upstream direction, s_j decreases in the downstream direction.

4.4.3 Track length normalization

A train route is composed of a sequence of station sections and line sections. Here "station section" refers to a sequence of connected blocks within a single station starting and ending at so-called station boundaries, and "line section" refers to a sequence of connected blocks within a single-track or double-track line, as the examples shown in Fig. 4.5. In practice, trains are assigned different routes, and the lengths of different station sections within a station might be different. The length differences make the multi-train trajectory optimization problem more complicated.

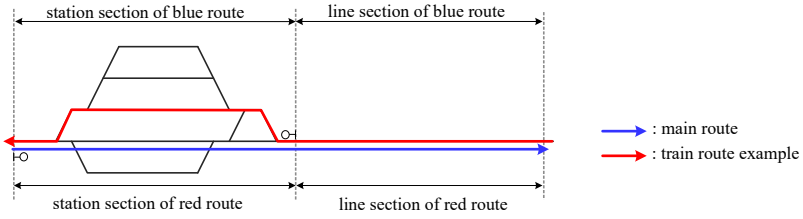

Figure 4.5: Examples of station sections, line sections and a main route.

A normalization parameter vector λ_i ($i \in \mathbf{I}$) is adopted to normalize section lengths. The normalization follows 3 steps. First, define station boundaries to divide the single-track corridor into two types, station regions and line regions. Generally, the station regions are the areas with parallel phases. For instance, station $z+1$ in Fig. 4.4 contains phases 11–12 and 13–14. The line regions in this paper are single-track sections. For a train $i \in \mathbf{I}$, denote by Stationsec_i^z the station section that train i uses at station $z \in \mathbf{Z}_i$, and by $\text{Linesec}_i^{z,z+1}$ the line section on train $i \in \mathbf{I}$'s route between station z and $z+1$ ($z, z+1 \in \mathbf{Z}_i$).

Second, define a main route in the downstream direction. The main route covers the whole corridor, and the kilometer points of the main route are continuous and increase in the downstream direction. Denote by $\text{Stationsec}_{\text{main}}^z$ the station section on the main route at station $z \in \mathbf{Z}$, and by $\text{Linesec}_{\text{main}}^{z,z+1}$ refers to the line section within the main route between station z and $z+1$ ($z, z+1 \in \mathbf{Z}$).

Last but not least, a normalization parameter vector $\lambda_i = [\lambda_{\text{Stationsec}_i^z}, \lambda_{\text{Linesec}_i^{z,z+1}}, \lambda_{\text{Stationsec}_i^{z+1}}, \lambda_{\text{Linesec}_i^{z+1,z+2}}, \ldots]^T$ ($i \in \mathbf{I}$) is used to scale train routes with respect to the reference 'main route'. The value of the normalization parameter at different station sections and line sections are different. For a station section in train $i \in \mathbf{I}$'s route at station $z \in \mathbf{Z}_i$,

$$\lambda_{\text{Stationsec}_i^z} = \frac{L_{\text{Stationsec}_i^z}}{L_{\text{Stationsec}_{\text{main}}^z}}, \ \forall\, i \in \mathbf{I}, z \in \mathbf{Z}_i, \tag{4.14}$$

where $L_{\text{Stationsec}_i^z}$ and $L_{\text{Stationsec}_{\text{main}}^z}$ are respectively the lengths of Stationsec_i^z and $\text{Stationsec}_{\text{main}}^z$.

For a line section on train $i \in \mathbf{I}$'s route between adjacent stations z and $z+1$ ($z, z+1 \in \mathbf{Z}_i$),

$$\lambda_{\text{Linesec}_i^{z,z+1}} = \frac{L_{\text{Linesec}_i^{z,z+1}}}{L_{\text{Linesec}_{\text{main}}^{z,z+1}}},\ \forall\, i \in \mathbf{I}, z, z+1 \in \mathbf{Z}_i, \tag{4.15}$$

where $L_{\text{Linesec}_i^{z,z+1}}$ and $L_{\text{Linesec}_{\text{main}}^{z,z+1}}$ are respectively the lengths of $\text{Linesec}_i^{z,z+1}$ and $\text{Linesec}_{\text{main}}^{z,z+1}$.

λ_i is used in the formulation of cost function and dynamic constraints of the MTTO model to scale the section lengths. The section lengths will be re-scaled again in the final solution for each train, so that the computed trajectories respect the actual route lengths.

4.4.4 Multiple-phase optimal control problem formulation

A multiple-phase optimal control problem is one where the trajectory consists of a collection of phases (Rao et al., 2003). In general, any particular phase has a cost function, a dynamic model, path constraints, boundary conditions, and event constraints. But it is not mandatory. The complete trajectory is obtained by properly linking adjacent phases via linkage conditions. Similarly, the total cost functional is the sum of the cost functionals within each phase. The optimal trajectory is then found by minimizing the total cost functional subject to the constraints within each phase and the linkage constraints connecting adjacent phases. In the following, we describe the details of the multiple-phase optimal control problem formulation of the MTTO model.

Notations:

r:	a phase $r \in \mathbf{R}, \mathbf{R} = \{1, \ldots, R\}$, R is the total number of phases;
$s_0^{(r)}$, $s_f^{(r)}$:	the initial and terminal location of phase r, $s_0^{(r)} < s_f^{(r)}$;
$\mathbf{A}$:	the set of adjacent phases, $\mathbf{A} = \left\{(m,n) \middle| s_f^{(m)} = s_0^{(n)}, m, n \in \mathbf{R}\right\}$;
$\mathbf{I}^{(r)}$:	the set of trains passing through phase r, $\mathbf{I}^{(r)} \subseteq \mathbf{I}$, train $i \in \mathbf{I}^{(r)}$ if phase r is within train i's route;
$x_i^{(r)}(s)$:	the state vector of train $i \in \mathbf{I}^{(r)}$ in phase r, $x_i^{(r)}(s) = [v_i^{(r)}(s),\ t_i^{(r)}(s)]^T$, containing train i's speed and time;
$u_i^{(r)}(s)$:	the control vector of train $i \in \mathbf{I}^{(r)}$ in phase r, $u_i^{(r)}(s) = [f_i^{(r)}(s),\ b_i^{(r)}(s)]^T$, containing train i's traction and braking forces;
$V_i^{\max,(r)}(s)$:	the speed limit of train i in phase r;
$R_{line,i}^{(r)}(s)$:	the line resistance caused by the constant gradient within phase r;
ξ_i:	direction indicators, $\xi_i = 0$ if $i \in \mathbf{I_d}$, otherwise $\xi_i = 1$;

$\lambda_i^{(r)}$: the normalization parameter, $\lambda_i^{(r)}$ equals the value of λ_i in phase r;
$D^{\min}_{i,s_f^{(m)}}, D^{\max}_{i,s_f^{(m)}}$: the lower and upper bound of the dwell time of train i at $s_f^{(m)}$, $s_f^{(m)}$ is a stop point, $m \in \mathbf{R}$.

The multiple-phase optimal control problem formulation of the MTTO model is:

$$\text{Minimize} \quad J = \sum_{r=1}^{R} J^{(r)}, \tag{4.16}$$

$$J^{(r)} = \sum_{i \in \mathbf{I}^{(r)}} J_i^{(r)}, \quad J_i^{(r)} = \begin{cases} \omega_i^{(r)} \cdot t_i^{(r)}(s_f^{(r)}) + \lambda_i^{(r)} \int_{s_0^{(r)}}^{s_f^{(r)}} f_i^{(r)}(s)\, ds, & \text{if } i \in \mathbf{I_d}, \\ \omega_i^{(r)} \cdot t_i^{(r)}(s_0^{(r)}) + \lambda_i^{(r)} \int_{s_0^{(r)}}^{s_f^{(r)}} f_i^{(r)}(s)\, ds, & \text{if } i \in \mathbf{I_u}, \end{cases} \tag{4.17}$$

subject to the dynamic constraints:

$$\begin{cases} \dfrac{dv_i^{(r)}(s)}{ds} = (-1)^{\xi_i} \lambda_i^{(r)} \dfrac{\theta_1 f_i^{(r)}(s) - \theta_2 b_i^{(r)}(s) - R_{train,i}(v_i^{(r)}) - R_{line,i}^{(r)}(s)}{\rho_i \cdot m_i \cdot v_i^{(r)}(s)}, \\ \dfrac{dt_i^{(r)}(s)}{ds} = (-1)^{\xi_i} \lambda_i^{(r)} \dfrac{1}{v_i^{(r)}(s)}, \end{cases} \quad \forall r \in \mathbf{R}, i \in \mathbf{I}^{(r)}, \tag{4.18}$$

the path constraints:

$$\begin{cases} 0 \le f_i^{(r)}(s) \le F_i^{\max}, \\ 0 \le b_i^{(r)}(s) \le B_i^{\max}, \\ 0 \le f_i^{(r)}(s) \cdot v_i^{(r)}(s) \le P_i^{\max}, \\ 0 \le v_i^{(r)}(s) \le V_i^{\max,(r)}(s), \\ \mathbf{A}_i^{\min} \le \dfrac{dv_i^{(r)}(s)}{dt_i^{(r)}(s)} \le \mathbf{A}_i^{\max}, \end{cases} \quad \forall\, r \in \mathbf{R}, i \in \mathbf{I}^{(r)}, \tag{4.19}$$

the phase boundary conditions (if any):

$$\begin{cases} v_{i,z,e}^{\min} \le v_i^{(r)}(k_{i,z,e}) \le v_{i,z,e}^{\max}, \\ t_{i,z,e}^{\min} \le t_i^{(r)}(k_{i,z,e}) \le t_{i,z,e}^{\max}, \end{cases} \quad \forall\, r \in \mathbf{R}, i \in \mathbf{I}^{(r)}, k_{i,z,e} \in \mathbf{K_{TCS}}_i \cap \{s_0^{(r)}, s_f^{(r)}\}, \tag{4.20}$$

the event constraints (if any):

$$\begin{cases} \left(t_i^{(r)}(q) - t_j^{(r)}(q)\right)^2 \ge h_s^2, \\ \qquad \forall\, r \in \mathbf{R}, (i,j) \in \mathbf{I_s} : i,j \in \mathbf{I}^{(r)}, q \in \mathbf{Signal}_{i,j} \cap \{s_0^{(r)}, s_f^{(r)}\}, \\ \left(t_i^{(r)}(q) - t_j^{(r)}(q)\right)^2 \ge h_o^2, \\ \qquad \forall\, r \in \mathbf{R}, (i,j) \in \mathbf{I_o} : i,j \in \mathbf{I}^{(r)}, q \in \mathbf{StationSignal}_{i,j} \cap \{s_0^{(r)}, s_f^{(r)}\}, \\ \left(t_i^{(r)}(s_0^{(r)}) - t_j^{(r)}(s_0^{(r)})\right)\left(t_i^{(r)}(s_f^{(r)}) - t_j^{(r)}(s_f^{(r)})\right) \ge \sigma, \\ \qquad \forall\, r \in \mathbf{R}, (i,j) \in \mathbf{I_o} : i,j \in \mathbf{I}^{(r)}, [s_0^{(r)}, s_f^{(r)}] \in \mathbf{SingleTrack}_{i,j}, \end{cases} \tag{4.21}$$

and the linkage conditions of all adjacent phases:

$$\begin{cases} v_i^{(m)}(s_f^{(m)}) - v_i^{(n)}(s_0^{(n)}) = 0, \\ D^{\min}_{i,s_f^{(m)}} \leq t_i^{(n)}(s_0^{(n)}) - t_i^{(m)}(s_f^{(m)}) \leq D^{\max}_{i,s_f^{(m)}}, \end{cases} \quad \forall (m,n) \in \mathbf{A}, i \in \mathbf{I}^{(m)} \cap \mathbf{I}^{(n)}. \tag{4.22}$$

The MTTO model aims at minimizing the sum of the cost functions over all phases. Each phase $r \in \mathbf{R}$ has its own cost function and constraints for the train(s) belonging to $\mathbf{I}^{(r)}$, if $\mathbf{I}^{(r)}$ is not empty. More specifically, the cost functions (4.17) represent the optimization targets of minimizing the total delay and energy consumption of train(s) going through phase r. Every single train's cost function $J_i^{(r)}$ is developed based on Equation (4.6). For train $i \in \mathbf{I_u}$, which goes from $s_f^{(r)}$ to $s_0^{(r)}$, $t_i^{(r)}(s_f^{(r)})$ refers to the departure time of train i from $s_f^{(r)}$, and $t_i^{(r)}(s_0^{(r)})$ refers to the arrival time at $s_0^{(r)}$, so $J_i^{(r)}$ uses $t_i^{(r)}(s_0^{(r)})$ in the first term.

The dynamic constraints (4.18) are stated with s as the independent variable, representing the dynamic differential equations. $(-1)^{\xi_i}$ is adopted to eliminate the influence of travelling directions. $\lambda_i^{(r)}$ is adopted for the normalization of section lengths. The path constraints (4.19) represent the operational constraints of vehicle characteristics, speed limits and riding comfort. The boundary conditions (4.20) represent the time and speed restrictions at timetable points if phase r's initial or terminal point is a timetable point. The event constraints (4.21) are developed based on (4.7) to avoid conflicts and separate trains. Constraints (4.21) are required if $\mathbf{I}^{(r)}$ includes more than one train.

In addition, the linkage conditions (4.22) are to make sure that the train's speed-distance and time-distance trajectories are continuous. If the linkage point of two successive phases is a stop point of a train i, $t_i^{(m)}(s_f^{(m)})$ and $t_i^{(n)}(s_0^{(n)})$ represent the arrival or departure times of train i at $s_f^{(m)}$, and $D^{\min}_{i,s_f^{(m)}}, D^{\max}_{i,s_f^{(m)}}$ are the minimum or maximum dwell times of train i at $s_f^{(m)}$. Otherwise, $D^{\min}_{i,s_f^{(m)}} = D^{\max}_{i,s_f^{(m)}} = 0$.

The multiple-phase optimal control problem can be solved with a pseudospectral method. In general, pseudospectral methods transcribe the continuous-time optimal control problem into a discrete nonlinear programming problem, after which nonlinear programming solvers are adopted to directly solve the problem.

4.4.5 Driving strategies and weight factors

A weight factor $\omega_i^{(r)}$ is used in cost functions (4.17) to balance delay recovery and energy saving. The weight factor $\omega_i^{(r)}$ should be determined firstly before adopting the pseudospectral methods to solve the MTTO model. Different weight factors contribute to different optimization results. The effect of weight factor values is discussed in (Wang and Goverde, 2016c). In this paper, $\omega_i^{(r)} = 10^4$ is used for delay recovery,

which gives more priority to delay recovery than to energy saving (note the difference in scale of time and energy), while weight factor $\omega_i^{(r)} = 10^2$ is adopted for energy saving, which gives more priority to energy saving than to delay recovery.

The priorities of delay recovery and energy saving of different trains at different running sections are different. In case of delays, three driving strategies can be considered:

1. *Delay-recovery strategy*: This strategy is used to make up delays and drive the train as fast as possible. Weight factor $\omega_i^{(r)} = 10^4$ if train i uses the delay-recovery strategy in the running section where phase r belongs to.

2. *Energy-saving strategy*: This strategy is adopted for energy-efficient driving that makes full use of given running times. Weight factor $\omega_i^{(r)} = 10^2$ if train i uses the energy-saving strategy strategy in the running section where phase r belongs to.

3. *On-time strategy*: This strategy makes the train return to the schedule. Weight factor $\omega_i^{(r)} = 10^2$ if train i uses the on-time strategy in the running section where phase r belongs to. In addition, the TCS arrival time window at the next stop is reset as a time point constraint, such as [scheduled arrival time, scheduled arrival time]. The energy-saving strategy uses a time window constraint for arrival at the next stop while the on-time strategy uses a time point constraint which commands the train to arrive at the scheduled time. In general, the energy-saving strategy is used if the train has increased travel time due to waiting for a meeting another delayed train, while an on-time strategy is adopted if the train is able to reach the next stop on time.

A driving strategy selection algorithm is designed to select proper driving strategies for each train and each running section. By selecting the driving strategies, weight factors of the MTTO model are set.

The first step is to estimate potential meeting stations. As mentioned in Section 4.3, the stations within the overlap parts of TCS time regions of opposite trains are potential meeting stations. Different meet plans produce different delay propagations. The first step of the driving strategy selection algorithm is to find a meeting plan, that produces minimal total estimated delays. Train delays are estimated by assuming the trains follow the FCFS (first-come, first-served) principle, the delayed trains run at maximum power, and other trains follow their schedules if their operations are not affected by delays. For detailed delay estimation methods, we recommend the works by Goverde (2007, 2010). The best meeting station for train i is represented by m_i. Two parameters η_{i,m_i} and $\beta_{i,z}$ are adopted for later driving strategy setting. η_{i,m_i} represents the estimated meeting time at m_i. $\beta_{i,z}$ refers to the secondary delay caused by the meeting event at m_i. For stations before m_i, $\beta_{i,z} = 0$ because train i is not affected by the meeting event yet. For stations after m_i, $\beta_{i,z} = \max\{t^{\min}_{i,m_i,a}, t^{\min}_{j,m_i,a}\} - t^{\min}_{i,m_i,a}$, which equals the secondary delay at station m_i.

Algorithm Driving Strategy Selection

Estimate meeting stations

For all trains $i \in \mathbf{I}$ and stations $z \in \mathbf{Z}_i$

for all $k \in \mathbf{M}_i$

assume k is a station where i meets an opposite train j;

estimate the total delays with k as the meeting station;

end

find the meeting station $m_i \in \mathbf{M}_i$, that produces minimal total estimated delays;

let $\eta_{i,m_i} = \max\{t^{\min}_{i,m_i,a}, t^{\min}_{j,m_i,a}\}$;

if z is a station before m_i,

$\beta_{i,z} = 0$;

else

$\beta_{i,z} = \eta_{i,m_i} - t^{\min}_{i,m_i,a}$;

end

End For

Set driving strategies

For all train $i \in \mathbf{I}$ and station $z \in \mathbf{Z}_i$

if $t^{\min}_{i,z,a} + \beta_{i,z} > S_{i,z,a}$,

train i uses the delay-recovery strategy in the running section before station z;

else

train i uses the on-time strategy in the running section before station z;

end if

if $z = m_i$,

if $t^{\min}_{i,z,a} < \eta_{i,m_i}$,

train i uses the energy-saving strategy in the running section before station z;

else if $t^{\min}_{i,z,a} = \eta_{i,m_i}$ and $t^{\min}_{i,z,a} < S_{i,z,a}$,

train i uses the delay-recovery strategy in the running section before station z;

end

end

end if

End For

The second step is to set the driving strategies. It contains two loops. The first loop is to preset driving strategies for every train and every running section. It is done by comparing the lower bounds of the TCS time windows plus the estimated secondary delays with the scheduled times. $t^{\min}_{i,z,a} + \beta_{i,z} > S_{i,z,a}$ means that the train cannot return back to schedule at station z even with the minimal running time. Therefore, a delay-recovery strategy is adopted to reduce delays. If $t^{\min}_{i,z,a} + \beta_{i,z} \leq S_{i,z,a}$, the train has sufficient running time to reach the next stop, thus an on-time strategy is used in the running section before station z. The second loop is designed to adjust the driving strategies for the running sections just before the estimated meeting station m_i. If $t^{\min}_{i,z,a} < \eta_{i,m_i}$, train i arrives first and shall wait for another train. Hence, train i has extra time margin for energy-efficient driving. So an energy-saving strategy is selected before the meeting station. If $t^{\min}_{i,z,a} = \max\{t^{\min}_{i,m_i,a}, t^{\min}_{j,m_i,a}\}$ and $t^{\min}_{i,z,a} < S_{i,z,a}$, train i may get an early arrival at m_i to let the opposite delayed train leave the station earlier. Therefore a delay recovery strategy is selected.

Two examples of the driving strategy selection algorithm are presented in Fig. 4.6. The yellow lines represent the sum of lower bounds of TCS time windows and estimated secondary delay caused by meeting events. By comparing yellow lines and scheduled paths, different driving strategies are selected for different running sections.

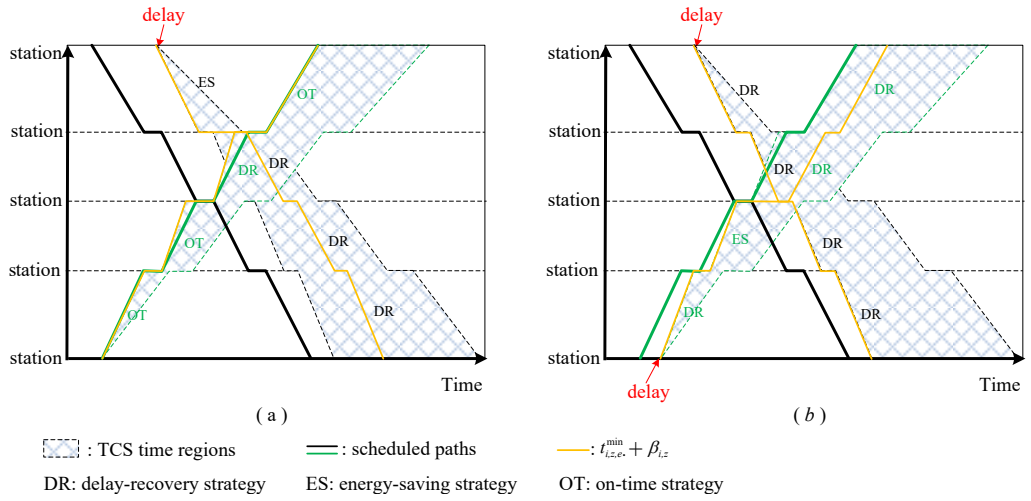

Figure 4.6: Demonstration for the driving strategy selection algorithm.

4.5 Case studies

A single-track corridor between Schagen (Sgn) and Den Helder (Hdr) in the north of the Netherlands is adopted for the case study, see Fig. 4.7. The infrastructure data is provided by the infrastructure manager ProRail. There are 4 stations along this corridor: Schagen (Sgn), Anna Paulowna (Ana), Den Helder Zuid (Hdrz), and Den Helder (Hdr). The infrastructure characteristics consist of a description of all

track sections, points, speed signs, gradients and signals over the entire track layout. Two trains operate on this corridor each half hour, one in each direction. The static parameters of the train used in this case study are listed in Table 4.1. The traction force and train resistance curves are shown in Fig. 4.8. Since the braking rate is the only accessible data characterizing the braking behavior, we let the braking force be equal to the braking rate times train mass.

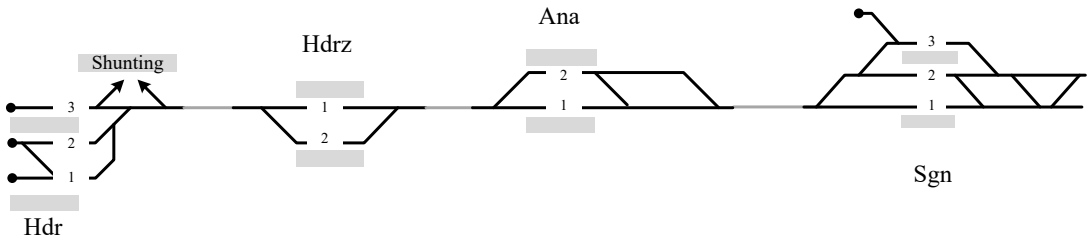

Figure 4.7: The partial single-track corridor used in the case study.

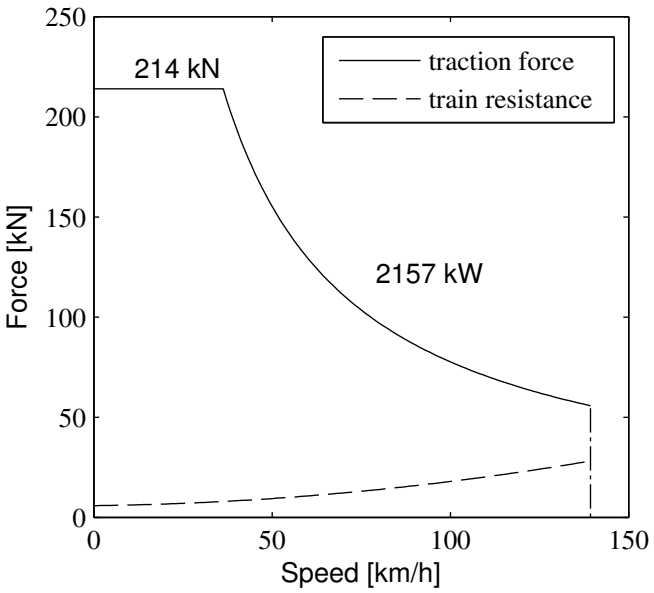

Figure 4.8: Traction force and line resistance of Intercity train.

Table 4.1: Basic parameters of Intercity train.

Property	Value
Train mass [t]	391
Rotating mass factor [-]	1.06
Maximum traction power [kW]	2157
Maximum traction force [kN]	214
Maximum braking deceleration [m/s^2]	-0.66

Table 4.2 shows the arrival and departure times of a pair of trains from opposite directions within the basic half-hour pattern. T_1 represents the train from Hdr to Sgn

Table 4.2: Basic arrival and departure times of two opposing trains (repeating each 30 min).

	Train T_1 from Hdr to Sgn			Train T_2 from Sgn to Hdr		
	Arrival time (mm:ss)	Departure time (mm:ss)	Track	Arrival time (mm:ss)	Departure time (mm:ss)	Track
Hdr	–	04:00	2	26:00	–	3
Hdrz	06:30	07:00	2	21:30	22:00	1
Ana	14:00	15:00	1	14:00	15:00	2
Sgn	20:30	–	1	–	07:00	2

and T_2 represents the opposite train. The second and third columns show the arrival and departure times. This timetable is based on the timetable in use in 2016. The two trains are scheduled to meet at Ana station, and the dwell time there is 1 minute. The scheduled dwell times at other stations are 0.5 minute. The last column of Table 4.2 shows the planned tracks at the stations. T_1 and T_2 use different tracks at station Hdr, Hdrz, Ana and Sgn, so that the four stations can be adopted as meeting stations.

4.5.1 Two-train trajectory optimization

The corridor between Sgn and Hdr uses a periodic timetable. Two opposite trains operate on this corridor each half hour. We first tested our proposed method with two trains within a basic half-hour pattern in 4 cases within total 9 different initial delays as shown in Table 4.3. The scheduled Case assumes the two trains operate according to the given timetable. Case A and B discuss the situation that one train follows the schedule whereas another train has initial delays, Case C considers the situation that both trains have initial delays. Initial delays were added to train T_1 and T_2 at their departure station Hdr and Sgn, respectively. The TCSs for both trains were calculated first. Each TCS consists of time and speed limits at every station. The speed limits at the stop points are 0. The time windows were calculated with the method from Section 4.3. It is assumed a minimal dwell time of 0.5 minute and maximal dwell time of 5 minutes. The multi-train trajectory optimization method in Section 4.4 was used to find the optimal energy-efficient delay recovery trajectories within the TCSs. The parameters in (4.21) were set as $h_s = 120$ s, $\sigma = 5$ s and $h_o = 15$ s. The value of h_s is set according to the network statement 2017 by ProRail (2017). Default headway norms are used that should be sufficient for the final timetable to be conflict-free and contain some buffer. The value of h_o ensures enough time interval for signal clearing and route setting. σ is a positive value to avoid any crossover of opposite trains' path. A pseudospectral method is applied for solving the multiple-phase optimal control problem. There exist several commercial and free packages that implement the pseudospectral method. We adopted GPOPS (Rao et al., 2010) with the Radau Pseudospectral Method as the solver. The experiments were carried out with GPOPS 4.1 on a laptop equipped with a 3.2 GHz Pentium R processor. As for the parameter settings of GPOPS, we used 'complex' as the string to indicate the differentiation method, a tolerance of 1e-3, an iteration of 2, and didn't use autoscaling. The explanation of the parameters can be found in (Rao et al., 2011).

Table 4.3: Initial delays of two opposite trains T_1 and T_2.

	Scheduled	Case A			Case B			Case C		
	Case	a	b	c	a	b	c	a	b	c
Delay of T_1 at Hdr [min]	0	0	0	0	5	10	15	3	6	12
Delay of T_2 at Sgn [min]	0	5	10	15	0	0	0	12	9	3

Fig. 4.9 shows the speed profiles and time-distance paths of the two on-time trains. Fig. 4.10-4.12 present the results of the 9 different initial delays. Each figure has three subplots considering three combinations of initial delays. Within each subplot, the top-left plot is the optimized speed profile of train T_1 from left to right, the lower-left plot is the optimized speed profile of train T_2 from right to left. The solid black lines represent the optimized speed profiles and the red horizontal lines refer to the static speed limits. The driving strategies for each running sections are identified with 'DR', 'ES' and 'OT' in the figures. 'DR', 'ES' and 'OT' are respectively the abbreviations of delay-recovery strategy, energy-saving strategy and on-time strategy. The right plot shows the optimized time-distance paths, where the solid black lines refer to the optimized results, the dashed red lines are the planned linearized time-distance paths, and the gray regions are the time regions of train T_1 and T_2 formed by their TCSs. The gray vertical lines represent the first home signals outside stations at both sides, so that the segments between two close gray vertical lines are stations with multiple tracks. Train time-distance paths are only allowed to intersect within the station areas. Table 4.4 shows the optimized results of the Scheduled Case, Case A, B and C. The 2nd column presents the output delays of train T_1 at station Sgn. The 3rd column shows the energy consumption to drive T_1 from Hdr to Sgn. The 4th and 5th columns show the delays of train T_2 at station Hdr and the energy consumption to drive T_2 from Sgn to Hdr. The 6th column is the sum of delays of T_1 at Sgn and T_2 at Hdr. The 7th column gives the energy consumption of T_1 and T_2 in the single-track corridor between Hdr and Sgn. The last column gives the computation times. Within the 2nd, 4th and 6th columns, upward arrows and downward arrows mean that the output delays are increased (↑) or decreased (↓) compared with the initial delays (the delays of train T_1 at Hdr, and of train T_2 at Sgn).

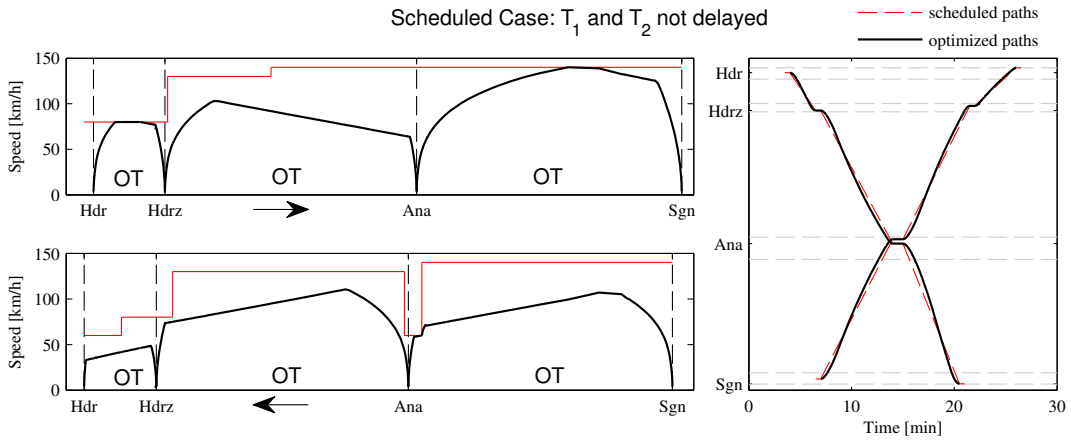

Figure 4.9: Scheduled Case: speed curves and time-distance paths of T_1 and T_2 (T_1 from left to right, T_2 from right to left).

Taking an overall look of Fig. 4.9-4.12, the train speeds stay below the speed limits and trains stop at every planned stop point, which means the optimized results ensure safe travelling speeds and accurate stops. The time-distance paths show that the two

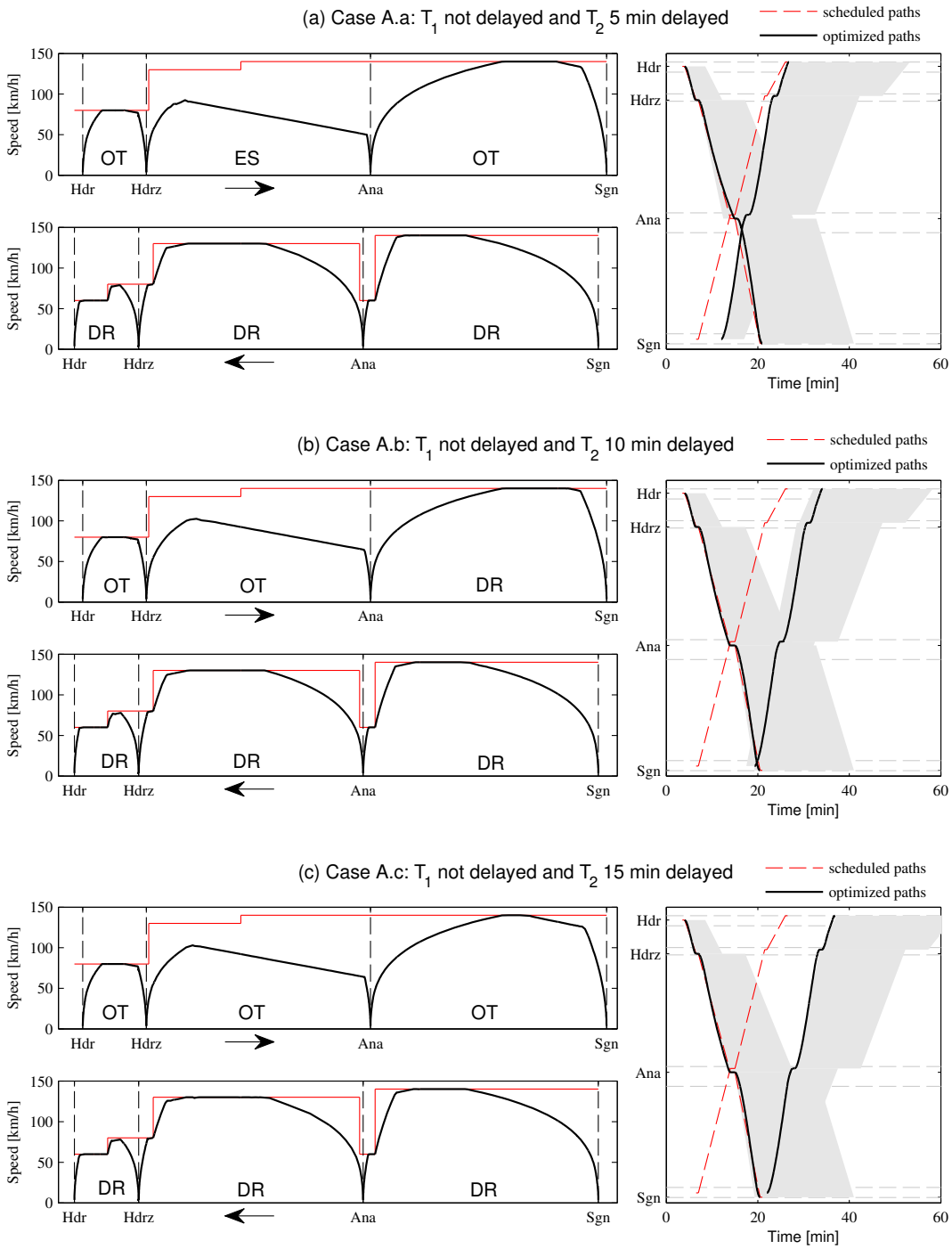

Figure 4.10: Case A: speed profiles and time-distance paths of T_1 and T_2 (DR: delay-recovery strategy; ES: energy-saving strategy; and OT: on-time strategy.).

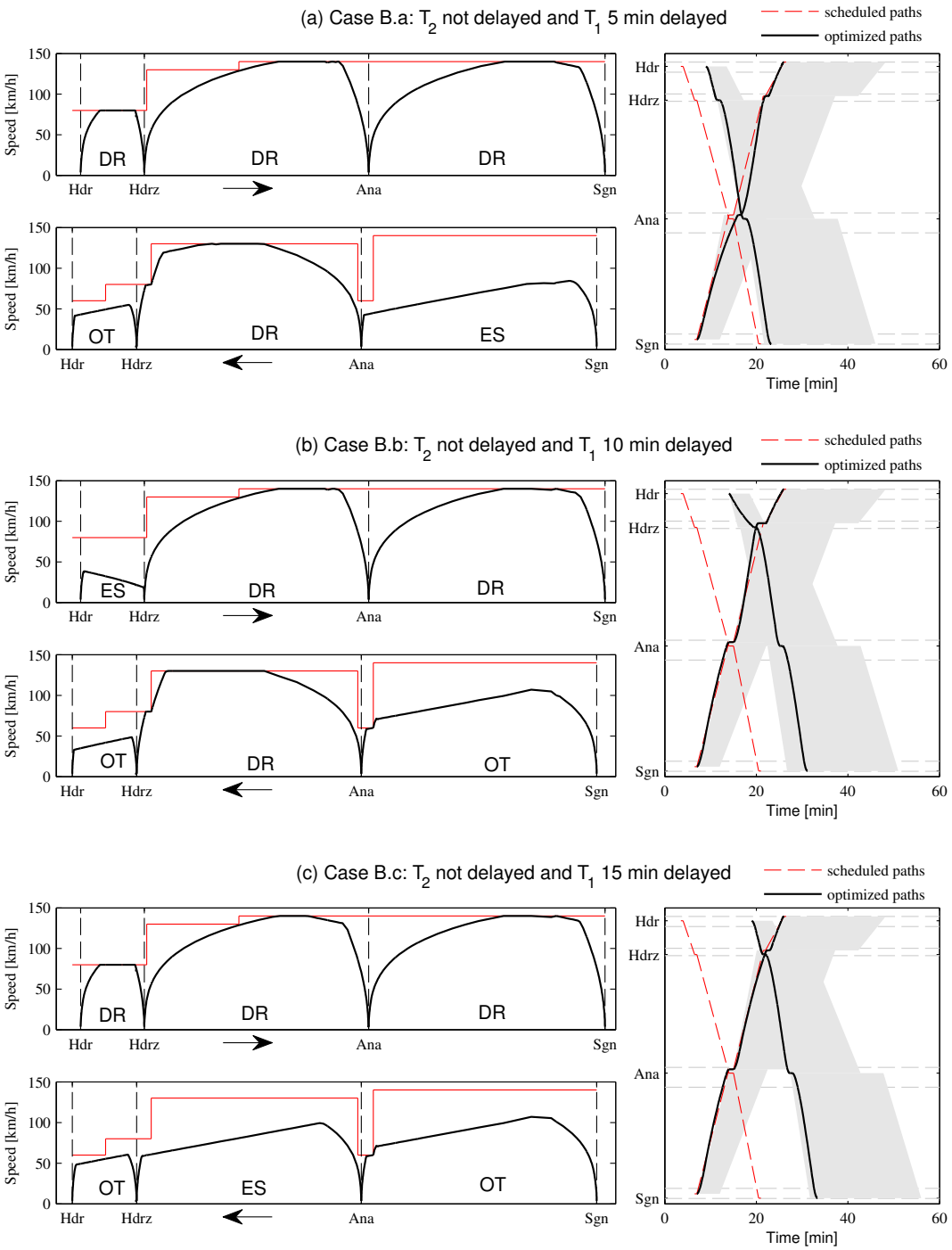

Figure 4.11: Case B: speed profiles and time-distance paths of T_1 and T_2 (DR: delay-recovery strategy; ES: energy-saving strategy; and OT: on-time strategy.).

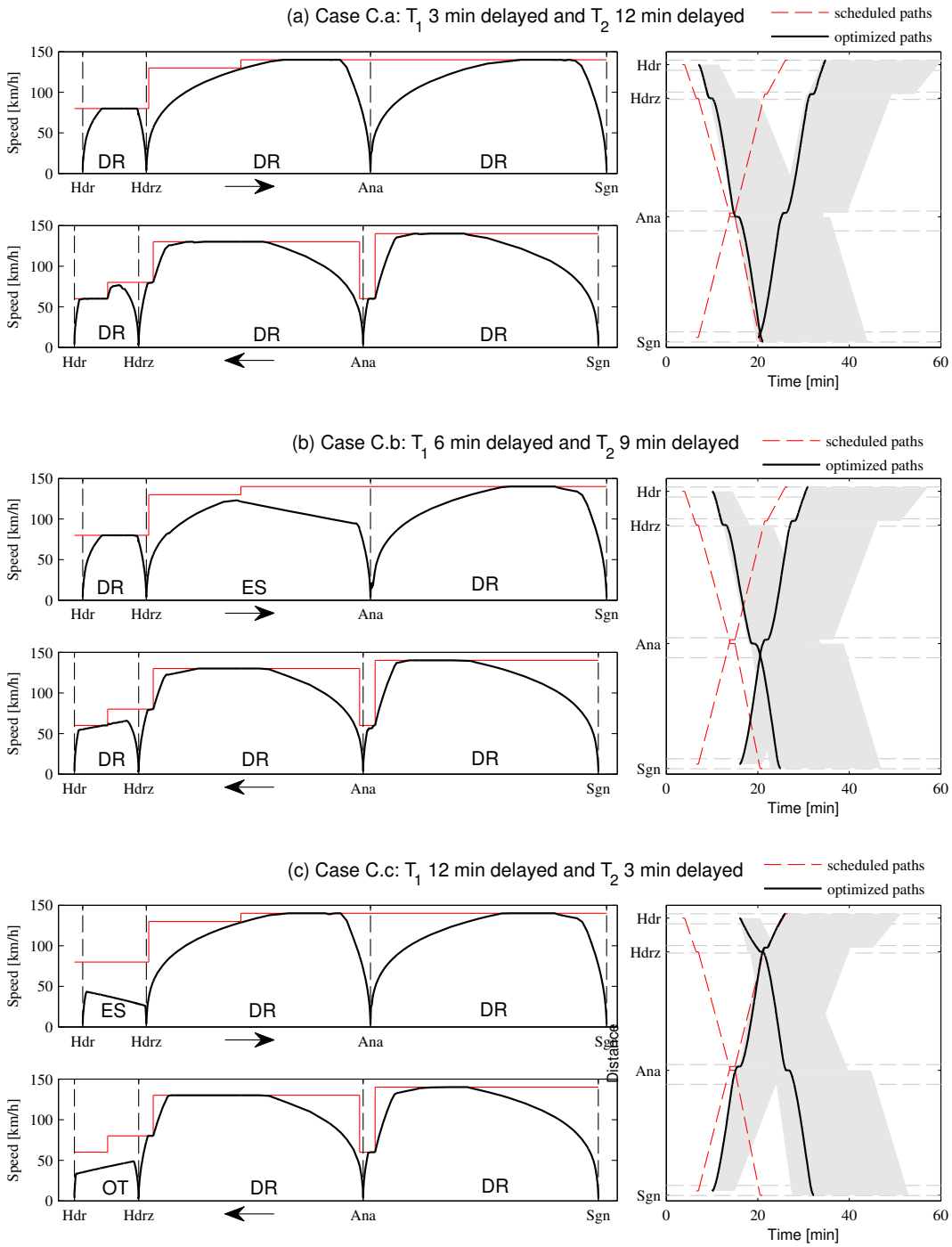

Figure 4.12: Case C: speed profiles and time-distance paths of T_1 and T_2 (DR: delay-recovery strategy; ES: energy-saving strategy; and OT: on-time strategy.).

trains cannot follow the scheduled paths under delay conditions. But the optimized time-distance paths stay within the TCSs, and they only cross each other in station areas, so no conflicts occur between them. In Fig. 4.9, T_1 and T_2 have no delays. The on-time driving strategy is used during every running section. The optimal control regimes between every two stops include using maximum traction during the outbound processes, maximum braking force for the inbound processes, and in between possible cruising and coasting before braking to save energy, which matches the theoretical driving strategy following from application of the PMP.

Fig. 4.10 shows the results in the case that only T_2 has delays (Case A). T_2 uses the delay recovery strategy over all the corridor between Hdr and Sgn. The optimized control regimes consist of maximum traction during the outbound processes, maximum braking force for the inbound processes, and cruising at maximum allowed speed. No coasting is used so that the delayed train can move as fast as possible and get back to schedule gradually. Train T_1 has no delay at Hdr station, however gets influenced by the delays of train T_2. In Fig. 4.10 (a) that T_2 is 5 min delayed at Sgn station, T_1 and T_2 meet at station Ana. The optimized meeting time is late than the scheduled meeting time. Train T_1 uses the energy-saving strategy and coasts more during the running between Hdrz and Ana. T_1 speeds up after Ana to make up the delay caused by the delayed meeting event. Fig. 4.10 (b) and (c) show the cases that the optimized meeting station is changed to Sgn when T_2 has bigger delays. The new meeting station is beneficial for minimizing delays, because train T_2 would waste time waiting for T_1 and cause a future delay of T_2 if T_1 and T_2 meet at the scheduled meeting station. In Fig. 4.10 (b), T_1 adopts the delay recovery strategy and arrives at station Sgn a few seconds before the scheduled arrival time, so that T_2 is able to leave Sgn as soon as possible after 10 min delay. Fig. 4.10 (c) shows the case that T_2 is 15 min delayed and T_1 can follow its schedule and arrive at Sgn before the delayed T_2.

Fig. 4.11 (a), (b) and (c) present the optimized results in case that T_1 has different initial delays at Hdr, while T_2 departs on-time from Sgn. When T_1 is 5 min delayed (Fig. 4.11 (a)), the trains meet at station Ana, T_1 uses the delay recovery strategy with less coasting and more cruising at maximum speeds to reduce delays. T_2 is delayed to meet train T_1 at station Ana, but the delay is recovered in the following journey. In Fig. 4.11 (b) and (c), the two trains meet at station Hdrz. Train T_2 follows the scheduled paths during the section between Sgn and Ana. Then it speeds up to arrive earlier (Fig. 4.11 (b)) or slows down to arrive later (Fig. 4.11 (c)) than the scheduled time at station Hdrz, so that T_1 can use the released section between Hdrz and Ana. In Fig. 4.11 (b), train T_1 is even secondarily delayed because of waiting for entering the open track between Hdrz and Ana. However, T_2 is able to return back to the scheduled times at station Hdr in all three cases (a), (b) and (c).

Fig. 4.12 shows the optimized results that both trains are delayed from their departure stations (Case C). Both train's trajectories in the three scenarios are different. But the delayed trains tend to use control regimes of maximum traction, cruising at maximum speeds and maximum braking to reduce delays. Only within the sections before the

meeting stations, the train might coast more to anticipate for the meeting events. For instance, T_1 uses the delay-recovery strategy in the running sections between Hdr and Ana in Fig. 4.12 (b), and between Hdr and Hdrz in Fig. 4.12 (c). Overall, we see that our algorithm can calculate speed and time-distance trajectories for two opposite trains. The trajectories avoid conflicts between the two trains by adjusting running times, dwell times and meeting stations. The speed profiles illustrate the three different driving strategies of the delay-recovery, energy-saving and on-time strategy, for different delay scenarios.

Table 4.4 presented the numerical results of the 10 scenarios. In general, we see an increase on the total energy consumption comparing the delay and no-delay situations. However there are exceptions when the delays of a single train may increase due to waiting for the meeting events. For instance, the delay of train T_1 increases in Case B (b) because of meeting T_2 at Hdrz. The total delay is reduced comparing the output delay and initial delay. The reason is the use of the delay-recovery strategy, which makes the train run as fast as possible and costs a lot of energy consumption. But the energy-saving and on-time strategies reduce the energy consumption. Take Case B (c) as an example, T_2 uses the energy saving strategy on the running section between Ana and Hdrz and the on-time strategy on the other two running sections. Train T_2 uses less energy consumption comparing with the scheduled case. The average computation time of the 10 scenarios is 73.92 s, while the minimal computation time is 40.1 s and the maximum number is 95.44 s. The computations are carried out on a laptop equipped with a 3.2 GHz Pentium R processor.

4.5.2 Discussion

Compared to the single-train trajectory optimization method, the multi-train trajectory optimization method is able to avoid conflicts between trains. Take Case C (b) as an example, where T_1 and T_2 both have initial delays at Hdr and Sgn. Fig. 4.13 presents a comparison of the results computed by the STTO method and the MTTO method. The optimized results by applying the STTO method aim at reducing delays. The two trains travel at the maximum speeds in order to get back to schedule as quickly as possible. However, the two trains meet at the single-track corridor between Ana and Sgn, which is forbidden. The MTTO method is able to avoid conflicts and lets the trains meet at a station region. Second, the proposed method allows a change of meeting locations. The driving strategy selection algorithm first estimates potential meeting locations, and accordingly selects best driving strategies for different running sections. The optimal meeting location and time are found by the MTTO method together with the optimal speed curves. The optimal meeting location and time enable a reduction of delay propagation. Last but not last, the proposed algorithm balances the energy saving and delay recovery requirements. Once a train is delayed, the first priority is to reduce delays instead of reducing energy consumption. The energy consumption is

Table 4.4: Optimization results of two opposite trains T_1 and T_2.

	Train T_1		Train T_2		Total output delay [s]	Total energy consumption $\times 10^8$ [J]	CPU time [s]
	Output delay [s]	Energy consumption $\times 10^8$ [J]	Output delay [s]	Energy consumption $\times 10^8$ [J]			
Scheduled Case	0	6.8961	0	5.2385	0	12.135	40.10
Case A	0	7.0096	49.08 $\downarrow$	10.334	49.08 $\downarrow$	17.344	62.37
	-3.01 $\downarrow$	7.6046	488.60 $\downarrow$	10.019	485.59 $\downarrow$	17.624	69.39
	0	7.0188	649.49 $\downarrow$	10.244	649.49 $\downarrow$	17.262	82.20
Case B	161.88 $\downarrow$	9.9800	0	6.0571	161.88 $\downarrow$	16.032	94.82
	639.63 $\uparrow$	9.1691	0	7.4422	639.63 $\uparrow$	16.611	75.11
	770.53 $\downarrow$	9.9930	0	4.9765	770.53 $\downarrow$	14.970	95.44
Case C	41.32 $\downarrow$	10.393	532.62 $\downarrow$	10.226	573.95 $\downarrow$	20.619	63.42
	268.70 $\downarrow$	7.9454	288.93 $\downarrow$	10.432	557.63 $\downarrow$	18.378	91.20
	705.66 $\downarrow$	9.1626	0 $\downarrow$	9.7704	705.66 $\downarrow$	18.933	74.13

only reduced in the cases that the train is on-time or the train has to wait for another train.

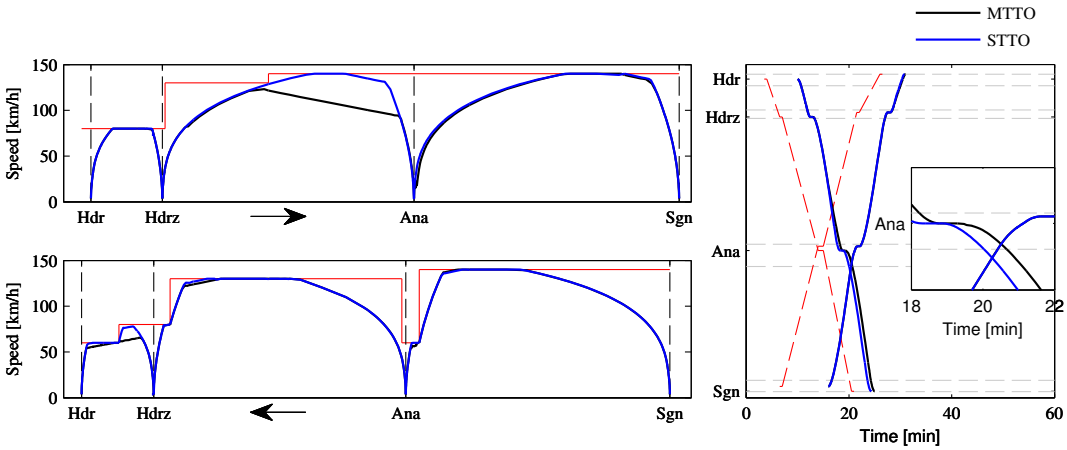

Figure 4.13: Case C (b): speed profiles and time-distance paths of T_1 and T_2 computed by the MTTO method (black lines) and STTO method (blue lines).

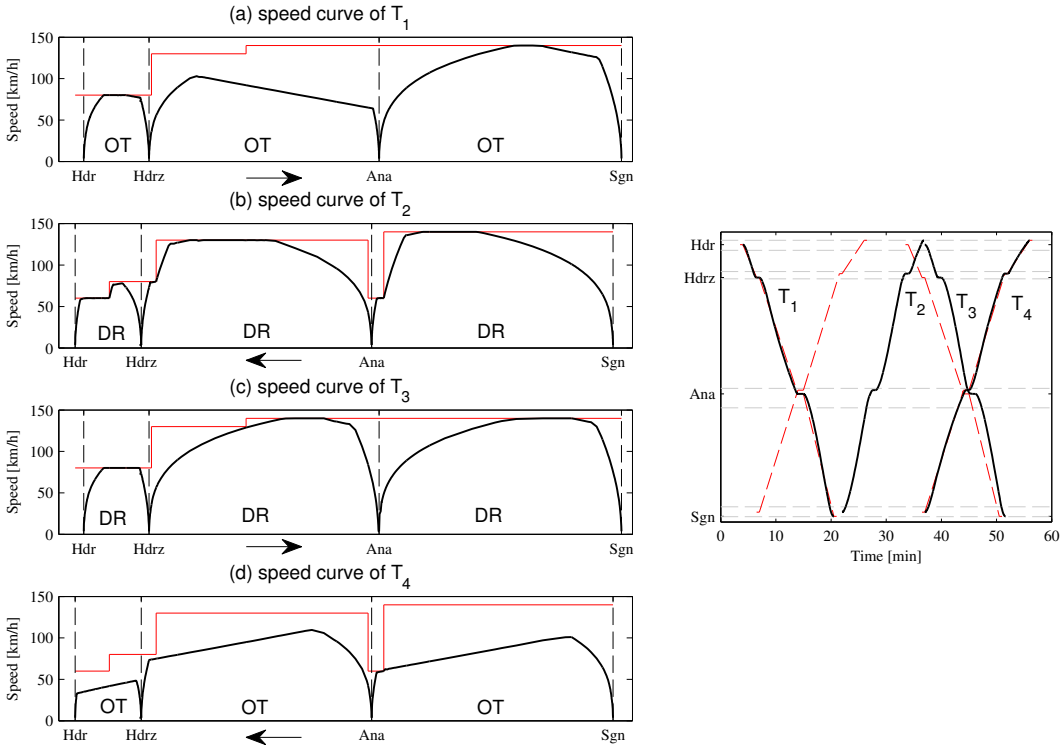

Figure 4.14: Case A (c): speed profiles and time-distance paths of T_1, T_2, T_3 and T_4 (DR: delay-recovery strategy; ES: energy-saving strategy; and OT: on-time strategy.).

Section 4.5.1 discussed the train trajectory optimization for two delayed opposite trains on a single-track line. However, the delays may propagate to other trains in the next half-hour pattern. For instance, in Case A (c) T_2's delay will be propagated to the

next half-hour pattern. In that case, it is necessary to take into account all affected trains. Fig. 4.14 shows the results of four trains within a hour pattern using the multi-train optimization model. Train T_2 is 15 min delayed at station Sgn (Case A(c)). T_3 is affected by T_2 and gets delayed at Hdr but it speeds up during the remaining journey and the delay is reduced gradually. Fig. 4.14 shows that the time-distance paths of the four trains only meet within station areas, which shows that the multi-train optimization method produces feasible trajectories. The computation time for the four-train case is 131.76 s.

4.6 Conclusions

This paper proposed a novel method of multi-train trajectory optimization. Traditional train speed profile optimization focuses on one single-train from one stop to another stop, but the method proposed by us is able to compute trajectories for multiple trains simultaneously. We developed a multi-train trajectory optimization method with a multi-phase optimal control problem formulation for trains on single-track lines. The model consists of the dynamic behavior and operational constraints for multiple trains, as well as constraints to avoid conflicts between trains. A pseudospectral method was adopted for solving the problem. By jointly optimizing trains' energy consumption and delay recovery, the method computes a feasible schedule with optimal meeting locations and associated speed profiles simultaneously. Case studies of two opposite trains running on a Dutch single-track corridor showed that our method is able to produce speed and time-distance trajectories for the opposite trains. The trajectories avoid conflicts between two trains by adjusted running times, dwell times and meeting stations. The speed profiles consider energy-efficient driving as well as delay recovery requirements using the three different driving strategies of delay-recovery, energy-saving and on-time running for different delay scenarios. Finally, a case study of multi-train trajectory optimization was presented that computes speed profiles and schedules for four trains at the same time.

The proposed method can be used in practice to combine conflict detection and resolution with energy-efficient driving. It provides feasible schedules as well as energy-efficient speed profiles, which gives a new approach to rescheduling and timetable design.

Bibliography

Albrecht, A., Howlett, P., Pudney, P., Vu, X., Zhou, P., 2016a. The key principles of optimal train control-part 1: Formulation of the model, strategies of optimal type, evolutionary lines, location of optimal switching points. Transportation Research Part B: Methodological 94, 482–508.

Albrecht, A., Howlett, P., Pudney, P., Vu, X., Zhou, P., 2016b. The key principles of optimal train control-part 2: Existence of an optimal strategy, the local energy minimization principle, uniqueness, computational techniques. Transportation Research Part B: Methodological 94, 509–538.

Albrecht, A., Koelewijn, J., Pudney, P., 2011. Energy-efficient recovery of delays in a rail network. In: Proc. 2011 Australasian Transport Research Forum.

Albrecht, A. R., Howlett, P. G., Pudney, P. J., Vu, X., Zhou, P., 2015. Energy-efficient train control: the two-train separation problem on level track. Journal of Rail Transport Planning & Management 5 (3), 163–182.

Albrecht, T., 2009. The influence of anticipating train driving on the dispatching process in railway conflict situations. Networks and Spatial Economics 9 (1), 85–101.

Cacchiani, V., Huisman, D., Kidd, M., Kroon, L., Toth, P., Veelenturf, L., Wagenaar, J., 2014. An overview of recovery models and algorithms for real-time railway rescheduling. Transportation Research Part B: Methodological 63, 15–37.

Caimi, G., Fuchsberger, M., Laumanns, M., Schüpbach, K., 2011. A multi-level framework for generating train schedules in highly utilised networks. Public transport 3 (1), 3–24.

Corman, F., D'Ariano, A., Pacciarelli, D., Pranzo, M., 2009. Evaluation of green wave policy in real-time railway traffic management. Transportation Research Part C: Emerging Technologies 17 (6), 607–616.

D'Ariano, A., Pranzo, M., Hansen, I. A., 2007. Conflict resolution and train speed coordination for solving real-time timetable perturbations. IEEE Transactions on Intelligent Transportation Systems 8 (2), 208–222.

Goverde, R. M., 2007. Railway timetable stability analysis using max-plus system theory. Transportation Research Part B: Methodological 41 (2), 179–201.

Goverde, R. M., 2010. A delay propagation algorithm for large-scale railway traffic networks. Transportation Research Part C: Emerging Technologies 18 (3), 269–287.

Higgins, A., Kozan, E., Ferreira, L., 1996. Optimal scheduling of trains on a single line track. Transportation research part B: Methodological 30 (2), 147–161.

Jovanović, D., Harker, P. T., 1991. Tactical scheduling of rail operations: the scan i system. Transportation Science 25 (1), 46–64.

Luthi, M., 2009. Improving the efficiency of heavily used railway networks through integrated real-time rescheduling. Ph.D. thesis, ETH Zurich.

Mazzarello, M., Ottaviani, E., 2007. A traffic management system for real-time traffic optimisation in railways. Transportation Research Part B: Methodological 41 (2), 246–274.

Meng, L., Zhou, X., 2011. Robust single-track train dispatching model under a dynamic and stochastic environment: a scenario-based rolling horizon solution approach. Transportation Research Part B: Methodological 45 (7), 1080–1102.

ProRail, 2017. Network statement 2017. Https: //www.prorail.nl /sites /default /files.

Rao, A., Benson, D., Darby, C., Mahon, B., Francolin, C., Patterson, M., Sanders, I., Huntington, G., 2011. User' s manual for gpops version 4. x: A matlab software for solving multiple-phase optimal control problems using hp–adaptive pseudospectral methods. University of Florida, Gainesville, 1–32.

Rao, A. V., Benson, D. A., Darby, C., Patterson, M. A., Francolin, C., Sanders, I., Huntington, G. T., 2010. Algorithm 902: GPOPS, a matlab software for solving multiple-phase optimal control problems using the gauss pseudospectral method. ACM Transactions on Mathematical Software 37 (2), 22.

Rao, A. V., et al., 2003. Extension of a pseudospectral legendre method to non-sequential multiple-phase optimal control problems. In: presented as paper AIAA. Vol. 5634. pp. 11–14.

Scheepmaker, G. M., Goverde, R. M., Kroon, L. G., 2017. Review of energy-efficient train control and timetabling. European Journal of Operational Research 257 (2), 355–376.

Szpigel, B., 1973. Optimal train scheduling on a single track railway. Operational Research 34 (4), 343–352.

Umiliacchi, S., Nicholson, G., Zhao, N., Schmid, F., Roberts, C., 2016. Delay management and energy consumption minimisation on a single-track railway. IET Intelligent Transport Systems 10 (1), 50–57.

Wang, P., Goverde, R. M. P., 2016a. Multiple-phase train trajectory optimization with signalling and operational constraints. Transportation Research Part C: Emerging Technologies 69, 255–275.

Wang, P., Goverde, R. M. P., 2016b. Train trajectory optimization of opposite trains on single-track railway lines. In: 2016 IEEE International Conference on Intelligent Rail Transportation (ICIRT). Birmingham, UK, pp. 23–31.

Wang, P., Goverde, R. M. P., 2016c. Two-train trajectory optimization with a green wave policy. Transportation Research Record, 2546.

Wang, P., Goverde, R. M. P., Ma, L., 2015. A multiple-phase train trajectory optimization method under real-time rail traffic management. In: 2015 IEEE 18th International Conference on Intelligent Transportation Systems. IEEE, Las Palmas, Spain, pp. 771–776.

Wang, Y., De Schutter, B., van den Boom, T. J., Ning, B., 2013. Optimal trajectory planning for trains–a pseudospectral method and a mixed integer linear programming approach. Transportation Research Part C: Emerging Technologies 29, 97–114.

Wang, Y., Ning, B., Cao, F., De Schutter, B., van den Boom, T. J., 2011. A survey on optimal trajectory planning for train operations. In: 2011 IEEE International Conference on Service Operations, Logistics, and Informatics (SOLI). pp. 589–594, beijing, China.

Yang, L., Li, K., Gao, Z., Li, X., 2012. Optimizing trains movement on a railway network. Omega 40 (5), 619–633.

Ye, H., Liu, R., 2016. A multiphase optimal control method for multi-train control and scheduling on railway lines. Transportation Research Part B: Methodological 93, 377–393.

Yin, J., Tang, T., Yang, L., Gao, Z., Ran, B., 2016. Energy-efficient metro train rescheduling with uncertain time-variant passenger demands: An approximate dynamic programming approach. Transportation Research Part B: Methodological 91, 178–210.

Yin, J., Yang, L., Tang, T., Gao, Z., Ran, B., 2017. Dynamic passenger demand oriented metro train scheduling with energy-efficiency and waiting time minimization: Mixed-integer linear programming approaches. Transportation Research Part B: Methodological 97, 182–213.

Yun, B., Tinkin, H., Baohua, M., 2011. Train control to reduce delays upon service disturbances at railway junctions. Journal of Transportation Systems Engineering and Information Technology 11 (5), 114–122.

Zhao, N., Roberts, C., Hillmansen, S., Nicholson, G., 2015. A multiple train trajectory optimization to minimize energy consumption and delay. IEEE Transactions on Intelligent Transportation Systems 16 (5), 2363–2372.

Chapter 5

Multi-train trajectory optimization for energy-efficient timetabling

5.1 Introduction

Improving energy efficiency is an important issue for railways to reduce their contributions to climate change further as well as to save and enlarge competition advantages involved, even though rail is already more energy efficient than most other transport modes. One promising means of improving energy efficiency is to optimize train operations by using energy-efficient driving strategies, which does not need extra investment for more infrastructure. Even with a small amount of energy saved in each train run, the total energy costs saved by the whole railway network are huge. This leads to research on energy-efficient train trajectory optimization (ETTO) by using optimal control theory to find the optimal trajectory (speed-distance profile) and driving strategies of a train that minimize energy consumption caused by the train movements (Howlett and Pudney, 1995).

The impact of train operation on energy savings depends on the running times given in the timetable. A running time between two stations contains two parts, the technically minimum running time and the running time supplement. The running time supplement is the extra running time on top of the technically minimum running time between two stations which is included in the timetable primarily to manage disturbances in operations and to recover from small delays (Scheepmaker and Goverde, 2015). However, if a train is punctual then these supplements can be used for energy-efficient driving. Therefore, the train trajectory and timetable are closely related and both of them have a direct influence on the energy-efficiency of train operations. To obtain global optimality of the whole system, the relationship between the train trajectory and timetable cannot be neglected.

The research on energy-efficient train trajectory optimization and energy-efficient time-tabling has been studied for decades. There are comprehensive surveys on

relevant areas, which include Wang et al. (2011), Albrecht et al. (2016), Scheepmaker et al. (2017), and Yang et al. (2016). Wang et al. (2011) reviewed the numerical approaches for solving the train trajectory optimization problem. Albrecht et al. (2016) focused on the state-of-the-art of using the Pontryagin's Maximum Principle (PMP) to find the key principles of optimal train control. Scheepmaker et al. (2017) and Yang et al. (2016) provided surveys on the energy-efficient train control and energy-efficient train timetable problems, where Scheepmaker et al. (2017) focused on general railway systems, and Yang et al. (2016) focused on urban rail. The literature review presented below focuses on ETTO for multiple trains and energy-efficient timetable adjustment.

5.1.1 Review of multi-train trajectory optimization

Most of the existing studies on ETTO focus on optimizing single train movements. Multi-train trajectory optimization (MTTO) has just drawn attention in recent years. The purpose of MTTO is to optimize multiple train movements together with a shared objective, and to find optimal control strategies for every involved train. Yang et al. (2012) provided a mathematical model for multiple trains on a railway network. The model aims at minimizing total energy consumption and running times of all trains, while satisfying the constraints to ensure the feasibility of multi-train operations, which include headway constraints, vehicle speed limit constraints, passenger riding comfort constraints, and dwell time constraints. The control strategies of every involved train are the decision variables of the multi-train model. A genetic algorithm (GA) integrated with simulation was designed to find the optimal control strategies. Li and Lo (2014a,b) proposed a multi-train model for metro lines. The model uses the switching time and speeds of control regimes (acceleration, cruising, coasting, and braking) as the decision variables, aims at minimizing the net energy consumption of multiple trains, and takes into account constraints of the number of trains, cyclist times, switching times, turnaround times, vehicle speed limits and dwell times. In Li and Lo (2014a), a GA method was designed to find optimal switching time and speeds and jointly optimize the timetables and speed profiles. In Li and Lo (2014b), the model is transformed to a convex optimization problem by using a linear approximation method, and solved using the Kuhn-Tucker conditions for dynamic train scheduling. Su et al. (2014) formulated an integrated energy-efficient optimization model to realize the optimal control of multi-trains. The model is for a railway corridor with one type of cyclic train operation. The model aims at minimizing the energy consumption caused by traction, and takes into account the cycle time, train dynamic movements, traction and braking forces, and speed limits constraints. The headway between adjacent cyclic operations is first determined according to the passenger demands. Then an iteration algorithm is used to find the optimal cycle time and the optimal number of trains, which minimize the timetable's energy consumption. The optimal control strategy for each train is computed by an independent optimal train-control algorithm. Zhou et al. (2017) incorporated train speed control into the timetable design process. A space-time-speed grid network for joint train routing, timetabling and trajectory optimization

is constructed as a path finding problem, which is solved by a dynamic programming algorithm.

As shown in the literature, researchers have proven that the MTTO has benefits in solving timetabling or rescheduling problems because the MTTO approaches optimize multi-train movements simultaneously, which achieves a global optimization of energy and capacity usage while taking into account the operational interactions between adjacent trains. However, although the majority of previous MTTO models take train control strategies as the decision variables (Yang et al., 2012; Li and Lo, 2014a,b; Su et al., 2014), they are computed separately by independent single-train trajectory optimization methods. Besides, train movement processes are simplified, such as assuming the same train routes, constant traction and braking forces, and the same type of rolling stock. Further improvements can be achieved by optimizing train control strategies simultaneously and considering more practical train movement processes.

5.1.2 Review of energy-efficient timetable adjustment

The quality of a railway timetable can be measured by several key performance indicators (KPIs): journey time efficiency, timetable feasibility, robustness, and energy efficiency (Goverde et al., 2016). Among those KPIs, energy efficiency is a secondary objective, particularly in dense railway networks, and can, therefore, be considered as a fine-tuning step after the time allowances have been set based on feasibility and robustness. The scientific literature on railway timetabling mainly considers macroscopic optimization models. The periodic event-scheduling problem model introduced by Serafini and Ukovich (1989) has been widely applied in cyclic timetabling (Peeters, 2003; Hansen and Pachl, 2014). Graph-based models (Yang et al., 2009; Cacchiani et al., 2008) and mixed integer linear programming (MILP) models (Cacchiani and Toth, 2012; Brännlund et al., 1998) were developed for generating non-cyclic timetables. Those macroscopic optimization models focus on finding optimal train orders, but are not concerned about how to the get accurate input parameters, such as running times, to set up the macroscopic model, while energy-efficient timetabling requires a microscopic level of details (Caimi et al., 2011).

Albrecht and Oettich (2002) proposed an approach of dynamic schedule synchronization and energy saving in rapid rail transit systems. They used a simulation model to compute the energy utilization for each discretized running time between two consecutive stops of a train. Then they calculated the optimal timetable with dynamic programming, in which train running times are dynamically modified, so that the probability of passenger connections is increased and the overall energy consumption of train operation remains low. Scheepmaker and Goverde (2015) developed an EZR model (energy-efficient operation or in Dutch 'EnergieZuinig Rijden') to find the energy-efficient trajectory of an individual train trip. The EZR model was adopted to analyze energy efficiency of the practical train movements and the real-world timetable. Their results show that using a more uniform allocation of the running

time supplements leads to extra energy savings and an improvement on punctuality compared to the method of tightening the timetable. Su et al. (2013) developed an optimization model that determines both an energy-efficient driving strategy and an optimal distribution of the running time supplements in the timetable. The authors first explicitly calculated the energy efficient train control strategy per trip. Then the model distributes the running time supplements among consecutive trips in order to minimize the total energy consumption. Goverde et al. (2016) proposed a three-level timetable design method, which constructs a stable robust conflict-free timetable with optimal train orders first and then adjusts time supplements for energy-efficiency. The time supplements are re-allocated on the principle of being beneficial for energy-saving train operation, taking into account the stochastic dwell times.

The approaches in (Scheepmaker and Goverde, 2015; Goverde et al., 2016; Albrecht and Oettich, 2002; Su et al., 2013) follow a similar process, by iteratively adjusting running time allocations and computing energy-efficient trajectories for every individual running time allocation. They emphasize that a good allocation of running time supplements is beneficial for timetable energy efficiency.

This paper contributes to a novel approach of energy-efficient timetabling that is developed from a train trajectory optimization view. The method we propose is to improve the energy efficiency of an existing timetable, which (1) focuses on a timetable for a railway corridor, (2) calculates energy-efficient speed profiles for every train in the timetable, taking into account the practical situation that trains use different routes and platforms at stations, constraints of train dynamic movements, vehicle characteristics, varying speed limits and gradients, and interactions between trains; and (3) is capable of adjusting running time allocation and producing a new energy-efficient timetable. The proposed approach integrates the train trajectory optimization and energy-efficient timetabling, which does not need pre-calculations of the relationships between running times and energy consumptions like the methods in (Scheepmaker and Goverde, 2015; Goverde et al., 2016; Su et al., 2013). Compared to the integrated methods on the timetable design level (Yang et al., 2012; Li and Lo, 2014a,b; Kraay et al., 1991), the proposed approach provides a more microscopic description of train movements and more accurate results of energy-efficient speed profiles.

The method is based on an existing timetable. It improves the timetable's energy efficiency by adjusting arrival and departure times. In detail, first the given timetable is converted into flexible arrival and departure time window constraints, which are described as a timetable constraint set (TCS). Then an ETTO method is developed to find the optimal energy-efficient time-distance paths within those TCSs. The ETTO method include two parts: one is a single-train trajectory optimization (STTO), which focuses on optimizing an individual train movement within the relaxed arrival and departure time windows, and the other is a multi-train trajectory optimization, which computes multi-train trajectories simultaneously with a shared objective of minimizing multi-train energy consumption and an additional target of eliminating

conflicts between trains. The STTO and MTTO are re-formulated as a multiple-phase optimal control problem (Rao, 2003), which has the advantage of accurately incorporating varying gradients, curves and speed limits and different train routes. It is then solved by a pseudospectral method (Rao et al., 2010). The multiple-phase optimal control problem formulation and the pseudospectral method have been used in (Wang and Goverde, 2016a) for single train trajectory optimization, in (Wang and Goverde, 2016c) for two following trains in the same direction, and in (Wang and Goverde, 2016b) to two opposite trains on single-track lines. This paper extends the methods to optimize trajectories for multiple trains on a railway corridor composed of single and/or double tracks, and implements the trajectory optimization method in energy-efficient timetable adjustment. The proposed approach is demonstrated by application to two case studies of opposite-trains running on a Dutch partially single-track railway corridor and following-trains running on a Dutch double-track railway corridor. The results show that our method is able to produce optimal energy-efficient speed profiles and improve the energy efficiency of a timetable.

The remainder of the paper is organized as follows: Section 5.2 provides a description of the energy-efficient timetabling problem and an introduction to the energy-efficient timetabling strategy. Section 5.3 presents the train trajectory optimization method. Section 5.4 presents the modelling and solution methods for the train trajectory optimization problem. Section 5.5 illustrates the approach in case studies. Finally Section 5.6 ends the paper with conclusions.

5.2 Energy-efficient timetabling problem

5.2.1 Problem description

Energy-efficient timetabling aims at finding a timetable for one or more trains on a railway corridor or network that allows as much as possible energy-efficient driving (Scheepmaker et al., 2017). The total running time of each train over the corridor may be pre-specified or may still have to be determined. In both cases, the aim is to determine the running time between each pair of consecutive stops for each train such that the total energy consumption of the involved trains is minimal.

The energy-efficient timetabling method proposed in this paper is a fine-tuning step by adjusting the arrival and departure times of an existing timetable to improve its energy efficiency. The focus is a timetable for a railway corridor, see the example shown in Fig. 5.1. The timetable lists the times when a service is scheduled to arrive at and depart from specified locations. The railway corridor may consist of single-track and/or double-track lines. Trains involved in this timetable are in the same and/or different directions. The stations in the downstream direction are named with successive numbers $1,2,\ldots,Z$. Denote by $\mathbf{Z} = \{1,2,...,Z\}$ the set of stations where Z is the number of stations between K_0 and K_f. Denote by $\mathbf{I_{all}}$ the set of trains operating

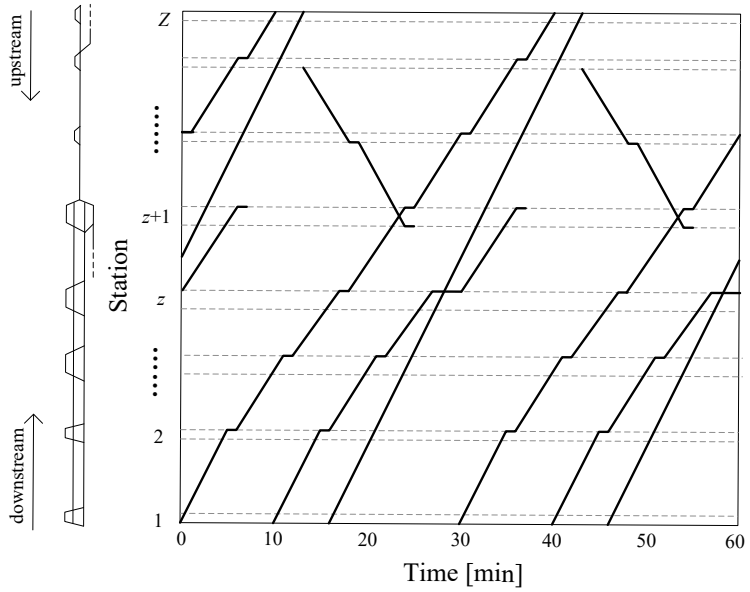

Figure 5.1: A timetable example for a railway corridor.

on this corridor, $\mathbf{I_d}$ the set of trains in the downstream direction from station 1 to Z and $\mathbf{I_u}$ the set of trains in the upstream direction from station Z to 1, and $\mathbf{Z}_i$ the stations on train $i \in \mathbf{I_{all}}$'s journey. Define the train sets $\mathbf{I_o} = \{(i,j)|\ i \text{ and } j \text{ are from opposite directions}, i,j \in \mathbf{I_{all}}\}$ and $\mathbf{I_s} = \{(i,j)|\ i \text{ and } j \text{ are in the same direction}, i,j \in \mathbf{I_{all}}\}$.

5.2.2 Energy-efficient timetabling strategy

The proposed energy-efficient timetabling strategy includes two steps:

Step 1: Relax the timetable by converting the time targets to time window constraints;

Step 2: Find optimal arrival/departure/passing-through (A/D/P) times and optimal energy-efficient speed profiles within those time windows.

The first step is to relax the given timetable. A timetable indicates strict time targets of arrival, departure and pass-through events for all involved trains. To adjust the allocation of running time supplements, the time targets of all the trains in intermediate stations are converted into time window constraints. Every train's first and last station maintain their original arrival and departure times so that the timetables of adjacent regions are not influenced. The lower bounds of the time windows represent the earliest possible A/D/P times assuming the train leaves the first station on the scheduled time. The upper bounds represent the latest possible A/D/P times in order to arrive at the last station on time. The lower bounds are computed with technical minimum running (dwell) times in the train's travel direction, while the upper bounds are computed with technical minimum running (dwell) times backwards. An example of time windows of a single train is shown in Fig. 5.2.

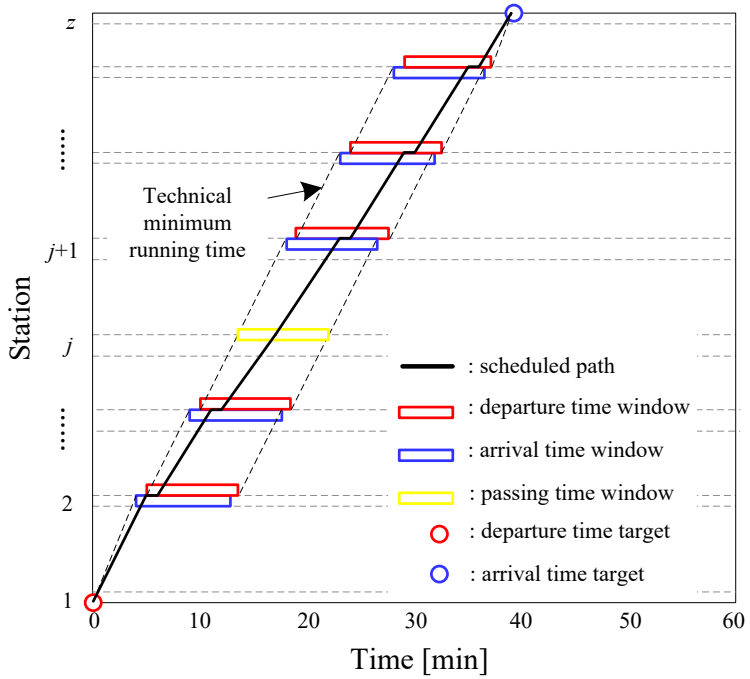

Figure 5.2: An example of time targets and time windows of a single train.

The time windows and corresponding speed windows are formulated with a timetable constraint set (TCS), which is a sequence of time and speed constraints at timetable points (stations). We classify a train's event at a station into three types: arrival, departure and pass-through. Denote by e an event, $e \in \{a,d,p\}$ where a refers to arrival, d refers to departure, and p refers to pass-through. For train $i \in \mathbf{I_{all}}$, the TCS is written as

$$\mathbf{TCS}_i = \left\{ \left(k_{i,z,e}, [t^{\min}_{i,z,e}, t^{\max}_{i,z,e}], [v^{\min}_{i,z,e}, v^{\max}_{i,z,e}] \right) \right\}_{z \in \mathbf{Z}_i}, \tag{5.1}$$

where $k_{i,z,e}$ is the location for train i at station z of event e, and $t^{\min}_{i,z,e}$, $t^{\max}_{i,z,e}$, $v^{\min}_{i,z,e}$ and $v^{\max}_{i,z,e}$ are respectively the lower and upper bounds of time and speed for e at $k_{i,z,e}$. Define $\mathbf{K_{TCS}}_i$ as the set of timetable points of train i. If $k_{i,z,e}$ is a stop station, the speed window $[v^{\min}_{i,z,e}, v^{\max}_{i,z,e}] = [0,0]$, and $k_{i,z,a} = k_{i,z,d}$. If $k_{i,z,e}$ is a pass-through station, $v^{\min}_{i,z,e}$ and $v^{\max}_{i,z,e}$ are respectively the lower and upper passing-through speeds.

Albrecht et al. (2013) proposed a train path envelope (TPE) to describe the time and speed constraints at timetable points, signals, and conflict points. The TPE is allocated to one train only and the TPEs do not overlap each other, so that as long as a train stays in its TPE there will be no conflicts. In this paper we allow overlapping TCSs while the conflicts are resolved with the multi-train trajectory optimization algorithm (Section 5.3).

Step 2 is to find optimal energy-efficient A/D/P times and speed profiles within those time windows. The reason of keeping A/D/P times within the time windows produced by step 1 is to avoid changing train sequences. Consequently, the journey times and

capacity usage are not influenced. A train trajectory optimization method (Section 5.3) is developed to find optimal energy-efficient A/D/P times and speed profiles.

5.3 Train trajectory optimization method

A single-train trajectory optimization (STTO) is developed firstly to find every single train's optimal energy-efficient A/D/P times and speed profiles within the train's TCS. In order to re-allocate the running times, the STTO no longer focuses on the train movements between two adjacent stops like the classical ETTO problem does (Khmelnitsky, 2000; Howlett, 2000; Liu and Golovitcher, 2003), but it concerns the whole corridor between the first and last station, which may contain a few intermediate stops and passing-through stations. Note that the TCSs, as well as the trajectories computed by the STTO, can not promise conflict-free train paths. Therefore it is necessary to do conflict detection. The conflict detection is by checking the overlaps in blocking diagrams (Goverde et al., 2016). If there are any overlaps in blocking diagrams, a multi-train trajectory optimization (MTTO) is applied to jointly compute the conflicting trains' trajectories. The MTTO eliminates conflicts between trains.

In summary, the train trajectory optimization method follows the three steps to find optimal A/D/P times and speed profiles:

Step 1: Compute the speed profiles and time-distance paths for every single train separately with the STTO;

Step 2: Conflict detection. If there is no conflict between the time-distance paths computed in Step 1, then take the time-distance paths from Step 1 as the output, otherwise go to Step 3;

Step 3: Compute the speed profiles and time-distance paths for the conflicting trains simultaneously with the MTTO, and output the computed time-distance paths.

The train trajectory optimization model is extended based on the the optimal control model presented in (Wang and Goverde, 2016a). Denote by $\mathbf{I}$ the set of trains which require speed profiles. If $\mathbf{I}$ only contains one train, the following model is the STTO model. If $\mathbf{I}$ contains more than one train, it becomes a MTTO model.

The cost function is to minimize the total energy costs of the trains in $\mathbf{I}$, that is

$$\min \qquad J = \sum_{i \in \mathbf{I}} J_i, \quad J_i = \int_{K_i^0}^{K_i^f} f_i(s_i)\, ds_i, \tag{5.2}$$

subject to the operational constraints of every single train $i \in \mathbf{I}$

$$\begin{cases} \dfrac{dv_i(s_i)}{ds_i} = \dfrac{\theta_1 f_i(s_i) - \theta_2 b_i(s_i) - R_{train,i}(v_i) - R_{line,i}(s_i)}{\rho_i \cdot m_i \cdot v_i(s_i)}, \\ \dfrac{dt_i(s_i)}{ds_i} = \dfrac{1}{v_i(s_i)}, \end{cases} \tag{5.3}$$

$$\begin{cases} 0 \le f_i(s_i) \le F_i^{\max}, \\ 0 \le b_i(s_i) \le B_i^{\max}, \\ 0 \le f_i(s_i) \cdot v_i(s_i) \le P_i^{\max}, \\ 0 \le v_i(s_i) \le V_i^{\max}(s_i), \\ A_i^{\min} \le \dfrac{dv_i(s_i)}{dt_i(s_i)} \le A_i^{\max}, \end{cases} \tag{5.4}$$

$$\begin{cases} v_{i,z,e}^{\min} \le v_i(k_{i,z,e}) \le v_{i,z,e}^{\max}, \\ t_{i,z,e}^{\min} \le t_i(k_{i,z,e}) \le t_{i,z,e}^{\max}, \quad \forall\, z \in \mathbf{Z}_i,\ k_{i,z,e} \in \mathbf{K}_{\mathbf{TCS}_i}, \end{cases} \tag{5.5}$$

$$D_{i,z}^{\min} \le t_i(k_{i,z,d}) - t_i(k_{i,z,a}) \le D_{i,z}^{\max}, \quad \forall\, z \in \mathbf{Z}_i,\ k_{i,z,a}, k_{i,z,d} \in \mathbf{K}_{\mathbf{TCS}_i}. \tag{5.6}$$

$$\frac{t_i(k_{i,z,d})}{6} - \left\lfloor \frac{t_i(k_{i,z,d})}{6} \right\rfloor = 0, \quad \forall\, z \in \mathbf{Z}_i. \tag{5.7}$$

The STTO model (**I** only includes one train) is to minimize the cost function (5.2), subject to constraints (5.3)-(5.7). The cost function (5.2) reflects the objective of minimizing energy consumption, where K_i^0 and K_i^f are respectively the start and end positions of train i's journey, s_i is the traversed distance [m], and $f_i(s_i)$ is the traction force [kN].

Equations (5.3) are the differential equations of train movements. Distance is adopted as the independent variable because gradients and speed limits occur as functions of distance rather than of time. In equations (5.3), $v_i(s_i)$ is the velocity of train i [m/s], ρ_i is the rotating mass factor, m_i is the mass of train i [t], $b_i(s_i)$ is the braking force of train i [kN], $R_{train,i}(v_i) = \alpha_i + \beta_i \cdot v_i + \gamma_i \cdot v_i^2$ is the train resistance force [kN] with coefficients α_i, β_i and γ_i, $R_{line,i}(s_i)$ is the line resistance force [kN], which is a function of position and consists of grade resistance and curve resistance, $t_i(s_i)$ is the traversed time of train i [s], and $\theta_1, \theta_2 \in \{0,1\}$ are two binary parameters with $\theta_1 \cdot \theta_2 = 0$.

Equations (5.4) are the path constraints of train i's vehicle performance parameters, speed limit and riding-comfort. $F_i^{\max}$, $B_i^{\max}$ and $P_i^{\max}$ are the upper bound of traction force, maximum braking force and maximum traction power of train i. The maximum traction force equals $\min\{F_i^{\max}, P_i^{\max}/v_i(s_i)\}$. $V_i^{\max}(s_i)$ is the speed limit at position s_i, including static and temporary speed restrictions. $A_i^{\min}$ and $A_i^{\max}$ are the lower and upper bound of acceptable acceleration.

Equations (5.5) are the event constraints which represent that the A/D/P times and speeds should respect the time and speed constraints of every timetable point in $\mathbf{K}_{\mathbf{TCS}_i}$. Equation (5.6) represents the dwell time constraints. The dwell times are restricted by the minimal and maximal dwell times, where the minimal dwell times should provide sufficient time for boarding and alighting. In (5.6), $D_{i,z}^{\min}$ and $D_{i,z}^{\max}$ are the minimal and maximal dwell times of train i at station z. Equation (5.7) defines the departure times as integral multiples of 6 seconds (in some countries 30 seconds or 60 seconds) for more precise information to drivers and dispatchers. In Equation (5.7), the unit of $t_i(k_{i,z,d})$ is in seconds. $\lfloor \cdot \rfloor$ refers to rounding down to the nearest whole unit.

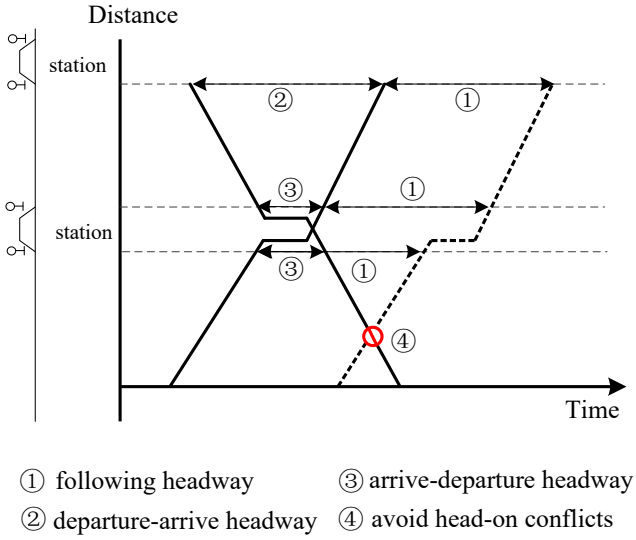

Figure 5.3: Necessary headways between trains.

If **I** contains more than one train, Equations (5.2)-(5.7) become parts of a MTTO model, which aims minimizing the cost function (5.2). The cost function (5.2) reflect the target of minimizing the energy costs for all the involved trains. The MTTO model optimizes the multi-train trajectory together, so that it is necessary to avoid conflicts between trains, as well as satisfy the operational constraints for every individual train (5.3)-(5.7). Three more types of constraints should be noticed:

1. a time interval between every two adjacent trains in the same direction is required for safe train separation (Fig. 5.3 ①),
2. for opposite trains, there are two important types of headway requirements: (i) "depart-arrive" headway, the headway between the departure of a train and the arrival of an opposing train from the same line (Fig. 5.3 ②); and (ii) "arrive-depart" headway, the headway between the arrival of a train and the departure of an opposing train towards the same line (Fig. 5.3 ③), and
3. opposite trains cannot travel on a single-track section between two adjacent stations at the same time, otherwise a head-on conflict occurs (Fig 5.3. ④).

The three conflict-avoiding constraints can be formulated as

$$\begin{cases} \big(t_i(q)-t_j(q)\big)^2 \geq h_s^2, & \forall (i,j) \in \mathbf{I_s}, q \in \mathbf{Signal}_{i,j}, \\ \big(t_i(q)-t_j(q)\big)^2 \geq h_o^2, & \forall (i,j) \in \mathbf{I_o}, q \in \mathbf{StationSignal}_{i,j}, \\ \big(t_i(l_0)-t_j(l_0)\big)\,\big(t_i(l_f)-t_j(l_f)\big) \geq \sigma, & \forall (i,j) \in \mathbf{I_o}, [l_0,l_f] \in \mathbf{SingleTrack}_{i,j}. \end{cases} \tag{5.8}$$

The first inequality represents the safe following headway constraint for trains in the same directions. Denote by $\mathbf{Signal}_{i,j}$ the set of signals on both train i and j's journeys for $i,j \in \mathbf{I_s}$, $t_i(q)$ and $t_j(q)$ refer to the time of train i and j passing through signal

$q \in \mathbf{Signal}_{i,j}$, and h_s is the minimal headway time between two successive trains in the same directions. The left hand sides of the first two equations are squared to include the influence of train sequences.

The second inequality is for safe "depart-arrive" or "arrive-depart" headway constraints. $\mathbf{StationSignal}_{i,j}$ is the set of signals at station boundaries on both train i and j's journeys for $i, j \in \mathbf{I_o}$. h_o is the minimum "depart-arrive" or "arrive-depart" headway time. Here "station signal" refers to a signal at station boundaries, either the inbound side or the outbound side. The point where the headway time applies is usually the station but we put the headway times at station signals. The reason is that trains may use different platforms which correspond to different phases in the multiple phase optimal control problem formulation, that is introduced later. We want to keep the headway constraints at one location where both i and j are passing through to simplify the formulation.

If the timetable is a periodic timetable, conflict-avoiding constraints shall take into account that the trains run every T_{period} (cycle time in seconds) (Hansen and Pachl, 2014). So that the first two equations in (5.8) become

$$\begin{cases} h_s^2 \leq \big(t_i(q) - t_j(q)\big)^2 \leq (T_{\text{period}} - h_s)^2, \forall (i,j) \in \mathbf{I_s}, q \in \mathbf{Signal}_{i,j} \\ h_o^2 \leq \big(t_i(q) - t_j(q)\big)^2 \leq (T_{\text{period}} - h_o)^2, \forall (i,j) \in \mathbf{I_o}, q \in \mathbf{StationSignal}_{i,j}. \end{cases} \tag{5.9}$$

The third inequality in (5.8) is used to avoid any crossover of two trains' time-distance paths on single-track segments in order to avoid head-on conflicts between two opposite trains. Define any section between l_0 and l_f, which opposite trains are allowed to use, as a single-track. $\mathbf{SingleTrack}_{i,j}$ is the set of single-tracks on both train i and j's journeys for $i, j \in \mathbf{I_o}$. $[l_0, l_f]$ refers to a piece of single track (l_0 and l_f are the start and end locations). $t_i(l_0)$, $t_i(l_f)$, $t_j(l_0)$ and $t_j(l_f)$ refer to the time of train i and j passing through l_0 and l_f, and σ is a positive value close to 0 representing a safe margin for train separation.

In summary, the MTTO model minimizes the cost function (5.2), subject to constraints (5.3)-(5.8) (or (5.9)), where $\mathbf{I}$ includes more than one train.

5.4 Modelling and solution methods

This section presents the modelling and solution methods for the MTTO since the STTO modelling and solution methods has already been published in (Wang and Goverde, 2016a). The advantage of the MTTO presented in Section 5.3 is that it enables optimizing the energy consumption of multi-trains together with constraints to avoid conflicts between trains. However, it gives rise to three key questions.

First, Equations (5.3) are the differential equations of the train movements. Every train's traversed distance is taken as the independent variable of its own differential

equations. However, the trains' traversed distances are not always the same since they are in different directions or follow different routes, as the example of red and blue routes show in Fig. 5.4. It is necessary to unify the independent variable in order to formulate train movements together.

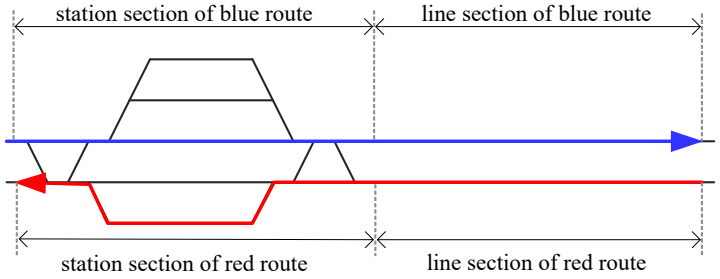

Figure 5.4: Example of two trains following different routes.

Second, trains are assigned different routes. Let "station sections" be sequences of connected blocks within a single station starting and ending at so-called station boundaries, and "line sections" be sequences of connected blocks within a single-track or double-track line (examples of station sections and line sections are shown in Fig. 5.4). Each train route is composed of a sequence of station sections and line sections, guiding the train through each station and each line. An accurate route model is the fundamental base of computing the train trajectories. However, trains are assigned different routes, while the lengths of different station sections within a station might be different, and the lengths of different line sections within a double-track line might also be different. The length differences make the multi-train trajectory optimization more complicated.

Last but not least, different trains have different speed limits and gradients since they travel on different routes, and the speed limits and gradients change along train routes. Besides, the MTTO model contains a lot of time and speed constraints at timetable points (in Equations (5.5)-(5.7)) and signals (in Equations (5.8)-(5.9)). How to deal with the varying speed limits and gradients and time and speed constraints at specific points is a difficult question.

This section provides solutions to these three questions. The independent variable is firstly unified, the section lengths are normalized, and the MTTO model is re-formulated as a multiple-phase optimal control problem to capture the varying speed limits and gradients and time and speed constraints.

5.4.1 Unification of the independent variable

Take distance s as the independent variable, which increases in the downstream direction. Let

$$ds_i = ds, \quad ds_j = -ds, \quad \forall\, i \in \mathbf{I_d}, j \in \mathbf{I_u}.$$

$ds_j = -ds$ because train j is in the upstream direction.

5.4.2 Normalization of section lengths

Our model takes into account the actual situation that trains use different routes and different tracks at stations, whilst the route lengths might be different. A normalization vector λ_i ($i \in \mathbf{I}$) is adopted for every station section or line section of train $i \in \mathbf{I}$ to normalize section lengths. With the introduction of λ_i, we scale all routes with respect to a fixed reference 'main route', so that all routes have unified and continuous kilometer points. λ_i is used in the formulation of cost function and dynamic constraints to scale the section lengths. The section lengths will be re-scaled again in the final solution for each train, so that the computed trajectories respect the actual route lengths.

The normalization follows 3 steps:

Step 1: Define station boundaries to divide the railway corridor into station regions and line regions.

Step 2: Define a main route in the downstream direction. The main route covers the whole corridor, and the kilometer points of the main route are continuous.

Step 3: Get the information of the lengths of every station section and line section of all the train routes and the main route, and compute λ_i for each section.

For a station section in train $i \in \mathbf{I}$'s route at station $z \in \mathbf{Z}_i$,

$$\lambda_{\text{Stationsec}_i^z} = \frac{L_{\text{Stationsec}_i^z}}{L_{\text{Stationsec}_{\text{main}}^z}},\ \forall\, i \in \mathbf{I}, z \in \mathbf{Z}_i, \tag{5.10}$$

where Stationsec_i^z refers to the station section, which train i uses at station z, $\text{Stationsec}_{\text{main}}^z$ refers to the station section on the main route at station j, $L_{\text{Stationsec}_i^z}$ and $L_{\text{Stationsec}_{\text{main}}^z}$ are respectively the lengths of Stationsec_i^z and $\text{Stationsec}_{\text{main}}^z$.

For a line section on train $i \in \mathbf{I}$'s route between adjacent stations z and $z+1$ ($z, z+1 \in \mathbf{Z}_i$),

$$\lambda_{\text{Linesec}_i^{z,z+1}} = \frac{L_{\text{Linesec}_i^{z,z+1}}}{L_{\text{Linesec}_{\text{main}}^{z,z+1}}},\ \forall\, i \in \mathbf{I}, z, z+1 \in \mathbf{Z}_i, \tag{5.11}$$

where $\text{Linesec}_i^{z,z+1}$ refers to the line section on train i's route between station z and $z+1$, $\text{Linesec}_{\text{main}}^{z,z+1}$ refers to the line section within the main route between station z and $z+1$, $L_{\text{Linesec}_i^{z,z+1}}$ and $L_{\text{Linesec}_{\text{main}}^{z,z+1}}$ are respectively the lengths of $\text{Linesec}_i^{z,z+1}$ and $\text{Linesec}_{\text{main}}^{z,z+1}$.

5.4.3 Multiple-phase optimal control problem formulation

The multiple-phase optimal control problem divides the railway corridor into multiple segments. Each segment is a phase, where any particular phase has its own cost function (minimizing energy costs), dynamic model (train dynamic movement model), path constraints (vehicle characteristics, speed limits, and riding comfort), boundary conditions (time and speed constraints at timetable points), and event constraints (to avoid conflicts). The complete trajectory is then obtained by properly linking adjacent phases via linkage conditions (continuous speeds and times). The total cost function is the sum of the cost functions within each phase. The optimal trajectory is then found by minimizing the total cost functional subject to the constraints within each phase and the linkage constraints connecting adjacent phases. The advantages of this modelling method are multiple: it gives an accurate description of varying speed limits and gradients and the time and speed restrictions at timetable points.

Assume that the infrastructure data combine track information such as speed, gradient, the signalling system (location of signals) and operational information like routes and timetable points. The first step is to divide the railway corridor into several segments. The division-points are one of three types:

1. *Critical points of speed limits and gradients.* The points of changing speed limits or gradients are used to partition the whole corridor, so that each interval has a unique speed limit and gradient value.

2. *Timetable points* that have time or speed limitations indicated by every train's TCS.

3. *Signal positions in both directions*. The signaling system consists of a series of railway signals that divide a railway line into a series of sections, or "blocks", which are important elements in managing train movements. For example, each block can only be occupied by one train at a time.

Fig. 5.5 gives an example, where the corridor is divided into 16 segments. Each segment between two adjacent division-points is a phase for the multiple-phase optimal control problem. Within each phase, the gradient and speed limit are constant, but their values may be different from the ones in other phases. The boundary points of a phase also might be a timetable point or a signal, where time and/or speed restrictions apply on the train operations.

Denote by $r \in \mathbf{R} = \{1,\ldots,R\}$ a phase, R is the number of phases of this railway corridor, $s_0^{(r)}$ the initial location of phase r, and $s_f^{(r)}$ the terminal location of phase r, $s_0^{(r)} < s_f^{(r)}$. Define $\mathbf{A} = \left\{(m,n)|s_f^{(m)} = s_0^{(n)}, m,n \in \mathbf{R}\right\}$ as the set of adjacent phases, and $\mathbf{I}^{(r)}$ as the set of trains passing through phase r, $\mathbf{I}^{(r)} \subseteq \mathbf{I}$. Let $v_i^{(r)}(s)$, $t_i^{(r)}(s)$ be train

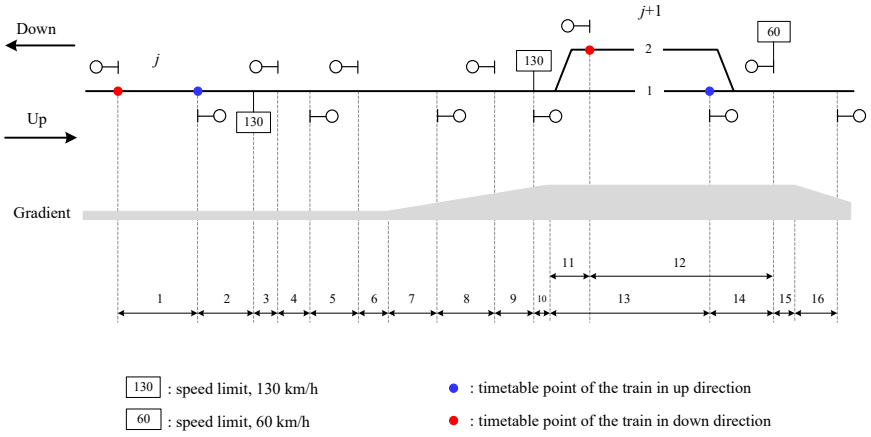

Figure 5.5: Example of partitioning in phases.

i's speed and time in phase r, $f_i^{(r)}(s)$, $b_i^{(r)}(s)$ be train i's traction and braking forces in phase r, $V_i^{\max,(r)}(s)$ be the speed limit of train i in phase r, and $R_{line,i}^{(r)}(s)$ be the line resistance caused by the constant gradient within phase r. ξ_i and $\lambda_i^{(r)}$ are introduced for later mathematical formulations. $\xi_i = 0$ if $i \in \mathbf{I_d}$, otherwise $\xi_i = 1$, and $\lambda_i^{(r)}$ equals the value of λ_i in phase r.

The MTTO model is re-formulated as a multiple-phase optimal control problem:

$$\begin{aligned} \text{Minimize} \quad J &= \sum_{r=1}^{R} J^{(r)}, J^{(r)} = \sum_{i \in \mathbf{I}^{(r)}} J_i^{(r)}, \\ J_i^{(r)} &= \lambda_i^{(r)} \int_{s_0^{(r)}}^{s_f^{(r)}} f_i^{(r)}(s)\, ds, \end{aligned} \tag{5.12}$$

subject to the dynamic constraints:

$$\begin{cases} \dfrac{dv_i^{(r)}(s)}{ds} = (-1)^{\xi_i}\lambda_i^{(r)} \dfrac{\theta_1 f_i^{(r)}(s) - \theta_2 b_i^{(r)}(s) - R_{train,i}(v_i^{(r)}) - R_{line,i}^{(r)}(s)}{\rho_i \cdot m_i \cdot v_i^{(r)}(s)}, \\ \dfrac{dt_i^{(r)}(s)}{ds} = (-1)^{\xi_i}\lambda_i^{(r)} \dfrac{1}{v_i^{(r)}(s)}, \end{cases} \quad \forall\ r \in \mathbf{R}, i \in \mathbf{I}^{(r)}, \tag{5.13}$$

the path constraints:

$$\begin{cases} 0 \le f_i^{(r)}(s) \le F_i^{\max}, \\ 0 \le b_i^{(r)}(s) \le B_i^{\max}, \\ 0 \le f_i^{(r)}(s) \cdot v_i^{(r)}(s) \le P_i^{\max}, \\ 0 \le v_i^{(r)}(s) \le V_i^{\max,(r)}, \\ A_i^{\min} \le \dfrac{dv_i^{(r)}(s)}{dt_i^{(r)}(s)} \le A_i^{\max}, \end{cases} \quad \forall\ r \in \mathbf{R}, i \in \mathbf{I}^{(r)}, \tag{5.14}$$

the boundary conditions (if any):

$$\begin{cases} v_{i,z,e}^{\min} \le v_i^{(r)}(k_{i,z,e}) \le v_{i,z,e}^{\max}, \\ t_{i,z,e}^{\min} \le t_i^{(r)}(k_{i,z,e}) \le t_{i,z,e}^{\max}, \\ \frac{t_i^{(r)}(k_{i,z,d})}{6} - \left\lfloor \frac{t_i^{(r)}(k_{i,z,d})}{6} \right\rfloor = 0, \end{cases} \quad \forall\, r \in \mathbf{R}, i \in \mathbf{I}^{(r)}, k_{i,z,e} \in \mathbf{K}_{\mathbf{TCS}_i} \cap \{s_0^{(r)}, s_f^{(r)}\}, \tag{5.15}$$

the event constraints (if any):

$$\begin{cases} \left(t_i^{(r)}(q) - t_j^{(r)}(q)\right)^2 \ge h_s^2, \\ \qquad\qquad \forall\, r \in \mathbf{R}, (i,j) \in \mathbf{I_s} : i,j \in \mathbf{I}^{(r)}, q \in \mathbf{Signal}_{i,j} \cap \{s_0^{(r)}, s_f^{(r)}\}, \\ \left(t_i^{(r)}(q) - t_j^{(r)}(q)\right)^2 \ge h_o^2, \\ \qquad\qquad \forall\, r \in \mathbf{R}, (i,j) \in \mathbf{I_o} : i,j \in \mathbf{I}^{(r)}, q \in \mathbf{StationSignal}_{i,j} \cap \{s_0^{(r)}, s_f^{(r)}\}, \\ \left(t_i^{(r)}(s_0^{(r)}) - t_j^{(r)}(s_0^{(r)})\right)\left(t_i^{(r)}(s_f^{(r)}) - t_j^{(r)}(s_f^{(r)})\right) \ge \sigma, \\ \qquad\qquad \forall\, r \in \mathbf{R}, (i,j) \in \mathbf{I_o} : i,j \in \mathbf{I}^{(r)}, [s_0^{(r)}, s_f^{(r)}] \in \mathbf{SingleTrack}_{i,j}, \end{cases} \tag{5.16}$$

and the linkage conditions of all adjacent phases:

$$\begin{cases} v_i^{(m)}(s_f^{(m)}) - v_i^{(n)}(s_0^{(n)}) = 0, \\ D_{i,s_f^{(m)}}^{\min} \le t_i^{(n)}(s_0^{(n)}) - t_i^{(m)}(s_f^{(m)}) \le D_{i,s_f^{(m)}}^{\max}, \end{cases} \quad \forall (m,n) \in \mathbf{A}, i \in \mathbf{I}^{(m)} \cap \mathbf{I}^{(n)}. \tag{5.17}$$

The cost function (5.12) aims at minimizing the cost functions over all phases, $J^{(r)}$ is the sum of the cost function(s) of the train(s) going through phase r. A single train's cost function $J_i^{(r)}$ aims at minimizing energy consumption within phase r. Each phase $r \in \mathbf{R}$ adopts the dynamic constraints (5.13) to represent the dynamic movements of train(s) going through segment $[s_0^{(r)}, s_f^{(r)}]$. The dynamic constraints are stated with s as the independent variable. $(-1)^{\xi_i}$ is adopted to eliminate the influence of travelling directions. $\lambda_i^{(r)}$ is adopted for the normalization of section lengths. Path constraints (5.14) are used to represent the operational constraints of vehicle characteristics, speed limits and riding comfort. Inequalities (5.15) work as the boundary conditions of phase r if $k_{i,z,e} \in \mathbf{K}_{\mathbf{TCS}_i}$ is the initial or terminal point of that phase. Timetable points are adopted as division-points, so phase r's initial or terminal point might be a timetable point, where time and speed restrictions on train operations apply. For a phase that has more than one train going through, event constraints (5.16) are required to avoid conflicts between trains. They are developed based on (5.8) or (5.9).

The linkage conditions (5.17) are to make sure that the train's speed-distance and time-distance trajectories are continuous. If the linkage point of two successive phases is a stop point of a train i, $t_i^{(m)}(s_f^{(m)})$ and $t_i^{(n)}(s_0^{(n)})$ represent the arrival and departure times of train i at $s_f^{(m)}$, and $D_{i,s_f^{(m)}}^{\min}, D_{i,s_f^{(m)}}^{\max}$ are the lower bound and upper bound of dwell times of train i at $s_f^{(m)}$ and $s_0^{(n)}$. Otherwise, $D_{i,s_f^{(m)}}^{\min} = D_{i,s_f^{(m)}}^{\max} = 0$.

5.4.4 Pseudospectral method

GPOPS (Rao et al., 2010) is adopted to solve the multiple-phase optimal control problem. GPOPS is a MATLAB software program for solving multiple-phase optimal control problems using the pseudospectral method. In general, pseudospectral methods transcribe the continuous-time optimal control problem into a nonlinear programming problem, after which a nonlinear programming solver is adopted to directly solve the problem. GPOPS uses the Radau pseudospectral method (Garg, 2011), which takes the Legendre-Gauss-Radau (LGR) points for collocation of the dynamic constraints, and for quadrature approximation of the integrated Lagrange cost term. The Lagrange polynomial approximation of the state, however, uses the LGR points plus the final point. In addition, GPOPS offers a function that implements an hp-adaptive mesh refinement algorithm that iteratively determines a mesh that accurately distributes the collocation points. GPOPS transcribes the continuous-time multiple-phase optimal control problem into a discrete NLP problem. The resulting NLP is then solved by SNOPT (Gill et al., 2005). For detailed mathematical descriptions, we recommend Wang and Goverde (2016a); Rao et al. (2010); Ye and Liu (2016).

5.5 Case studies

The proposed approach is applied in case studies on a Dutch single-track corridor and a double-track corridor. The infrastructure data is provided by the Dutch infrastructure manager Prorail. The infrastructure characteristics consist of a description of all track sections, points, speed signs, gradients and signals over the entire track layout. The single-track rail corridor is about 20 km long, between Den Helder (Hdr) and Schagen (Sgn) in the north of the Netherlands, see Fig. 5.6 (a). There are 4 stations along this corridor: Den Helder (Hdr), Den Helder Zuid (Hdrz), Anna Paulowna (Ana), and Schagen (Sgn). The double-track corridor is between Utrecht-'s-Hertogenbosch, which is one of the busies rail lines in the Netherlands. This railway corridor is about 50 km long, including two main tracks, divided into one long corridor for each traffic direction, 8 passenger stations: Utrecht (Ut), Utrecht Lunetten (Utl), Houten (Htn), Houten Castellum (Htnc), Culemborg (Cl), Geldermalsen (Gdm), Zaltbommel (Zbm) and 's-Hertogenbosch (Ht) (Fig. 5.6 (b)).

Fig. 5.7 shows the pre-defined timetables for the single-track and the double-track corridor (one direction from Ht to Ut). The time-distance diagrams are based on the timetables in use in 2016, which are periodic timetables with train services repeating every half hour. The trains in black solid lines in Fig. 5.7 are chosen for the case studies as the traffic within half hour timetables. On the double-track corridor, the trains in different directions are independent from each other, so only the trains from Ht to Ut are taken into account. By optimizing the six trains' time paths, the timetables for the whole day are optimized. To simplify the illustration, we name the trains as T_1 (regional train from Hdr to Sgn), T_2 (regional train from Sgn to Hdr), T_3 (regional train

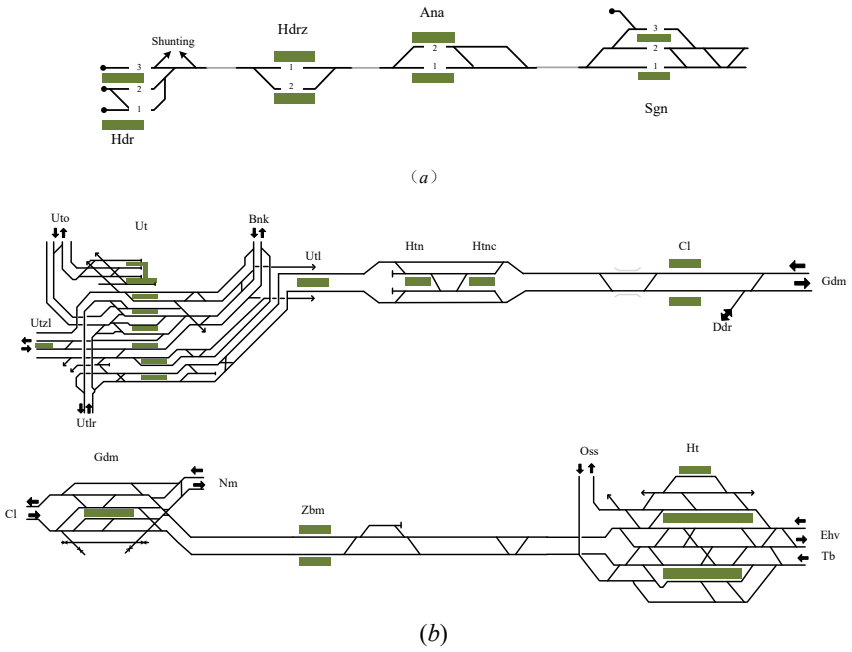

Figure 5.6: The partial single-track and double-track corridors used in the case studies.

from Gdm to Ut), T_4 (regional train from Ht to Ut), T_5 (intercity train from Ht to Ut) and T_6 (intercity train from Ht to Ut), as shown in Fig. 5.7. The light blue rectangles in Fig. 5.7 refer to multi-track lines, where the trains use different tracks. Trains use the same tracks on the other regions. On the single-track corridor between Hdr and Sgn, T_1 and T_2 operate in different directions and the two trains are scheduled to meet at Ana station. The double track corridor has two intercity trains (T_5 and T_6) and two regional trains (T_3 and T_4) running in the direction from Ht to Ut, and T_5 overtakes T_4 at Gdm station.

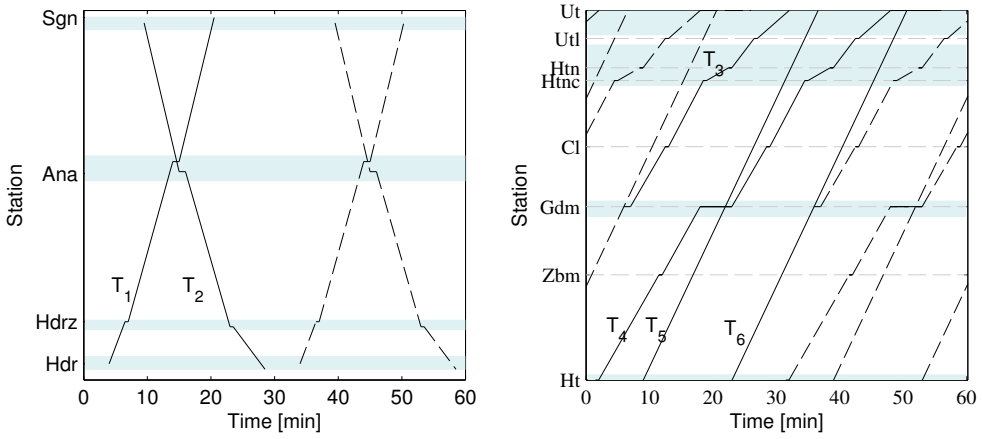

Figure 5.7: Original timetables of single-track and double track corridors.

The static parameters of the regional and intercity trains are listed in Table 5.1. The traction force and train resistance curves are shown in Fig. 5.8. Since the braking rates

are the only accessible data characterizing the braking behavior, we let the braking force be equal to the braking rate times train mass.

Table 5.1: Basic parameters of Regional and Intercity train.

Property	Value	
	Regional	Intercity
Train mass [t]	220	391
Rotating mass factor [-]	1.06	1.06
Maximum traction power [kW]	1918	2157
Maximum traction force [kN]	170	214
Maximum braking deceleration [m/s^2]	-0.8	-0.66

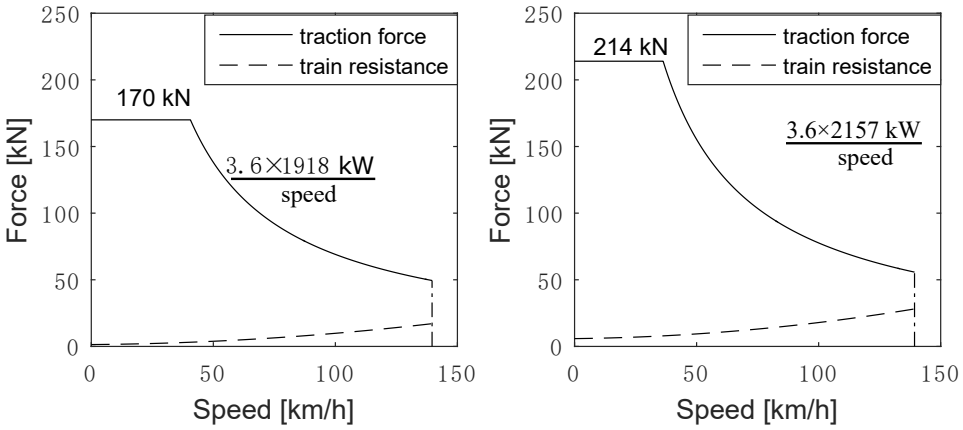

Figure 5.8: Traction force and line resistance of Regional and Intercity train.

The proposed methods were tested in two scenarios. The first is the scheduled scenario. The STTO is adopted to compute the speed profiles of the six trains separately, which assumes the trains operate according to the given timetables. Arrival and departure target points constraints are used to model the trains' punctuality. The second scenario is the energy-efficient timetable adjustment case. The A/D/P time target constraints are converted to time window constraints first, then the STTO is adopted to compute the speed profiles and time paths of the six train separately. After that, the conflicts are detected by checking the overlaps on blocking diagrams. If there are conflicts between the train paths, the MTTO method is adopted to re-compute the speed profiles and time-distance paths of the conflicting trains.

The TCS time windows of train T_1, T_2, T_3 and T_4 are presented in Fig. 5.9. The TCSs T_5 and T_6 are composed by scheduled departure and arrival times. The running times of T_5 and T_6 between Ht and Ut are the same as the ones provided by the original timetable. The timetables we study are periodic timetables, so Equations (5.9) are used by the MTTO model to ensure enough headways between trains. The parameters in Equations (5.8) and (5.9) were set as $T_{\text{period}} = 1800$ s, $h_s = 120$ s, $h_o = 15$ s, and $\sigma = 5$ s. The value of h_s is set according to the network statement 2017 by Prorail (ProRail,

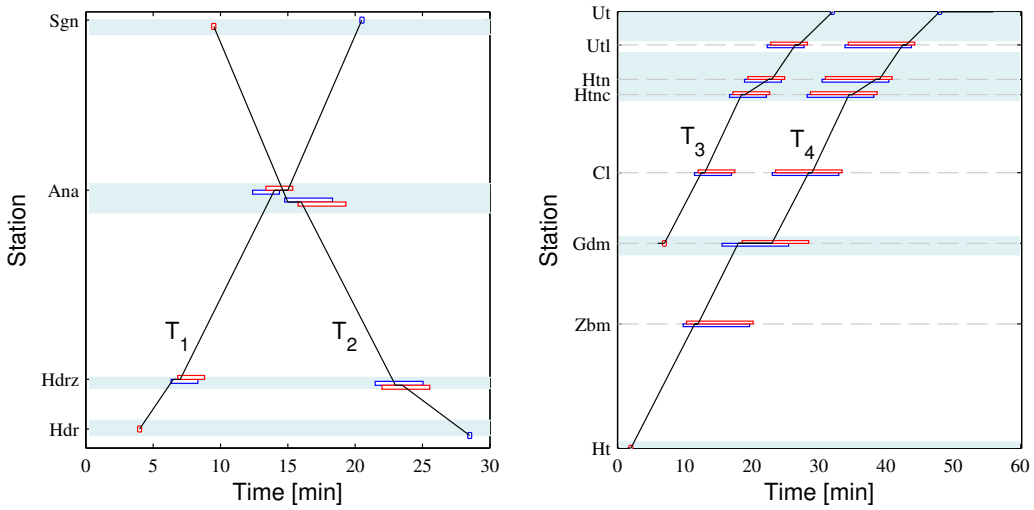

Figure 5.9: TCS time windows of train T_1, T_2, T_3 and T_4 (red rectangles refer to departure time windows, the blue rectangles refer to arrival time windows).

2017). We use default headway norms that should be sufficient for the final timetable to be conflict-free and contain some buffer. This can be checked by computing the blocking time diagram for the final solution to prove that the timetable is conflict-free, or if not to increase some headway times in the same manner as presented in Bešinović et al. (2016). The value of h_o ensures enough time interval for signal clearing and setting. σ is a positive value to avoid any crossover of opposite trains' path. The dwell time windows at the meeting station, Ana, and the overtaking station, Gdm, are respectively [1 min, 2 min], and [3 min, 6 min]. The minimal and maximal dwell times at other stations are 0.5 min and 1 min.

The experiments were carried out with GPOPS 4.1 on a laptop equipped with a 3.2 GHz Pentium R processor. As for the parameter settings of GPOPS, we used 'complex' as the string to indicate the differentiation method, a tolerance of 1e-3, an iteration of 2, and didn't use autoscaling. The explanation of the parameters can be found in (Rao et al., 2011).

Fig. 5.10, 5.11, 5.12 and Table 5.2 present the optimized results for the two trains, T_1 and T_2, on the single-track corridor. Fig. 5.13, 5.14, 5.15 and Table 5.3 present the optimized results for the four trains, T_3, T_4, T_5 and T_6, on the double-track corridor.

Timetable analysis: Table 5.2 and 5.3 present the arrival and departure times of the original timetables and the optimized timetables. The optimized arrival and departure times are slightly different from the ones indicated by the original timetables. The departure times are integral multiples of 6 seconds because of the restriction of Equation (5.7). The optimized dwell times of train T_1 and T_2 at Ana are 1 minute. The optimized dwell times of T_4 at Gdm are respectively 3 minutes by using STTO, and 4 minutes by using MTTO. In addition to that, the optimized dwell times at the other stations of all trains are 0.5 minutes. The results show that short dwell times are beneficial for energy-efficiency. The MTTO provides 1 minute longer dwell time of

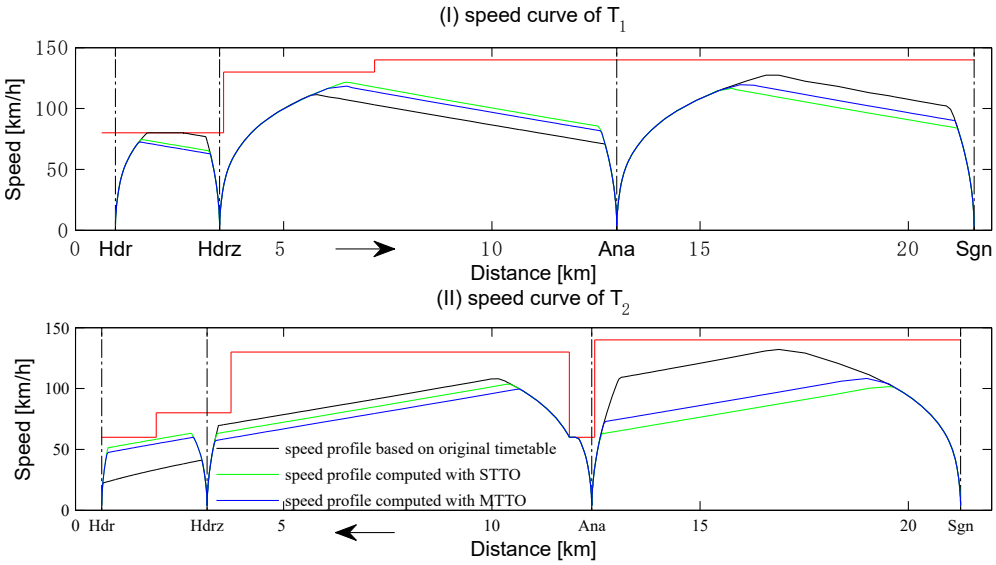

Figure 5.10: Speed profiles for trains on the single-track corridor.

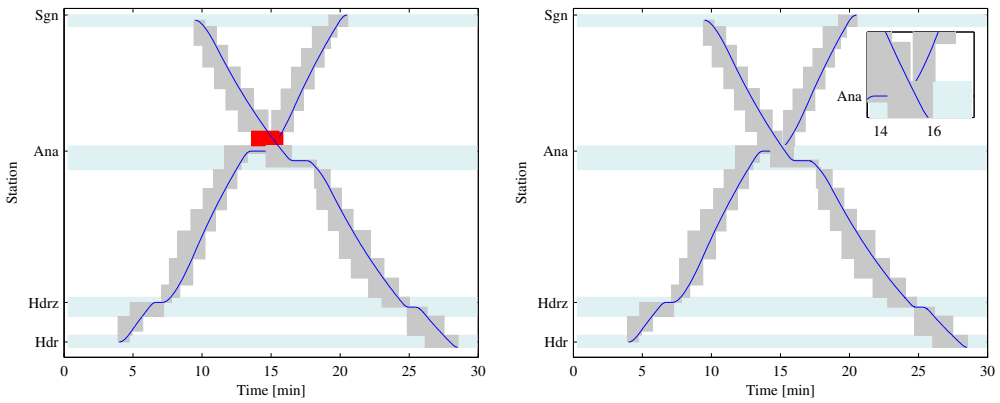

Figure 5.11: Blocking time diagrams of train T_1 and T_2 computed by STTO (left) and MTTO (right) (red refers to conflicts).

Table 5.2: The original and optimized timetables, and their computation times and energy consumptions for the single-track corridor.

	Train	Event	Hdr	Hdrz	Ana	Sgn	Computation time [s]	Energy consumption [J]	Energy saving	Conflicts
Original timetable	T_1	A	–	06:30	14:00	20:30	–	6.9378×10^5	–	no
		D	04:00	07:00	15:00	–				
	T_2	A	28:30	23:00	15:00	–	–	5.4670×10^5	–	no
		D	–	23:30	16:00	09:30				
STTO	T_1	A	–	06:42	13:30	20:30	28.61	6.4663×10^5	7.29%	yes
		D	04:00	07:12	14:30	–				
	T_2	A	28:30	25:00	16:36	–	13.93	4.1349×10^5	24.37%	yes
		D	–	25:30	17:36	09:30				
MTTO	T_1	A	–	06:42	13:42	20:30	81.12	6.4364×10^5	4.34%	no
		D	04:00	07:12	14:42	–				
	T_2	A	28:30	24:48	16:00	–		4.1366×10^5	24.34%	no
		D	–	25:18	17:00	09:30				

*A: arrival time, [mm:ss]; D: departure time, [mm:ss].

Table 5.3: The original and optimized timetables, and their computation times and energy consumptions for the double-track corridor.

	Train	Event	Ht	Zbm	Gdm	Cl	Htnc	Htn	Utl	Ut	Computation time [s]	Energy consumption [J]	Energy saving
Original timetable	T_3	A	–	–	–	12:30	18:30	22:30	26:30	32:00	–	3.9658×10^5	–
		D	–	–	07:00	13:00	19:00	23:00	27:00	–			
	T_4	A	–	11:30	18:00	28:30	34:30	38:30	42:30	48:00	–	7.3417×10^5	–
		D	02:00	12:00	23:00	29:00	35:00	39:00	43:00	–			
	T_5	A	–	–	–	–	–	–	–	37:00	–	1.2394×10^6	–
		D	09:00	–	–	–	–	–	–	–			
	T_6	A	–	–	–	–	–	–	–	51:00	–	1.2391×10^6	–
		D	23:00	–	–	–	–	–	–	–			
STTO	T_3	A	–	–	–	13:00	20:00	22:48	27:18	32:00	18.79	3.2810×10^5	17.27%
		D	–	–	07:00	13:30	20:30	23:18	27:48	–			
	T_4	A	–	11:42	19:00	28:30	36:00	38:48	43:12	48:00	49.76	5.7409×10^5	21.8%
		D	02:00	12:12	22:00	29:00	36:30	39:18	43:42	–			
	T_5	A	–	–	–	–	–	–	–	37:00	31.31	1.2394×10^6	0%
		D	09:00	–	–	–	–	–	–	–			
	T_6	A	–	–	–	–	–	–	–	51:00	32.83	1.2391×10^6	0%
		D	23:00	–	–	–	–	–	–	–			
MTTO	T_4	A	–	12:00	20:00	30:00	36:42	39:30	43:00	48:00	256.13	6.3550×10^5	13.4%
		D	02:00	12:30	24:00	30:30	37:12	40:00	43:30	–			
	T_5	A	–	–	–	–	–	–	–	37:00		1.2394×10^6	0%
		D	09:00	–	–	–	–	–	–	–			

*A: arrival time, [mm:ss]; D: departure time, [mm:ss].

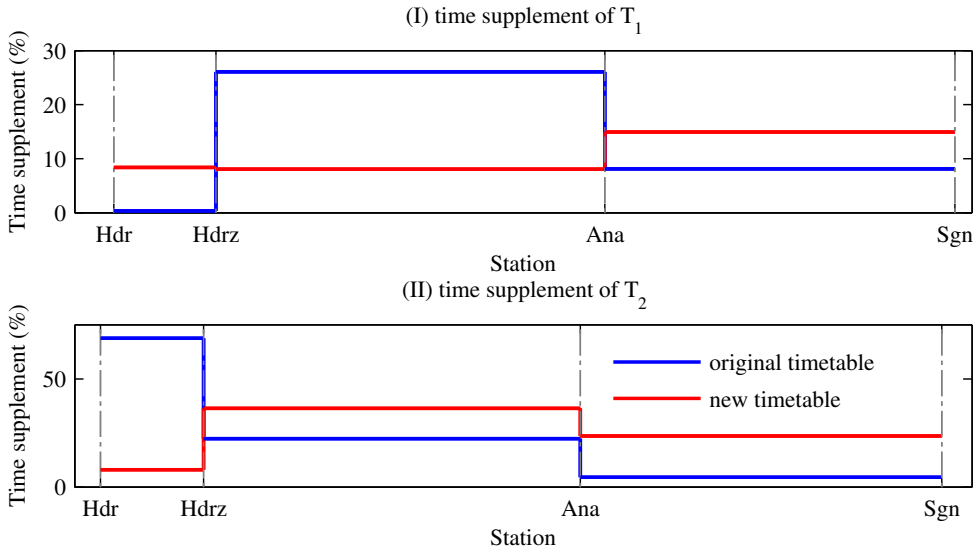

Figure 5.12: Time supplements of the original timetable and optimized timetable for trains on the single-track corridor.

tain T_4 at Gdm to satisfy the constraint (5.8) and to eliminate conflicts between T_4 and T_5, see Fig. 5.14.

Speed profile analysis: Fig. 5.10 shows the speed profiles of train T_1 from left to right, and train T_2 from right to left. Fig. 5.13 shows the speed profiles of T_3, T_4, T_5 and T_6. In Fig. 5.10 and 5.13, the red horizontal lines represent the static speed limits, the black lines refer to the energy-efficient speed profiles based on the original timetable, the green lines represent the optimized speed profiles within TCS windows computed with the STTO model, and the blue lines represent the optimized speed profiles computed with the MTTO model.

The optimal speed profiles, computed by both STTO and MTTO (as shown in Figs. 5.10 and 5.13), satisfy the energy-efficient train control theory by the application of PMP (Howlett and Pudney, 1995): the control regimes between every two stops include using maximum traction during the outbound processes, maximum braking force for the inbound processes, cruising at maximum speeds, and coasting before braking for energy saving. Train speeds do not exceed the static varying speed limits. The trains are capable of accelerating after entering high speed regions and decelerating to low speeds before getting in low speed areas. The trains stop at every planned stop point, which includes not only the first and last stations of the corridor, but also the intermediate stops, such as Hdrz, Ana (for train T_1 and T_2), Zbm, Gdm, Cl, Htnc, Htn, and Utl (for train T_3, T_4, T_5 and T_6). It shows that both STTO and MTTO can handle time and speed constraints at intermediate stations. The MTTO method is capable of optimizing the trajectories of trains on different directions and different routes.

Blocking time diagram analysis: Fig. 5.11 and 5.14 present the blocking time diagrams, which are computed according to the optimized results using STTO (left) or MTTO (right). Both in Fig. 5.11 and 5.14, the light-blue rectangles represent station

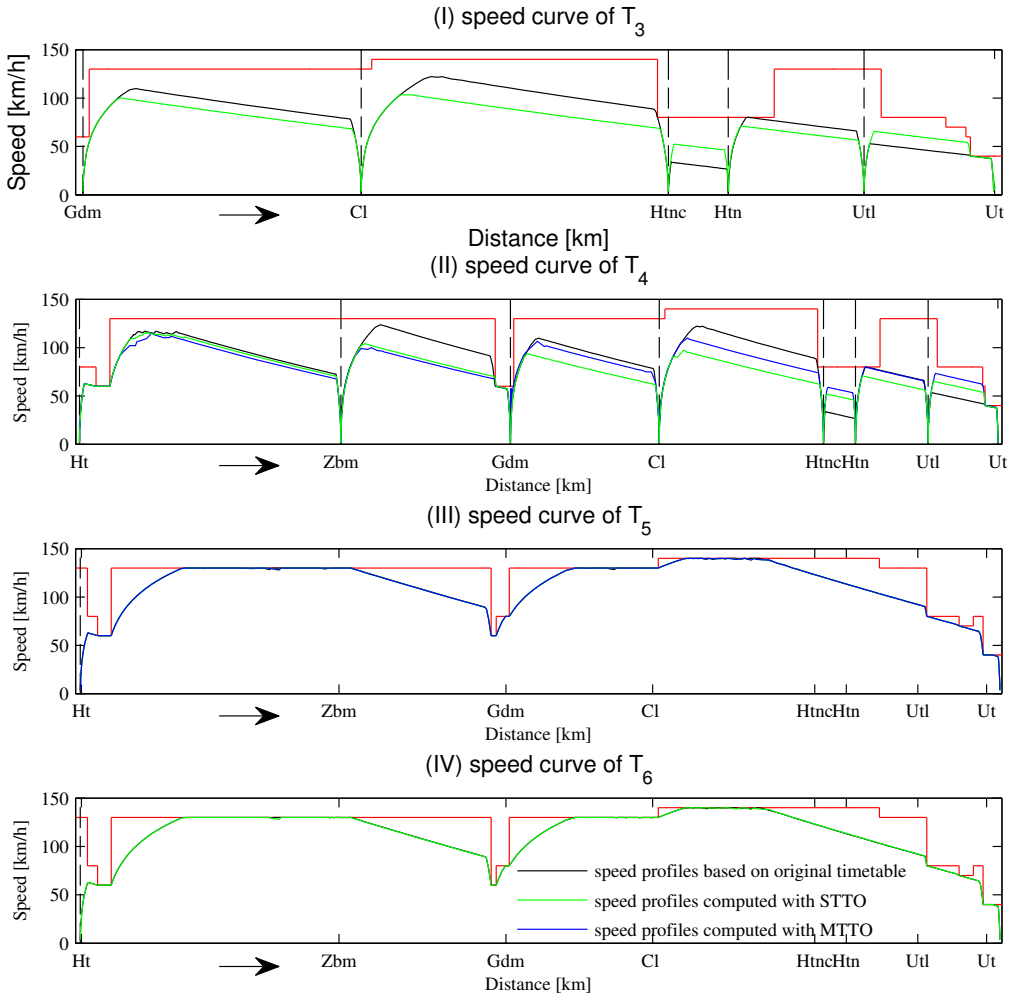

Figure 5.13: Speed profiles for trains on the double-track corridor.

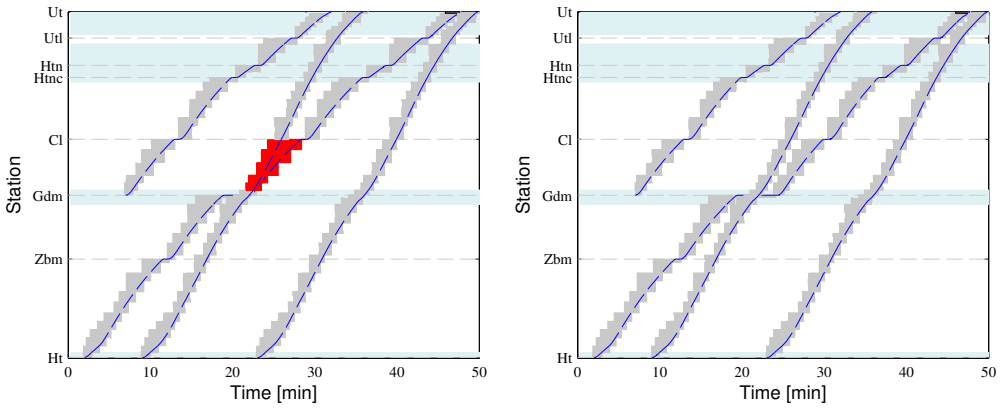

Figure 5.14: Blocking time diagrams of train T_3, T_4, T_5 and T_6 computed by STTO (left) and MTTO (right) (red refers to conflicts).

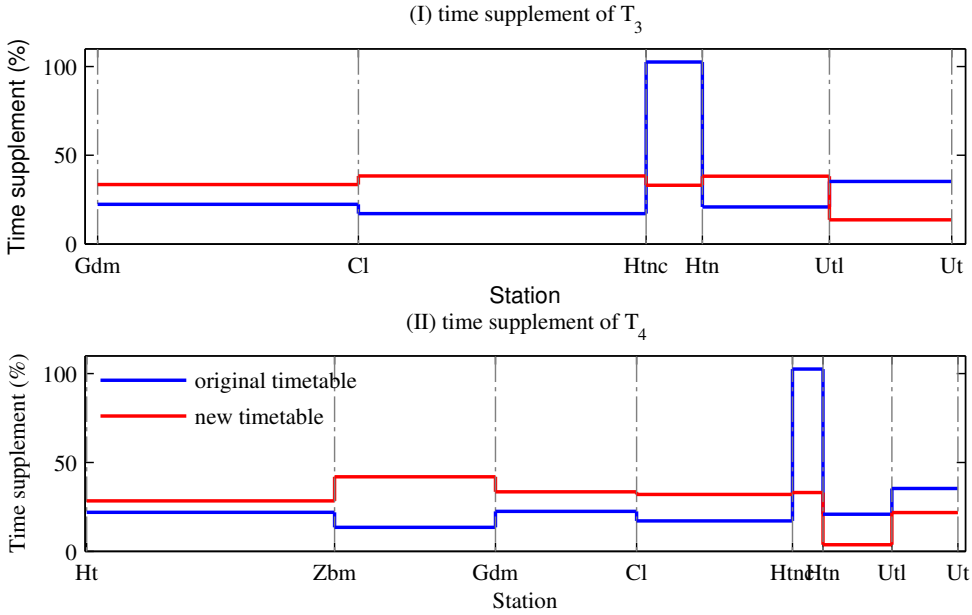

Figure 5.15: Time supplements of the original timetable and optimized timetable for trains on the double-track corridor.

areas with multiple tracks. The blocking time diagrams are only allowed to intersect within the station areas.

As the blocking time diagrams shown in Fig. 5.11 on the left, T_1 and T_2's blocking times intersect at the single-track line between Sgn and Ana, which is not feasible. Therefore the MTTO method is adopted to compute new conflict-free time paths. The right plot in Fig. 5.11 shows that the blocking time diagrams for T_1 and T_2 overlap at station Ana, which has two parallel tracks. T_1 uses track 1 while the opposing train uses track 2, so the conflict is eliminated with the optimized results.

In Fig. 5.14, the left plot presents an overlap of the blocking times of train T_4 and T_5 on the section between Gdm and Cl. Both T_4 and T_5 leave Gdm at 00:22:00, thus there is no sufficient headway between the moments that the trains start using the section between Gdm and Cl. Therefore, the MTTO is adopted to re-compute the trajectories for T_4 and T_5. The results are shown in the right plot of Fig. 5.14, where train T_4 leaves Gdm at 00:24:00, causing no conflicts with T_5.

Time supplement and energy consumption analysis: Fig. 5.12 and 5.15 present the time supplements of the original and optimized timetables for T_1, T_2, T_3 and T_4. The time supplements of T_5 and T_6 are not discussed herein, because their running times between Ht and Ut are the same as the ones provided by the original timetable.

It can be seen that the time supplements are re-allocated. The re-allocation of time supplements has a direction influence on speed profiles and energy consumptions. Trains coast more on the sections with more running time supplements. As reported in Table 5.2 and 5.3, the energy consumption of trains T_1-T_4 are decreased by 4.34%, 24.34%, 17.27% and 13.4%. In addition, the optimized dwell time of train T_4 at Gdm

is 4 minutes, so that T_4 got 1 minute more running time compared to the original timetable. The extra running time is beneficial to energy saving. The STTO is able to save more energy consumption than the MTTO model, however, computing the trajectories separately may cause conflicts. The MTTO saves less energy consumption but eliminates the conflicts.

Computation time analysis: The computation times are reported in Tables 5.2 and 5.3. The STTO is able to compute trajectories for each train within a short time (less than 1 minute to compute a trajectory for a train running on a 50 km long corridor). The MTTO causes longer computation times, compared to the STTO, since the MTTO model contains more variables.

5.6 Conclusions

This paper proposed a novel energy-efficient timetabling strategy. This strategy is achieved by adjusting the arrival and departure times of an existing timetable to improve its energy efficiency using train trajectory optimization. The train trajectory optimization method proposed by us integrates two types, a single-train trajectory optimization, and a multi-train trajectory optimization. The STTO focuses on one single-train's trip, which is able to compute the energy-efficient trajectory for a trip containing not only two stops but also intermediate stops or passing-through stations, while the classical train trajectory optimization methods only solve the problem with a train from one stop to another stop. If the STTOs generate conflicts then a MTTO method is applied. The MTTO model optimizes multiple trains' trajectories simultaneously. It aims at minimizing all trains' energy consumption, and concerns the train dynamic behavior and operational constraints for every individual train, as well as constraints to avoid conflicts between trains. The STTO and MTTO models are re-formulated as a multiple-phase optimal control problem and solved by a pseudospectral method. Both STTO and MTTO are adopted in finding the optimal speed profiles and conflict-free time paths, which in turn changes the arrival and departure times of the existing timetable, and improves the timetable's energy efficiency. Case studies of two half-hour timetables on a Dutch single-track corridor and a double-track corridor suggested that our method is able to produce energy-efficient timetables.

Future research aims at integrating the train trajectory optimization in timetable design. Along with the proposed MTTO model, the following extensions should be addressed: (1) a scheduling model to find optimal train orders; and (2) dynamic headway constraints to ensure a feasible timetable.

Bibliography

Albrecht, A., Howlett, P., Pudney, P., Vu, X., Zhou, P., 2016. The key principles of optimal train control—part 1: Formulation of the model, strategies of optimal type, evolutionary lines, location of optimal switching points. Transportation Research Part B: Methodological 94, 482–508.

Albrecht, T., Binder, A., Gassel, C., 2013. Applications of real-time speed control in rail-bound public transportation systems. IET Intelligent Transport Systems 7 (3), 305–314.

Albrecht, T., Oettich, S., 2002. A new integrated approach to dynamic schedule synchronization and energy-saving train control. WIT Transactions on the Built Environment 61.

Bešinović, N., Goverde, R. M. P., Quaglietta, E., Roberti, R., 2016. An integrated micro–macro approach to robust railway timetabling. Transportation Research Part B: Methodological 87, 14–32.

Brännlund, U., Lindberg, P., Nöu, A., Nilsson, J., 1998. Allocation of scarce track capacity using Lagrangian relaxation. Transportation Science 32, 358–369.

Cacchiani, V., Caprara, A., Toth, P., 2008. A column generation approach to train timetabling on a corridor. 4OR: A Quarterly Journal of Operations Research 6 (2), 125–142.

Cacchiani, V., Toth, P., 2012. Nominal and robust train timetabling problems. European Journal of Operational Research 219 (3), 727–737.

Caimi, G., Fuchsberger, M., Laumanns, M., Schüpbach, K., 2011. A multi-level framework for generating train schedules in highly utilised networks. Public Transport 3 (1), 3–24.

Garg, D., 2011. Advances in global pseudospectral methods for optimal control. Ph.D. thesis, University of Florida.

Gill, P. E., Murray, W., Saunders, M. A., 2005. SNOPT: An SQP algorithm for large-scale constrained optimization. SIAM Review 47 (1), 99–131.

Goverde, R. M. P., Bešinović, N., Binder, A., Cacchiani, V., Quaglietta, E., Roberti, R., Toth, P., 2016. A three-level framework for performance-based railway timetabling. Transportation Research Part C: Emerging Technologies 67, 62–83.

Hansen, I. A., Pachl, J., 2014. Railway timetabling and operations. Eurailpress.

Howlett, P., 2000. The optimal control of a train. Annals of Operations Research 98 (1), 65–87.

Howlett, P., Pudney, P., 1995. Energy-efficient train control. Springer, london, UK.

Khmelnitsky, E., 2000. On an optimal control problem of train operation. IEEE Transactions on Automatic Control 45 (7), 1257–1266.

Kraay, D., Harker, P. T., Chen, B., 1991. Optimal pacing of trains in freight railroads: model formulation and solution. Operations Research 39 (1), 82–99.

Li, X., Lo, H. K., 2014a. An energy-efficient scheduling and speed control approach for metro rail operations. Transportation Research Part B: Methodological 64, 73–89.

Li, X., Lo, H. K., 2014b. Energy minimization in dynamic train scheduling and control for metro rail operations. Transportation Research Part B: Methodological 70, 269–284.

Liu, R., Golovitcher, I. M., 2003. Energy-efficient operation of rail vehicles. Transportation Research Part A: Policy and Practice 37 (10), 917–932.

Peeters, L., 2003. Cyclic railway timetable optimization. Ph.D. thesis, Erasmus Universiteit Rotterdam, Rotterdam, the Netherlands.

ProRail, 2017. Network statement. Https: //www.prorail.nl /sites /default /files.

Rao, A., Benson, D., Darby, C., Mahon, B., Francolin, C., Patterson, M., Sanders, I., Huntington, G., 2011. User's manual for gpops version 4. x: a matlab software for solving multiple-phase optimal control problems using hp-adaptive pseudospectral methods. University of Florida, Gainesville.

Rao, A. V., 2003. Extension of a pseudospectral legendre method to non-sequential multiple-phase optimal control problems. In: 2003 AIAA Guidance, Navigation, and Control Conference and Exhibit. Austin, USA, pp. 11–14.

Rao, A. V., Benson, D. A., Darby, C., Patterson, M. A., Francolin, C., Sanders, I., Huntington, G. T., 2010. Algorithm 902: GPOPS, a matlab software for solving multiple-phase optimal control problems using the gauss pseudospectral method. ACM Transactions on Mathematical Software 37 (2), 22.

Scheepmaker, G. M., Goverde, R. M. P., 2015. The interplay between energy-efficient train control and scheduled running time supplements. Journal of Rail Transport Planning & Management 5 (4), 225–239.

Scheepmaker, G. M., Goverde, R. M. P., Kroon, L. G., 2017. Review of energy-efficient train control and timetabling. European Journal of Operational Research 257 (2), 355–376.

Serafini, P., Ukovich, W., 1989. A mathematical model for periodic scheduling problems. SIAM Journal on Discrete Mathematics 2 (4), 550–581.

Su, S., Li, X., Tang, T., Gao, Z., 2013. A subway train timetable optimization approach based on energy-efficient operation strategy. IEEE Transactions on Intelligent Transportation Systems 14 (2), 883–893.

Su, S., Tang, T., Li, X., Gao, Z., 2014. Optimization of multitrain operations in a subway system. IEEE transactions on intelligent transportation systems 15 (2), 673–684.

Wang, P., Goverde, R. M. P., 2016a. Multiple-phase train trajectory optimization with signalling and operational constraints. Transportation Research Part C: Emerging Technologies 69, 255–275.

Wang, P., Goverde, R. M. P., 2016b. Train trajectory optimization of opposite trains on single-track railway lines. In: 2016 IEEE International Conference on Intelligent Rail Transportation (ICIRT). pp. 23–31, birmingham, UK.

Wang, P., Goverde, R. M. P., 2016c. Two-train trajectory optimization with a green-wave policy. Transportation Research Record: Journal of the Transportation Research Board (2546), 112–120.

Wang, Y., Ning, B., Cao, F., De Schutter, B., van den Boom, T. J., 2011. A survey on optimal trajectory planning for train operations. In: 2011 IEEE International Conference on Service Operations, Logistics, and Informatics (SOLI). pp. 589–594, beijing, China.

Yang, L., Li, K., Gao, Z., 2009. Train timetable problem on a single-line railway with fuzzy passenger demand. IEEE Transactions on fuzzy systems 17 (3), 617–629.

Yang, L., Li, K., Gao, Z., Li, X., 2012. Optimizing trains movement on a railway network. Omega 40 (5), 619–633.

Yang, X., Li, X., Ning, B., Tang, T., 2016. A survey on energy-efficient train operation for urban rail transit. IEEE Transactions on Intelligent Transportation Systems 17 (1), 2–13.

Ye, H., Liu, R., 2016. A multiphase optimal control method for multi-train control and scheduling on railway lines. Transportation Research Part B: Methodological 93, 377–393.

Zhou, L., Tong, L. C., Chen, J., Tang, J., Zhou, X., 2017. Joint optimization of high-speed train timetables and speed profiles: A unified modeling approach using space-time-speed grid networks. Transportation Research Part B: Methodological 97, 157–181.

Chapter 6

Real-time train trajectory optimization in driver advisory system development

6.1 Introduction

Railway systems have become more and more busy with the growth of traffic demand in many countries. The increased density raises the difficulties of assuring efficient train operations. Trains are operated by human drivers. Their primary goal is to ensure train safety and maintain the schedule (arrival and departure times). Experienced drivers are able to save energy consumption and ensure passenger comfort. But different drivers have different driving skills. It is hard to achieve an efficient train operation especially when the train is interrupted by unexpected events. To improve the performance of train drivers, an in-cab system could be installed, which provides train drivers with information and driving advice and helps them to drive the train in an efficient manner. These systems are called Driver Advisory Systems (DASs).

There are several DASs on the market. Panou et al. (2013) provide a detailed review of the methods and features of existing DASs. Some DASs just provide drivers with timetable information and other generic advice on paper or on a screen. Those DASs are generally onboard tools, independently from the traffic management system. Typical examples are German and Swiss electronic timetables. They are the only systems that are in widespread use today. More complex systems provide drivers with dynamic advice on how to drive the train pursuant to a pre-defined timetable. For instance, LEADER ON-BOARD (Knorr-bremse, 2009) is a driver advisory system that helps train drivers operate their trains in a smooth and energy-efficient manner. LEADER calculates optimal speed profiles and continuously displays speed recommendations as well as information, such as milepost, gradients, and upcoming stations, based on the train's current position and pre-defined timetable. Energymiser

(Albrecht et al., 2011) is also a driver advisory system that aims at maintaining the pre-defined schedule while reducing energy consumption. Energymiser minimizes energy consumption using a control strategy based on optimal control theory. The advice includes driving regime changes, along with speed recommendations. GreenSpeed (Curis, 2017) advises the train to travel in a low speed before the signal changing from red to green so that the train glides right through successive green signals. Recently, advanced systems have been proposed that aim at optimizing traffic flow for the railway network as a whole. The systems consist of two parts, that a traffic management system that dynamically re-plans the timetable to avoid conflicts, a connected driver advisory system that provides advice in order to drive the trains in accordance with the new plan. AF (Mehta et al., 2010) and CATO (Tschirner et al., 2013) are typical examples of such C-DASs.

Future DASs shall provide not only static timetable information but also dynamic driving advice, such as speed recommendations, driving regimes, and so on. The information and advice shall be continuously adjusted in real time and ensure that the drivers are supplied with the best possible advice for punctual arrival with minimal energy consumption. Future DASs shall also include functions to connect with the traffic management system. So the advice is in accordance with the real-time traffic plan. The fundamental requirements for a DAS are:

1. To provide advisory information to the drivers in order to follow the schedule (or minimize delays) and to improve energy efficiency and passenger comfort.
2. To respect speed restrictions for train's safety.
3. To respect time restrictions, given by a pre-defined timetable or a real-time traffic plan.
4. To monitor the movement of the train so that the advice is properly updated.

The most critical factor in railway traffic is safety. For a DAS this means, that it must not conflict with information from the signals and the automatic train protection system. Meanwhile, the DAS shall advise a train to run at safe speeds under speed restrictions. The DAS shall also maintain the pre-defined or re-planned timetable. A DAS always strives to keep the train on time, thereby maximizing punctuality and optimizing traffic flow. Only if the train is within the planned time slots, the available slack time is used for energy efficient driving. If the train deviates from its schedule, the DAS should assist drivers to get the delayed train back to schedule as soon as possible.

To achieve those targets, an advisory trajectory over the train route is required. The trajectory includes information of advised driving regimes, speed and time over distance. The trajectory is the foundation of providing driving advice that assists the driver to pursue the pre-defined or re-planned timetable. The DAS should be able to

obtain the train state (location, time, and speed) in real time to allow correct advice to be defined and displayed. It is also important to monitor the differences between the actual state and the advised location, time, and speed. When the train state does not match the advised one, the advice is not followed well by train drivers. New advice should be re-calculated according to the driver's behavior and the actual environment if the deviations exceed some threshold.

Some existing DASs have adopted optimal control theory to compute the advisory trajectory. However, there are still some challenges faced by the trajectory computation methods. The first challenge is that the trajectory computation is an optimization problem with multiple objectives and multiple constraints. The optimization objectives for an on-time and delayed train are different. The objective for the on-time train is to save energy consumption while the delayed train needs to reduce delays. The trajectory should respect a large number of constraints. For instance, the timetable constraints, vehicle characteristic limits, and riding comfort restrictions. It is also anticipated to apply certain time and speed restrictions at signals to avoid yellow and red signals as much as possible and make the train travel under green signals in order to improve the driving efficiency. Usually, it should be avoided that a train has to come to a standstill and wait in front of certain switches to make space for other trains within dense yards or junctions. Such time and speed restrictions at critical locations (signals, switches) should be taken into account while computing the advisory trajectory.

Current trajectory computation methods that have been applied in DASs are mainly based on the Pontryagin's Maximum Principle (PMP) and the dynamic programming method. The PMP is an indirect method, which has been widely adopted in the trajectory optimization problem (Milroy, 1980; Cheng and Howlett, 1992; Howlett and Pudney, 2012). The optimal train control strategy following from application of the PMP to a long journey on a flat track with sufficient running time supplement consists of a sequence Acceleration with maximal traction–Cruising–Coasting–Braking with maximal effort (Cheng and Howlett, 1992; Howlett and Pudney, 2012; Milroy, 1980). For a train operating on a track with varying speed limits and gradients, the optimal control strategy is a sequence of these optimal regimes where the succession of regimes and their switching points also depend on the speed limits and gradients (Howlett, 1996; Khmelnitsky, 2000; Liu and Golovitcher, 2003; Pudney and Howlett, 1994). The trajectory optimization then is to find the optimal switching points and sequence of driving regimes. The dynamic programming algorithm is a popular algorithm to find the optimal sequence of driving regimes (Haahr et al., 2017). The dynamic programming algorithm firstly constructs a speed profile graph which consists of a lot of possible driving regimes at different locations, then a search algorithm is used to find the optimal sequence of driving regimes among the speed profile graph. The optimal sequence of regimes costs the least energy. The speed profile graph should be comprehensive and fully consider all possibilities. Otherwise, it is not able to produce solutions with high quality. Besides, finding the optimal sequence of driving regimes is a difficult problem except for simple cases such as a single speed limit and flat track

(Albrecht et al., 2016a,b). Especially, it is very challenging for such algorithms to take into account the time and speed restrictions at critical locations (signals, switches).

In this paper, we implement a different trajectory optimization method into a new DAS development. The DAS is named ETO (Energy-efficient Train Operation). The trajectory optimization is formulated as a multiple-phase optimal control problem and is solved by a pseudo-spectral method. The advantages of this modelling method are multiple: it gives an accurate description of varying speed limits and gradients; the pre-planned or re-planned timetables can be taken into account; the time and speed constraints at intermediate stations, signals, and switches can be satisfied; and minimizing energy consumption or minimizing delays as the optimization targets provides benefits for energy-efficient and on-time driving. Our previous work (Wang and Goverde, 2016) has implemented the trajectory optimization method to find the optimal trajectory for a train running under all green signals. As regards the practical implementation, a lot of practical issues should be taken care of: which section requires an advisory trajectory (due to the CPU power limitation, it is not possible to compute the trajectory over the whole journey at once), how to prepare data for the automatic trajectory computation, and how to convert the trajectory to driving advice. Those questions are answered in the following sections.

The key benefit of ETO is advice on how to achieve an efficient usage of energy as well as maintain the pre-planned or re-planned schedule. In addition to the situation that the train travels on-time, two more practical problems are taken into account by ETO: how to get back to the schedule when the train has a delay, and how to deal with the situation that the trains do not follow ETO's advice. To solve the first problem, the trajectory calculation method inside ETO adopts a pseudo-spectral method to find the optimal train control strategy. It aims at an energy-efficient driving behavior when the train has sufficient time supplements, and focuses on reducing delays when the train is late. The second problem the trains do not follow the provided advice which leads to deviations between the practical train running time-distance path and the advised time-distance path. ETO is able to respond to the time deviations, and offers re-optimized speed profiles and re-computed driving advice to eliminate the deviations.

The main contributions presented in this paper are:

1. Description of a prototype DAS, ETO, which provides energy-efficient and on-time advice and responds to deviations from the advised time-distance path,
2. Description of ETO's framework, data formats, functions and the underlying mathematical models, and
3. Demonstration of the ETO system in a laboratory environment with real-world instances.

The remainder of the paper is organized as follows: Section 6.2 provides a general description of a driver advisory system, including the functionalities and system

architecture alternatives. Section 6.3 introduces ETO's framework and its sub-modules. Section 6.4 presents the underlying mathematical models of trajectory computation. Section 6.5 describes the functions of the advice generation module. Section 6.6 presents the test environment and illustrates the approach in case studies. Finally Section 6.7 ends the paper with conclusions.

6.2 General DAS description

A driver advisory system aims at providing advice and information to drivers to optimize traffic flow and in some cases energy efficient driving. The operational concept of a DAS generally considers three DAS variants, Standalone, Networked and Connected:

1. A standalone DAS (S-DAS) provides train drivers with predefined timetable information and driving advice. Usually, the standalone DAS is an onboard application with predefined route geography and timetable data loaded into the system, independent of a traffic management system. The advice is calculated dynamically according to train delays and the predefined timetable.

2. A networked DAS (N-DAS) is a driver advisory system that is capable of communicating with one or more railway undertaking control centers, thus enabling provision of data to the train, including updates for schedule or routing information, though these are generally not in near real time.

3. A connected DAS (C-DAS) provides train drivers with real-time schedule information and driving advice. Usually, the connected DAS is linked to a traffic management system that can calculate new train timings (real-time traffic plan) to avoid conflicts and communicate them to the DAS. The DAS dynamically updates advice in order to drive the trains in accordance with the real-time traffic plan.

A connected DAS is a promising development by connecting a rail traffic management system and every single train in order to optimize real-time traffic flow and energy efficiency. The ON-TIME project proposed a cascading loop of real-time traffic management and train control as given in Fig. 6.1 (ON-TIME, 2014; Quaglietta et al., 2016). The outer control loop is a traffic management system (TMS), which collects real-time traffic state from different sensors, computes the real-time traffic plan and translates for each train into a train path envelope (TPE). The train path envelope is basically defined over each signal and timetable release point of a train run. Inside this envelope, the DAS control loop I computes an advisory trajectory and re-computes it if the deviations exceed some threshold. The trajectory shall be described as sequences of driving regimes as function of position and time with additional speed information. In DAS control loop II, the driving advice is determined in order to follow the advisory

trajectory or get back to the trajectory in case of deviations. In DAS control loop III, a driver or ATO implements the advice and reacts to external disturbances like weather impact or train faults, the ATP system supervises independently that any safety restrictions are respected by the advice implementation.

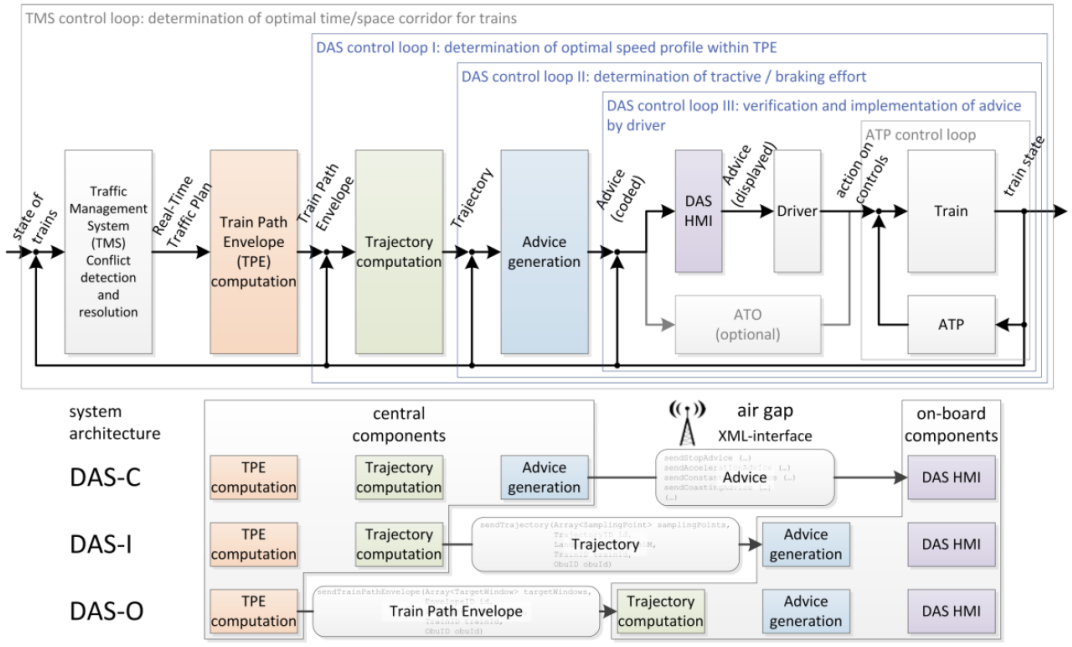

Figure 6.1: Real-time traffic management and train control framework & driver advisory system architecture (ON-TIME, 2014).

6.2.1 Functionality descriptions

The DAS control loops receive the train path envelope from the rail traffic management module. Within the train path envelope, a trajectory shall be computed, which best fulfills the objectives given in a predefined objective function. The train path envelope is a series of targets for each train at specific positions such as station platform stops, signals or switches, based on estimated earliest and latest passing times and speed limits (Albrecht et al., 2013; ON-TIME, 2014; Wang and Goverde, 2016). The targets are defined by triples of position, time and speed. Two kinds of targets are distinguished:

1. Target points: indicating that a train must reach a target position at the specified time and speed,

2. Target windows: indicating that a train must reach a target position within a time window and speed window.

Target points are mostly implemented at stop locations, indicating specific arrival/departure times and speeds. Target windows are adopted to indicate the earliest and latest time

(speed) constraints at intermediate stations, signals and so on. It must be guaranteed, that the train path envelope should be drivable and the advisory trajectory should respect the train path envelope. For a mathematical description, classify a train's event at a station into three types: arrival, departure and pass-through. Denote by e an event $e \in \{a, d, p\}$, where a refers to arrival, d refers to departure, and p refers to pass-through. The train path envelope is written as a series of target points and windows

$$\text{TPE} = \left\{ (p_{j,e}, [\underline{t}_{j,e}, \bar{t}_{j,e}], [\underline{v}_{j,e}, \bar{v}_{j,e}]) \right\}_{j=1}^{m}, \tag{6.1}$$

where $p_{j,e}$ is the location for a train at the j-th TPE point of event e, $j \in \{1, 2, \ldots, m\}$, m is the number of TPE locations (stations, signals, switches) along train's route. $\underline{t}_{j,e}$, $\bar{t}_{j,e}$, $\underline{v}_{j,e}$, and $\bar{v}_{j,e}$ are respectively the minimum and maximum time and speed limits at $p_{j,e}$. If $\underline{t}_{j,e} = \bar{t}_{j,e}$ and $\underline{v}_{j,e} = \bar{v}_{j,e}$, then $p_{j,e}$ has a target point constraint. Otherwise, it is a target window constraint.

In case the TMS wants to have the train operate under green signals, time window constraints at signals are taken into account by the train path envelope. The lower bounds of time windows are the earliest possible times for the train to pass through signals when the signals are green (Wang and Goverde, 2016). In case of a conflicting train path, a time constraint at a conflict point can be applied in the train path envelope to restrict the train movement.

The trajectory is computed by the trajectory computation module, which best fulfills the objectives given by predefined objective functions. The trajectory shall be described as sequences of driving regimes as a function of position and time with additional speed information. The trajectory has to respect technical limits and tolerances set by infrastructure managers. For example, static and temporary line speed limits, vehicle parameter restrictions, and train dynamic movement restrictions. The trajectory has to maintain the timetable or the real-time traffic plan. Only if the train is within the planned time slots, the train has the ability to save energy consumption by using the extra running time.

As regards the advice presented to drivers, in most vehicles, the driver controls traction and braking efforts. Some vehicles are equipped with systems for automatic cruise control (Junaid and Wang, 2006; Dong et al., 2010). In that case, the driver can set the speed which the automatic speed controller will try to follow. It can be summarized that the advice given to drivers could include:

1. The advisory traction/braking efforts.
2. The advisory driving regimes. The following regimes are possible: (a) acceleration with maximal traction; (b) acceleration with partial traction; (c) coasting; (d) cruising at a constant speed; (e) braking with maximal effort; (f) braking with partial effort; (g) stop; (h) departure; and (i) end-of-advice. The regimes could be given together with the parameters of traction/braking efforts, speed or time information.

3. The speed recommendations, such as the advisory speed at the current position or time, the target speed with the current driving regime.

4. The time-keeping information, which is related to the state of timetable adherence. The information could include the up-to-date timetable, the estimated delays, the distance/time to reach the next timetable point.

5. Decision-support information, which is used by drivers for making decisions. The information could include the gradient profile, the recommended speed profile, the deviation from the recommended trajectory, the energy usage and so on. Generally, the choice on the kind of advice must be made under careful consideration of human factors and safety requirements.

6.2.2 System architecture alternatives

The modules within the DAS loops could be allocated in the traffic control center (TCC) or the train. The system architecture can be classified into three alternatives by the distribution of intelligence (Fig. 6.1):

1. DAS-C (Central): The trajectory and advice are computed centrally. The advice is sent to on-board components for display purpose.

2. DAS-I (Intermediate): The trajectory is computed centrally and transmitted to the train. The advice is computed according to the advisory trajectory from central components and displayed on-board.

3. DAS-O (On-board): Central components compute the train path envelope and transmit it onboard. on-board components compute the advisory trajectory and advice and display.

The three alternatives have different requirements in train state monitoring and communications. Under the DAS-C alternative, no specific positioning sensors need to be accessed on-board. The train state is determined by the track-side system for traffic state monitoring and it is available to the TCC. Under the DAS-I and DAS-O alternatives, the speed and position values are measured on-board. They should be transmitted regularly to the TCC in order to improve traffic state monitoring. The three alternatives respectively transmit the advice, trajectory, and train path envelope from the TCC to the on-board units (OBUs). Under the DAS-C alternative, the driving advice is computed centrally and transmitted to the OBUs. The driving advice should be transmitted together with a position or time reference, at which the advice becomes valid and the duration of the validity of the advice. Regular reliable communication between the TCC and OBUs is required to provide the advice. Under the DAS-I alternative, the trajectory is computed centrally and transmitted to the OBUs. The permitted deviations for the trajectory (upper bound/lower bound) can be also included

in order to give information to the train driver on how close the train is referring to the TPE boundaries in order to avoid conflicts with surrounding trains. The permitted deviations must never exceed the TPE boundaries. Under the DAS-O alternative, the entire train path envelope is communicated to the OBUs. Trajectory and advice are computed on-board. Only the changes to the real-time traffic plan require a completely new train path envelope. Partial TPE updates might happen if the train is delayed or affected by other trains.

6.3 ETO overview

This section provides an overview of the ETO (Energy-efficient Train Operation) System. At the current stage, ETO is a prototype DAS that collects information about the train state (location, time, and speed) in real time, and then computes and displays driving advice for an efficient train movement. The main characteristics of ETO can be summarized as:

1. It has two versions, Standalone and Connected.
2. It provides advice regarding current and approaching speed recommendations and driving regimes, as well as estimated times of arrival at coming timing points.
3. It advises drivers how to achieve, from a given current location and with a specific destination arrival time, an energy-efficient or delay-recovery (if the train has a delay) train operation.
4. It respects speed restrictions, and takes into account varying gradients and curves.
5. It takes into account the train path envelope constraints, not only the arrival and departure times, but also time restrictions at other timetable points, signals, and conflict points (switches).
6. It automatically responds to deviations of the actual time-distance path from the advised one, and re-computes and updates speed profiles and advice, ensuring that the driver is supplied with the best possible advice for punctual arrival with minimal energy consumption.

ETO may be used as a Standalone DAS and as a Connected DAS. The architectures of the two versions are shown in Fig. 6.2. As a Standalone DAS, ETO computes a train path enveloped based on a pre-defined timetable in store. The Connected ETO shall be connected to a traffic management system. The train path envelope is received from the traffic management system. The two versions have four common modules,

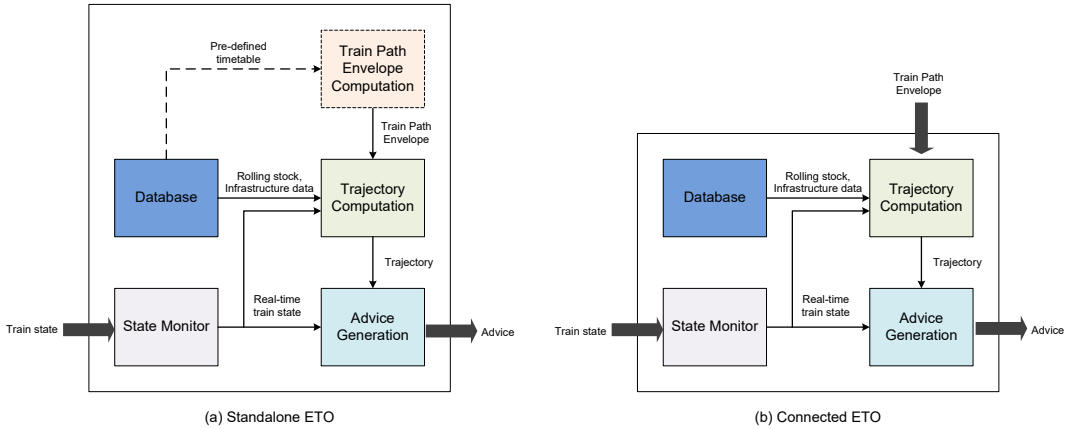

Figure 6.2: The Frameworks of the Standalone ETO and the Connected ETO.

Database, State Monitor (SM), Trajectory Computation (TC), and Advice Generation (AG).

The Database includes the rolling stock and infrastructure data, which are related to trajectory computation (see Section 6.4). The Standalone ETO also has the pre-defined timetable in stored, which is sent to the TPE Computation module to come up with a train path envelope consisting of pre-planned time constraints.

The State Monitor is responsible for collecting real-time data relative to the train movement (location, time, and speed). The data are collected continuously in a regular time interval and recorded as a train state history file. At every sampling point, the data is sent to the trajectory computation module and the advice generation module, so that the advisory trajectory and driving advice are updated according to the real-time train state.

The Trajectory Computation module computes the advisory train trajectory. The trajectory consists of sequences of driving regimes, recommended speeds, times and recommended traction/braking efforts as function of position. The trajectory is computed by optimal control theory with the objectives of maintaining timetables (real-time traffic plans) and improving energy efficiency (see Section 6.4).

The Advice Generation module computes driving advice in accordance with the trajectory from the TC module. Currently, ETO just provides all possible advice, including speed, driving regime recommendations, time-keeping information, and so on (see Section 6.5).

6.4 Trajectory computation

The trajectory computation (TC) module computes the advisory trajectory and re-computes it if the actual train movement deviates over some threshold. The trajectory computation module consists of a cascade of sequenced steps shown in Fig. 6.3.

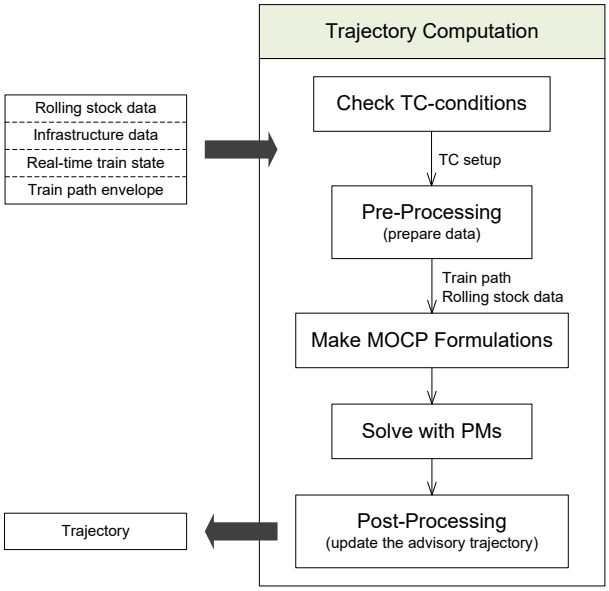

Figure 6.3: The trajectory computation cascade.

The trajectory computation process begins with collecting input data from different sources. The input data contains the rolling stock and infrastructure data from the database, the real-time train state data from the State Monitor, and the train path envelope from the TPE Computation module. Next, the TC-conditions are checked to determine if a new trajectory should be computed. If a new trajectory is required, the pre-processing step gets data prepared for the train trajectory computation. The trajectory computation is formulated as a multiple-phase optimal control problem (MOCP) and solved with a pseudospectral method (PM). The new computed trajectory is sent to the post-processing step to be integrated with the existing trajectory and added with new information for the later advice generation.

6.4.1 Check TC-conditions

The train path envelope from the TPE Computation module generally includes time and speed restrictions over a couple of running sections (the sections between stations). The aim of the TC module is to find the trajectory within the TPE optimizing certain objectives. For the sake of the limitation of CPU power, the TC module does not compute the trajectory for the whole TPE at once, but instead, it computes a trajectory for a partial TPE at one time to the next target point. The partial TPE is dynamically updated and constructed within the TC module (mainly by the pre-processing step) in accordance with the train state and the train path envelope from the TPE computation module. A new trajectory is computed if one of the TC-conditions hold. The TC-conditions are:

1. The TC module receives an updated train path envelope from the TPE Computation module.

2. The train is approaching a next running section.
3. The train is moving on a running section which does not have an advisory trajectory computed yet.
4. The actual time-distance path deviates from the advised time-distance path over some threshold (e.g. 10 s).

TC-condition 1 happens if the TMS produces a re-planned timetable so that the TPE Computation module comes up with a new corresponding train path envelope. The TC module should adjust the trajectory to follow the new timetable. TC-condition 2 prepares a trajectory for the coming running section in advance. TC-condition 3 happens in the case that the ETO is started up while the train has already left a station. A trajectory for the running section, where the train is located, is required. TC-condition 4 takes into account that the train movement does not exactly follow ETO's advice due to any reason. A new trajectory for the remaining section (from the current train location to the next stop) is required if the deviation is over some threshold to provide updated realistic advice. The new trajectory always starts from a departure location (TC-condition 1, 2 and 3) or the current train location (TC-condition 4) and ends at the next arrival location. The arrival location is taken as the terminal of the trajectory because the speed window at an arrival point is fixed as [0,0], the lower bound of the arrival time window equals the planned arrival time (to avoid earlier arrival), and the upper bound is equal to the planned arrival time if the train is on time, or lager than the planned arrival time if the train is delayed, however the TC algorithm always tries to minimize delays (see Section 6.4.3). The relatively strict constraints would avoid any influence on the train running in remaining sections.

A data structure called TC-setup is adopted to decide if a new trajectory shall be computed by the following steps after the TC-condition checking. The TC-setup contains a mark, named as New Trajectory Flag (NTF), and the speed and time restrictions at the start and terminal locations of the new trajectory. If NTF is true, then the time and speed restrictions become valid and the following steps are executed to compute a new trajectory. If NTF is false, then there is no requirement for a new trajectory, the time and speed restrictions are invalid and the following steps would not be executed. The time and speed restrictions at the start and terminal locations of the new trajectory are formulated as

$$\mathrm{TC}_{\mathrm{setup}} = \{(p_k, [\underline{t}_k, \bar{t}_k], [\underline{v}_k, \bar{v}_k])\}_{k \in \{start, end\}}, \tag{6.2}$$

where p_{start} and p_{end} are respectively the start and terminal locations of the new trajectory. $[\underline{t}_k, \bar{t}_k]$ and $[\underline{v}_k, \bar{v}_k]$ $(k \in \{start, end\})$ are the corresponding speed and time constraints at p_{start} and p_{end}.

The values of the time and speed windows in Equation (6.2) are different in different cases. As for TC-condition 1 and 3, p_{start} and p_{end} are respectively the departure and arrival locations of the current running section. As for TC-condition 2, p_{start} and

p_{end} are respectively the departure and arrival locations of the approaching running section. The time and speed windows equal the time and speed windows at p_{start} and p_{end} within the original train path envelope from the TPE Computation module. As for TC-condition 4, p_{start} refers to the current train location, p_{end} is the next arrival location. $\underline{v}_{start}$ and $\bar{v}_{start}$ equal the train current speed, $\underline{t}_{start}$ and $\bar{t}_{start}$ are equal to the current time, $[\underline{v}_{end}, \bar{v}_{end}]$ and $[\underline{t}_{end}, \bar{t}_{end}]$ equal the arrival time and speed constraints at p_{end} within the train path envelope from the TPE Computation module.

6.4.2 Pre-processing

The pre-processing step prepares data for trajectory calculation. The trajectory calculation relies on the input data about the rolling stock (the traction/braking characteristics of the train; the train mass and length; the train resistance parameters; the riding comfort acceptance), infrastructure (the static and temporary speed limits; the slopes, curves; the signals) and train path envelope. For the convenience of later trajectory calculation, two type of data structures, the rolling stock data structure and the train path structure, are constructed by the pre-processing step and sent to the next step of constructing MOCP formulations.

In general, the rolling stock XML data expressed in RailML format could be used (Nash et al., 2004). Currently, the rolling stock data is expressed in an XML format as the example in Fig. 6.4 in order to match the test environment (Section. 6.6). The rolling stock XML is specified with the name of the train composition and modeled by considering all relevant characteristics of the vehicles such as the mass, the rotating mass factor, the length, the maximum speed, the traction and braking characteristics, and the train resistance parameters. The MOCP formulation is able to deal with different types of traction and braking characteristics (see Section 6.4.3). Fig. 6.5 presents three examples of traction characteristics, which can be represented either by the maximum traction power, the maximum traction force, and the maximum braking rate.

```
<RollingStock>
        <Name> VIRM 12 (12 bakken) </Name>
        <Mass > 770 </Mass>
        <RotatingMassFactor> 1.06 </RotatingMassFactor>
        <Length> 188 </Length>
        <MaxSpeed> 160 </MaxSpeed>
        <TractionType> typeA </TractionType>
        <BrakingType> typeA </BrakingType>
        <CoastingA> -1,81999996584636E-6 </CoastingA>
        <CoastingB> -9,91999986581504E-5 </CoastingB>
        <CoastingC> -0,0201709996908903 </CoastingC>
        <TractionParamater>
                <MaxTractionForce> 214 </MaxTractionForce>
                <MaxTractionPower>1918</MaxTractionPower>
        </TractionParamater>
        <BrakingParamater>
                <MaxBrakingDeceleration> 0.66 </MaxBrakingDeceleration>
        </BrakingParamater>
</RollingStock>
```

Figure 6.4: Snippet of the XML of the rolling stock data.

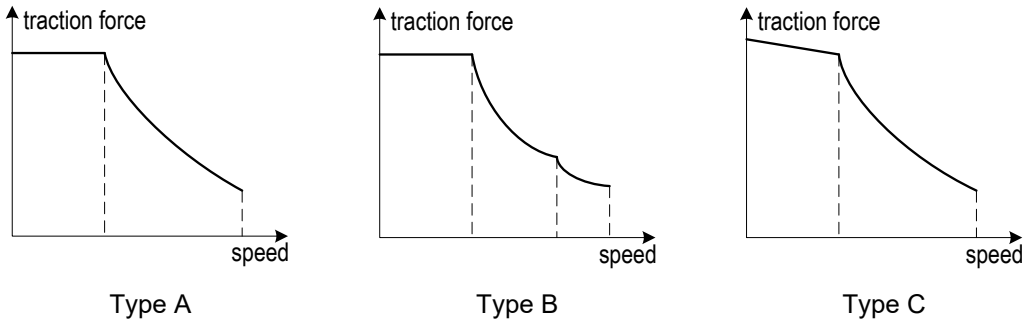

Figure 6.5: Three types of traction characteristics.

The train path structure contains the information about speed limits, gradients, curves, and time/speed constraints at p_{start}, p_{end} and TPE points between p_{start} and p_{end}. A demonstration of constructing the train path structure is presented in Fig. 6.6.(a). The TC-setup provides the time and speed windows at p_{start} and p_{end}. It is adopted to find the TPE piece between p_{start} and p_{end}. The TPE piece shall include the time and speed constraints at p_{start} and p_{end}. Especially, if p_{start} does not belong to the original TPE from the TPE computation module (TC-condition 4), the time and speed constraints at p_{start} must be added into the TPE piece. The TPE piece must be driveable, i.e. the train has the ability to run between two TPE targets within the technical minimal running time, otherwise it is not possible to find a trajectory within the TPE piece. The time windows of the TPE piece are adjusted by extending their upper bounds if the TPE piece is not driveable. The extended upper bounds guarantee that the train has sufficient running time. After determining the TPE piece, the infrastructure information is combined with the TPE piece, which results in the train path structure. The infrastructure information is a sequence of infrastructure points (speed/gradients changing points, signals) with additional values about speed limits, gradients, and signal states. Note that the speed limits take into account the train length by extending the lower speed limits before a speed increase by the train length. So that the train will only accelerate after its rear has safely passed the lower speed limit, see the example in Fig. 6.6.(b).

A part of the train path XML is presented in Fig. 6.7. The train path structure is formulated as a table which is arranged by an increasing sequence of locations (unit: m) with information about the speed limit (unit: km/h), gradient (unit: ‰), curve (unit: m), time window constraints (hh:mm:ss) and speed window constraints (unit: km/h). Each location has a special type identified by the 'TPEPoint' or 'InfraPoint'. The 'TPEPoint' means that the location is a TPE point. An additional mark is included in 'TPEPoint' type which identifies the types of the TPE point (D: departure, A: arrival, P: passing-through). If the location is a TPE point, there are a time window and a speed window constraint which indicate the time and speed restrictions for the train to go through that location. Type 'InfraPoint' means that the location is a changing point of speed limit, gradient or curve. The numbers within <SpeedLimit></SpeedLimit>, <Gradient></Gradient> and <Curve></Curve>

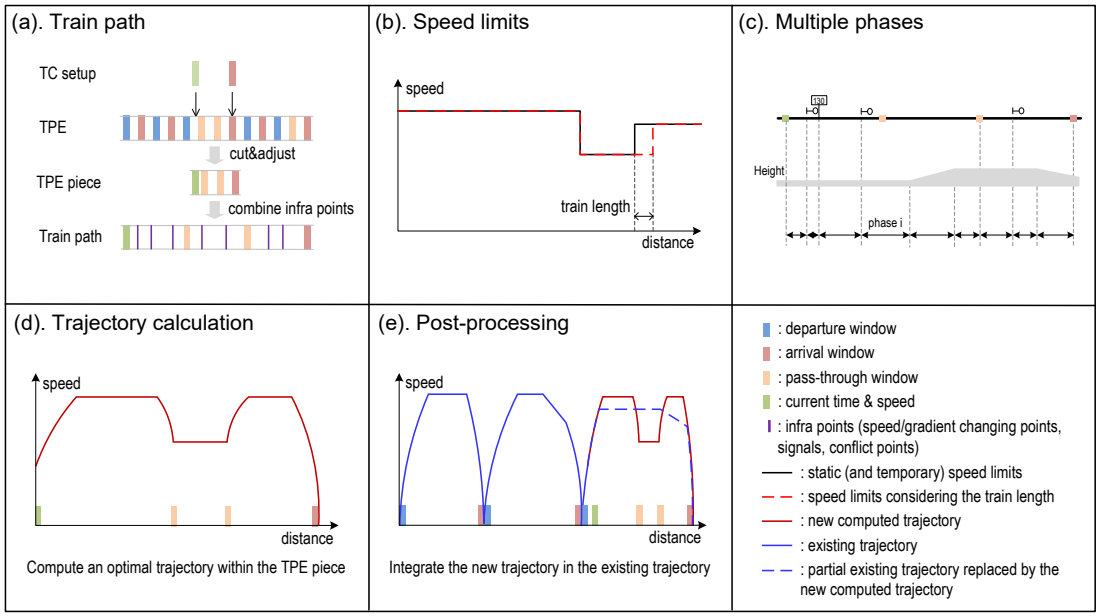

Figure 6.6: Demonstrations of data and functions within the trajectory computation module.

are the values form this InfraPoint point to the next InfraPoint point. The benefits of this train path formulation are obvious: it saves data space usage by combining the TPE and infrastructure information into one file and matches with the multiple-phase optimal control problem formulation for train trajectory computation (see Section 6.4.3).

```
<TrainPath>
        <TrainPathNode><Number> 1 </Number><Location> 0 </Location><Type> TPEPoint (D) </Type>
                <Speedlimit> 40 </Speedlimit><Gradient> 0 </Gradient><Curve> 0 </Curve>
                <TimeWindow> [08:02:00,08:02:00] </TimeWindow><SpeedWindow> [0,0] </SpeedWindow></TrainPathNode>
        <TrainPathNode><Number> 2 </Number><Location> 36 </Location><Type> InfraPoint </Type>
                <Speedlimit> 40 </Speedlimit><Gradient> 2 </Gradient><Curve> 0 </Curve>
                <TimeWindow></TimeWindow><SpeedWindow></SpeedWindow></TrainPathNode>
        <TrainPathNode><Number> 3 </Number><Location> 556 </Location><Type> InfraPoint </Type>
                <Speedlimit> 60 </Speedlimit><Gradient> 2 </Gradient><Curve> 0 </Curve>
                <TimeWindow></TimeWindow><SpeedWindow></SpeedWindow></TrainPathNode>
        <TrainPathNode><Number> 4 </Number><Location> 986 </Location><Type> TPEPoint  (P) </Type>
                <Speedlimit> 60 </Speedlimit><Gradient> 2 </Gradient><Curve> 0 </Curve>
                <TimeWindow> [08:02:30,08:03:30] </TimeWindow><SpeedWindow> [30,60] </SpeedWindow></TrainPathNode>
</TrainPath>
```

Figure 6.7: Snippet of the XML of the train path.

6.4.3 MOCP formulation and PMs

MOCP formulation

The train trajectory optimization is formulated as a multiple-phase optimal control problem. The MOCP formulation partitions the train route into multiple segments. The division points are the points within the train path structure (constructed by the pre-processing step). The segment between any two adjacent division-points is a phase

of the multiple-phase optimal control problem. Fig. 6.6 (c) gives an illustration of the multiple phases. Within each phase, the gradient and speed limit are constant, and the boundary points might be TPE points or signals, where time and/or speed restrictions apply to the train operations.

The multiple-phase optimal control problem is one where the trajectory consists of a collection of phases. In general, any particular phase has a cost function, a dynamic model, path constraints, boundary conditions, and event constraints. The complete trajectory is obtained by properly linking adjacent phases via linkage conditions. Similarly, the total cost functional is the sum of the cost functionals within each phase. The optimal trajectory is then found by minimizing the total cost functional subject to the constraints within each phase and the linkage constraints connecting adjacent phases. The trajectory computation is formulated as a multiple-phase optimal control problem:

$$\text{Minimize} \quad J = \sum_{r=1}^{R} J^{(r)}, \tag{6.3}$$

subject to the dynamic constraints:

$$\begin{cases} \dfrac{dv^{(r)}(s)}{ds} = \dfrac{\theta_1 f^{(r)}(s) - \theta_2 b^{(r)}(s) - R_{train}(v^{(r)}) - R^{(r)}_{line}(s)}{\rho \cdot m \cdot v^{(r)}(s)}, \\ \dfrac{dt^{(r)}(s)}{ds} = \dfrac{1}{v^{(r)}(s)}, \end{cases} \quad \forall \ r \in \{1,\ldots,R\}, \tag{6.4}$$

the path constraints:

$$\begin{cases} 0 \le f^{(r)}(s) \le F^{\max}, \\ 0 \le b^{(r)}(s) \le B^{\max}, \\ 0 \le f^{(r)}(s) \cdot v^{(r)}(s) \le P^{\max}, \\ 0 \le v^{(r)}(s) \le V^{\max,(r)}, \\ A^{\min} \le \dfrac{dv^{(r)}(s)}{dt^{(r)}(s)} \le A^{\max}, \end{cases} \quad \forall \ r \in \{1,\ldots,R\}, \tag{6.5}$$

the boundary conditions (if any):

$$\begin{cases} \underline{v}_{j,e} \le v^{(r)}(p_{j,e}) \le \bar{v}_{j,e}, \\ \underline{t}_{j,e} \le t^{(r)}(p_{j,e}) \le \bar{t}_{j,e}, \end{cases} \forall\, r \in \{1,\ldots,R\}, \quad p_{j,e} \in K_{\text{TPE piece}} \cap \{s_0^{(r)}, s_f^{(r)}\}, \tag{6.6}$$

and the linkage conditions of all adjacent phases:

$$\begin{cases} v^{(r_1)}(s_f^{(r_1)}) - v^{(r_2)}(s_0^{(r_2)}) = 0, \\ t^{(r_1)}(s_f^{(r_1)}) - t^{(r_2)}(s_0^{(r_2)}) = 0, \end{cases} \quad \forall (r_1, r_2) \in A. \tag{6.7}$$

The cost function (6.3) aims at minimizing the cost functions over all phases. R is the number of phases, $r \in \{1,\ldots,R\}$ is a phase, $J^{(r)}$ is the cost function of phase r

(see more details in Section 6.4.3), and J is the overall cost function of the trajectory optimization problem. For a phase $r \in \{1,\ldots,R\}$, $s_0^{(r)}$ denotes the initial location of phase r, and $s_f^{(r)}$ denotes the terminal location of phase r, $s_0^{(r)} < s_f^{(r)}$.

The dynamic constraints (6.4) are adopted by each phase $r \in \{1,\ldots,R\}$ to represent the dynamic movements within $[s_0^{(r)}, s_f^{(r)}]$. In Equations (6.4), s is the traversed distance [m], $s \in [s_0^{(r)}, s_f^{(r)}]$; $v^{(r)}(\cdot)$ is the train velocity in phase r [m/s]; ρ is the rotating mass factor; m is the train mass [t]; $f^{(r)}(\cdot)$ is the traction force in phase r [kN]; $b^{(r)}(\cdot)$ is the braking force in phase r [kN]; $R_{train}(v^{(r)}) = \alpha + \beta \cdot v^{(r)} + \gamma \cdot v^{(r)2}$ is the train resistance force [kN] with coefficients α, β and γ; $R_{line}^{(r)}(\cdot)$ is the line resistance force caused by the constant gradient within phase r [kN]; $t^{(r)}(\cdot)$ is the traversed time in phase r [s]; and $\theta_1, \theta_2 \in \{0,1\}$ are two binary parameters with $\theta_1 \cdot \theta_2 = 0$.

The path constraints (6.5) are used to represent the operational constraints of vehicle characteristics, speed limits, and riding comfort. $F^{\max}$, $B^{\max}$ and $P^{\max}$ are the maximum traction force, maximum braking force and maximum traction power. $V^{\max,(r)}$ is the speed limit of phase r, including static and temporary speed restrictions. $A^{\min}$ and $A^{\max}$ are the lower and upper bound of acceptable acceleration. The first two equations in the path constraints (6.5) are the formulation of the traction characteristic of Type-A in Fig. 6.5. As regards other types, they can also be represented with similar equations.

In (6.6), $K_{TPEpiece}$ is the set of TPE points within the TPE piece constructed by the pre-processing step in Section 6.4.2. Inequalities (6.6) work as the boundary conditions of phase r if $p_{j,e}$ is a TPE point within the TPE piece as well as the initial or terminal point of phase r. The TPE points are adopted as division-points, so phase r's initial or terminal point might be a TPE point, where time and speed restrictions on train operations apply.

The linkage conditions (6.7) are to make sure that the train's speed-distance and time-distance trajectories are continuous, where $A = \left\{(r_1, r_2) | s_f^{(r_1)} = s_0^{(r_2)}, r_1, r_2 \in \{1,\ldots,R\}\right\}$, which refers to the set of adjacent phases.

The trajectory optimization minimizes cost function (6.3) subject to (6.4-6.7). The pseudospectral method (Rao, 2003; Garg, 2011) transcribes the optimal control problem into an nonlinear programming (NLP) problem, and then solves it with an NLP solver.

Objective functions

The trajectory calculation has two different optimization targets, minimizing delay and minimizing energy consumption, for different circumstances. Minimizing delay is used if the train is delayed and cannot reach the target on time or does not have enough running time. The objective then is to run as fast as possible so that the train is able to

reach p_{end} with the least delay. The cost function for a phase $r \in \{1,\ldots,R\}$ is

$$J^{(r)} = \int_{s_0^{(r)}}^{s_f^{(r)}} \frac{1}{v^{(r)}(s)}\, ds. \tag{6.8}$$

The time window at the arrival location p_{end} has $\underline{t}_{end} \leq \bar{t}_{end}$, so that the train is not allowed to arrive earlier than the scheduled time $\underline{t}_{end}$ ($\underline{t}_{end}$ equals the planned arrival time), but is provided with sufficient time to arrive at p_{end} ($\bar{t}_{end}$ is bigger than the estimated earliest arrival time).

Minimizing energy consumption is chosen if the train has some time supplements. The cost function then is

$$J^{(r)} = \int_{s_0^{(r)}}^{s_f^{(r)}} f^{(r)}(s)\, ds. \tag{6.9}$$

The time window at p_{end} has $\underline{t}_{end} = \bar{t}_{end}$ for computing an energy-efficient trajectory so that the train arrives just at the planned arrival time.

Pseudospectral method

A Radau pseudospectral method (Garg, 2011) is chosen to solve the train trajectory optimization problem. In general, pseudospectral methods transcribe the continuous-time optimal control problem into a nonlinear programming problem, after which a nonlinear programming solver is adopted to directly solve the problem. The Radau pseudospectral method takes the Legendre-Gauss-Radau (LGR) points for collocation of the dynamic constraints, and for quadrature approximation of the integrated Lagrange cost term. The Lagrange polynomial approximation of the state, however, uses the LGR points plus the final point. It transcribes the continuous-time multiple-phase optimal control problem into a discrete NLP problem. The resulting NLP is then solved by SNOPT. For detailed mathematical descriptions, we recommend Rao et al. (2010); Wang and Goverde (2016); Ye and Liu (2016).

6.4.4 Post-processing

After an optimal trajectory is found, a post-processing step is applied, to generate advice at every sampling point (every 1 second) and integrate the new computed trajectory within the existing trajectory.

The solution computed by the pseudospectral method includes sequences of speed, time and distance at LGR points. The linear interpolation method is applied to compute the speed, time and distance at sampling points (Fig. 6.8). Meanwhile, additional information is added to every sampling point for later advice generation. The information at every sampling point contains

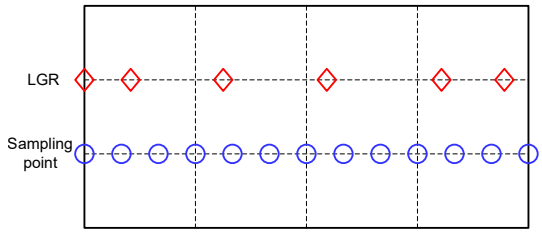

Figure 6.8: Schematic diagram of LGR points and sampling points.

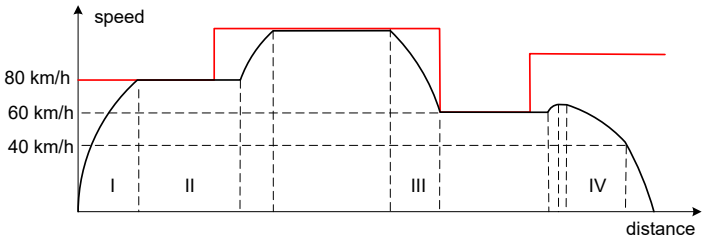

I: driving regime: acceleration with maximal traction; target speed: 80 km/h
II: driving regime: cruising at 80 km/h; target speed: 80 km/h
III: driving regime: braking with maximal effort; target speed: 60 km/h
IV: driving regime: coasting; target speed: 40 km/h

Figure 6.9: An example of the advisory target speeds.

1. The *time*;

2. The *distance*;

3. The *optimal speed*;

4. The *traction/braking effort*;

5. The *driving regime*, which include: (a) acceleration with maximal traction; (b) acceleration with partial traction; (c) coasting; (d) cruising at a constant speed; (e) braking with maximal effort; (f) braking with partial effort; (g) stop; (h) departure; and (i) end-of-advice;

6. The *target speed*; the target speed is the speed that the train wants to achieve at the end of the current driving regime. An example of target speeds is shown in Fig. 6.9. If the current advisory driving regime is acceleration, coasting, or braking, the target speed is the speed at the location of the next driving regime switch point.

7. The *distance to the approaching driving regime*;

8. The *time to the approaching driving regime*; and

9. The *distance to the approaching TPE point*.

The new computed trajectory between p_{start} and p_{end} is integrated within the existing trajectory, as the example shown in Fig.6.6 (e). The new trajectory replaces the existing trajectory if this section between p_{start} and p_{end} already got one. Otherwise, the new trajectory is combined with the existing trajectory.

6.5 Advice generation

The advice generation module computes the advice based on the real-time train state and the advisory trajectory. The real-time train state data provides real-time location, time, and speed. The advisory trajectory provides advice at every sampling point. The real-time train state enables the advice updated properly at every sampling point.

Currently, ETO provides three types of advisory information: *current advisory information*, *approaching advisory information*, and *state analysis information*. The purpose of providing current advisory information is that the driver knows what ETO is proposing at the current location of the train. Approaching advisory information allows the driver to prepare for any future change in advisory information. The state analysis information is helpful for the analysis of the energy consumption and delay status.

The current advisory information mainly contains the current advisory driving regime, the current target speed, the current optimal speed, and the current advisory traction/braking effort. The approaching advisory information can be classified into two types, the approaching driving regimes, and the approaching TPE points. The time and distance until the coming driving regime and TPE point are all delivered for better guidance to the drivers. More specifically, the approaching advisory information mainly contains the approaching driving regime, the distance to the approaching advisory driving regime, the time to the approaching advisory driving regime, the approaching timetable point, the approaching timetable point event, the distance to the approaching TPE point, and the expected delay at the approaching TPE point. The current state analysis information includes the current time deviation, the current speed deviation, the current energy used, and the current expected energy used. The current time deviation refers to the deviation from the advised time at the current location. The current speed deviation refers to the deviation of the current speed from the advised optimal speed at the current location. The current energy used is the energy that the train has used from the starting time of the ETO system. The current expected energy used is the energy that would be used if the train exactly follows the advisory trajectory from this current position.

The advice information and the speed profiles are presented on ETO's display and updated dynamically at every sampling point to support drivers making decisions. Future development includes the choice of proper information to be displayed and the visualization.

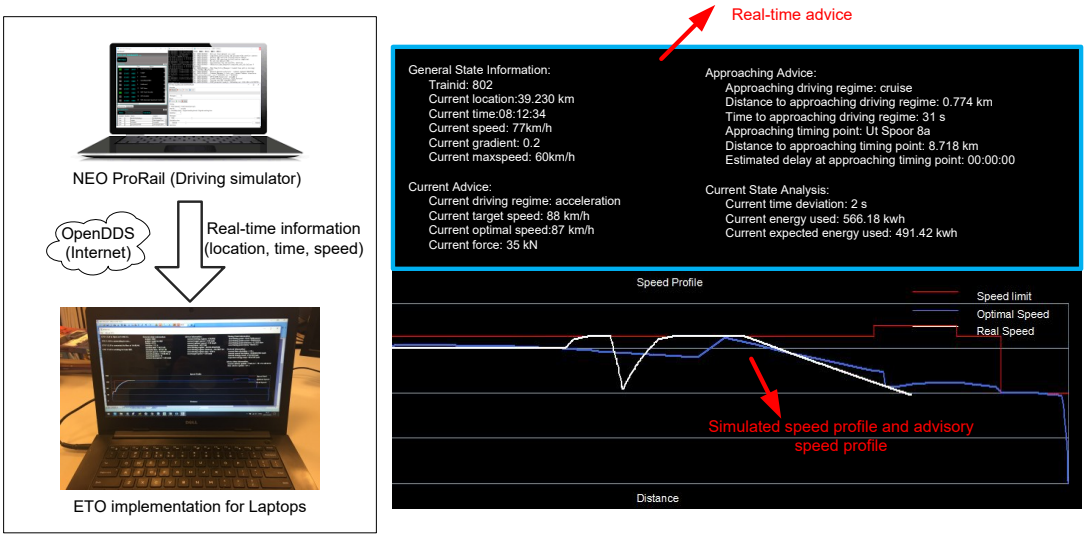

Figure 6.10: Test Environment for the ETO system (right) and Advisory information and speed profiles on ETO's display (left).

6.6 Test scenarios

6.6.1 Software technical aspects and test environment

The ETO prototype is developed in the Visual Studio platform using C++. Fig. 6.10 presents an example of ETO's display. The current display of ETO is just for the laboratory tests, which does not consider the human factors and user-friendliness yet, but presents all real-time advisory information and speed profiles. The trajectory calculation module requires a few seconds of computation times to find an optimal trajectory. During the computation process for a new trajectory, ETO assumes the existing trajectories to provide advice until a new trajectory is ready.

The ETO system has been tested in a laboratory environment. The test framework is shown in Fig. 6.10, where ETO runs on a laptop and is connected to the NEO simulation system using the Data Distribution Service (DDS) middleware (Pardo-Castellote, 2003). The rolling stock, infrastructure, and timetable data are stored in a database, assuming that ETO works alone without a connection to a traffic management system. The real-time information about train locaitons, times, and speeds are from the NEO system. NEO is being developed for the Dutch railway infrastructure manager ProRail and the Dutch Railways NS. NEO provides the function of simulating train movements and signalling system, and delivers simulated train locations, times and speeds to the ETO system in real time via OpenDDS. OpenDDS (Computing, 2009) is an open source C++ implementation of the DDS. It is an Object Management Group (OMG) machine-to-machine standard that aims to enable scalable, real-time, dependable, high-performance and interpretable data exchanges using a publish-subscribe pattern.

6.6.2 Test cases

This section demonstrates the approach with two different cases: case A provides a demonstration of energy-efficient driving while case B offers an example of delay-recovery driving. Case A assumes that a freight train travels on a short running section (4570 m) between two stops. The given running time contains enough time supplements so that coasting regimes are expected for energy saving. Case B assumes that an intercity train runs on the long corridor (around 50 km) from 's Hertogenbosch (Ht) to Utrecht (Ut). The given running time is smaller than the technical minimal running time, so the train is late compared to the planned arrival time at Ut station.

ETO and NEO are adopted for the two cases with ETO providing the advice information and NEO providing the simulated train locations, times and speeds in every 1 second. The test scenarios assume that NEO does not follow ETO's advice, but simulates the train behavior on its own way. The purpose is to test how ETO responses to the situation that the advice is not followed. Besides, ETO does not have access to the information about signal states at the current stage, but NEO does. Therefore the simulated train movements are influenced by the signalling system. ETO was carried out on a laptop equipped with a 3.2 GHz Pentium R processor. The time deviation threshold is 10 seconds, which means ETO re-computes the trajectory if the simulated train running time deviates more than 10 seconds from the advised time-distance path, either 10 seconds early or 10 seconds late.

The advisory speed profiles and simulated speed trajectories for the two cases are shown in Figs. 6.11 and 6.12 respectively. In each figure, the upper plot shows the advised speed profile (solid blue line), the simulated speed profile (dashed black lines) by NEO, and the speed limits (red horizontal lines). The top plots also contain several green crosses, which refer to the locations where new trajectories for the remaining sections were computed. The reasons for re-computation, the computation times (CPU time) and estimated delays at the last stations based on the new computed trajectories, are reported in a rectangular block. The bottom plots show all the advised speed profiles computed by the ETO system. They are represented in different colors, each color represents one individual speed profile. The solid parts are used for the advice generation, while the dashed lines are not used, but are replaced with new speed profiles. All the solid lines on the bottom plots comprise the advised speed profile on the top plots.

The advised speed profile in Fig. 6.11, ETO suggests the freight train to accelerate during the outbound process, and then cruise at the maximum allowed speed 40 km/h. The train speed must stay below 40 km/h until the train's tail passes the region with speed limit 40 km/h. After that, the freight train is suggested to accelerate, cruise at 60 km/h, and then coast for a while before braking. Because the given running time is longer than the technical minimal running time. Coasting is encouraged to save energy consumption. The simulated speed profile is provided by the NEO system, its speeds are higher than the advise speeds in the middle of this running section. Therefore

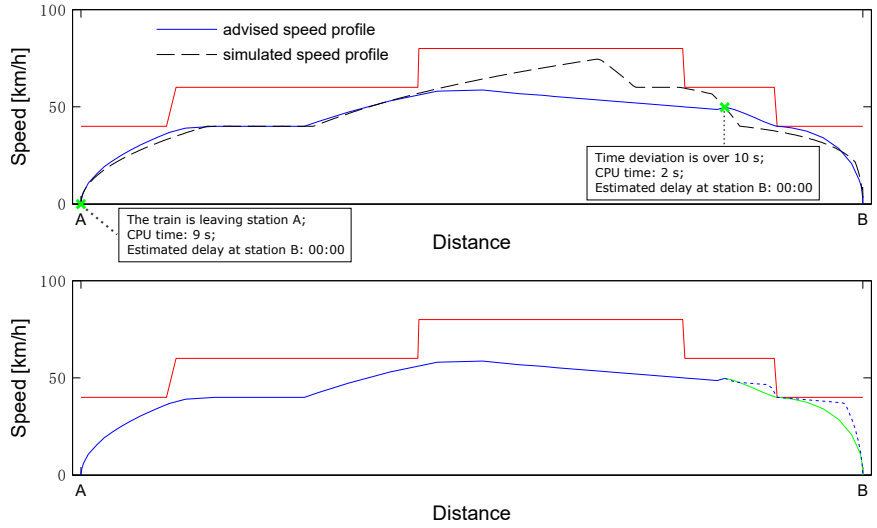

Figure 6.11: The advised speed profiles and practical speed profiles of a freight train between A and B.

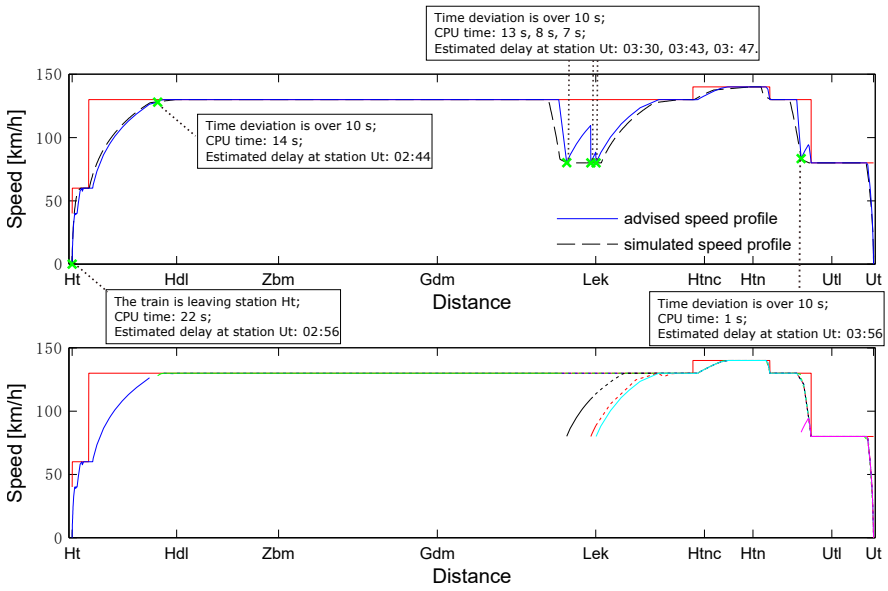

Figure 6.12: The advised speed profiles and practical speed profiles of an Intercity train between Ht and Ut.

the train goes earlier than the advised time-distance path. At location 3761.1 m, the simulated time is 10 s earlier than the advised one, so that a new trajectory from 3761.1 m to the arrival point is re-computed. The new trajectory suggests the train to use less braking force since the train is ahead of the schedule and coasting would lead to an early arrival. The computation times for the two trajectories (from the departure point to the arrival point and from the location of 3761.1 m to the arrival point) are respectively 9 s and 2 s.

In Fig. 6.12, the intercity train is advised to use the full acceleration and braking and travel at the maximum speed because the given running time is shorter than the technical minimal running time. The train will be late at the arrival station. Thus the delay-recovery strategy is adopted. In the beginning, the simulated speed curve did not take into account the safety of the train tail, which accelerates immediately after the train head passed through the low speed limits. Therefore the simulated running time gets 10 s ahead of the advisory profile at 2607.3 m, and a new trajectory from 2607.3 m to Ut station is re-computed by ETO. In the middle, the simulated speed profile meets a yellow 8 signal, and the train brakes to 80 km/h. ETO finds that the train travels at a lower speed than the advised speed (130 km/h). It re-computes the trajectory and advises the train to accelerate and come back to 130 km/h again because the train is already late. At 43438.4 m, the simulated speed profile brakes earlier than advised, which would cause a further delay at the Ut station. ETO recomputes a new trajectory from 43438.4 m to Ut, and advises the train to accelerate a little bit before braking to reduce the delay. The computation times for each trajectory are shown in Fig. 6.12. For the 50 km corridor, the longest computation time is 22 s and the shortest is 1 s. The values of the expected delays are updated with every new trajectory.

Throughout all the advised speed profiles, the train speeds stay below the speed limits. The advisory speed profiles advise the driver to regulate train speed at the varying speed limits via decelerating before low speed limits and accelerating before high speed limits, where the trains only accelerate after the entire train passed the low speed limits. The trains stop at the planned stop target positions, which means that safety and accurate stops are guaranteed if the driver follows the advisory speed profiles. The advised speed profiles give the priority to the delay recovery, and try to get the trains back to schedule as soon as possible. Energy efficient driving is suggested if the train has sufficient running times. The test scenarios show that the ETO system can provide advisory trajectories within short computation times. It is also able to respond to the time deviations between the actual and advisory time-distance paths.

6.7 Conclusions

A prototype new train driver advisory system ETO (energy-efficient train operation) has been presented in this paper. We have provided answers of how to design a DAS system, how to advise the drivers to efficiently control the train with minimal energy

consumption and get the train back to its timetable in case of delays, and how to dynamically update the trajectory and the advice if the actual train movement does not follow the advisory information.

The article presents an overview of the ETO system. ETO consists of two versions: Standalone ETO and Connected ETO. The functions and the underlying mathematical models of the trajectory computation and advice generation modules are described in details. The test scenarios are presented to show the performances of Standalone ETO.

In the future, we will focus on further development of the ETO system: an interface considering human factors and user-friendliness, future tests with consideration of the signalling system and interaction between multiple trains, and a connection to a rail traffic management system.

Bibliography

Albrecht, A., Howlett, P., Pudney, P., Vu, X., Zhou, P., 2016a. The key principles of optimal train control—part 1: Formulation of the model, strategies of optimal type, evolutionary lines, location of optimal switching points. Transportation Research Part B: Methodological 94, 482–508.

Albrecht, A., Howlett, P., Pudney, P., Vu, X., Zhou, P., 2016b. The key principles of optimal train control—part 2: Existence of an optimal strategy, the local energy minimization principle, uniqueness, computational techniques. Transportation Research Part B: Methodological 94, 509–538.

Albrecht, A., Koelewijn, J., Pudney, P., 2011. Energy-efficient recovery of delays in a rail network. In: Proceedings of 2011 Australasian Transport Research Forum. Adelaide, Australia, pp. 1–7.

Albrecht, T., Binder, A., Gassel, C., 2013. Applications of real-time speed control in rail-bound public transportation systems. IET Intelligent Transport Systems 7 (3), 305–314.

Cheng, J., Howlett, P., 1992. Application of critical velocities to the minimisation of fuel consumption in the control of trains. Automatica 28 (1), 165–169.

Computing, O., 2009. Inc. opendds developer's guide. Http://download. ociweb. com/OpenDDS/OpenDDS-latest. pdf.

Curis, 2017. Greenspeed. Http://www.cubris.dk/what-is-greenspeed/.

Dong, H., Ning, B., Cai, B., Hou, Z., 2010. Automatic train control system development and simulation for high-speed railways. IEEE circuits and systems magazine 10 (2), 6–18.

Garg, D., 2011. Advances in global pseudospectral methods for optimal control. Ph.D. thesis, University of Florida, Gainesville, USA.

Haahr, J. T., Pisinger, D., Sabbaghian, M., 2017. A dynamic programming approach for optimizing train speed profiles with speed restrictions and passage points. Transportation Research Part B: Methodological 99, 167–182.

Howlett, P., 1996. Optimal strategies for the control of a train. Automatica 32 (4), 519–532.

Howlett, P., Pudney, P., 2012. Energy-efficient train control. Springer.

Junaid, K. M., Wang, S., 2006. Automatic cruise control modeling-a lattice pwl approximation approach. In: Intelligent Transportation Systems Conference, 2006. ITSC'06. IEEE. IEEE, pp. 1370–1375.

Khmelnitsky, E., 2000. On an optimal control problem of train operation. IEEE Transactions on Automatic Control 45 (7), 1257–1266.

Knorr-bremse, 2009. Leader, driver advisory system. Http:// www.knorr-bremse.com/media/documents/railvehicles/product_broschures/extra/ Leader_1220_EN.pdf.

Liu, R., Golovitcher, I. M., 2003. Energy-efficient operation of rail vehicles. Transportation Research Part A: Policy and Practice 37 (10), 917–932.

Mehta, F., Rößiger, C., Montigel, M., 2010. Latent energy savings due to the innovative use of advisory speeds to avoid occupation conflicts. In: 2010 International Conference on Computer System Design and Operation in the Railway and other Transit Systems (COMPRAIL 2010). Southampton, UK, pp. 99–108.

Milroy, I. P., 1980. Aspects of automatic train control. Ph.D. thesis, Loughborough University, Leicestershire, UK.

Nash, A., Huerlimann, D., Schütte, J., Krauss, V. P., 2004. Railml† a standard data interface for railroad applications. WIT Transactions on The Built Environment 74.

ON-TIME, 2014. Best practice, recommendations and standardisation. Deliverable ONT-WP01-DEL-003.

Panou, K., Tzieropoulos, P., Emery, D., 2013. Railway driver advice systems: Evaluation of methods, tools and systems. Journal of Rail Transport Planning & Management 3 (4), 150–162.

Pardo-Castellote, G., 2003. Omg data-distribution service: Architectural overview. In: 23rd International Conference on Distributed Computing Systems Workshops. Rhode Island, USA, pp. 200–206.

Pudney, P., Howlett, P., 1994. Optimal driving strategies for a train journey with speed limits. The Journal of the Australian Mathematical Society. Series B. Applied Mathematics 36 (01), 38–49.

Quaglietta, E., Pellegrini, P., Goverde, R. M. P., Albrecht, T., Jaekel, B., Marlière, G., Rodriguez, J., Dollevoet, T., Ambrogio, B., Carcasole, D., et al., 2016. The on-time real-time railway traffic management framework: A proof-of-concept using

a scalable standardised data communication architecture. Transportation Research Part C: Emerging Technologies 63, 23–50.

Rao, A. V., 2003. Extension of a pseudospectral legendre method to non-sequential multiple-phase optimal control problems. In: AIAA Guidance, Navigation, and Control Conference and Exhibit. Austin, USA, pp. 11–14.

Rao, A. V., Benson, D. A., Darby, C., Patterson, M. A., Francolin, C., Sanders, I., Huntington, G. T., 2010. Algorithm 902: GPOPS, a matlab software for solving multiple-phase optimal control problems using the gauss pseudospectral method. ACM Transactions on Mathematical Software 37 (2), 22.

Tschirner, S., Andersson, A. W., Sandblad, B., 2013. Improved railway service by shared traffic information. In: 2013 IEEE International Conference on Intelligent Rail Transportation (ICIRT). Beijing, China, pp. 117–122.

Wang, P., Goverde, R. M. P., 2016. Multiple-phase train trajectory optimization with signalling and operational constraints. Transportation Research Part C: Emerging Technologies 69, 255–275.

Ye, H., Liu, R., 2016. A multiphase optimal control method for multi-train control and scheduling on railway lines. Transportation Research Part B: Methodological 93, 377–393.

Chapter 7

Conclusions and recommendations

This thesis is motivated by the challenges in improving energy-efficiency of train operations outlined in Chapter 1. The main objectives are to develop the modelling and solution methods for the train trajectory optimization problem to improve the model accuracy and the computation time, to apply the methods in a train driver advisory system development, and to develop a multi-train trajectory optimization method to solve the delay recovery and the energy-efficient timetabling problem. Several research questions are stated under the research objectives, which are answered throughout Chapters 2-6. This chapter summarises the answers. First, the main conclusions are synthesised from the perspectives in Section 7.1. Section 7.2 recommends future research directions and practical recommendations.

7.1 Main findings and conclusions

The modelling and solution methods for train trajectory optimization

The train trajectory optimization problem was formulated as a multiple-phase optimal control problem, which answers the question of *how to formulate an accurate model for the train trajectory optimization problem*. The train path envelope (TPE) was adopted to characterize the timetable restrictions on train movements. The restrictions include the time and speed constraints (targets or windows) at stops, passing-through stations, and other timetable relevant locations. The multiple-phase optimal control problem divides the whole train trajectory into multiple segments. The division-points include critical points of speed limits or gradients and curves, timetable points, conflict points, and signal locations. Each divided segment is a phase, where any particular phase of an optimal control problem has its own cost function (minimizing energy costs or delays), dynamic model (train dynamic movement model), path constraints (vehicle characteristics, speed limits, and riding comfort), and boundary conditions (time and speed constraints at timetable points, conflict points, and signal locations). The complete trajectory is then obtained by properly linking adjacent phases via linkage

conditions. The total cost function is the sum of the cost functions within each phase. The optimal trajectory is then found by minimizing the total cost functional subject to the constraints within each phase and the linkage constraints connecting adjacent phases. The advantages of this modelling method are multiple: it gives an accurate description of varying speed limits and gradients, and the time and speed restrictions at timetable points, conflict points and signal location; and it allows flexibility in minimizing energy consumption and delays.

A Pseudospectral method was used to transcribe the multiple-phase optimal control problem to a nonlinear programming problem (NLP), and then solve it within by NLP solvers. That is the answer to the question of *which solution approach can be used to solve the train trajectory optimization in short time*. The Pseudospectral method transcribes the continuous-time optimal control problem into an NLP problem. The resulting NLP problem can be solved by nonlinear optimization algorithms. There are several well-developed packages that implement the Pseudospectral method, in which GPOPS was adopted in this research, that is, a Matlab-based open source tool that uses the Radau Pseudospectral Method to solve the multiple-phase optimal control problem. Experiments showed that the Pseudospectral method is able to compute the optimal driving strategy within a short time, even for the train running on a corridor with complex speed limits and gradients.

Multi-train trajectory optimization method

A multi-train trajectory optimization (MTTO) method was proposed to answer the question of *what are feasible modelling and solution methods for the multi-train trajectory optimization problem*. The MTTO model aims at minimizing all involved trains' energy costs or delays, with the consideration of every single train's operational constraints (dynamic movement model, vehicle characteristics, speed limits, TPE constraints, etc.), as well as the requirements of avoiding conflicts between trains. The MTTO model is then reformulated as a multiple-phase optimal control problem and solved with the Pseudospectral method.

The key features of the MTTO method are: the MTTO method optimizes multi-train trajectories simultaneously for energy-efficient or less delayed train movements; it is flexible since the trains can be in the same and opposite directions, use different rolling stock compositions, speed limits, timetable constraints, routes and station platforms; and the MTTO method ensures safe interactions between trains since it includes constraints to keep safe headways between adjacent trains and to avoid conflicts. Compared to the single-train trajectory optimization (STTO) methods, the MTTO method has the advantage of characterising the interaction between trains and allowing multi-train cooperations. This method was adopted in the research of energy-efficient delay recovery and energy-efficient timetabling.

Energy-efficient delay recovery methods

A single-train delay recovery strategy was proposed with consideration of signalling constraints, which answers the question of *how can we ensure a single train gets back to its schedule with less energy consumption, as well as efficiently respond to signal systems, when the train is delayed*. The single-train delay recovery strategy was developed on basis of the proposed STTO method, with the TPE representing the timetable constraints, the STTO formulated as a multiple-phase optimal control problem, and the Pseudospectral method solving the problem. If the train is later than the schedule times, the strategy aims at reducing delays and getting the train back to its schedule as soon as possible. If the train runs on-time, the objective is to reduce energy costs. The influence from signal systems on train operations is taken into account. A signal response policy and a green wave policy are proposed for different circumstances of available signal information. The signal response policy ensures that the train makes correct and quick responses to different signalling aspects in case that only limited available information about one signal in rear of the train ahead. The green wave policy avoids yellow signals in case that a full prediction is available about the signal aspect timings in rear of the train ahead. Experimental results showed that, compared to the signal response policy, having access to predictive information of the leading train and the green wave policy are more beneficial for saving energy consumption and reducing train delays.

A multi-train delay recovery method was proposed based on the multi-train trajectory optimization approach. It provides an answer to the question of *how can we avoid yellow and red signals and the stop/start behavior with a multi-train cooperation method, when the train operations are interrupted by unexpected events*. The multi-train delay recovery method can reduce delays and energy consumption by multi-train cooperation. The primary goal of the multi-train delay recovery method is to reduce delays and delay propagation. Energy saving relays on making use of waiting times (waiting times are caused by avoiding conflicts with delayed trains). For the trains running in same directions, the green wave policy was used to reduce the chance of meeting yellow signals and thus avoid inefficient stop/start behavior. For the trains in opposite directions, a strategy of selecting best driving strategy for each running section and best meeting stations of opposite trains was proposed, which is beneficial for delay recovery and energy-efficient driving.

In general, the energy-efficient delay recovery methods are capable of reducing delay propagation, saving energy consumption, and avoiding inefficient stop/start behaviors.

Energy-efficient timetabling

This thesis proposed a novel method of energy-efficient timetable adjustment on the train trajectory optimization level, to answer the question of *how can we improve the timetable's energy efficiency with the trajectory optimization method*. The energy-efficient timetabling is achieved by using the trajectory optimization method to adjust

the arrival and departure times of an existing timetable with the purpose of improving the timetable's energy efficiency. The given timetable is converted into flexible arrival and departure time window constraints first, then the STTO method is adopted to compute the energy-efficient speed profiles and time paths of the trains involved in the timetable separately. After that, detect conflicts. If there are conflicts between the time paths, the MTTO method is adopted to re-compute the speed profiles and time paths, while eliminating the conflicts.

Experiments showed that the method jointly optimizes train trajectories and the timetable. The arrival and departure times of an existing timetable are shifted by the trajectory optimization methods, so that the time supplements are optimally allocated for energy efficient operation.

Driver advisory system development

A prototype of a new train driver advisory system ETO (energy-efficient train operation) has been presented in this thesis with the application of the proposed trajectory optimization method. This gives an answer to the question of *how can we implement the proposed train trajectory optimization method into a driver advisory system*. ETO's framework is presented in this thesis, as well as the functions and the underlying mathematical models of the sub-modules within the framework.

ETO advises drivers how to achieve, from a given current location and with a specific destination arrival time, an energy-efficient or delay-recovery (if the train has delays) train operation. ETO takes into account the train path envelope constraints, not only the arrival and departure times, but also time restitutions at other timing points and conflict points. ETO respects speed restrictions, and takes into account varying gradients and curves. ETO automatically responses to the deviations of the actual time-distance path from the advised one, and re-computes and updates speed profiles and advice, ensuring that the driver is supplied with the best possible advice for punctual arrival with minimal energy consumption. The test scenarios showed that ETO has advantages on real-time performance, and accurate computations.

7.2 Future research directions and practical recommendations

In this section, we recommend several directions for future research and practical recommendations.

The first suggestion for future research is to explore more on the topic of energy-efficient train operations. Improving energy consumption through optimizing train operations is a good option, since it does not need investment on extra infrastructure. Research on energy-efficient train operations can be carried out from two aspects,

off-line planning and real-time traffic management. The off-line planning includes line planning, timetable design, and rolling stock scheduling. Improving energy efficiency can play a significant roll during the off-line planning processes, however, which have not drawn enough attention yet. Meanwhile, real-time traffic management directly influences the energy consumption of train operations. Investing in novel traffic management and train control methods in order to save energy consumption is essential.

The second suggestion for future research is to explore more efficient solution methods for the train trajectory optimization method. The train trajectory optimization requires short computation time since it is an important part of the driver advisory systems (DASs) for real-time trajectory computation. The proposed algorithms provide an accurate modelling method for the train trajectory optimization problem. The Pseudospectal method is capable of solving the problem within a short time, for instances, which produces an optimal trajectory within 30 seconds for a train run on a 50 km long corridor. Future research on shortening the computation time without reducing the accuracy of solutions is still an important issue. This thesis provided a direction of using direct methods in solving the train trajectory optimization problem, which improves the computation speed and can be further improved for more efficient solution methods.

A third future research direction is to take into account the human factors issue when designing a driver advisory system since human drivers still play an important role. In this thesis, ETO's advice and user interface have not taken into account human factors. It is necessary to perform future research on considering and testing human factors in relation to the proposed ETO system and understand how do human drivers react to the advice information and how to design a user-friendly interface.

A fourth future research direction is to investigate how to implement the DASs in a mainline railway system. ATO (Automatic Train Operation) systems have been used in real-world metro lines. However, train operations on mainlines are more complicated compared to the operations on metro lines. The mainlines contain more rolling stock types, more complex network layouts, and more complex service plans, which arises the difficulties of developing a practicable DAS. We provided a flexible modelling method for trajectory optimization, which can handle varying speed limits and gradients, flexible timetable constraints, route changes, signal constraints and so on. Further investigation in the trajectory optimization methods with consideration of more practical factors is necessary for future DAS implementation.

Last but not least, connecting the DASs to a rail traffic management system (TMS) is highly recommended. In this thesis, the ETO system is tested with a static timetable. ETO can be easily connected to a TMS. It is interesting to test the effectiveness of the proposed ETO system in more practical situations. For instances, how does ETO respond to an updated timetable or new route? How does ETO provide real-time traffic information to drivers? Answering these questions entails development of analysis,

modelling and simulation tools to improve and test the feasibility and performance related to the driver advisory system.

Summary

Even though rail is more energy efficient than most other transport modes, the enhancement of energy efficiency is an important issue for railways to reduce their contributions to climate change further as well as to save costs and enlarge competition advantages involved. This thesis is motivated by the challenges in improving energy-efficiency of train operations. The main objectives are to develop the modelling and solution methods for the train trajectory optimization problem to improve the model accuracy and the computation time, to apply the methods in a train driver advisory system development, and to develop a multi-train trajectory optimization method to solve the delay recovery and the energy-efficient timetabling problem.

First, the train trajectory optimization was formulated as a multiple-phase optimal control problem and solved by a pseudospectral method. The multiple-phase optimal control problem divides the whole train trajectory into multiple phases. The optimal trajectory is then found by minimizing the total cost functional of all phases subject to the constraints within each phase and the linkage constraints connecting adjacent phases. The multiple-phase optimal control problem gives an accurate description of varying speed limits and gradients, and the time and speed restrictions at timetable points, conflict points and signal location; and it allows flexibility in minimizing energy consumption and delays. A pseudospectral method was used to transcribe the multiple-phase optimal control problem to a nonlinear programming (NLP) problem, and then solve it within by NLP solvers. Experiments showed that the pseudospectral method is able to compute the optimal driving strategy within a short time, even for a train running on a corridor with complex speed limits and gradients.

Secondly, a multi-train trajectory optimization method was proposed. The multi-train trajectory optimization method optimizes multi-train trajectories simultaneously for energy-efficient or less delayed train movements. The multiple trains can be in the same and opposite directions, and use different rolling stock compositions, speed limits, timetable constraints, routes and station platforms. Safe interactions between trains are guaranteed by the multi-train trajectory optimization method, since constraints to keep safe headways between adjacent trains and to avoid conflicts are taken into account. This method was adopted in the research of energy-efficient delay recovery and energy-efficient timetabling.

Third, we investigated the energy-efficient delay recovery methods both from the perspectives of single-train and multi-train movements. For a single delayed train,

the single-train delay recovery strategy aims at reducing delays and getting the train back to schedule as soon as possible. The influence from signal systems on train operations is taken into account. A signal response policy and a green wave policy are proposed for different circumstances of available signal information. The signal response policy ensures that the train makes correct and quick responses to different signalling aspects in case of only limited available information about one signal in rear of the train. The green wave policy avoids yellow signals in case that a full prediction is available about the signal aspect timings in rear of the train ahead. Experimental results showed that, compared to the signal response policy, having access to predictive information of the leading train and the green wave policy are more beneficial for saving energy consumption and reducing train delays. Besides, a multi-train delay recovery method was proposed, which reduces delays and energy consumption by multi-train cooperation. The primary goal of the multi-train delay recovery method is to reduce delays and delay propagation. Energy saving relies on making use of extra running times caused by avoiding conflicts with delayed trains. For the trains running in the same direction, the green wave policy was used to reduce the chance of meeting yellow signals and thus avoid inefficient stop/start behavior. For the trains running in opposite directions, a strategy of selecting best driving strategy for each running section and best meeting stations of opposite trains was proposed, which is beneficial for delay recovery and energy-efficient driving.

Fourth, we proposed a novel method of energy-efficient timetable adjustment on the train trajectory optimization level. The energy-efficient timetabling is achieved by using the trajectory optimization method to adjust the arrival and departure times of an existing timetable with the purpose of improving the timetable's energy efficiency. The given timetable is converted into flexible arrival and departure time window constraints first, then the trajectory optimization method is adopted to compute the energy-efficient speed profiles and time paths of the trains involved in the timetable. Experiments showed that the method jointly optimizes train trajectories and the timetable. The arrival and departure times of an existing timetable are shifted by the trajectory optimization methods, so that the time supplements are optimally allocated for energy efficient operation.

Fifth, a prototype of a new train driver advisory system, ETO (energy-efficient train operation), has been presented in this thesis with the application of the proposed trajectory optimization method. ETO advises drivers how to achieve an energy-efficient or delay-recovery train operation. ETO takes into account not only the arrival and departure times, but also time restitutions at other timing points and conflict points. ETO respects speed restrictions, and takes into account varying gradients and curves. ETO automatically responses to the deviations of the actual time-distance path from the advised one, and re-computes and updates speed profiles and advice, ensuring that the driver is supplied with the best possible advice for punctual arrival with minimal energy consumption. The test scenarios showed that ETO has advantages for real-time performance, and have accurate computations.

In summary, this thesis demonstrated that train trajectory optimization methods can be successfully applied to improving energy efficiency of railway systems.

Samenvatting

Alhoewel railvervoer energiezuiniger is dan de meeste andere vervoermodaliteiten, is een verdere energiebesparing belangrijk voor de spoorwegen om hun aandeel in de klimaatverandering verder te verminderen en bovendien de kosten te verlagen en daarmee de concurrentiepotitie te verbeteren. Dit proefschrift is gemotiveerd door de uitdagingen van energiezuinig rijden van treinen. Dit proefschrift richt zich op het bepalen van de optimale trajectorie van een trein, d.w.z. het snelheidsprofiel van een trein met het daarbij behorende tijdwegpad. De hoofddoelen zijn de ontwikkeling van modellen en oplossingsmethoden voor het treintrajectorie optimaliseringsprobleem met betere modelnauwkeurigheid en rekentijden, het toepassen van die methoden in de ontwikkeling van een rijadviessysteem, en de ontwikkeling van een multi-treintrajectorie optimaliseringsmethode voor het optimaal inhalen van vertragingen en het berekenen van energiezuinige dienstregelingen.

Allereerst is de treintrajectorieoptimalisatie geformuleerd als een multi-fase optimaal besturingsprobleem en opgelost met een pseudospectrale methode. Het multi-fase optimale besturingsprobleem verdeelt de hele treintrajectorie in meerdere fases. De optimale trajectorie wordt dan gevonden door minimalisering van de totale kosten over alle fases onder de beperkingen in iedere fase en de extra beperkingen die de opeenvolgende fases aan elkaar koppelen. Het multi-fase optimale besturingsprobleem geeft een nauwkeurige beschrijving van de wisselende snelheidsgrenzen en hellingen alsmede de tijd- en snelheidsrestricties op dienstregelingspunten, conflictpunten en seinposities, en het geeft flexibiliteit in het minimaliseren van energiegebruik en vertragingen. Een pseudospectale methode is gebruikt om het multi-fase optimale besturingsprobleem te transformeren naar een niet-lineair programmeringsprobleem (NLP pobleem) en dat op te lossen met een NLP-oplossingsmethode. Experimenten hebben laten zien dat de pseudospectrale methode de optimale rijstrategie in korte tijd kan berekenen, zelfs voor een trein die rijdt op een corridor met complexe snelheidsgrenzen en hellingen.

Ten tweede is een multi-treintrajectorie optimaliseringsprobleem voorgesteld. Het multi-treintrajectorie optimaliseringsprobleem optimaliseert meerdere treintrajectoriën tegelijkertijd voor energiezuinig rijden of minder vertraagde treinbewegingen. De treinen kunnen zowel in dezelfde als in de tegengestelde richting rijden, en gebruik maken van verschillende materieelsamenstellingen, snelheidsgrenzen, dienstregelings-beperkingen, rijwegen en perronsporen. Veilige interacties tussen treinen worden

gewaarborgd in het multi-treintrajectorie optimaliseringsprobleem doordat beperkingen voor veilige volgafstanden en voorkomen van conflicten tussen achtereenvolgende en kruisende treinen zijn meegenomen. Deze methode is gebruikt in de onderzoeken naar energiezuinig vertragingsherstel en energiezuinige dienstregelingen.

Als derde hebben we methoden onderzocht voor energiezuinig vertragingsherstel vanuit het perspectief van zowel enkele treinen als multi-trein bewegingen. Voor een enkele vertraagde trein beoogt de enkele-trein vertragingsherstelstrategie de vertraging te reduceren en de trein zo snel mogelijk weer naar het plan terug te brengen. De invloed van seinsystemen op de treinafwikkeling is meegenomen. Een seinresponsie tactiek en een groene-golf tactiek zijn voorgesteld voor verschillende omstandigheden van beschikbare seininformatie. De seinresponsie tactiek garandeert dat de trein juist en snel reageert op verschillende seinbeelden in het geval dat slechts informatie over één sein verderop beshikbaar is. De groene golf tactiek vermijdt gele seinen in het geval dat een volledige voorspelling beschikbaar is over de seinbeeldtijdstappen achter de voorliggende trein. Experimentele resultaten laten zien dat toegang hebben tot voorspellende informatie over de voorliggende trein in combinatie met de groene golf tactiek beter is voor energiebesparing en vertragingen dan de seinresponsie tactiek. Daarnaast is een multi-trein vertragingsherstelmethode voorgesteld, die vertragingen en energiegebruik reduceert door samenwerking tussen de treinen. Het primaire doel van de multi-trein vertragingsherstelmethode is om vertragingen en vertragingsvoortplanting te verminderen. Energiebesparing kan worden behaald door gebruik te maken van extra rijtijd door anticipatie op het voorkomen van conflicten met vertraagde treinen. Voor treinen in dezelfde richting is de groene golf tactiek gebruikt om de kans op een geel sein te verminderen en daarmee inefficiënt stop-start gedrag te voorkomen. Voor tegengestelde treinen is een selectieprocedure voorgesteld dat de beste rijstrategie voor ieder baanvak bepaalt alsmede de beste ontmoetingsstations waar tegemoetkomende treinen elkaar kunnen passeren. Dit is voordelig voor zowel vertragingsherstel als energiezuinig rijden.

Als vierde hebben we een nieuwe methode voorgesteld voor energiezuinige dienstregelingsaanpassingen op het niveau van treintrajectorieoptimalisering. De energiezuinige dienstregeling wordt bereikt door de treintrajectorieoptimaliseringmethode te gebruiken om de aankomst- en vertrektijden van een bestaande dienstregeling aan te passen met als doel om het energiegebruik van de dienstregeling te verbeteren. De gegeven dienstregeling wordt eerst geconverteerd naar flexibele tijdvensters voor de aankomst- en vertrektijden, waarna de trajectorieoptimaliseringmethode wordt toegepast om energiezuinige snelheidsprofielen en tijdwegpaden te berekenen van de treinen in de dienstregeling. Experimenten laten zien dat de methode de treintrajectoriën en dienstregeling gezamenlijk optimaliseert. De aankomst en vertrektijden van een bestaande dienstregeling worden verschoven door de treintrajectorieoptimaliseringmethode zodat de rijtijdspelingen optimaal worden verdeeld voor energiezuinig rijden.

Als vijfde is in dit proefschrift een prototype machinistadviessysteem, ETO (Energiezuinige Trein Operatie), gepresenteerd waarin de voorgestelde treintrajectorieoptimalisering wordt toegepast. ETO adviseert machinisten over een energiebesparende of vertragingsherstellende treinafhandeling. ETO houdt rekening met alle tijdvensterbeperkingen, niet alleen de aankomst- en vertrektijden, maar ook tijdrestricties op andere dienstregelingspunten en conflictpunten. ETO respecteert snelheidsbeperkingen en wisselende hellingen en boogstralen. ETO reageert automatisch op afwijkingen van de geadviseerde tijdwegpaden, en herberekent en vernieuwt de snelheidsprofielen en adviezen, zodat de machinist continu het best mogelijke advies krijgt voor punctueel en energiezuinig rijden. De testscenarios lieten zien dat ETO voordelig is voor de real-time prestaties en de berekeningen nauwkeurig zijn.

Samenvattend demonstreert dit proefschrift dat treintrajectorieoptimaliseringmethoden succesvol kunnen worden toegepast voor energiebesparing van railsystemen.

About the author

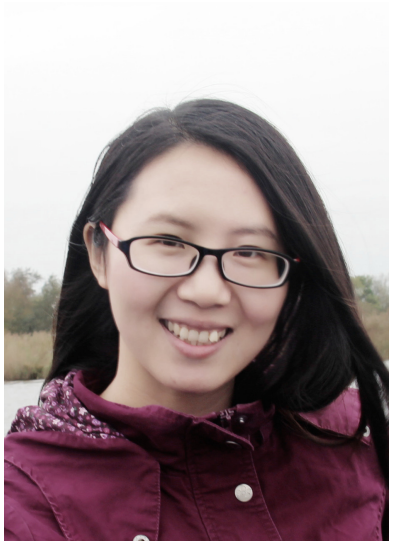

Pengling Wang was born in China in 1989. She graduated in Electric Power System and Automation at Southwest Jiaotong University in 2011. In the same year, she started her master of Power Electronics and Power Drives at Southwest Jiaotong University, under the supervision of Prof. Chunyang Chen and Prof. Xiaoyun Feng. After one year of master study, in 2012, she started her Ph.D research in Control Theory and Science, under the supervision of Prof. Lei Ma. The research topic was about "Multi-Train Operation Optimization and Control for Railway Traffic Conflict Detection and Resolution". In 2017, she received a Doctor degree of Control Science and Engineering.

In 2014 she came to the Netherlands, and she joined the Transportation and Planning section at Delft University of Technology. Here she started a new Ph.D. research in train trajectory optimization. This research was funded by the Chinese Scholarship Council and the Dutch Infrastructure manager ProRail, and under the supervision of Prof. Rob M.P. Goverde and Prof. Serge Hoogendoorn. Now she is a post-doc researcher at TU Delft, working on test algorithms for train driver advisory systems.

Her research interests include real-time railway system management, train operation optimization and control, and driver advisory systems.

Publications

Journal articles

1. **Wang P**, Goverde, R M P. (2017). Multi-train trajectory optimization for energy efficiency and delay recovery on single-track railway lines. Transportation Research Part B: Methodological, 105, 340-361.

2. Lin X, Wang Q, **Wang P**, Sun P, Feng X. (2017). Energy-efficient operation problem of a freight train considering the long-distance steep downhill. Energies, 10(6): 794.

3. **Wang P**, Goverde R M P. (2016). Multiple-phase train trajectory optimization with signalling and operational constraints. Transportation Research Part C: Emerging Technologies, 69: 255-275.

4. **Wang P**, Goverde R M P. (2016). Two-train trajectory optimization with a green-wave policy. Transportation Research Record: Journal of the Transportation Research Board, 2546: 112-120.

5. **Wang P**, Ma L, Goverde R M P, Wang Q. (2016). Rescheduling trains using Petri nets and heuristic search. IEEE Transactions on Intelligent Transportation Systems, 17(3): 726-735.

6. **Wang P**, Ma L, Wang Q, Feng X. (2015). Analysis of train operation conflict based on train group model using petri nets. Journal of the China Railway Society, 3: 002. (In Chinese)

7. **Wang P**, Wang Q, Cui H, Feng X. (2013). Automatic train control algorithm for train tracking. Journal of Southwest Jiaotong University, 6: 012. (In Chinese)

8. **Wang P**, Lin X, Li Y, Feng X. (2012) Energy saving train operation optimization with adaptive genetic algorithm. Computer Simulation, 29(11): 350-354. (In Chinese)

Working articles

1. **Wang P**, Goverde R M P. (2017). Multi-train trajectory optimization for energy-efficient timetabling.

2. **Wang P**, Goverde R M P. (2017). Real-time trajectory optimization in train driver advisory system development.

Conference articles

1. **Wang P**, Goverde R M P. (2017). Development of the train driver advisory system ETO. 5th IEEE International Conference on Models and Technologies for Intelligent Transport Systems (MT-ITS). Napoli, Italy.

2. **Wang P**, Goverde R M P. (2017). Multi-train trajectory optimization method for energy-efficient timetable adjustment. 7th International Conference on Railway Operations Modelling and Analysis (Raillille). Lille, France.

3. **Wang P**, Goverde R M P. (2016). Train trajectory optimization of opposite trains on single-track railway lines. 2016 IEEE International Conference on Intelligent Rail Transportation (ICIRT). Birmingham, UK: 23-31.

4. **Wang P**, Goverde R M P. (2015). Two-train trajectory optimization with a green-wave policy. Transportation Research Board, Washington DC, USA.

5. **Wang P**, Goverde R M P, Ma L. (2015). A multiple-phase train trajectory optimization method under real-time rail traffic management. 2015 IEEE 18th International Conference on Intelligent Transportation Systems (ITSC). Las Palmas, Spain: 771-776.

6. **Wang P**, Goverde R M P, Ma L. (2015). Train trajectory optimization with signalling constraints. Conference on Advanced Systems in Public Transport (CASPT 2015), Rotterdam, the Netherlands.

7. **Wang P**, Wang Q, Ma L, Feng X. (2013). Real-time train speed regulation with consideration of over-speed protection. 2013 32nd Chinese Control Conference (CCC). Xian, China: 8141-8146.

8. **Wang P**, Lin X, Li Y. (2012). Optimization analysis on the energy saving control for trains with adaptive genetic algorithm. 2012 International Conference on Systems and Informatics (ICSAI), Yantai, China: 439-443.

TRAIL Thesis Series

The following list contains the most recent dissertations in the TRAIL Thesis Series. For a complete overview of more than 150 titles see the TRAIL website: www.rsTRAIL.nl.

The TRAIL Thesis Series is a series of the Netherlands TRAIL Research School on transport, infrastructure and logistics.

Wang, P., *Train Trajectory Optimization Methods for Energy-Efficient Railway Operations*, T2017/12, December 2017, TRAIL Thesis Series, the Netherlands

Weg, G.S. van de, *Efficient Algorithms for Network-wide Road Traffic Control*, T2017/11, October 2017, TRAIL Thesis Series, the Netherlands

He, D., *Energy Saving for Belt Conveyors by Speed Control*, T2017/10, July 2017, TRAIL Thesis Series, the Netherlands

Bešinović, N., *Integrated Capacity Assessment and Timetabling Models for Dense Railway Networks*, T2017/9, July 2017, TRAIL Thesis Series, the Netherlands

Chen, G., *Surface Wear Reduction of Bulk Solids Handling Equipment Using Bionic Design*, T2017/8, June 2017, TRAIL Thesis Series, the Netherlands

Kurapati, S., *Situation Awareness for Socio Technical Systems: A simulation gaming study in intermodal transport operations*, T2017/7, June 2017, TRAIL Thesis Series, the Netherlands

Jamshidnejad, A., *Efficient Predictive Model-Based and Fuzzy Control for Green Urban Mobility*, T2017/6, June 2017, TRAIL Thesis Series, the Netherlands

Araghi, Y., *Consumer Heterogeneity, Transport and the Environment*, T2017/5, May 2017, TRAIL Thesis Series, the Netherlands

Kasraian Moghaddam, D., *Transport Networks, Land Use and Travel Behaviour: A long term investigation*, T2017/4, May 2017, TRAIL Thesis Series, the Netherlands

Smits, E.-S., *Strategic Network Modelling for Passenger Transport Pricing*, T2017/3, May 2017, TRAIL Thesis Series, the Netherlands

Tasseron, G., *Bottom-Up Information Provision in Urban Parking: An in-depth analysis of impacts on parking dynamics*, T2017/2, March 2017, TRAIL Thesis Series, the Netherlands

Halim, R.A., *Strategic Modeling of Global Container Transport Networks: Exploring the future of port-hinterland and maritime container transport networks*, T2017/1, March 2017, TRAIL Thesis Series, the Netherlands

Olde Keizer, M.C.A., *Condition-Based Maintenance for Complex Systems: Coordinating maintenance and logistics planning for the process industries*, T2016/26, December 2016, TRAIL Thesis Series, the Netherlands

Zheng, H., *Coordination of Waterborn AGVs*, T2016/25, December 2016, TRAIL Thesis Series, the Netherlands

Yuan, K., *Capacity Drop on Freeways: Traffic dynamics, theory and Modeling*, T2016/24, December 2016, TRAIL Thesis Series, the Netherlands

Li, S., *Coordinated Planning of Inland Vessels for Large Seaports*, T2016/23, December 2016, TRAIL Thesis Series, the Netherlands

Berg, M. van den, *The Influence of Herding on Departure Choice in Case of Evacuation: Design and analysis of a serious gaming experimental set-up*, T2016/22, December 2016, TRAIL Thesis Series, the Netherlands

Luo, R., *Multi-Agent Control of urban Transportation Networks and of Hybrid Systems with Limited Information Sharing*, T2016/21, November 2016, TRAIL Thesis Series, the Netherlands

Campanella, M., *Microscopic Modelling of Walking Behavior*, T2016/20, November 2016, TRAIL Thesis Series, the Netherlands

Horst, M. van der, *Coordination in Hinterland Chains: An institutional analysis of port-related transport*, T2016/19, November 2016, TRAIL Thesis Series, the Netherlands

Beukenkamp, W., *Securing Safety: Resilience time as a hidden critical factor*, T2016/18, October 2016, TRAIL Thesis Series, the Netherlands

Mingardo, G., *Articles on Parking Policy*, T2016/17, October 2016, TRAIL Thesis Series, the Netherlands

Duives, D.C., *Analysis and Modelling of Pedestrian Movement Dynamics at Large-scale Events*, T2016/16, October 2016, TRAIL Thesis Series, the Netherlands

Wan Ahmad, W.N.K., *Contextual Factors of Sustainable Supply Chain Management Practices in the Oil and Gas Industry*, T2016/15, September 2016, TRAIL Thesis Series, the Netherlands

Liu, X., *Prediction of Belt Conveyor Idler Performance*, T2016/14, September 2016, TRAIL Thesis Series, the Netherlands

Gaast, J.P. van der, *Stochastic Models for Order Picking Systems*, T2016/13, September 2016, TRAIL Thesis Series, the Netherlands